

**FUNCTIONAL ORGANIZATION OF THE MONKEY  
VISUAL CORTEX FOR STEREOSCOPIC DEPTH.**

Daniel Lewis Adams.

PhD. Thesis.

University College London.

September 1997.

ProQuest Number: 10017388

All rights reserved

INFORMATION TO ALL USERS

The quality of this reproduction is dependent upon the quality of the copy submitted.

In the unlikely event that the author did not send a complete manuscript and there are missing pages, these will be noted. Also, if material had to be removed, a note will indicate the deletion.



ProQuest 10017388

Published by ProQuest LLC(2016). Copyright of the Dissertation is held by the Author.

All rights reserved.

This work is protected against unauthorized copying under Title 17, United States Code.  
Microform Edition © ProQuest LLC.

ProQuest LLC  
789 East Eisenhower Parkway  
P.O. Box 1346  
Ann Arbor, MI 48106-1346

## Contents

Abstract .....	5
Acknowledgements.....	7
Introduction	
Section 1	
The perception of depth	
Historical review of stereoscopic vision.....	9
The meeting of projections from the eyes .....	15
The random dot stereogram .....	17
Local and global stereopsis .....	18
Psychoanatomy .....	19
Ocular dominance .....	20
Ocular interaction .....	22
Disparity tuning.....	23
The functions of different types of disparity tuned cell.....	30
Other types of disparity .....	31
Psychophysics .....	34
The correspondence problem .....	37
Colour and stereopsis .....	37
Isoluminance studies.....	38
Spatial frequency .....	40
Orientation and stereopsis .....	41
Stereoscopic depth constancy .....	42
Computational models .....	44
Stereoblindness .....	47
Primate lesion studies .....	50
Effects of abnormal visual experience on binocular vision .....	51
Section 2	
The physiology of the V3 complex	
Orientation tuning in the V3 complex.....	55
Colour cells in the V3 complex .....	56
Real-motion cells.....	58
Gaze dependent cells .....	59
Section 3	
Anatomy of stereopsis	
Anatomical description of the prestriate areas .....	62
Cytochrome oxidase divisions within the visual cortex .....	64
"What" and "where" pathways .....	67
Materials and methods	
Pharmacology .....	73
Surgery .....	75
Perfusion .....	76
Optics.....	77
Physiology .....	78
Categorization of cell properties	
Receptive field data statistics .....	84
Receptive field characteristics.....	85
Response characteristics .....	86
The detection of cell grouping .....	90

Anatomical tracing and histological procedures .....	90
Histology.....	92
Cortical reconstructions .....	95
Results	
Section 1	
Electrophysiological data	
Allocation of cells to visual areas .....	103
The properties of cells in the V3 complex .....	105
a) Orientation selectivity tuning.....	105
b) Direction selectivity .....	111
c) Wavelength selectivity.....	120
d) Clustering of cells with similar properties .....	123
e) Binocular properties.....	126
f) Disparity tuning .....	130
Proportions of disparity cells.....	139
Properties of disparity tuned cells .....	140
Orientation and direction tuning .....	142
Length tuning.....	144
Receptive field eccentricity .....	144
Vertical disparity .....	146
Functional organization of disparity tuned cells .....	149
Comparison with V2 .....	169
Section 2	
Anatomical Data	
Introduction.....	174
Description of the visual areas .....	175
Injection sites .....	176
Cortical projections of V3. ....	177
The projections of V3A .....	185
Comparison of V3 and V3A. ....	197
The projections of DP. ....	198
Discussion	
Section 1	
Physiology	
Introduction.....	208
Orientation and direction .....	209
Non-classical orientation/direction cells .....	209
Comparison of V2 and the V3 complex .....	210
Orientation and disparity .....	213
Topography of the V3 complex .....	214
Disparity selective cells in the prestriate areas. ....	217
Proportions of disparity tuned cell types.....	219
Vertical disparity selectivity .....	220
Unorthodox disparity cells.....	222
Quantitative depth selectivities .....	224
Motor and sensory systems.....	225
Form vision.....	226
Section 2	
Anatomy	

Introduction.....	228
Pathways in the visual cortex .....	228
Connections of the V3 complex .....	231
"What" and "Where" pathways.....	233
Oculomotor systems .....	234
Parietal connections .....	235
Patchiness of connections .....	237
General conclusions .....	238
Appendix A	
General model of cell response to different stimulus directions	
Description of the models .....	240
Model optimisation .....	241
Statistical analysis of models .....	245
References .....	247

## Abstract

Our own, and other previous studies of V3 and V3A (two visual areas constituting the V3 complex) have shown it to contain many orientation tuned cells with strong binocular interactions (Zeki 1978b; Burkhalter and Van Essen 1986; Felleman and Van Essen 1987). This, and the area's M dominated cortical input, led us to choose the V3 complex as a likely candidate for an area specialized in the processing of stereoscopic depth. Thus, the aim of this study was to record from single cells in V3 and V3A and determine their selectivity for stereoscopic depth. The responses of cells in these two areas were examined and the distribution of disparity tuned cells was compared with that in area V2, which has all modalities of vision represented in it. The results show that the V3 complex contains a high percentage of disparity tuned cells and that these are also orientation or direction tuned. Thus, these cells are detecting the horizontal disparity of visual features. Previously defined classes of disparity tuned cell (Poggio and Fischer 1977; Poggio *et al.* 1988) were found in both the V3 complex and parts of V2. In agreement with previous studies, (Burkhalter and Van Essen 1986; Hubel and Livingstone 1987) disparity tuned cells were found in the thick stripes of V2.

The second part of this study was to examine brains injected with anatomical tracing agents to discover the cortical connections of the V3 complex and an area on the dorsal prelunate gyrus (DP) which receives an input from V3A. Results showed that the areas injected V3, V3A and DP have extensive connections with each other and with areas dealing with other attributes of vision. The results demonstrate that the V3 complex projects form and stereoscopic depth information to parietal and temporal

areas which use this information for the analysis of more complex visual attributes.

## Acknowledgements

This piece of work would not have been possible without the help of a number of people, primarily, my supervisor Professor Zeki, whose wisdom encouragement and advice was invaluable. I would also like to express my gratitude to Dr. Stuart Shipp for sharing his enthusiasm and expertise during experimental work as well as his critical reading of the manuscript, Grant Wray and John Romaya for technical and computer assistance and Mark Rayan and Anne Fitzpatrick for histological tutoring and help. I would also like to thank my colleagues, Konstantinos Moutoussis, Andreas Bork and Ludovica Marini for being good company and sharing the work load during experiments that usually lasted 24 hours a day for an entire week.

I am also grateful to the BBSRC, Wellcome Trust and latterly the Department of Social Security for providing the funds necessary for the completion of this thesis.

# Introduction

## Section1

### The perception of depth

The ability to judge depth is an important faculty of visual animals; it provides them with knowledge of distance with respect to the organism and distances of objects with respect to one another and hence prepares them for making appropriate motor responses. It is of evolutionary importance because it greatly aids the hunting and capture of prey as well as the safe navigation of animals in their environment. Psychophysical studies indicate that the perceptual transformation from two to three dimensions relies on two types of cues: cues for monocular depth, and stereoscopic cues for binocular disparity. At distances greater than about 50m the retinal images from each eye are virtually identical, so depth must be judged using monocular cues. There are at least five types of monocular depth cue:

1. *Previous familiarity.* If we know from experience something about the size of an object we can judge the object's distance.
2. *Interposition.* If one object is partially hidden from view by another object we assume the hidden object is further away.
3. *Linear and size perspectives.* Parallel lines appear to converge with distance. The greater the convergence of lines, the greater the impression of distance. The visual system interprets the convergence as depth by assuming that the lines remain parallel.
4. *Distribution of shadows and illumination.* Patterns of light and dark can give the impression of depth. The shading on objects implies different inclinations to the light source and on the whole, brighter shades of colours tend to be seen as nearer.

5. *Motion (or monocular movement) parallax.* As we move our heads from side to side, the image projected by an object in the visual field moves across the retina. Nearby objects seem to move quickly and in the opposite direction to our movement, whereas distant objects move slowly.

All of the above cues (except the fifth) are used by artists to endow their paintings with a sense of depth. This impression of depth can be so convincing to the brain that if some paintings (particularly those containing a great deal of linear perspective cues) are viewed monocularly, the visual system will make convergent and divergent eye movements that match those that would be made when viewing the real three dimensional scene (Enright 1987).

Objects viewed at distances smaller than about 50m project a slightly different image onto each retina because the eyes are separated horizontally. This difference (called disparity) can be used by the visual system as a powerful depth cue. The analysis of disparity to produce depth vision is called stereopsis.

#### Historical review of stereoscopic vision

The history of ideas about vision is documented back to the time of the Greeks, who, following an idea by Empedoclés (5th century BC), believed that light leaves the eye in the form of a cone made up of straight rays and these rays gain knowledge of the world by "feeling" objects rather like an invisible hand. The information gained is then transported back to the eye and brain to generate visual sensations. Recently it has been commented that this idea of active vision is more akin to reality than the idea of a passive "camera like" visual system.

The first breakthrough in visual optics was the work of an Arabic scholar by the name of Alhazen (965-1040). He firmly rejected the emanation theory of vision proposed by the Greeks and in his book "The Book of Optics" (Kitāb al-manāzīr) (Alhazen 1989). He proposed that the visual scene is projected as a two dimensional inverted image onto the retina. Realising that the image would be inverted and reversed, he suggested that it was corrected by a further refraction from the back of the eye to form a corrected image on the optic disc. Many years later, Johannes Kepler (1571-1630) concluded that there was no basis for the second inversion proposed by Alhazen and suggested that the image was rectified by a mental process. The realization that the visual image was projected onto the retina as a two dimensional representation caused people to wonder how the flat image on the retina was transformed into a three dimensional precept of the visual world. This problem was of particular concern to artists, whose main preoccupation was how to represent three dimensions on a flat canvas. Since stereoscopic cues cannot be used in paintings, the foci of these enquiries were based on monocular depth cues.

Although the rudiments of binocular vision had been observed by Euclid, who noticed that the eyes each have a slightly different view of the world, and Aristotle, who noted that when one eye is pressed with a finger, a double image is produced, binocular vision was not equated with depth perception. Thus the question arose "why do we have two eyes?" For many years (since the time of Alhazen) it was believed that two eyes were useful because if one becomes damaged, the other remains intact. This is not to say that the geometry of binocular optics was not studied; Alhazen himself described the way in which objects placed in front of or behind the fixation plane produce double images and those

that lie at, or close to, the fixation plane, i.e. on corresponding points, are fused to form a single image. With this observation, Alhazen described what we now know as the horopter, i.e. the plane in space at which objects can be seen as single fused images. Although Alhazen realized that this plane was not fronto-parallel, its precise geometry was not studied until 1818 by Vieth and Müller (Vieth 1818; Müller 1826). Similarly, Alhazen described a small area in space either side of the fixation plane, at which objects can still be seen as single and fused, this area is now known as Panum's fusional area, and its study had to wait until 1858 (Panum 1858).

Perhaps the earliest description of stereopsis was produced by Leonardo da Vinci (1452-1519); in his work *Trattato della pittura* (see Keele 1955; Strong 1979) he observed; "That a painting, though conducted with the greatest art and finished to the last perfection, both with regard to its contours, its lights, its shadows and its colours, can never show a rilievo equal to that of the natural object, unless these be viewed at a distance and with a single eye." taken from Wheatstone (1838). Here Leonardo implied that two dimensional pictures can only truly portray the real scene if that scene is devoid of stereoscopic depth cues. However, Leonardo did not show a full understanding of the finer points of stereopsis other than the idea that closing one eye transformed the visual world into an image more resembling that on a canvas.

In 1613 Franciscus Aguilon published his works on optics entitled *Opticorum libri sex*. His 6 books followed the work of Euclid, Alhazen and others with the addendum that depth perception is improved with binocular vision. This point was illustrated in Aguilon's book with an engraving by the artist Rubens which depicts a one eyed man under-

estimating the distance to an object held in front of him (reproduced in figure 1).



Figure 1.

Rubens' engraving depicting a one-eyed man underestimating the distance to an object held in front of him to portray the point that binocular vision is important for depth discrimination. Produced in 1613, it was commissioned by Franciscus Aguilon to illustrate his work *Opticorum libri sex* (Taken from Judson and van de Velde 1978).

Thus, the question "Why do we have two eyes?" was answered nearly two centuries after it was asked. Aguilon studied the geometry of binocular vision using the theorems of Euclid and coined the term "horopter" to describe the plane in space at which both fused and diplopic images appear to lie. The word horopter comes from the Greek "*horos*", meaning space and "*opter*", observer. The word horopter is still used today, but to describe a slightly different plane. Aguilon used the term to describe a fronto-parallel plane at the same distance from the observer as the fixation point. Today the horopter describes a plane in space, points lying on which appear fused to the observer. Rather than a fronto-

parallel plane, this produces a horizontal circle (the Vieth-Müller circle) which passes through the centres of both eyes (see figure 2).

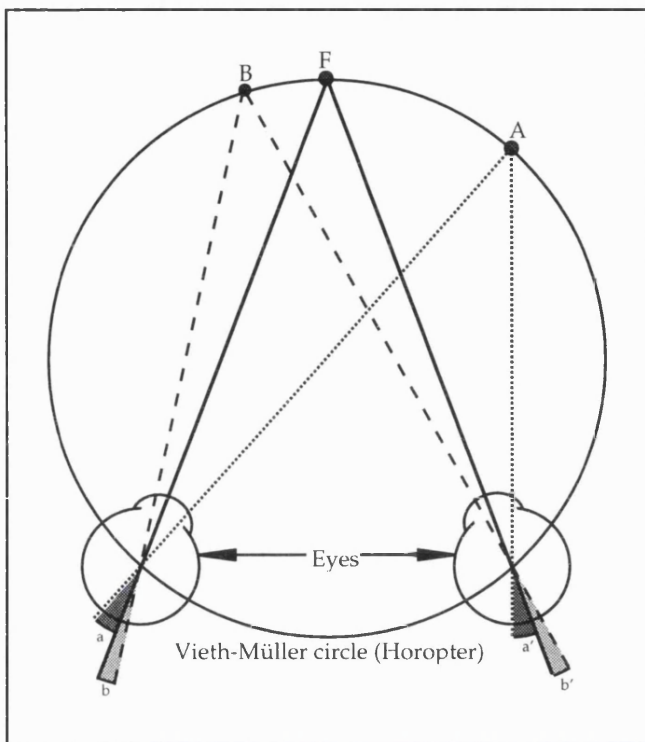


Figure 2.

Illustration of the Vieth-Müller circle or horofter. The figure represents a horizontal plane including both eyes and a fixation point (F). Points A and B lie on the Vieth-Müller circle. From Euclidean geometry, angles  $a = a'$  and  $b = b'$ . Thus the points A and B both project to corresponding retinal points and are seen as single fused images, as do all points that lie on the circle.

The Vieth-Müller circle was first described in a paper by Vieth (1818), although it was simultaneously studied by Müller (1826). They showed that all points projecting to corresponding retinal points form a circle that passes through the optic centres of both eyes. Vieth mistakenly generalized his theory of corresponding points in three dimensions to a sphere. His mistake was corrected by Prévost (1843) who showed that the theoretical horofter is in fact a toroid formed by sweeping the Vieth-Müller circle through the interocular axis.

The notion that binocular vision gives rise to depth perception was not further pursued until the 19th century when Charles Wheatstone (the inventor of the Wheatstone bridge) published a paper entitled: "Contributions to the physiology of vision. -Part the first: On some

remarkable, and hitherto unobserved, Phenomena of Binocular Vision" (Wheatstone 1838). He showed an understanding of stereoscopic depth perception and illustrated the phenomenon with the invention of the stereoscope. With this instrument, shown in Figure 3, two photographs of a scene taken 60-65mm apart, one from the position of each eye, are mounted onto a binocular like device such that the right eye sees only the picture taken from the right position and the left eye sees only the left picture. Fusion of the two images produces a three dimensional image.

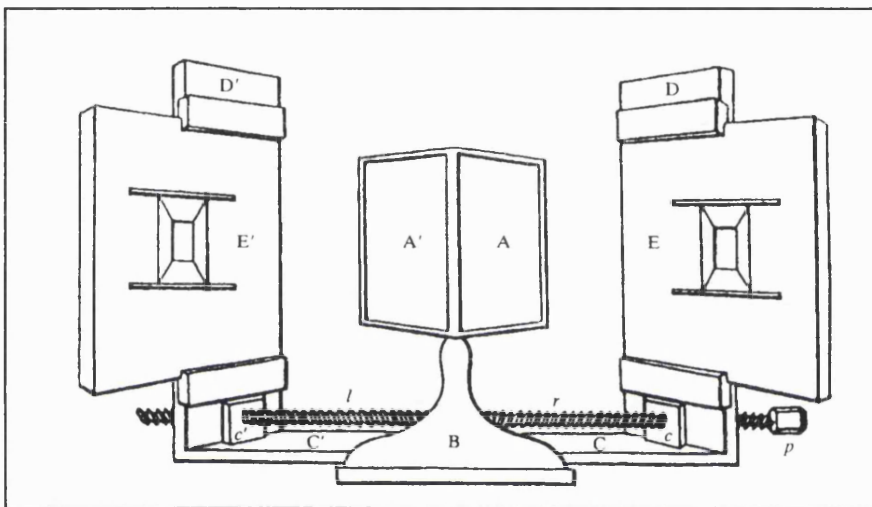


Figure 3.

A diagram of Wheatstone's stereoscopic apparatus. The two monocular images (E' and E) are reflected by mirrors (A' and A) placed close to the eyes of the viewer, so that each eye only sees one image. The two images are therefore superimposed and the viewer fuses them to produce a "solid" stereo image. (Taken from Wheatstone 1838).

Thus the stereoscope vividly demonstrates stereopsis by enabling convincing stereoscopic depth to be perceived from two-dimensional images. In Wheatstone's own words, "The preceding experiments render it evident that there is an essential difference in the appearance of objects when seen with two eyes, and when only one eye is employed, and that the most vivid belief of the solidity of an object of three dimensions arises from two different perspective projections of it being simultaneously presented to the mind." (p. 380). If the elements of

disparity in Wheatstone's stereoscopic pictures are examined it can be seen that corresponding elements in each picture are shifted towards or away from each other; the former causes a shift in depth in front of, and the latter behind, the viewer's fixation plane.

In 1858, Panum described a range of disparities within which two similar images, one in each eye, are perceived as a single image (Panum 1858). This plane (Panum's fusional area) is an area in depth that extends in front of and behind the fixation plane that corresponds to the region of binocular single vision. The images from the two eyes of all points within this area are said to be 'fused'. The front to back size of the area in depth is dependent upon a number of factors: it increases in a geometric way as the fixation plane become further away from the eyes but the visual angle subtended from the front of the area to the back remains constant, and it tends to increase in size towards the periphery of the visual field. It is also dependent on the nature of the stimulus and its background (Panum 1858; Ogle 1964).

### The meeting of projections from the eyes

In order that the two views of the world be unified to produce a single percept, information from both eyes must arrive at single cells in the brain. Although this concept seems obvious today, for a long time it was thought that the monocular images remained separate throughout the visual system and were combined "by a mental act" (Helmholtz 1893). Ramón y Cajal stood alone in his belief that inputs from corresponding parts of the two retinae converge on what he called "isodynamic cells" and it is this that forms the basis of unified binocular vision (Ramón y Cajal 1911). The location of the first binocular cells in the visual system has been sought for many years, since it is here that the intricacies of

binocular vision may be elucidated. Not unreasonably, Galen (175) and after him, Alhazen (1989), thought that the locus of binocular combination was the optic chiasm. During the Renaissance, René Descartes proposed that the optic fibres might converge on the pineal gland for unification (*Traité de l'Homme*). In fact the first possible site for unification of information from the two eyes is the lateral geniculate nucleus (LGN), where fibres from both eyes terminate having already been combined en-passage through the optic chiasm. The LGN is a nucleus comprising six layers. Physiological and anatomical examinations of the layers (Silva 1956) reveals them to contain cells that receive monocular inputs; layers 1, 4 and 6 receive projections from the contralateral eye and the others are exclusively innervated by the ipsilateral eye. Cells in these layers are also solely excited by their respective eye. Extensive connections exist between the layers of the LGN but these do not endow the cells with the property of binocularity (Guillery 1971). Thus, fibres leaving the LGN still carry monocular information. The next stage in the visual pathway is the primary visual cortex (striate cortex, area 17 or V1), more specifically layer 4c, the input layer. In 1959, Hubel and Wiesel proved Ramón y Cajal to be correct by demonstrating the existence of binocular cells in the cortex (Cajal's "isodynamic cells"). These cells first occur in V1 except in layer 4c. V1 is therefore the first locus where fusion of the two monocular images can occur (Hubel and Wiesel 1959). Quite why cells retain their exclusive monocularity until this stage, when they have had ample opportunity for generation of binocularity at previous parts of the visual system, is not known.

### The random dot stereogram

How does the brain know which parts of the monocular image correspond to the same object viewed by the other eye? This question (the correspondence problem, which we will return to) remains unresolved today but a great advance was made in 1960. Bela Julesz, a radar engineer, was working with wartime aerial photographs taken behind enemy lines. A technique used to spot camouflaged structures was to take two photographs from slightly different locations and view them with a stereoscope this way objects taller than their surroundings stand out in binocular depth. At the time, the prevalent view about the correspondence problem held by psychologists was that the brain first recognized an object in the monocular images, and then paired the two objects to produce single vision and stereoscopic depth. Working with stereoscopic images comprising few recognizable forms, Julesz knew this not to be the case. To demonstrate his observation he made images with a computer, similar to his stereoscopic aerial photographs but containing no recognizable forms. These "random dot stereograms" (RDS) comprise two random, yet correlated patterns of dots with a central portion of dots being shifted by an integer multiple of the dot size in opposite directions for each image (Julesz 1960). Fusion of the two images produces a powerful sensation of depth, the central portion being displaced in front of, or behind the surrounding texture, depending on the direction of the shift of that part of the texture with respect to the surround.

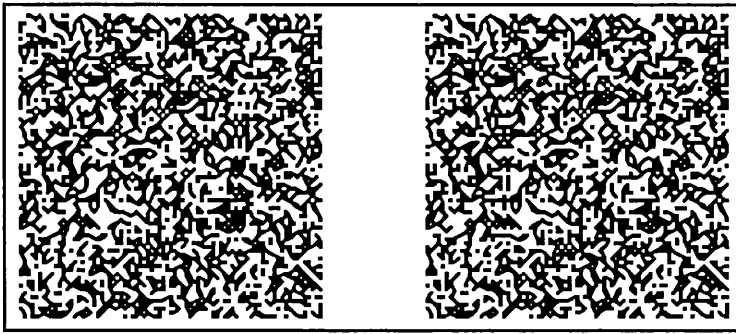


Figure 4.

An example of Julesz's original random dot stereogram. Diverging the eyes in such a way as to superimpose and fuse each monocular image produces the sensation of depth. In this figure, divergent viewing produces a smaller square displaced behind the plane of the paper.

These figures vividly demonstrate that, contrary to the predominant theory of the day, binocular depth perception does not require monocular form recognition and is an operation carried out quite "early" in the visual system. This revelation shifted the emphasis of neurophysiological research from problems in monocular form recognition to the search for binocular cells in the visual brain. It also introduced the notion of local and global stereopsis.

#### Local and global stereopsis

One of the most important consequences of the invention of the random dot stereogram was the revelation that monocular form or depth cues are not necessary for binocular fusion. Thus, the visual system must be using a very much more simple method of fusing binocular images than previously supposed. Since the many similar elements in a random dot stereogram could easily give rise to false matches, the system must be using more than just the form of the individual elements to produce binocular fusion. Thus, global stereopsis is the method the visual system uses to examine large portions of the monocular images and undertakes a cross correlation analysis, not only matching individual features but also taking into account their surrounding global

neighbourhood to disambiguate false matches (Julesz 1971; Julesz and Oswald 1978). Local stereopsis refers to the more classical kind of binocular fusion where, within Panum's fusional area, unique features in each monocular image are paired to resolve ambiguity (Julesz 1971; Julesz and Oswald 1978).

### Psychoanatomy

Since the depth features of random dot stereograms can only be seen when monocular information from each eye has converged onto a single cell, it can be said that all the neural machinery up to V1 is incapable of responding to stereoscopic depth. Thus, any perceptual effects produced by viewing stimuli presented as random dot stereograms must be produced in the cortex rather than the retina or LGN. The localization of perceptual effect using psychophysics was called psychoanatomy (Julesz 1971). Many types of random dot stereograms (both static and dynamic) have since been produced, each designed to exhibit a particular optical illusion or perceptual aftereffect. These studies are numerous and mostly draw the same conclusions, i.e. perceptual effects can be reproduced without the need for monocular features and must therefore be produced within the visual cortex. The first psychophysicist to employ disparity instead of luminance gradients for the presentation of optical illusions was Papert (1961). By presentation of common optical illusions, such as the Müller-Lyer lines<sup>1</sup>, Papert showed that the illusions persist when no monocular cues are present, thus demonstrating that the locus of the illusion is cortical rather than retinal or thalamic.

---

<sup>1</sup>The Müller-Lyer lines are a famous optical illusion constituting lines of identical length, one terminated at each end with an inwardly facing arrowhead, the other terminated by outwardly facing arrowheads. The line with outwardly facing arrowheads appears shorter than the other.

## Ocular dominance

The advent of single unit recording brought about a revolution in the study of the visual system. First applied in the primary visual cortex, cells were found that responded to stimuli presented to the animal (Hubel and Wiesel 1959). Cats were used at first, and later, because of their superior vision (especially colour vision) and the similarity of their visual system to humans, monkeys were recorded from. The relative influence of the two eyes on the response of a cell (ocular dominance) varies from cell to cell in V1 and a scheme of classification was devised (Hubel and Wiesel 1962). The stimuli used to categorize cells into these groups were presented to each eye in turn. Thus, it was not possible to find out how the responses of the cell might change when both eyes are stimulated simultaneously (binocular interaction). Cells in V1 were found to fit into one of seven groups: group 1 contains cells that are exclusively contralaterally driven, while group 7 cells are exclusively ipsilaterally driven, with all gradations in between.

Cells in these groups were found to fit into a columnar organization in the primary visual cortex, the ocular dominance columns. These robustly organized columns are only present in the primary visual cortex and comprise a patchwork of modules normal to the surface of that area, each eye supplying irregular stripes of cortex about half a millimetre wide. Ocular dominance columns remain one of the most solid findings in the visual system and have since been demonstrated anatomically and physiologically. The first anatomical demonstration was achieved by making lesions in single layers of the LGN and looking at the pattern of degenerated axon terminals in the striate cortex (Hubel and Wiesel 1969). Since the layers of the LGN contain monocular cells, the degeneration was restricted to the

monocular ocular dominance columns. Technical advances led to an improved anatomical method of visualization of ocular dominance columns involving the injection of a radio-labelled amino-acid (tritiated proline) into one eye. It was first achieved in the mouse (Grafstein and Laurenco 1973) and later emulated in the monkey (Wiesel *et al.* 1974). The amino-acid is transported from the retinal ganglion cells to the LGN and then transneuronally to striate cortex. Autoradiography of sections taken from striate cortex exhibit patches of dense transport of the amino acid in layer 4, corresponding to the domains that contain monocular cells. The 2 Deoxy-glucose (2DG) technique (Sokoloff 1977), when employed by Tootell *et al.* (1988a), also demonstrated, among other things, the pattern of ocular dominance columns in the striate cortex of the macaque. The 2DG technique is a method of showing a picture of functional activity; radioactive glucose ( $^{14}\text{C}$ -2-deoxy-*d*-glucose) is injected into the animal's circulation while it is presented with a visual stimuli. After viewing the stimuli for a few minutes in the paralysed and anaesthetized state (to prevent eye movements) the animal is killed and its brain sectioned. Areas that were very active directly before the animal's death contain more of the radioactive glucose and can be visualized by autoradiography. Thus, full field monocular stimulation of the animal will produce pictures of the ocular dominance columns in flat mounted sections, cut parallel to V1's surface. These techniques have established that the ocular dominance columns form a series of parallel bands, each 0.25 to 0.5 mm wide. They spread through all layers of the cortex and in each hemisphere a retinotopic map of the visual hemifield is represented twice, one within the left eye columns and one within the right. The bands tend to run  $90^\circ$  to the V1/V2 border in 'iso-eccentric stripes', thus mapping two circular visual fields onto the elliptical surface of the striate cortex (Hubel and Wiesel 1977; LeVay *et al.* 1985; LeVay and Voigt 1988).

Hubel and Wiesel suggested that the differing degrees of ocular dominance might, in some way, provide the basis for a depth sensitivity mechanism, the dominance characteristics being segregated so that each monocular component of an image could be compared to that of the other eye. This has so far proved not to be the case, and the functional significance (if any) of ocular dominance and its columnar organization in V1 in some (but not all<sup>2</sup>) animals with stereoscopic vision remains unclear.

### Ocular interaction

Aside from Hubel and Wiesel's ocular dominance characteristics, another type of binocular property exists for cells in the visual cortex. Since Hubel and Wiesel stimulated their cells monocularly, they did not find information relating to the binocular interactions of cells. When cells are driven binocularly their responses may change and are not predictable from the monocular responses. Zeki (1979) examined this property and devised a method of classification of binocular cells depending upon their response during binocular stimulation. Thus, cells were divided into six groups according to whether they were driven by one eye only (two categories), dominated by one eye (two categories), equally well driven by either eye (one category) or driven by simultaneous binocular stimulation only (one category). Using these categories, so called "ocular interaction histograms" could be plotted for populations of cells. When these histograms are plotted for particular visual areas one can see that nearly all cells in prestriate cortex, i.e. all cells beyond V1, are (i) binocular and (ii) produce differing degrees of binocular interaction. Thus all these prestriate areas are, in theory,

---

<sup>2</sup>The squirrel monkey (*Saimiri sciureus*) does not have ocular dominance columns in its primary visual cortex, yet its stereoscopic vision is comparable to primates that do. (Livingstone *et al.* 1995).

candidates for analysing stereoscopic depth. However, since disparity was not systematically varied in Zeki's study, cells that only respond at critical disparities may have been missed. It is this property that enables cells to be depth selective, and an area with a high proportion of these disparity selective cells would be a far more likely candidate for an area of depth specialization.

### Disparity tuning

The receptive fields of binocular cells in V1 were found to occupy corresponding areas on the two retinae and their response properties were qualitatively identical for both eyes (Hubel and Wiesel 1962). Stereoscopic vision requires more than the presence of binocular cells alone. In order to get information regarding the relative depths of objects from the fixation plane the system needs to be capable of fusing the images from both eyes and analysing the information derived from the small differences between each image. To achieve this one would expect some binocular cells to have receptive fields that are slightly non-corresponding, this receptive field disparity being in the order of a few minutes of arc, thus allowing the cells to respond maximally when slight disparities exist between the two monocular images. This is what makes cells disparity tuned.

The experimental stimulation of both receptive fields simultaneously will yield information regarding binocular interaction (facilitation or attenuation), but in order to stimulate cells at specific disparities a more elaborate regime is required. One solution in the paralysed animal is to superimpose both receptive fields on a screen using Risley bi-prisms and stimulate with a single moving bar (Pettigrew *et al.* 1968; Bishop *et al.* 1971). The setting on the prisms can then be

quantitatively varied to stimulate the cell over a range of retinal disparities. Another method is to leave the receptive fields separated and employ two stimuli, one for each receptive field (Henry *et al.* 1969). If the two stimuli are correctly positioned, the animal should fuse them and its visual system be presented with a single binocular stimulus. By varying the distance between the two stimuli one can change the disparity. The advantage of both of these techniques is that one can stimulate cells at specific disparities and if a cell's responses are sensitive to small changes in disparity, it shows that the cell is tuned to stimuli placed at a specific distance relative to the horopter.

The method of superimposing the receptive fields of a cell using prisms was employed by Pettigrew *et al.* (1968) in the striate cortex of the cat. Their major finding was that cells had greatly facilitated responses when stimulated by a single moving bar with their receptive fields superimposed; furthermore, some cells were exquisitely sensitive to the exact position of the receptive fields. Differences as small as 3 minutes of arc would greatly modify the cell's responses, and if disparity (i.e. the prism setting) was set to non optimal values, some cells' responses could be inhibited. Thus cells in cat striate cortex can be selective for disparity. If the disparities these cells are tuned to deviate from zero one can assume they are doing more than fusing the two retinal images to form the "cyclopean image"<sup>3</sup>. A population of cells whose responses are maximized over differing disparities would in effect be tuned to different positions in depth relative to the horopter.

---

<sup>3</sup>*Cyclopean image* is a term introduced by Bela Julesz (1971), it refers to the single binocular image we perceive from the fusion of two images and is named after the mythological Greek giant, Cyclops, who had a single eye in the middle of his forehead.

In order to measure differences in disparity tuning from cell to cell, the very small eye movements that occur, even after complete paralysis of the eye musculature, must be stopped, or measured and subtracted from the data. The methods of eye movement elimination in Bishop/Pettigrew's group were to plot the optic disks of each eye onto a screen and monitor their movement. This method is only possible in the cat because it, unlike the monkey, has reflective retinae; shining a bright light into the cat's eyes produces an image of its retinae on the tangent screen. Additionally, the eyes were immobilized by gluing the scleral margins to brass rings. With these measures in place the authors found a spread of optimal disparities of  $\pm 1^\circ$  (Nikara *et al.* 1968), most cells being tuned to points at or very close to zero disparity, i.e. the horopter.

Using the prism method of aligning receptive fields, Hubel and Wiesel were also looking for binocular cells (Hubel and Wiesel 1970), but in the monkey visual cortex. In order to keep track of eye movements they simultaneously recorded from a binocular V1 "reference" cell in the opposite hemisphere and repeatedly plotted its receptive fields, taking note of any movements. Since the receptive fields of V1 cells are small and well defined, any movement of the positions of the reference cell's receptive fields will correspond to eye movements, and can be removed from the data obtained from the investigating electrode. Unable to find binocular depth cells in area 17 (V1) they moved onto the territory of the prestriate cortex which at the time was thought to comprise two areas (18 and 19). Here they found a large proportion of cells (43%) whose responses were critically dependent upon the prism setting and were therefore disparity selective or "binocular depth cells". Hubel and Wiesel noted that although there was variation in horizontal disparity among cells, neighbouring cells often had similar disparity selectivities but

varying orientation selectivities. These groups of binocular depth cells were segregated from cells not concerned with depth and tentatively called depth columns. Hubel and Wiesel also noted that the disparity of a cell was related to its orientation selectivity, "The displacement of the field in one eye, relative to the field in the other, is usually at right angles to the receptive field orientation." (Hubel and Wiesel 1970). Thus only cells with near vertical orientation tuning will be tuned to horizontal disparity. Retrospective examination of this paper shows that the authors were recording from two areas, V2 and V3A; they found binocular depth cells in both, although they were unaware of this subdivision within the lunate sulcus at the time.

The spread of optimal disparities found by Bishop/Pettigrew's group (Barlow *et al.* 1967; Nikara *et al.* 1968) in cat striate cortex prompted Hubel and Wiesel to re-examine the stereoscopic mechanisms in that animal (Hubel and Wiesel 1973). Hubel and Wiesel's recordings from monkey striate cortex had shown there to be very little variation in receptive field disparities in V1; the great majority of cells had their fields in precise registration (only 5% showing detectable disparities) and they had found no convincing examples of binocular depth cells (Hubel and Wiesel 1970). In order to find out if the difference was a genuine species difference they recorded from the cat's striate cortex, controlling for eye movements by keeping a striate reference cell in the opposite hemisphere with which to compare disparities. Contrary to Bishop/Pettigrew's data they found very little variation in disparities and concluded that the main mechanisms subserving stereoscopic depth perception in the cat (as in the monkey) lie outside the striate cortex. The discrepancy between these two groups is probably down to their stimulation and field plotting techniques. Hubel and Wiesel defined disparity as the relative distance

between the receptive fields of a cell (taking eye movements into account), but Bishop/Pettigrew's group defined it as the prism setting required to produce a maximal response of a cell. It is possible that a cell may still not give a maximal response when its receptive fields have been perfectly superimposed. Rodieck recognized this problem in terminology (Rodieck 1971) and suggested that the term "incongruity" be used for receptive field disparity (i.e. non-corresponding locations of receptive fields), keeping the term "disparity" for response-defined disparity only. Since these early studies many disparity tuned cells have been found in cat and monkey striate cortex (Nelson *et al.* 1977; Poggio and Fischer 1977; Von der Heydt *et al.* 1978).

Once isolated, the best way to study a binocular depth cell is to plot a graph of horizontal stimulus disparity against the cell's response to that stimulus. For non-disparity tuned binocular cells such a graph will give rise to a broad curve, showing simply that the cell responds better to binocular stimulation than monocular. For a smaller proportion of binocular cells the curve will be a far more specific shape, showing that the cell is disparity tuned. Disparity tuned cells modulate their responses over a very narrow range of disparities and the type of modulation they show fits them into a scheme of classification devised by Poggio and Fischer (1977). This classification scheme divides cells into two groups, either near/far (asymmetric) or tuned. Figure 5 shows the response properties (in the form of disparity tuning curves) for their four types of disparity tuned cell.

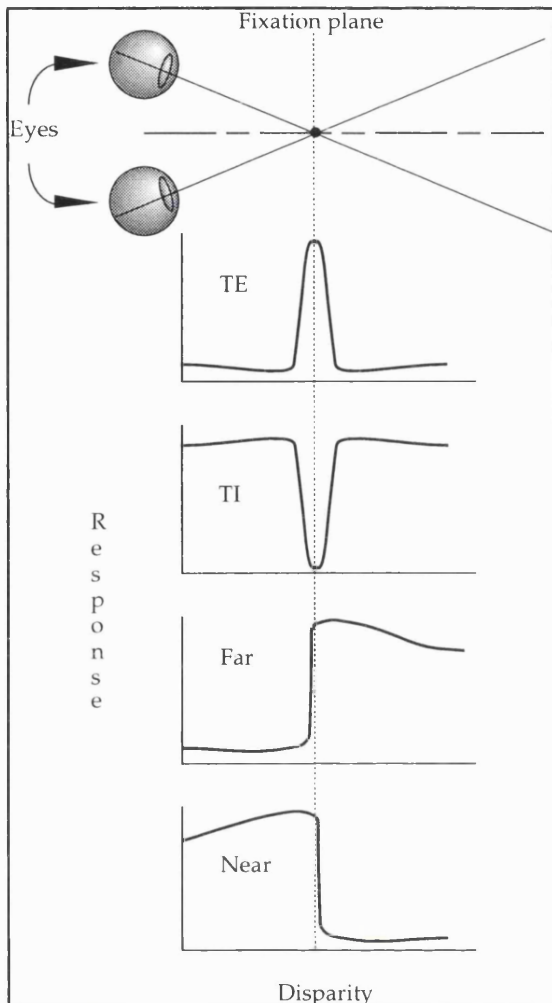


Figure 5.

Shapes of the disparity-response curves for the four types of disparity tuned cell described by Poggio and Fischer in their 1977 paper. TE, Tuned excitatory, TI, Tuned inhibitory. The Near and Far cells fall into the asymmetric category, and the TE and TI cells into the tuned category. The positions of the curves on the x axis are relative to the position of the fixation plane.

Poggio and Fischer's recording set-up had a number of advantages over previous ones that enabled them to find and classify these cells: firstly they recorded from the awake behaving monkey, trained to fixate a particular point while its receptive fields were plotted and stimuli presented. This carries the advantage that one always knows the position of zero disparity and eye movement problems were eradicated. Also the stimuli were presented in real depth relative to the depth of the fixation spot (i.e. the stimulus screen was moved towards or away from the animal) rather than using disparate stimuli or superimposing receptive fields, as had been used in the previous studies. An important feature of disparity tuned cells is the position of the optimal disparity relative to the

fixation plane. Poggio and Fischer found that most of their cells were tuned to points within  $\pm 0.5^\circ$  of the fixation plane. This corresponds to a real distance in depth of roughly  $\pm 3\text{cm}$  at their particular fixation distance, a value roughly equal to Panum's fusional area. They concluded that the range of optimal disparities they found (For TE and TI cells) was the neural correlate of Panum's fusional area (Poggio and Fischer 1977).

Since their 1977 study, Poggio *et al.* have found disparity tuned cells in both V2 and V3 (Poggio *et al.* 1985; Poggio *et al.* 1988). In their 1988 paper they enlarged their categories of disparity tuned cells to include the tuned near (TN) and tuned far (TF) types: these neurones have response profiles similar to the tuned excitatory type, but their responses occur at disparities between  $\pm 0.01^\circ$  to  $1.0^\circ$  thus, they differ from TE cells in their location, but not the width of their optimal response. These neurones are in a minority in V1 (14/31), increase in V2 (21/30) and are common in V3/V3A (23/26) (Poggio *et al.* 1988). The eccentricities of different types of disparity tuned cells were also studied by the authors but since the majority of the cells they investigated in V1 and V2 had their receptive fields within  $4^\circ$ , and all of their V3 cells were at eccentricities greater than  $4^\circ$ , they were not able to provide any strict correlation between eccentricity and stereotuning.

The proportions of the various types of disparity tuned cells in different areas have also been the subject of investigation and it has been shown to vary in different visual areas. The proportion of tuned cells versus asymmetric cells changes as the level of hierarchical processing is increased. In V1, V2 and V3 tuned cells and asymmetric cells are in equal proportions (Poggio *et al.* 1988), in V5 the proportion of asymmetric cells increases to 60% (Maunsell and Van Essen 1983a), in MST (V5A) the

proportion of asymmetric cells increases to about 90% (Roy *et al.* 1992) and in the lateral intraparietal area (LIP) the figure is 100% (Gnadt and Mays 1991).

#### The functions of different types of disparity tuned cell

Since "tuned" cells (TE, TI, TN and TF cells) are often present at the early stages of visual processing it has been suggested that they may be predominantly involved in the stereo-matching process to maintain accurate stereo fusion within Panum's fusional area (Trotter 1995). The width of tuning of TE/TI cells would therefore correspond to the limit of stereo acuity (Poggio and Fischer 1977). The asymmetric cells' function may be more to do with the control of convergent and divergent eye movements and to tell the visual system whether an object appearing outside Panum's fusional area is in front of or behind that plane (Poggio and Fischer 1977). Indeed the near and far cells in LIP have been shown to be modulated by vergence (Gnadt and Mays 1991) and this area projects to the superior colliculus, a region assigned to oculomotor control (Sparks 1986). Asymmetric cells, especially the near cells, may also have a function in the control of hand movements because they respond to stimuli nearer to the animal than the fixated object, and could be useful for the direction of hand movements toward that object. The changing proportions of tuned and asymmetric cells mentioned above suggests that the further up the parietal sequence of areas one progresses, the greater the involvement of motor function, be it ocular or manual.

### Other types of disparity

Disparity is a general term encompassing all types of difference between the two monocular images of an object. These differences may be further subdivided: position disparity is the shift in horizontal position that arises from an object being displaced from the fixation plane; orientation disparity is the perceived difference in orientation between each monocular image of a line which tilts in depth towards or away from the observer (illustrated in figure 6).

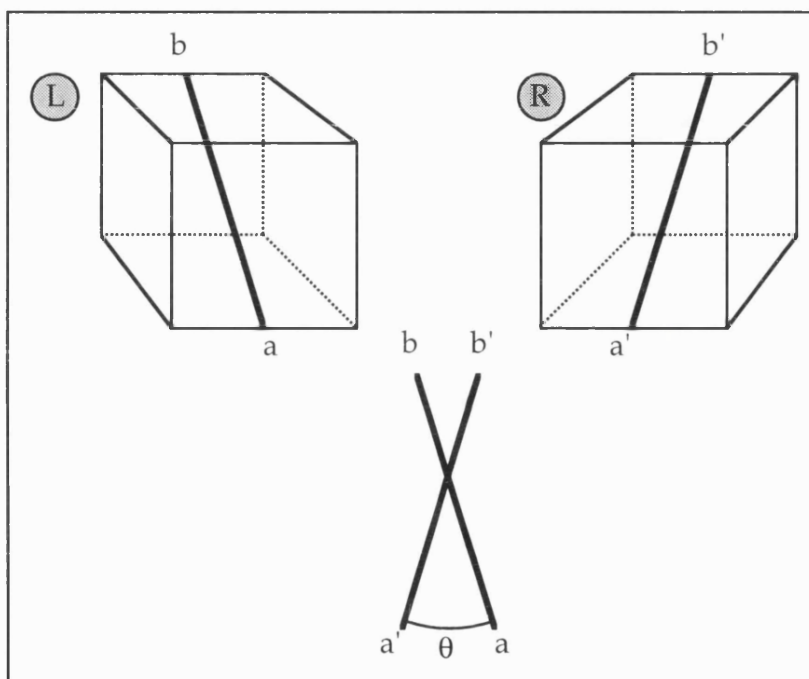


Figure 6.

Illustration of the orientation difference between each image on the retinae when a line tilted towards or away from the observer is viewed binocularly. L and R represent the (exaggerated) images on the left and right retinae of a single line tilted in depth, the cube is added to aid perspective viewing. By analysing the angle  $\theta$  the inclination of the line can be calculated and depth perceived.

Disparity curvature is the difference in perceived curvature between the two monocular images of a surface of a three dimensional object. Shapes rotated about their vertical axis cause disparity of horizontal width. Together these differences are analysed to produce a three dimensional percept of a solid object. As previously mentioned,

position disparity allows one to know the distance of an object from the fixation plane, but alone it gives no cues to the three dimensional form of an object. One of the constituents of three dimensional form is tilt in depth. Since we are capable of discriminating whether lines are rotated about a horizontal axis, one might expect to find cells selective for tilt in depth in the visual cortex. In effect, a cell selective for tilt in depth could comprise a cell whose two monocular receptive fields are each tuned to a slightly different orientation, hence the term "orientation disparity". Since our eyes are separated in a horizontal direction it is only possible to perceive tilt in depth when viewing vertically or near vertically oriented lines (neglecting all other depth cues). Cells of this type were indeed found in the cat's striate cortex (Blakemore 1970) and since in monkey V1 (Hanny *et al.* 1980).

So called "tilt in depth" cells give an optimal response when each eye is presented with a line slightly differing in orientation. Eye movements will cause problems when looking at this type of cell because cyclotorsion will make all cells appear to be selective for tilt in depth. Blakemore (1970) eliminated this possibility by recording from many cells in a single animal whose eyes were held still (by suturing them to firmly held metal rings) and demonstrating that the difference in the cell's preferred orientation between the two eyes varied significantly from cell to cell (Blakemore 1970). Another feature of these cells was that they were also selective for horizontal disparity, and their responses could be occluded if the optimal orientation disparity stimulus was not presented at the correct horizontal disparity. The existence of cells selective for tilt in depth in the macaque was disputed by Hubel (Hubel and Wiesel 1977) who maintained that the properties of each receptive field remain identical for all binocular cells. However, since striate cells have been

found that have opposite direction selectivities in each eye (Zeki 1982) it is not unreasonable to suggest that V1 cells may have slightly different orientation preferences for each eye.

Some cells have been found to mediate another attribute of stereoscopic vision, that is motion in depth (Pettigrew 1973; Regan and Beverley 1973; Zeki 1974a). Stimuli comprising a fixed disparity are perceived at a fixed depth but if disparity is changed while the stimulus is being viewed, motion in depth is perceived. The direction of 3 dimensional motion is dependent upon both the direction of the images in both eyes and the direction of change of disparity. By changing these parameters, trajectories of any direction can be produced. Pettigrew found cells in area 18 of the cat that signalled changing disparity (Pettigrew 1973), and later Cynader *et al* (1978) found cells in area 18 of cat's visual cortex that were selective for specific trajectories; perhaps unsurprisingly, the majority of cells found were selective for trajectories that would result in the stimuli coming close to, or actually hitting the animal (Cynader and Regan 1978). Zeki (1974a) found cells in V5 of the macaque that had opposite direction selectivities or each eye and would therefore respond maximally to movement towards, or away from, the animal (see figure 7).

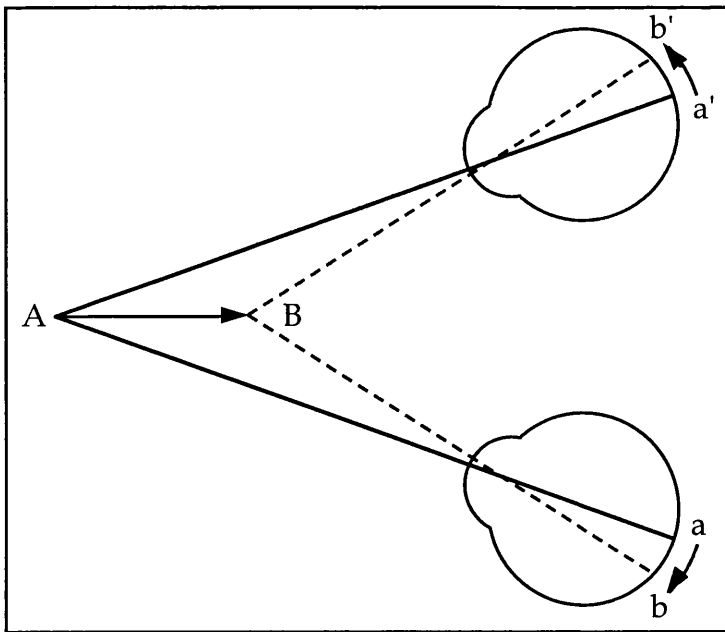


Figure 7.

Diagram to show that when a point at  $A$ , having its retinal images at  $a$  and  $a'$ , is displaced to  $B$ , having its images at  $b$  and  $b'$ , the displacement is in opposite directions in the two eyes (assuming no eye movements take place). Cells with opposite direction selectivities in each eye have been found in V5 (Zeki 1974a).

However, the existence of such motion in depth cells in monkey area V5 was disputed in 1983 (Maunsell and Van Essen 1983a) because, although they appeared to respond well to motion in depth when stimulated at trajectories far from the unit's optimal fixed disparity, their best response was still to motion in the fronto-parallel plane, i.e. at a fixed disparity. This may be true for some trajectory cells, but cannot stand for cells with opposite direction selectivities in each eye as reported by Zeki in V5 (Zeki 1974a). It has since been suggested that motion in depth is not analysed by single units, but by the change in output from many units, each tuned to a fixed disparity (Cumming 1995). Whether the outputs from these units would have to converge onto a single cell for the motion in depth to be perceived is unknown.

### Psychophysics

Stereopsis has been studied extensively by psychophysicists because it is an accessible attribute of vision to study in this way. The advent of the random dot stereogram inspired a deluge of studies because it contains pure disparity and can be manipulated easily to elucidate the

perceptual properties of stereopsis. The forms seen in random dot stereograms are also invisible monocularly and therefore, must be constructed once the visual signals have reached the cortex.

Various authorities have subdivided human stereopsis into categories; here I shall review each of these (sometimes overlapping) divisions formed mainly on the basis of psychophysical studies.

### *Local/global*

In order to prevent the false matching of the small black and white squares that constitute random dot stereograms, a type of stereopsis that examines more than the local features of the visual scene must exist. Julesz called this type of stereopsis "global" (Julesz 1971) because it has to take information from a large area of the visual field in order to prevent mismatching of the identical local features. Local stereopsis is therefore the mechanism required to perceive depth in the more classical stereoscopic scenes where there is no chance of false matching because each part of the monocular image is unique. Thus, the division of local and global stereopsis may be looked upon as an absence and presence respectively of interactions between different parts of the visual field at or beyond the initial disparity processing level. Although this classification of stereopsis was produced entirely on the basis of psychophysics it corresponds well to a physiological property of cells, i.e. their receptive field size. Cells with large receptive fields would be able to undertake global stereopsis because they can take information from larger areas of the visual field, whereas, for example, striate cells, which have very small receptive fields, would be better suited to the analysis of local stimulus features.

*Fine /coarse*

The division of stereopsis into fine and coarse is one of magnitude of disparity. A "fine" system would be capable of transforming small disparities into fused percepts of three dimensional objects. Disparities that exceed Panum's fusional area cause double vision. However, even when an image appears double due to its large disparity, it still carries a depth percept. Thus, the coarse system does not require fusion of the two monocular images in order to gain information about relative depth. Physiologically, this concept could correspond to the responses of different types of disparity tuned cell. Fine stereopsis could be signalled by "tuned" cells which respond specifically to disparities at or near to Panum's fusional area giving narrow response profiles. Large disparities will not stimulate "tuned" cells, but will cause "asymmetric" cells to respond because these cells are stimulated over a large range of disparities that exceeds the limits of the horopter, either in front of (near cells), or behind it (far cells).

*Cyclopean/noncyclopean*

Julesz coined the term cyclopean; it refers to visual stimuli that can only be perceived binocularly, for example, the contours present between areas of different disparity in a random dot stereogram. Essentially, cyclopean stimuli do not exist when viewed monocularly. The "cyclopean eye" is the concept of a system in the brain where the depth information is extracted by processing disparity. The cyclopean eye is therefore the part of the brain able to 'see' depth contours defined by disparity in random dot stereograms. A non-cyclopean stimuli will still appear on the cyclopean eye, but unlike the cyclopean image it will also appear in monocular images. This concept corresponds to the physiology of some disparity selective cells, which may respond to monocular

stimulation, but whose responses are only tuned when they are stimulated binocularly at the correct disparity.

### The correspondence problem

In order that two retinal images be fused, the brain has to decide which parts of each monocular image correspond to the same object viewed by the other eye. This is the correspondence problem. From Julesz's random-dot-stereogram studies in the 1960s, we know that binocular correspondence happens early in the visual system, i.e. before object recognition, and that the stimulus requirements necessary for correspondence (as well as stereoscopic depth) do not need to be sophisticated. The exact stimulus requirements necessary for correspondence have been studied psychophysically for many years.

### Colour and stereopsis

Several lines of evidence have suggested that colour is not used by the stereomatching system to achieve correspondence. An often used method of producing stereopsis is to view two images through red and green anaglyphs. One image, made up of red and white dots, is viewed through a green filter placed over one eye, producing a black and green pattern, and the other image, made up of green and white dots is viewed through a red filter producing a black and red pattern. The two patterns are superimposed, avoiding the need for divergence or crossing of the eyes (as in Julesz's random dot stereograms). When this is done, the region of the patterns containing disparate dots is seen standing out vividly in depth even though each eye sees it in a different colour. Thus it was suggested that colour cannot be important for the stereoscopic matching system (Ramachandran and Sriram 1972). Livingstone *et al* (Livingstone and Hubel 1987b) went one stage further than using

coloured filters to explore this phenomena; polarized filtered random dot stereograms containing different coloured dots (red, green, blue and yellow) were prepared and the coloured dots were arranged so that no spatially corresponding dots were of the same colour, the colours being shifted in one direction. The result was a stereogram that contained two cues: colour and position; the viewer could pair the dichoptically presented dots on the basis of their colour or their position. In this case colour based matching was possible, but the more common and preferable match was based on the position of the dots, producing an identical sensation of depth as when pure contrast random dot stereograms were used.

### Isoluminance studies

Isoluminance is used by psychophysicists (and physiologists) as a tool to present stimuli whose contours are visible due purely to chromatic (and not luminance) differences. Presenting various types of stimuli at isoluminance is a method of discovering what role the chromatic contrast sensitive system in the brain plays in the perception of the particular stimulus. A stimulus that is undetectable or whose detection is adversely affected when presented at isoluminance would probably be analysed by a part of the brain which cannot draw knowledge from chromatic contrast alone. Various experiments have been carried out using isoluminance and disparity, some of which have produced conflicting results.

Lu and Fender (1972) found that stereoscopic depth perception is difficult or absent in fine random dot stereograms composed of two isoluminant colours rather than black and white. Their stimuli were composed of 100 dot random dot stereograms, each dot subtending  $0.1^\circ$ .

They used various combinations of isoluminant colours but found depth perception to be severely compromised in every case (see also Gregory 1979). Conflicting results were produced by the 1974 study of Comerford who used low spatial frequency stimuli comprising a single disk shaped object on an isoluminant background and found only a marginal deterioration of stereoscopic depth perception at isoluminance. This disagreement led Livingstone and Hubel to study stereopsis and isoluminance; they suggested that the "P" system<sup>4</sup> was "depth blind" (Livingstone and Hubel 1988). They found that the exact luminance setting required to null stereoscopic depth in random dot and simple figure stereograms occurs over a very narrow range and varies markedly from subject to subject (Livingstone and Hubel 1987b). This factor may also help to explain why these studies arrived at conflicting conclusions, artefacts such as chromatic aberration and the presence of slight luminance-contrast borders may have contributed to the depth sensations reported at isoluminance. However, the discrepancy could be related to differences in spatial frequencies used in the stimuli. DeValois *et al.* (1988) have suggested that the visual system lacks a channel sensitive to high spatial frequency borders defined by chromatic contrast, making the fine random dot stereograms of Lu and Fender difficult to resolve (even monocularly). In conclusion, it is not possible to assign stereoscopic depth perception exclusively to either the "M" or "P" systems on the basis of these studies.

---

<sup>4</sup>The P system (which will be discussed in greater detail later) originates in the parvocellular layers of the LGN, the other layers being magnocellular (M) layers. Early recording from the LGN (Wiesel and Hubel 1966) showed that some P cells had the property of wavelength selectivity whereas those in the M layer did not. Other differences exist between the M and P systems and these will be discussed in a later section.

### Spatial frequency

Masking studies<sup>5</sup> involving stereopsis (Julesz and Miller 1975; Yang and Blake 1991) have shown that human depth perception can be compromised using masks with similar spatial frequencies to the target. This was shown by producing a random dot stereogram which had been band-pass filtered so that it contained a narrow range of spatial frequencies. One of the monocular random dot stereogram figures then had a mask of a particular spatial frequency noise added. It was found that if the spatial frequency of the noise differed from that of the stereogram elements by more than two octaves, stereopsis was unaffected. In this case one spatial frequency channel mediated the stereopsis while another was in a state of binocular rivalry. However, masking noise of a similar spatial frequency to the stereogram elements destroyed the stereoscopic appreciation of depth (Julesz and Miller 1975). Thus it was demonstrated that the stereoscopic system uses spatial frequency-specific channels.

Single random dot stereograms that contain two overlapping depth planes have also been prepared, but can only be fused if the two planes are presented with widely differing spatial frequency content (Mayhew and Frisby 1977). In these stereograms both depth planes can be perceived simultaneously, the nearer one appearing transparent. This demonstration that stereoscopic stimuli with different spatial frequencies can be perceived simultaneously at different depths also provides evidence that the processes involved in stereopsis are tuned for spatial frequency.

---

<sup>5</sup>The paradigm of masking uses two stimuli, a target and a mask; if perception of the target stimuli can be reduced by simultaneous, pre- or post-presentation of the mask, then the two stimuli must be processed by the same "perceptual module" in the visual system.

## Orientation and stereopsis

The orientation specificity of processes involved in stereopsis have been less well defined. Stereograms comprised of oriented lines (random line stereograms) were first prepared by Julesz (1971). In these studies the orientation of the lines was centred about the horizontal, therefore no tilt in depth due to orientational disparities was perceived. Julesz showed that the perception of depth could be destroyed if the (short) lines were rotated by  $\pm 15^\circ$  in one monocular image (Frisby and Julesz 1975a). The relation of line length and stereopsis was investigated in a subsequent paper, to find out if there was a constant orientation difference required to reduce depth perception, regardless of the length of the lines. The authors found that the longer the lines, the smaller the orientation difference required to degrade stereoscopic depth, thus "the critical factor underlying the depth reduction is not the orientation difference *per se*, but rather the vertical disparity which an orientation difference introduces into the display between the tips of corresponding lines." (Frisby and Julesz 1975b). In a similar study (Braddick 1979) lines centred about the vertical were used, therefore producing tilt in depth, the orientation difference between the two images required to reduce stereoscopic fusion was much larger, presumably because a vertical line requires more rotation to introduce a particular vertical disparity than a horizontal line. These investigations into the relationship between stimulus orientation and stereoscopic vision were unable to show whether the visual system uses orientation as a critical cue for correlation and depth perception and left a confused picture of the relationship between orientation and stereopsis. Perhaps a more salient approach to this line of investigation was taken more recently, where the interrelations between orientation and stereoscopic vision were investigated using a masking experiment. This experiment "...used the

masking paradigm to evaluate the orientation selectivity of the mechanisms mediating human stereopsis." (Mansfield and Parker 1993). The authors used spatially filtered stereo-pairs containing both orientation and spatial frequency information and masked one of the monocular figures with a binocularly uncorrelated mask of varying orientation. They found that the threshold for correct judgement of whether a central square was in front or behind the background of the stereogram was elevated most when masks of similar orientation to the stereogram were used. Masks of orthogonal orientation (but identical spatial frequency and contrast) were much less effective at masking stereopsis. Mansfield and Parker's results suggested that the masking of stereopsis depends on interactions between orientation tuned mechanisms. This conclusion shows a greater concordance between the mechanisms of stereopsis measured psychophysically in humans and the picture yielded by the previous studies of orientation selective disparity tuned cells found in cat (Barlow *et al.* 1967; Joshua and Bishop 1970) and monkey (Hubel and Wiesel 1970; Poggio and Fischer 1977) visual cortex.

### Stereoscopic depth constancy

The relationship between depth and retinal disparity is not a linear one; a fixed disparity will produce a greater sensation of depth with increased viewing distance. The perceived depth of a point with a given disparity from the fixation plane will increase proportional to  $1/\text{viewing distance}^2$ , i.e. the inverse square law (Ono and Comerford 1977). Thus, to calculate the depth difference between two points on a surface from binocular disparities, it is necessary to know the absolute (egocentric) viewing distance to the surface. This geometric fact poses the problem of stereoscopic depth constancy, i.e. how does the visual system scale retinal disparities with respect to the viewing distance. The traditional view of

how this is done is that cells receive an input from extraretinal signals (Helmholtz 1909), the convergence angle of the eyes rather than the accommodation effort (Ritter 1977), and use this information to scale horizontal disparities for viewing distance. Indeed the angle of gaze has been shown to affect the responses of cells in many visual parts of the brain. Spontaneous-activity modulation of about one third of dorsal lateral geniculate cells has been obtained by manipulation of the vergence angle with prisms in the awake behaving monkey (Richards 1968). In V1, disparity tuned cells have been found whose responses are modulated by the fixation distance, for example, a cell might display the responses of a near cell at a viewing distance of 40 cm but when tested for disparity at 20 and 80 cm it becomes poorly responsive and no longer tuned to disparity (Trotter *et al.* 1992). To eliminate other factors that could cause this modulation of response, i.e. accommodation effort, the vergence angle was also manipulated with prisms. In this case the vergence angle will be changed yet the accommodation effort will remain constant. If vergence angle rather than accommodation is responsible for the distance effect, the use of prisms should reproduce the same effects that occur with changing the distance of fixation; this was found to be the case.

The information about the vergence position of the eyes comes from proprioceptive receptors (muscle spindles) within the ocular musculature. Stretching of ocular muscle spindles has been shown to produce cortical responses in many parts of the visual brain, including V1 (Buisseret and Maffei 1977). The ocular muscle spindles travel in the ophthalmic branch of the trigeminal nerve. Experiments have been done to investigate the effects of sectioning this afferent in kittens and adult cats. Cutting one or both of these nerves in kittens produces permanent deficits in visual-motor coordination (Hein and Diamond 1983),

including an impairment of depth vision as revealed by behavioural tasks (Graves *et al.* 1987). The results of experiments in which a unilateral or bilateral lesions of the ophthalmic branch of the trigeminal nerve was made in adult cats are less demonstrative. Graves *et al.* found that the depth vision of some cats was more affected by unilateral deafferentation than others, whereas Fiorentini *et al.* (1985) found that unilateral deafferentation affected the depth discrimination of all adult cats. More recently, Trotter *et al.* (1993) found that unilateral deafferentation in the cat only affected depth discrimination when done between 3 and 13 weeks post-natal, and unilateral deafferentation only affected depth discrimination when done between 3 and 10 weeks (Trotter *et al.* 1993).

Thus, it is clear that cells at very early stages in the visual pathway respond (or modulate their responses) to extraretinal vergence signals, the purpose of which is presumably to enable egocentric distance calculation and the scaling of retinal disparities for viewing distance.

### Computational models

There is another method of computing the egocentric distance to the fixation point. It is based on a computational model that uses the viewing geometry of binocular vision, and follows from the work of Mayhew and Longuet-Higgins. For details of the full mathematical proofs, their papers should be consulted (Longuet-Higgins 1981; Longuet-Higgins 1982b; Longuet-Higgins 1982a; Mayhew 1982; Mayhew and Longuet-Higgins 1982). In principle, this model proves mathematically that, from the stereoscopic projection of three retinal points, it is possible to recover their three dimensional coordinates in egocentric space. Furthermore, these coordinates may be calculated without the need for any extraretinal information such as vergence angle or lens

accommodation (Longuet-Higgins 1981; Longuet-Higgins 1982b). The model requires the presence of cells tuned to both horizontal and vertical disparity, and a strong line of evidence that the brain uses this method (or a similar one) to scale relative disparities and produce depth constancy is the presence of these cells in the visual cortex (Barlow *et al.* 1967; Nikara *et al.* 1968; Gonzalez *et al.* 1993). The presence of cells tuned to vertical disparity was not given much attention until Mayhew's theory was proposed because it was the general belief that only horizontal retinal disparities contribute to stereoscopic depth perception. A well known exception to the above statement is an apparently paradoxical perceptual effect called the "induced effect". This effect, first described by Lippincott (1889) and extensively studied by Ogle (1964) is a perceptual distortion of the binocular field produced by the addition of a cylindrical magnifying lens to one eye with the axis of magnification in the vertical direction. The effect makes a frontoparallel surface appear tilted about its vertical axis, so as points on the same side of the surface as the eye over which the lens is placed, appear closer; exactly the same distortion that would be produced if the lens had been placed in front of the other eye with its axis of magnification in the horizontal direction. Thus, "The magnification in the vertical meridian *induces* an effect, as though the lens had been put before the other eye with the magnifying effect horizontal." (Ogle 1964).

The induced effect plainly shows that the visual system is not only capable of analysing vertical disparities but also that these disparities have a bearing on the perception of stereoscopic depth. Interestingly, most of the properties of the induced effect can be explained in terms of the computational model outlined above and produce further evidence for the brain's use of vertical disparities in the calculation of egocentric depth

(Mayhew 1982; Mayhew and Longuet-Higgins 1982). In point of fact, it was Helmholtz who first proposed a function of vertical disparities in depth vision (Helmholtz 1909). By conducting the simple experiment of arranging vertical plumb lines into a frontoparallel plane, he discovered that the addition of small gold beads to the lines facilitated their accurate positioning on the geometrical horopter. The only effect of the beads is to add extra vertical position cues so that the small vertical disparities produced by asymmetric fixation can be analysed. However, this observation was largely neglected because it could not be reproduced. Hillebrand (1893) is reported by Ogle (1962) to have tried to replicate Helmholtz's experiment and found no difference in placement of the lines with or without the beads. A possible explanation of this discrepancy is the fact that Hillebrand (and later Ogle himself) placed few beads on their lines, and these were located near the centres so that they appeared near the horizontal meridian, a locus in the visual field where vertical disparities are minimized.

More recently another line of evidence has arisen against this computational theory of stereoscopic depth constancy. It is based on a psychophysical experiment into the appreciation of the shape of a cylinder defined by a random dot stereogram (Cumming *et al.* 1991). The authors used random dot stereograms in this shape judgement task and showed that manipulations of vertical disparities had no effect on perceived three dimensional shape. However, manipulating the convergence angle of the eyes did affect the perceived shape of the cylinder, suggesting substantial changes in the subjects' scaling of horizontal disparities. They concluded that vertical disparities were not used to scale horizontal disparities for viewing distance, this being a function of extraretinal signals.

In summary, it can be certain that the visual system uses extraretinal signals to modulate the responses of single cells in the visual cortex, in theory these signals are all that is necessary for the system to produce accurate measurements of egocentric depth. Evidence from the induced effect and Helmholtz's horopter experiments provide good evidence that the visual system uses vertical disparities, indeed its cells are selectively tuned for vertical disparity, but the question arises; if extraretinal signals are all that is necessary to enable single cells to be selective for egocentric depth, why is a complex calculation undertaken to serve the same purpose without the use of these signals? Perhaps both mechanisms are used, the vergence angle not providing accurate enough information on its own. This implies a certain amount of redundancy, analogous to the multiple depth signalling mechanisms of binocular and monocular vision.

### Stereoblindness

There is a population of humans who have deficiencies in their stereoscopic vision. These people have been divided into various groups depending on the types of deficiency and accompanying strabismus (squint). In a 1970 study by Richards, stereoblindness was tested by presenting the subject with a random dot stereogram for a short period of time (80ms) and asking them whether the central portion of disparate dots was in front of, on, or behind the background. The short presentation time was used to prevent the subject from making convergent or divergent eye movements that might aid the depth detection task without the use of stereoscopic mechanisms. The stimuli were projected with polarized light to present each monocular stimuli to each eye exclusively and the subject wore glasses that were polarized in

perpendicular directions. Richards was able to identify three types of stereoblindness, characterized by an inability to distinguish crossed, uncrossed or zero disparities presented to one hemisphere (by presentation of the stimuli to one side of the fixation point). From this observation Richards suggested that there are three classes of disparity detector, those that detect uncrossed, zero and crossed disparities. Richards calculated that the probability of lacking one of these detectors and therefore having a stereoanomaly of this type is about 30% in the normal population. However, in a subsequent paper by the same author (Richards 1973) this clear cut theory of stereoanomalies was shown to be incomplete. This paper described the way in which stereoanomalies can be specific to the sign of luminance. A subject with an inability to discriminate crossed disparities for black on white stimuli, becomes unable to discriminate uncrossed disparities when tested with white on black stimuli. This phenomenon shows that there is more to stereoanomalies than the simple loss of a particular detector.

In order to investigate the location of stereoanomalous regions in the visual field, Richards and Regan (1973) devised a "stereo-perimetry" test. The test comprized a depth stimulus that could be moved within the subject's visual field while they fixated a stationary spot. The stimuli consisted of either a bar continuously oscillating in depth, or a stationary bar flashed for 100ms at either a crossed or uncrossed disparity. In an apparently normal subject, large areas of the visual field were found where the subject could not detect either crossed or uncrossed disparities when tested with the oscillating bar. However, these areas seemed normal when tested with the stationary flashed stimulus or if tested with a flashing and oscillating target. These results suggest a number of possible conclusions:

First, that the processing of motion in depth may be done separately to that for static depth, so it becomes possible to be "motion-in-depth blind" but retain good static depth vision. These "stereomotion scotomas" were described by Richards (1973) and further studied by Hong and Regan (1989) who found that some stereomotion scotomas were specific for the direction of motion in depth (towards or away from the subject). It has also been found that particular regions of the visual field that are static-depth stereoblind, may be sensitive to motion in depth when tested with a stimulus such as a rotating cylinder defined by disparity (Rouse *et al.* 1989).

Second, that disparity detectors (or disparity tuned cells) must be retinotopically organized in the cortex. If particular areas of the visual field (stereo scotomas) lack disparity detectors, the detectors must be arranged retinotopically, otherwise their loss would cause a global degradation of stereoacuity across the whole visual field.

Third, Richards and Regan concluded that the mechanisms for detecting uncrossed and crossed disparities must rely on separate neural circuitry. This conclusion is demonstrated by the fact that particular areas of the visual field may be blind to crossed disparities while others, in the same subject, may be blind to uncrossed disparities. Physiological evidence from "near" and "far" disparity tuned cells in the monkey visual cortex (Poggio and Fischer 1977; Poggio *et al.* 1988) supports this finding (see previous section on disparity tuned cells).

Unlike other visual abnormalities, e.g. akinetopsia (Zihl *et al.* 1983; Zeki 1991) and achromatopsia (Kolmel 1988; Zeki 1990), complete loss of depth perception is not commonly associated with a specific brain injury,

and stereoblindness following brain injury is quite rare. There are a few documented cases of patients with lesions to the parietal lobe who suffered complete loss of depth perception and one in particular (case 3 of Riddoch, 1917) who described his visual world as appearing as if "Everything seems to be really the same distance away." (Riddoch 1917). This patient, and another described by Smith and Holmes (1916), suffered their loss of depth vision in conjunction with a more disabling loss of spatial and self orientational vision. As well as their deficiency in stereoscopic vision it is obvious that they must have lost most, if not all, of their ability to judge depth from binocular and monocular cues. This visual disturbance is particularly associated with motor responses to visual stimuli, so that reaching to targets is severely impaired and patients have difficulty stabilising their eyes. Lesions producing an exclusive loss of stereopsis are less common and are not usually noticed during normal vision. They are often accompanied by more profound visual and visuomotor impairments (Datta *et al.* 1978). The lack of neurological injury patients with exclusively impaired stereopsis suggests that stereopsis is a wide spread property throughout the visual system and unlike colour and motion cannot be solely eliminated by ablation of a single area. The common association of stereoblindness and visuomotor impairment in neurological patients suggests that the parietal areas damaged in these patients may be performing motor functions in conjunction with depth discrimination.

### Primate lesion studies

Lesion studies on stereopsis have shown that after removal of the central 5° of the visual field from V1 or V2, stereo-thresholds for tasks requiring fine stereopsis (i.e. judgements of stereopsis within Panum's fusional area) increase by a factor of ten (Cowey 1985). Removal of large

portion of the inferotemporal cortex produced a 50% increase in stereo-thresholds for the same task. However, when the same monkeys were tested with tasks requiring coarse stereoscopic discriminations (i.e. judgements of the stereoscopic depth of unfused images) in random dot stereograms their performance was not affected by the V1 lesion and only slightly affected by the V2 and inferotemporal lesions. Thus, detection of large disparities does not require the foveal representation of the visual field in V1. Subcortical lesions of the rostral superior colliculi and pretectum (which also impaired the monkeys' eye movements) completely abolished their ability to perform the task. These monkeys were shown to have diplopia, i.e. they were unable to control vergence eye movements. The study of Ptito *et al.* (1992) showed that stereoscopic depth vision can be lost following lesions to areas 17 and 18 in the cat, yet other abilities such as offset acuity and brightness discrimination are not affected. Hence, in summary lesion studies have failed to provide evidence for a single area being involved in the processing of stereoscopic depth.

#### Effects of abnormal visual experience on binocular vision

Many experiments have been done on the development of neural circuitry involved with binocular vision. These studies have concentrated on modelling pathological human conditions such as strabismus (squint), anisometropia (unequal refraction in the two eyes), aphakia (absence of a lens) and cataracts (opacity of the lens), all of which can cause amblyopia (literally "blunt vision"), the symptoms of which are a deficit of vision in one eye. This is usually achieved by interfering with the input to one or both eyes. Eyes can be occluded, removed, sutured closed or misaligned with respect to each other by surgically deviating the eye by cutting the ocular musculature. Animals can also be

reared in the dark or have prism or magnifying goggles applied. These procedures can be done at various stages of development and have effects on visual performance and on the development of cells in the visual system from the LGN upwards.

The first of these studied was done by Hubel and Wiesel (1965a) who induced squint in kittens by lesioning their ocular musculature, then recorded from their striate cortex to assess the effect of the squint on populations of binocular cells there. They found that inducing a squint from birth permanently reduced the proportion of binocular cells responding to the strabismic eye from the normal 80%, down to 20%. Thus, binocular cells had been converted to monocular cells responding only to the non-deviated eye. They found that this change was mirrored in the anatomy of the ocular dominance columns, those for the strabismic eye were dramatically reduced in size due to the good eye "taking over". The same result has since been noted in monkeys (Baker *et al.* 1974). Occlusion rather than misalignment of an eye has a similar effect on the proportions of cortical binocular cells and the anatomy of V1's ocular dominance columns, and renders the occluded eye virtually blind. However, recovery may occur if the eye's vision is restored early enough (Wiesel and Hubel 1963; Blakemore 1976). In the monkey, monocular occlusion also reduces the size of striate cortex blobs that are dominated by the occluded eye (Trusk *et al.* 1990). The effects of binocular occlusion on the development of the visual system have been studied in dark reared kittens. It has been found that a period of dark rearing, comparable to that used in the monocular deprivation studies, has a less devastating effect on the cellular responses from the corresponding cortex. Dark reared cats retain a substantial number of cells responsive to stimulation of either eye, but still have a lack of binocular cells (Wiesel

and Hubel 1965; Blakemore and Van Sluyters 1975; Kaye *et al.* 1982). A similar loss of the proportions of binocular cells is found if prisms are used to deviate the visual axes in cats (Blakemore and Van Sluyters 1975; Smith *et al.* 1979) and in monkeys (Crawford and von Noorden 1979). This suggests that the process that degrades visual responses and causes the strong shift of ocular dominance during monocular deprivation, is not the lack of stimulation *par se*, but the lack of a balanced input from both eyes. All experiments involving monocular or binocular deprivation or deviation reduce the proportions of binocular cells and induce stereoblindness.

In order to investigate the effect of a temporal dissociation of the visual input to each eye, studies have been done on the effects of swapping a monocular occluder from eye to eye so that each eye gets a similar input of the same stimuli, but not at the same time (Hubel and Wiesel 1965a; Blakemore 1976). This interference has no effect on visual acuity in either eye, neither does it lead to an imbalance in the proportions of cells responding to either eye. However, it does cause a loss of binocular cells and causes stereoblindness. If the eyes are occluded for varying proportions of the time, the proportions of cells responding to stimuli in each eye changes to correspond to the amount of time each eye was left open (Tieman *et al.* 1983). In addition, the properties of cells responding to the eye occluded for a longer proportion of time showed degradation in their orientation tuning curves and their responses to motion that were not present in animals with equal eye occlusion.

In summary, normal visual development is critically dependent on normal visual experience during the early stages of vision, the so called "critical period". An imbalance of visual experience between the

eyes (be it caused by occlusion or deviation) during this time is severely detrimental, causing a loss of binocular cells, and cells responding to stimulation of the affected eye. Remaining cells show a reduction of their tightness of orientation tuning, sensitivity to visual motion and allotment of cortex. Presumably it is these cortical effects that cause the symptoms of amblyopia. The development of a full compliment of binocular cells requires simultaneous binocular vision with correct correspondence, anything less produces stereoblindness in humans and experimental animals.

The above experiments provide evidence for Hebb's rule for the development of synapses, proposed in 1949 by the Canadian psychologist Donald Hebb: "When an axon of cell A...excite[s] cell B and repeatedly or persistently takes part in firing it, some growth process or metabolic change takes place in one or both cells so that A's efficiency as one of the cells firing B is increased." (Hebb 1949)

## Section 2:

### The physiology of the V3 complex:

#### Orientation tuning in the V3 complex

Studies of the receptive fields of V3 complex neurones have found varying proportions of orientation selective, direction selective and unselective cells. One such study (Baizer 1982), using the awake behaving rhesus monkey, found the majority of V3 cells were unselective (52%) with 33% orientation selective, the rest (15%) being direction selective. These figures differ markedly from previous studies by Zeki (1978b; 1978c) where 88% of V3 cells were found to be orientation selective. It was recognized by Baizer that slightly different criteria for orientation selectivity were used for each of these studies. Zeki's criterion was that cells were considered orientation selective if "when tested with [moving or stationary] slits bars and edges, they showed an orientation preference and did not respond to the orthogonal orientation." (Zeki 1978c). Whereas, in order to be classified as orientation selective in Baizer's study, cells had to be "sensitive to the orientation of stationary stimuli." When Baizer used Zeki's criteria for orientation selectivity, the number of orientation selective cells in her sample went up to 48%, a number still far off the 88% from Zeki's experiments. Felleman *et al.* found 76% of V3 cells to be orientation selective in the paralysed preparation (Felleman and Van Essen 1987). The proportion of orientation selective cells found in V3A in Zeki's study was 81.2% (Zeki 1978c). Another study of the awake behaving monkey found 55% of V3A cells to be orientation tuned (Galletti and Battaglini 1989). All of these studies found the majority of cells in V3 and V3A were orientation selective except that of Baizer (Baizer 1982). The reason for the variation between studies is probably due to the differences in classification criteria.

Cells can be classified in one of two ways: quantitatively or qualitatively. Before the advent of modern computer based spike recording techniques, cells had to be classified qualitatively, usually by the passing of a slit of light over the receptive field and judging the response to different orientations by ear. The accurate measurement of responses in spikes per second and the plotting of orientation versus response curves has enabled experimenters to devise methods of quantitatively measuring orientation selectivity. The problem associated with quantitative measurements is that one has to decide on a threshold, above which cells are selective and below which they are not. The orientation index (o.i.) method has been applied to cells by a number of researchers, most of whom agree that cells can be considered orientation selective if their o.i. value is greater or equal to 0.7 and orientation biased if the index is between 0.5 and 0.7 (see results section for a detailed description of this index).

### Colour cells in the V3 complex

Qualitative studies of cells in the V3 complex have found it to be an area containing cells that are not selective for the wavelength of stimuli (Van Essen and Zeki 1978; Zeki 1978b; Baizer 1982; Zeki 1983). However, more recently Felleman *et al.* (1987) studied the receptive field properties of V3 cells and applied quantitative methods as criteria for the assignment of colour selectivity. These indices are numbers essentially derived by comparison of responses to most and least effective stimuli. Two indices were used, the colour index (c.i.) and the white index (w.i.). The c.i. is a comparison of the magnitude of response to the least effective wavelength with the most effective wavelength and has the formula:

$$c.i. = 1 - \frac{\text{Response to least effective monochromatic wavelength} - \text{background}}{\text{Response to most effective monochromatic wavelength} - \text{background}}$$

It yields values near 1 for selective cells and values near 0 for completely nonselective cells. The w.i. was used to express the relative response to

white light, this compares the response to photopically matched white light with that to the best monochromatic stimulus. Its formula is:

$$w.i. = 1 - \frac{\text{Response to white - background}}{\text{Response to most effective monochromatic wavelength - background}}$$

Thus, the w.i. gives high values for cells unresponsive to white light (i.e., selective for some wavelength over white light) and low values for cells as responsive to white as to the best monochromatic wavelength. Use of these quantitative measures provided Felleman and Van Essen with a figure of 21% (20/94) of V3 cells displaying wavelength selectivity (having a value of c.i. 0.7). The authors plotted c.i. against w.i. to produce a scatter histogram for their V3 cells. This showed that there was an even distribution of both indices and that there were no distinctly clustered subpopulations, suggesting that the majority of their cells had colour properties but only those over a certain threshold were classified as "colour selective". They further subdivided this population on the basis of the w.i. and classified 5 of their 20 "colour selective" V3 cells as "colour opponent" (w.i. > 0.7) and 15 as "colour biased" (w.i. < 0.7). An average colour tuning curve made by aligning all the preferred wavelengths on a wavelength versus response curve, showed that their population of "colour selective" cells had the following properties.

- 1) The most tightly tuned responses occur at the average preferred wavelength, showing a lack of variation of the preferred wavelengths for tuned cells.
- 2) The average response is about half the peak response, showing a lack of strong colour opponency from antagonistic cone inputs.
- 3) A range of bandwidths at half maximal response of 80-100nm compared to an average of about 25nm for colour selective cells in macaque striate cortex (Dow 1974; Poggio *et al.* 1975; Michael 1978b; Michael 1978a) and a range of 10 to 40nm in V4 (Zeki 1977a; Zeki 1980b; De Monasterio and Schein 1982; De Monasterio 1983).

Whether these "colour selective" cells in V3 are performing functions that are dependent on their broad preference to particular wavelengths or whether they just happen to have slight wavelength biases which are of no physiological importance remains an unresolved question. However, since other areas (V1 and V4) contain many cells that are much more selective for colour, the question arises: why have a few (5%) poorly wavelength selective cells in V3?

### Real-motion cells

When the physiology of the visual cortex is investigated in the awake behaving monkey it becomes possible to influence cellular responses by training the monkey to execute specific eye movements. The way eye position effects the responses of cells depends on the type of cells being recorded from. One type of cell that has its responses modulated by eye position is the "real-motion cell" (Galletti *et al.* 1984; Aicardi *et al.* 1987b; Galletti *et al.* 1988; Galletti *et al.* 1990). This type of cell uses information about eye movement and/or position to distinguish between the motion of an object through space and the translation of an image across the retina due to an eye movement. They respond maximally to motion of a correctly oriented stimulus over the receptive field but less to motion of the retinal image produced by a smooth pursuit eye movement that passes the cell's receptive field over a similar stationary stimuli. First discovered in small numbers in V1 and V2 (10-15%) (Galletti *et al.* 1984; Galletti *et al.* 1988), they were found to be present in a higher proportion (40%) in the V3 complex, where they are also orientation selective (Aicardi *et al.* 1987b; Galletti *et al.* 1990). There are two sources of eye movement information available to cells in the cortex: retinal and extraretinal. Retinal signals come from visual cells capable of detecting the movement of the whole visual field that occurs

when the eyes move, and extraretinal signals originate from proprioceptors in the eye musculature that are sensitive to the position and motion of the eyes themselves. In order to discover which of these two signals the V3 complex cells use to endow them with the property of real-motion sensitivity, Galletti *et al.* tested their real motion cells with two stimuli, a bar stimulus with a textured background or the same bar with a plain background. In theory, cells using retinal eye motion signals should not respond as well when there is no textured background to signal the eye movement to the cell, whereas those cells using extraretinal signals exclusively, should not be affected by the presence or absence of the textured background. This paradigm demonstrated that about half of the real-motion cells' responses in the V3 complex were increased with the textured background, suggesting that these cells receive a retinal input. However, some real-motion cells were found to exhibit their real-motion characteristics when tested in the dark (Galletti *et al.* 1990), showing that they must also receive extraretinal signals. The source of these extraretinal signals remains unknown but they may include proprioceptive information from the eye musculature and vestibular information to take head movements into account.

#### Gaze dependent cells

Another type of cell found in the V3 complex is the gaze dependent cell (Andersen and Mountcastle 1983; Aicardi *et al.* 1987a; Galletti and Battaglini 1989). Similar to the real-motion cell, this type of cell is commonly orientation selective and uses information regarding eye position. However, rather than signalling real motion, this cell's response is dependent upon animal's angle of gaze. When physically identical visual stimuli, at the cell's preferred orientation, are delivered to identical retinotopic positions (the cell's receptive field), different

responses are evoked; the magnitude of the response is dependent upon the direction in which the monkey is looking. The authors suggest that such a property would be very useful for building an internal map of real (rather than retinotopic) space which could then be used to stabilize visual perception despite eye movements. Galletti *et al.* (1989) found that about half of the cells they recorded from in V3A displayed the property of gaze-dependence, some of which were completely silent when stimulated at some gaze angles yet responded vigorously when stimulated at others. However, the majority responded to the stimulus at all gaze angles with a maximum response at one gaze angle. Most gaze dependent cells had their preferred gaze angle within the visual field hemisphere contralateral to the hemisphere being recorded from. Galletti *et al.* (1989) also found that- "gaze-dependent neurones seem to be segregated in restricted cortical regions, within area V3A, without mixing with non-gaze-dependent cells of the same area." This suggests a functional organization of this type of cell within V3A. Unlike the previously mentioned real-motion cells, gaze-dependent cells do not use retinal signals to convey eye position or movement. This was tested by placing prism in the line of sight of the monkey so that, although the stimulus appeared to be at a location corresponding to a non-responsive gaze angle, the eyes still pointed at part of the field corresponding to a good response gaze angle. When this was done, the cell still responded. In addition, cells retained their gaze-dependence in darkness, showing that the eye position rather than the stimuli position with respect to background cues, is the important factor.

The source of information necessary for cells in area V3A to modulate their responsivity with eye position that enables them to be gaze dependent has not been previously investigated. However, likely

candidates are: the frontal eye fields, area 7a and the intralaminar nuclei of the thalamus, which all contain neurones whose spontaneous firing rate in darkness is a function of eye position (Bizzi 1968; Sakata *et al.* 1980; Schlag-Rey and Schlag 1984).

### **Section 3:**

#### **Anatomy of stereopsis:**

##### **Anatomical description of the prestriate areas**

Area V3 was first described as a narrow strip of cortex immediately anterior to both dorsal and ventral V2 and representing the lower and upper visual fields respectively (Cragg 1969; Zeki 1969). The presence and individuality of V2, V3 and V3A were discovered by placing small lesions in the meridian representations of the striate cortex and finding areas of degeneration in the prestriate cortex. This method showed that areas of the visual field were represented in a number of loci within the prestriate cortex. Areas of degeneration following such V1 lesions were found in the posterior bank of the lunate sulcus, the fundus of the lunate sulcus and the anterior bank of the lunate sulcus. The exact location of these areas of degeneration depended on the location of the lesion within V1. These areas of degeneration represent the prestriate representation of the visual field in V2, V3 and V3A respectively. The boundaries of V3 and V3A were found by the technique of sectioning the splenium of the corpus callosum. Since parts of the visual field representing the vertical meridian are callosally connected (Whitteridge 1965; Pandya and Vignolo 1968), cells whose receptive fields encroach on the vertical meridian will suffer retrograde axonal degeneration when the corpus callosum is sectioned. This degeneration can be visualized in the cortex by means of the silver stain (Nauta and Gyax 1954; Fink and Heimer 1967). Section of the corpus callosum therefore produces patches of degeneration in the prestriate cortex that represent the vertical meridian. A patch at the striate prestriate border shows that V1 and V2's vertical meridian representations meet there. Two closely spaced patches at the medial part of the anterior bank of the lunate sulcus represent the border between V3

and V3A, and a further patch, roughly half way along the anterior bank of the lunate sulcus, corresponds to the vertical meridian representation of V4, and therefore the V3A/V4 border. It should be mentioned that these patches of degeneration following callosal section are not identical in their characteristics from area to area. The V1/V2 border's patch is small and well defined, reflecting the accurate topography of these areas. The patches of degeneration at the V3/V3A border spread over more cortex than those of V1/V2, and in V4 the degeneration occurs over large areas and varies from monkey to monkey, reflecting the coarse, disorderly topography in that area. When the results of V1 lesion studies and corpus callosum section studies were examined together, the representation and topography of the multiple prestriate areas was elucidated (Cragg 1969; Zeki 1969). Since then it has become possible to demonstrate anatomically the horizontal and vertical meridians in areas V2 and V3 simultaneously by combining the techniques of callosal section and the injection of anatomical tracing agents into the horizontal meridian representation in V1 in the same monkey (Zeki 1977b). Thus, it was confirmed that the horizontal meridian formed the border between V2 and V3 and the vertical meridian formed the V3/V3A border. This study left no doubt that both areas V2 and V3 are topographically organized and that both areas receive a direct input from V1.

As soon as the anatomical locations of the prestriate areas V2, V3, V3A, V4 and V5 were found, physiological investigations into their cells' specializations and topography could begin in earnest. These studies confirmed the topographic results from striate lesion and callosal section studies, the receptive fields of cells advancing towards, and then away from the vertical meridian as the electrode crossed the V1/V2 or V3A/V4 borders. However, a more interesting consequence of these

electrophysiological studies was the discovery that response properties and receptive field characteristics of cells suddenly changed as the borders were crossed (Zeki 1978a).

The V1/V2 border is characterized by a dramatic change in receptive field size, from very small in V1 to larger in V2. The response properties of cells also change as this border is crossed. V1 cells are quite often orientation selective, this orientation selectivity being arranged in a columnar fashion (Hubel *et al.* 1978). V2 also contains orientation selective cells, these being more widely spaced but of similar width to those in V1 (Tootell and Hamilton 1989). Direction selective cells are found mainly in layer 4b of V1, but in V2 they are restricted to the thick cytochrome oxidase stripes (Livingstone and Hubel 1988). As the electrode crosses the V2/V3 border, the size of receptive fields increases again and the proportions of wavelength and unoriented cells decreases, the majority of cells being orientation selective (Zeki and Sandeman 1976). V3 and V3A cells appear similar in response property and receptive field size (Zeki 1978b) but a dramatic change occurs at the V3A/V4 border. V4 cells have very large receptive fields and are commonly wavelength or colour selective (Zeki 1973). V4 and V5 are also distinct in their response properties, V5 contains no wavelength selective cells, the vast majority being direction selective and often prefer spots to long bars as long as they move in the cell's preferred direction (Zeki 1974b).

#### Cytochrome oxidase divisions within the visual cortex

The cytochrome oxidase method of staining demonstrates the inherent metabolic capacity of tissues and produces a picture of the metabolic architecture (Wong-Riley 1979).

When the macaque striate cortex is stained for the enzyme cytochrome oxidase, two parallel dark staining bands, corresponding to layers 4A and 4C, are produced and also an array of small oval shaped patches of denser staining known as "blobs" or "puffs" in layers 2 and 3 (Horton and Hubel 1981; Horton 1984). It seems that these cytochrome oxidase dense areas coincide with zones of direct geniculate excitatory input, for this is true not only of layers 4A and 4C but also of the blobs in layers 2 and 3 (Livingstone and Hubel 1982). When cut parallel to the surface, V1's distinct pattern of cytochrome oxidase blobs can be seen. In what had originally been thought of as an homogenous area containing orientation selective cells in columns (Hubel and Wiesel 1977), a pattern of cytochrome oxidase rich blobs was observed.

The blob pattern in V1 also marks out the distribution of functional classes of cells. As shown by direct recording (Livingstone and Hubel 1984), and later by 2-deoxyglucose studies (Tootell *et al.* 1988b), the blobs were shown to contain non-oriented wavelength selective cells whilst cells in the interblobs display orientation specificity. Thus, a functional specialization within V1 was discovered, the wavelength selective (non-orientation selective) cells being grouped together into cytochrome oxidase rich blobs, and the orientation selective cells, which are not concerned with wavelength, residing in the interblobs.

Similarly in V2, cytochrome oxidase staining revealed a pattern of dark stripes on a pale background, the stripes were of two varieties, thick and thin, roughly 1mm in width, running orthogonal to the V1/V2 boundary and forming three compartments: thick stripes, thin stripes and interstripes (Livingstone and Hubel 1982; Tootell *et al.* 1983; Wong Riley and Carroll 1984; Shipp and Zeki 1989). Again, these

cytoarchitectonic divisions were found to coincide with thalamic inputs from the pulvinar (Livingstone and Hubel 1982), but whereas the pulvinar input is mostly to layer 3, where the stain is darkest, the stripes extend through all layers. The connections between V1 and V2 tell us a great deal about the functional organization of the cytochrome architecture of the latter area; the connections follow a "like with like" principle. Thus, the blobs in later 2 and 3 of V1 connect with the thin stripes of V2, the interblobs of V1 project to interstripes of V2 (Livingstone and Hubel 1984) and the thick stripes of V2 receive their input from layer 4B of V1 (Livingstone and Hubel 1987a). Perhaps unsurprisingly, the functional properties of cells within V2's cytochrome oxidase stripes also conform to the "like with like" principle; cells in the thin stripes are concerned with wavelength, the interstripes' cells are orientation selective and the thick stripes harbour cells that are both orientation selective and/or direction selective (DeYoe and Van Essen 1985; Shipp and Zeki 1985; Hubel and Livingstone 1987).

### "What" and "where" pathways

In 1982 Ungerleider and Mishkin divided the visual cortex into two pathways, one for object vision and one for spatial vision, the so called "what" and "where" pathways. The "what" pathway is said to originate from the P<sub>b</sub> retinal ganglion cells terminating in the parvocellular ("P") layers of the lateral geniculate nucleus (LGN) and has general characteristics making it suitable for form and colour vision. The "where" pathway comes from P<sub>a</sub> retinal ganglion cells which terminate in the magnocellular ("M") layers of the LGN, it has characteristics making it more suitable for the analysis of dynamic form and motion. This separation of function has been extrapolated in the cortex so that the "what" pathway is said to comprise a hierarchical line of visual areas terminating ventrally in the temporal lobe and the "where" pathway a set of visual areas that progress dorsally into the parietal lobe (Ungerleider and Mishkin 1982). It has been suggested that the "what" pathway is capable of completely analysing the physical properties of a visual object and the "where" pathway executing spatial vision (Mishkin *et al.* 1983). The functions of these two pathways have been largely proposed from the results of lesion studies, which do produce complex deficits in either object recognition or the perception of space, depending on their location in either the dorsal or ventral pathway (Pohl 1973). More recent studies have shown this theory of visual cognition to be an over-simplification. The division of visual properties into object and spatial is not possible, for instance, the location or movement characteristics of an object can have a great deal to do with what it is. Additionally, areas in both the ventral and dorsal pathways have been shown to be "out of place" with respect to the "what" and "where" hypothesis, archetypally, V3 is in the dorsal pathway and an "M" fed area but contains a predominance of orientation selective cells making it specialized for form, i.e. "what" an

object is. From the "what" and "where" doctrine, one would expect to find disparity tuned cells in both pathways, because disparity information provides the brain with knowledge of spatial location and three dimensional form.

Stereo-tuned cells have been found in layer 4b of V1 (Poggio, G.F. personal communication to Hubel and Livingstone (1987)), the thick stripes of V2 (Hubel and Livingstone 1987) and V5 (Zeki 1974a; Maunsell and Van Essen 1983a), all areas (or modules) receiving their input from the "M" system. It been shown psychophysically that depth vision is compromised when the stimulus is shown at isoluminance (Lu and Fender 1972; Over *et al.* 1973; Gregory 1979; Livingstone and Hubel 1987b) presumably because isoluminant contours are not initially analysed by the "M" system. Most physiological studies have shown that stereotuned cells are not concerned with the wavelength or colour of the stimulus (Hubel and Livingstone 1987; Livingstone and Hubel 1988), but some (Burkhalter and Van Essen 1982; Burkhalter and Van Essen 1986; Gegenfurtner *et al.* 1995) have found that cells in area 18 (V2) can be "polymodal", i.e. selective for more than one visual attribute, e.g. colour/stereopsis, colour/direction and colour/orientation. Although most studies agree that orientation and disparity are often selected for by the same cell, these authors have suggested that V2 is an area which integrates colour and direction, and colour and disparity. However, they do state that cells "selective" for two stimulus attributes are usually poorly tuned to one or both of them (Gegenfurtner *et al.* 1995).

Areas sharing an "M" input with V5 are the thick stripes of V2 and the V3 complex. The thick cytochrome oxidase stripes of V2 receive their input from Layer 4b and project to V3, V3A and V5, comprising the

cortical "M" pathway. In V2, stereotuned cells are found, on the whole, in the thick stripes (Livingstone and Hubel 1988), a parcellation containing very few cells with colour specificity (Hubel and Livingstone 1987) and when V2 is ablated stereoscopic vision is severely compromised (Cowey and Porter 1979), Area V3, whose cells are predominantly orientation selective, receives its input from the thick stripes of V2 and also lacks colour cells (Zeki 1978b; Baizer 1982). V3 and the thick stripes of V2 contain high proportions of stereoscopic depth cells (Burkhalter and Van Essen 1982; Burkhalter and Van Essen 1986; Felleman and Van Essen 1987) and some cells have been found there that have very strong binocular interactions, for instance a cell in V3 may actually be inhibited by monocular stimulation yet respond well with binocular stimulation (Zeki 1979).

It is possible to selectively lesion the "M" or the "P" layers of the monkey LGN by individually injecting them with ibotenic acid. Monkeys can then be tested on pretrained tasks to discover their visual deficits. Lesions of the parvocellular layers produce deficits in stereopsis for fine patterns but have no effect on stereopsis in coarse patterns, and magnocellular layer lesions selectively compromise high temporal frequency flicker and motion perception but have little effect of stereopsis (Schiller and Logothetis 1990; Schiller *et al.* 1990). This evidence (along with evidence from isoluminance studies of stereopsis; see previous section) suggests that the parvocellular system processes disparity information from fine patterns defined by luminance contrast and coarse isoluminant patterns, and that both the parvocellular and magnocellular systems process disparity in coarse patterns defined by luminance contrast. The absence of a fine pattern isoluminant system (high spatial frequency "P" system) produces the deficits in stereopsis observed by Lu

and Fender (Lu and Fender 1972) who used isoluminant fine random dot stereograms, and the presence of the low spatial frequency isoluminant system (Parvocellular system) explains the seemingly antagonistic result of Comerford (Comerford 1974) who used coarse patterns for their disparity stimuli. Therefore, it is not possible to equate the "M" and "P" system with luminance and chromatic contrast respectively. Neither is it correct to assert that disparity is exclusively processed in the "M" system.

The evidence from isoluminance studies seems to suggest that stereoscopic depth selectivity is restricted to the "M" system, even that the "P" system is blind to depth. This suggestion was made by Livingstone and Hubel (1988) but since these conclusions disagree with those obtained from selectively lesioning the "M" and "P" layers of the LGN, a more detailed investigation of the response properties of the "M" and the "P" systems is required to resolve the disparity. As well as chromatic and luminance differences between the "M" and "P" systems, there is also a difference in their selectivity for spatial frequency (DeValois and DeValois 1988; DeValois 1991). Tootell *et al.* (1988) also showed this division with a 2DG experiment using high and low spatial frequency stimuli and imaging the activities of blobs and interblobs in V1 (Tootell *et al.* 1988c). These authors argue that the primary distinction between ("P" fed) blobs and ("M" fed) interblobs is one of spatial frequency; blobs contain cells tuned for low spatial frequency (coarse detail) and interblobs contain cells tuned for high spatial frequency (fine detail). They state that the differences in chromatic and orientation tuned responses between "M" and "P" regions are a direct consequence of the spatial frequency differences. Thus, blobs are more often wavelength selective because their cells operate as colour opponent for low spatial frequency stimuli and are unresponsive to high spatial frequencies. Similarly, the interblob

cells are more tightly tuned for orientation because their cells are selective for higher spatial frequencies. Both theories produce similar divisions of labour within the cortex, the "M" system dealing with motion and orientation signals (high spatial frequency) and the "P" system dealing with both wavelength and luminance contrast signals (low spatial frequency). However, recordings made from the magnocellular layers of the LGN (Logothetis *et al.* 1990) have shown that they can respond (weakly) to chromatically defined borders, showing that even this division of labour is not absolute.

## Materials and methods:

This study was done on 29 Cynomolgus monkeys, (*Macaca fascicularis*), a species of old world monkey.

Monkey Name.	Number of Units.		Injection Target.
	Disparity Tested.	Total.	
SP14			HRP into V3A
SP15			HRP into V3A
SP28			HRP into V3A
SP44			HRP into V3
MP2			HRP into DP
MP3			HRP into DP
VG30	19	57	HRP into V3
VG31	7	93	HRP into V4
VG32	5	8	
VG33	3	124	
VG34	16	57	HRP into V3
VG35	35	59	HRP into V3
VG36	9	18	HRP into DP, Pro. into V4
VG37	17	61	Pro. into DP, HRP into V4
VG38	15	89	
VG39	21	42	HRP into DP
VG40	0	16	
VG41	0	63	
VG42	4	59	HRP into DP
VG43	2	32	
VG44	17	60	HRP into V4A
VG45	50	93	
VG46	28	85	
VG47	6	81	
VG48	0	44	HRP into VVC
VG49	0	100	HRP into VVC
VG50	4	99	HRP into VVC
VG51	47	91	
VG52	82	130	
VG53	33	156	
<b>Total units:</b>	<b>420</b>	<b>1717</b>	

Table 1.

This table details all the animals from which units were recorded or anatomical tracer injections made. VVC refers to ventral visual cortex, a region of cortex under investigation in a concurrent study.

Males weighing from 2 to 4Kg were used for physiological recording and/or the injection of anatomical tracing agents. Animals were recorded from for 24 hours a day for five days and the anatomical tracing agent injected on the second or third day. Due to a low success rate of V3 complex injections, the particular brains used in this study (MP2, MP3, SP14, SP15, SP28 and SP44) were injected and digitized by previous researchers working in this laboratory and my role was to prepare reconstructions from this material using computer software developed by J. Romaya in this laboratory (Romaya and Zeki 1985), and examine the connections of these brains.

All invasive procedures and recording sessions were done under full anaesthesia. At the end of the experiment the animal was killed with an overdose of anaesthetic, perfused through the heart and its brain removed and sectioned so that electrode tracks could be reconstructed and the distribution of anatomical tracing agents determined. Animals were housed and all procedures were done in accordance with Home office regulations under the Animals (Scientific Procedures) Act 1986.

### Pharmacology

Before removal from their cages the animals were anaesthetized with 40mg ketamine i.m. ("Vetalar" Parke-Davis). This fast acting, short term agent allows the animal to be weighed, shaved and a cannula chronically inserted into the saphenous vein; during this procedure additional 20mg doses of ketamine may be required. Once cannulated, a long term anaesthetic was administered to the animal. Careful selection of the anaesthetic is critical to the experiment. The agent used must eliminate the possibility of the animal feeling any pain and render it unconscious, yet not affect the responses of cells in the visual cortex.

Ideally the anaesthetic should have a large therapeutic range and be safe over long periods of time. In the earlier experiments sodium pentobarbitone ("Sagatal" Rhône Mérieux) was used at an initial dose of between 0.7 and 1.0 mg i.v. with supplementary doses of about 0.1 mg/hour i.v. administered at two to four hourly intervals, but because of problems with "build up" of anaesthetic over time causing overdose dangers (barbiturates accumulate in fatty tissues, thus reducing the effective dose over time) a safer agent was selected. A combination of propofol ("Diprivan" Zeneca) 4-12 mg/Kg/hr i.v. infusion, and the morphine analogue-sufentanil citrate (Janssen), 3-8 µg/Kg/hr i.v. infusion, was used. Propofol is used in human surgery and is fast acting and quickly metabolized. It has a very large therapeutic range, provides deep anaesthesia and is best administered as a continuous infusion (Waugaman and Foster 1991). The opioid provides supplementary pain relief because, although propofol is a good anaesthetic, it only provides total surgical anaesthesia when used in conjunction with an analgesic (Jansen *et al.* 1990). Once anaesthetized the monkey was intubated or (in later experiments) the trachea cannulated to allow artificial respiration.

The following drugs were also administered:

The steroid, dexamethasone sodium phosphate ("Decadron" David Bull Laboratories) Initial dose 8mg i.m. 12 hours before the experiment, followed by 4mg i.m. every 12 hours, to guard against cerebral oedema and consequent herniation.

A systemic antibiotic, chloramphenicol ("Intramycetin" Parke-Davis) 300mg/day i.m. & s.c., to prevent infection.

The anti-secretory agent, glycopyrronium bromide ("Robinol" A.H. Robins) 0.04mg/day i.v., to prevent the formation of saliva and mucus which could block the tracheal tube.

### Surgery

Once sufficiently anaesthetized (verified by the absence of muscle tone, eye blink and pedal flexion reflexes) and before the neuromuscular blocking agent was administered, the surgical procedure was started. In chronic experiments the operation was done under aseptic conditions. The animals head was held by means of ear bars and a mouth bar and the scalp cut and retracted to expose the skull. A small hole was then made with a dental drill and enlarged with rongeurs to expose an area of dura about 100mm<sup>2</sup>. The dura was then very carefully removed with dural-scissors to expose the delicate cortical surface beneath. The exposure was usually made to incorporate the lunate sulcus, a useful landmark for the placement of electrode penetrations which can usually be found about 15mm dorsal and anterior to the occipital crest. Depending on the type of electrode penetration to be used (normal or tangential), the exposure was either fitted with a clear plastic recording chamber fixed onto the skull with dental cement and filled with 2% agar, or just covered with agar. The absence of the recording chamber allows a greater range of penetration angles, a requirement for tangential penetrations. The purpose of the agar was to maintain stability of the electrode by preventing pulsations of the cortex. Since the position of the electrode penetration was of critical importance in these experiments, a dissecting microscope (Zeiss) was employed to visualize the cortical surface through the agar.

After surgery the monkey was maintained under anaesthesia and the neuromuscular blocking agent, pancuronium bromide ("Pavulon" Organon Teknika) was administered with an initial dose of  $100\mu\text{g}/\text{Kg}$  and then as a continuous i.v. infusion of  $60\mu\text{g}/\text{Kg}/\text{hr}$ . The neuromuscular blocker was used to minimize eye movements. Since the respiratory musculature is also paralysed the animal has to be ventilated; this was achieved with a "Harvard" ventilator, the stroke volume of which had been calculated according to the animal's weight ( $11.6\text{cm}^3/\text{Kg}$ ). To monitor the animal's state of anaesthesia, heart rate, end-tidal  $\text{CO}_2$  and rectal temperature were monitored with a Datex Cardiocap ECG/gas analyser machine and kept within safe limits<sup>6</sup> by adjustment of the infusion pump rate, respiration rate and heated blanket thermostat respectively. The Cardiocap machine was set up with an alarm system to warn the experimenter if the animal's vital signs reach non-optimum values. In order to maintain the animal under anaesthesia the following additional precautions were taken hourly: the tracheal tube was aspirated by insertion of a suction tube to reduce the build-up of mucus and the infusion line and cannulation was checked.

## .c2.Perfusion

At the end of the recording session the animal was given a fatal overdose of Sagatal with 25000 units of heparin ("Monoparin" CP) to prevent blood clots, and perfused. The thoracic cavity was opened and the descending aorta was clamped to reduce the volume of the vascular circuit to be perfused. A large bore needle was inserted and clamped into the left ventricle and the right atrium was incised to produce an open circuit through which the animal could be perfused. First 2 litres of warm

---

<sup>6</sup>End tidal  $\text{CO}_2$  was maintained at between 3 and 4%, ideally 3.5%.  
The animal's core temperature was kept as close to  $37.5^\circ\text{C}$  as possible.  
A safe range for heart rate is between 100 and  $150\text{min}^{-1}$ .

saline containing 25000 units of heparin ("Monoparin" CP) was passed through until it ran clear. This was followed by 4% paraformaldehyde in phosphate buffer. The fixative was run through for 30-40 minutes. Too long an exposure to paraformaldehyde degrades the peroxidase activity of HRP but some fixation is necessary to allow smooth cutting of frozen sections and bind the peroxidase within the cell bodies and terminals to which it has been transported (Mesulam 1982). After fixing, the paraformaldehyde was rinsed out with 2l each of 4°C 10, 20 and 30% sucrose solutions in phosphate buffer after which the brain was removed and stored at 4°C in 30% buffered sucrose solution until no longer buoyant (usually about 40 hours). It was important that all the paraformaldehyde was removed because it interferes with both the cytochrome oxidase and HRP staining procedures (Courville and Saint Cyr 1978; Rosene and Mesulam 1978).

### Optics

The eyelids were sutured or taped open and the pupils were dilated with 1% atropine eye drops (Schering-Plough) to allow visualization of the retinas, and the eye lids retracted with 10% phenylephrine drops (Richard Daniel & Son). Gas permeable neutral density contact lenses were fitted to prevent drying of the corneas - a major limiting factor on the quality and therefore length of experiments. Streak retinoscopy was used to determine the power of auxiliary lenses required to focus the eyes on a monitor at a distance of about 1.5m in front of the monkey. The positions of the foveas were then plotted onto the monitor with a reversible ophthalmoscope and these positions saved onto floppy disc. Since monkeys' foveas are not always easily visualized, retinal blood vessel landmarks were also plotted because they are much easier to relocate when replotting the eyes to check for eye movements. The

accuracy of retinal landmark plotting was estimated to be within  $\pm 1$  degree. Landmarks were replotted between cells and any eye movements recorded. During the experiment the eyes were regularly irrigated with hypertonic saline and 0.05% Chloramphenicol eye drops ("Snophenicol" Chauvin) were applied every 12 hours to prevent infections. At the first sign of the conjunctiva becoming opaque due to drying of the eyes, the lenses were removed and the eyes closed. Closing the eyes did not always restore the transparency of the corneas, so regular irrigation of the eyes with hypertonic saline was of critical importance.

### Physiology

Extracellular recordings of electrical activity were made with platinum-gold plated tungsten-in-glass microelectrodes (Merrill and Ainsworth 1972) of low impedance ( $1M\Omega$  at 1KHz) and 10-12  $\mu\text{m}$  exposed tip length. These electrodes, when used in conjunction with the spike discriminator, enable both single and small groups of cells to be recorded from. The electrode was advanced with a Burleigh "inchworm" microdrive which can make steps as small as  $0.5\mu\text{m}$ . However, since the diameter of a cell body in the cortex averages 20-30 $\mu\text{m}$  the electrode was advanced at least  $50\mu\text{m}$  between recording sites to ensure that a new cell had been encountered. The fine adjustment on the microdrive was used to "fine tune" the signal from a particular cell. Amplification equipment consisted of a "Neurolog" NL 100 headstage preamplifier and various Neurolog modules (NL 104 AC Preamplifier NL 125 Filters, NL 200 spike trigger, NL 606 Latch counter). Spikes were displayed on a tektronics RM 565 oscilloscope fitted with a type 3A9 amplifier and relayed over a loud speaker. A spike counter was fed by a spike discriminator which passed all the spikes greater than a particular amplitude set by the experimenter. Thus single or small groups of cells were recorded from. The output

from the spike counter was digitized to form the input to a Commodore Amiga 2000 microcomputer programmed (by J.R. Romaya) with software capable of displaying the continuous spike rate as a histogram (bin width 20ms) and saving portions of this histogram to floppy disk. The same computer was also programmed to present pre-recorded sets of stimuli to the monkey and automatically save the portion of spike activity that corresponded to the "in field" period, i.e. the time period during which the stimulus occupied the receptive field.

Two types of penetration, referred to above, were made through the cortex. Figure 8 shows the types of penetration on a horizontal section taken through the occipital cortex. In order to record from V3 a normal penetration (a) was employed, first entering V1 then passing through the white matter into V2, across the lunate sulcus and into V3 or V3a. The functional architecture of V2 (to be described later) makes electrode tracks that run parallel to the surface desirable, so recordings from V2 were made at the edge of the operculum at an angle tangential to the surface of the cortex (b). Tangential penetrations enabled recording from a number of V2's cytochrome oxidase stripes in succession. Tangential penetrations through V3a and V3 were also possible (c). Although harder to achieve, they are of interest because they enable one to see whether the properties of cells change as the electrode is advanced through the area in different directions. Multiple electrode penetrations were made into the cortex (up to six) and, to identify individual tracks and depths of cells, one or more electrolytic lesions were made in each track by passing current through the recording electrode ( $7\mu\text{A}$  for 7 seconds, tip positive).

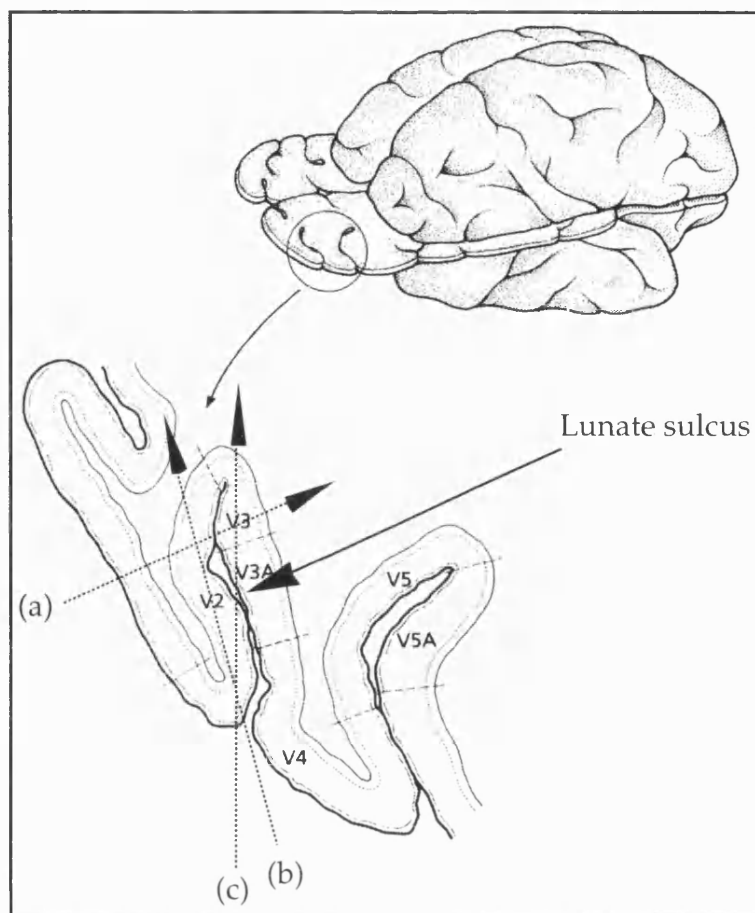


Figure 8.

An illustration of the types of electrode penetration used. A horizontal section is shown with three electrode approaches marked on as lines a, b and c.

Visual stimuli were generated on a colour TV monitor (Grundig BCG155) by the Amiga computer. Using the computer, stimuli of various shapes, sizes and colours could be presented on different coloured back grounds and moved either manually (by means of a track ball) for receptive field plotting or by the computer for running pre-programmed stimuli trials.

Receptive fields were plotted manually by presenting the best stimulus and determining the outermost point where a response can be reliably elicited. The borders were drawn orthogonal to the direction of motion of the stimulus as it was moved towards the receptive field

centre, a process repeated four times to produce a rectangular receptive field. The field positions were saved onto floppy disk by the Amiga computer.

The many types of pre-programmed trials were each designed to test the cell's selectivity for a particular stimulus attribute. Trials to test orientation selectivity presented the receptive field with a bar at a set of orientations, the steps could be varied from  $5^\circ$  to  $45^\circ$ , the bar could be moving (perpendicular to its orientation) or stationary and the bar and background, although usually black and white, could be of any one of 255 colours. Each orientation was tested at least 3 times in a random sequence and the average response for each orientation calculated. The test for wavelength presented the cell with bars of roughly isoluminant colours, moving or stationary at the cell's preferred orientation (if any) and usually on a black, white or isoluminant grey background. Isoluminance was determined by the minimum motion technique (Anstis and Cavanagh 1983) on three representative human subjects; it was assumed that human and monkey do not have isoluminant points that differ markedly. Each colour was presented at least 3 times and average responses taken. The test for disparity tuning presented each of the cell's receptive fields with a vertical (or near vertical) bar moving in a horizontal direction or a short bar or spot moving in a vertical direction. The stimuli were presented at various disparities and averages taken over 3 trials for each disparity (a more detailed description of the disparity stimulus can be found later). Since any property of the stimulus could be varied with the computer a great variety of tests could be custom made, e.g. speed, length, size, direction, shape and stimulus background/foreground colour.

In general two methods for stimulating at various disparities were available: the first used one stimulus for both receptive fields. For this method (Pettigrew *et al.* 1968; Bishop *et al.* 1971) a single bar was passed through both receptive fields having first superimposed them with Risley bi-prisms, disparity was varied by changing the prism settings. The other method (first described by Henry, Bishop and Coombs (1969)) was to keep the receptive fields widely separated and to stimulate with two identical stimuli, one for each eye. By changing the distance between the two stimuli it was possible to simulate the changes in disparity associated with viewing stimuli in frontoparallel planes other than that of the horopter (the fixation plane). In the cases where the receptive fields of each eye overlapped on the screen, red and green filters (anaglyphs) were put over the animals eyes and the corresponding stimuli were presented in red and green so that each eye only saw one of the two stimuli. This method was used in the present study because disparity can be quantitatively and accurately measured if it is a distance between two stimuli on a screen rather than a prism setting. The prisms also produce distortions to the image which can not be easily corrected.

Figure 9 illustrates the method used in this study for stimulating at various disparities. Figure 9i is a representation of the paths of light during normal vision. The animal fixates point (b) in space. The points (a) and (c) are in front of, and behind the fixation plane respectively and are therefore seen as disparate. Since disparity is defined as a visual angle, the disparities of these points will be twice the visual angle subtended between b' to a' and b' to c' respectively. Figure 9ii represents the paralysed monkey's eyes. Each eye has its own fixation point (b and b) so if identical stimuli are placed at each of these corresponding points, the fused image of both stimuli will appear to be at the horopter (zero

disparity). Identical stimuli placed at the non corresponding points (a) or (c), will be seen with retinal disparities  $2(b' \text{ to } a')^\circ$  or  $2(b' \text{ to } c')^\circ$  respectively, so the fused images of these stimuli will appear to be in front of or behind the horopter.

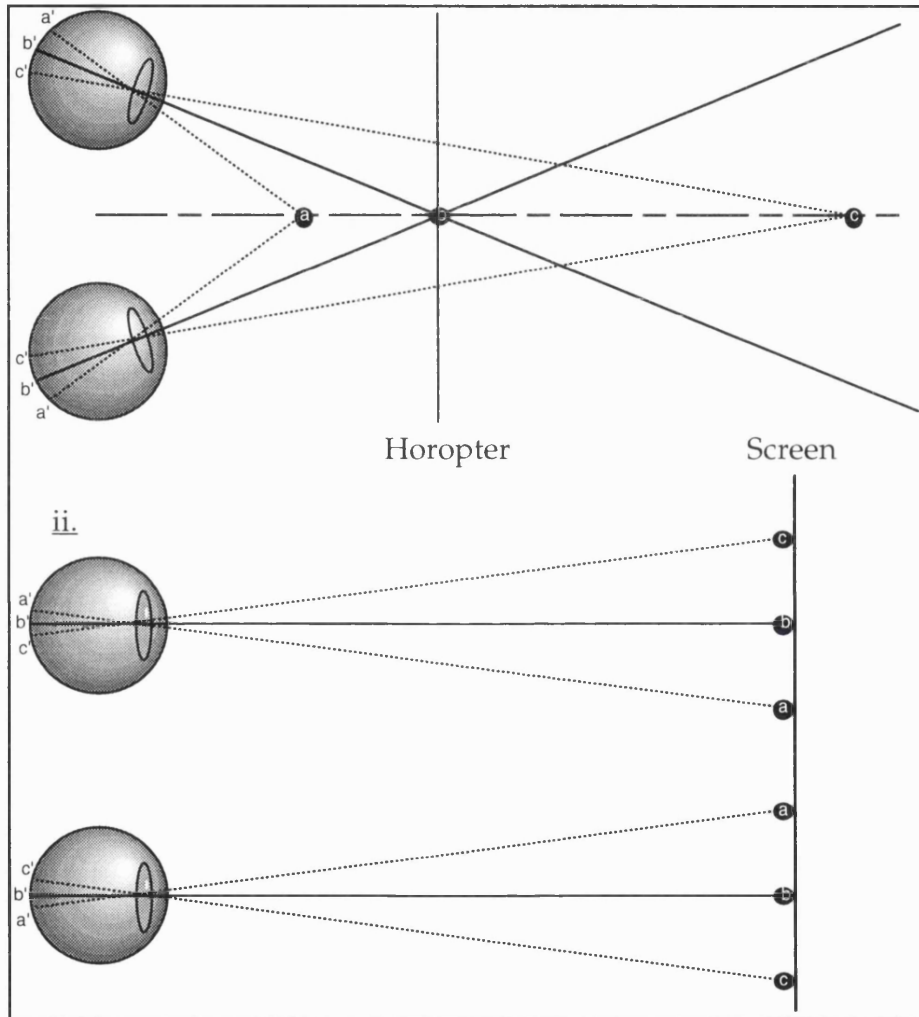


Figure 9.

The method of stimulating cells with varying disparity. i) Shows how disparity occurs during normal vision of points a, b and c at different locations in depth. ii) Shows how these disparities can be produced in the paralysed monkey using points a, b and c on a fronto-parallel fixation screen.

## Categorization of cell properties:

### Receptive field data statistics (John Romaya, personal communication)

The receptive field data was stored on computer as a set of four vertices for each receptive field. Each vertex is stored as an  $x$ ,  $y$  co-ordinate pair. The  $x$  co-ordinate represents position right (positive) or left (negative) of the vertical meridian and the  $y$  co-ordinate represents position above (positive) or below (negative) the horizontal meridian. These data are obtained by moving a flat screen along a circular track which thus describes a cylinder. The axis of the cylinder forms a vertical line which passes through the centre of the head of the monkey. As a result a polar co-ordinate system is mapped to a Cartesian co-ordinate system and for the purposes of this study all quantities such as receptive field size, area, etc. are calculated as though the receptive field vertex co-ordinates were true Cartesian co-ordinates. It is acknowledged that this process does introduce a distortion of the receptive field characteristics. This distortion is negligible at or near the horizontal meridian but increases with distance from the horizontal meridian so that at  $30^\circ$  above or below the horizontal meridian there is an exaggeration of up to 15% in the calculation of receptive field area, corresponding to an overestimate of 7.5% in receptive field size. This distortion is due to plotting the receptive fields on a cylinder rather than a sphere and affects the  $y$  co-ordinates only. In addition there is a local distortion caused by plotting the receptive fields on a plane surface rather than on a cylinder. Typically we use a plotting area approximately 40cm wide at a distance of 114cm. The maximum local distortion at the edges in this case is 1.5%.

### Receptive field characteristics

- 1) The receptive field size is calculated as the square root of the area and is a value in degrees.
- 2) The receptive field area is calculated as the surface area of the polygon formed by the Cartesian co-ordinates of the four receptive field vertices. It is a value in degrees squared.
- 3) The receptive field eccentricity is calculated as the distance of the Cartesian co-ordinates of the centre of mass of the receptive field from the fovea.
- 4) The receptive field shift is the angular distance in degrees between the receptive field centres of two consecutive recorded cells. The shift is also normalized using the electrode depths of the two cells to give a shift per 100 microns of cortex so if, for example, the distance between two successive cells is 200 microns the shift will be calculated as half the distance between the centres of their receptive fields.
- 5) Receptive field scatter is a measure of deviation from perfect topographic mapping and is calculated for short sequences of cells which may be reasonably expected to display a progressive drift in position along the sequence. A simple model of topographic mapping is assumed whereby the predicted centre of each receptive field lies on a straight line in the visual field and the position of the centres along the line progress according to the electrode depth. This problem can be resolved mathematically by performing two linear regressions: electrode depth versus cell centre x co-ordinate and electrode depth versus cell centre y co-ordinate. These regressions combine to give a predicted centre position

for each electrode depth. For each cell the distance of the centre of the field from the predicted position is calculated and this is the scatter for that cell.

### Response characteristics

#### Quantitative measurement:

All cells encountered were tested for their selectivity for orientation, direction, wavelength composition, length, binocularity and disparity. Some cells were further tested for colour, texture in depth, speed and form from motion (using texture). In order to get a quantitative measurement of a cell's selectivity, the following index was calculated by the computer:  $I = 1 - \frac{(worst - base)}{(best - base)}$  (Burkhalter and Van Essen 1986). This compared the best and worst responses for each attribute, after subtraction of the baseline firing rate (average firing rate between trials, when the screen was blank). The more selective a cell's response, the higher the index, up to an index value of 1; beyond 1, the selectivity was accompanied by overt inhibition. An index of 0.7 or higher was taken to indicate "strong" selectivity for the attribute tested; values between 0.5 and 0.7 indicated a bias. With indices higher than 1, the ability to compare the selectivity of different cells was lost: the stronger the inhibition, the higher the index, but, in the presence of that inhibition, the stronger the response to the best stimulus, the lower the index. We used the index in our classification, leaving out of account all cells in which the standard error bars of the best and the worst responses overlapped (see Van Essen and Burkhalter (1986)). The index classification system took into account the response of the cell to only two of the many conditions tested. We therefore did not blindly follow the index classification, but examined the computer-stored results of all of

the cell's responses, and also the notes taken at the time of the test, before it was classified as selective for one attribute or the other.

Cells were placed in the following qualitative categories:

*Orientation*

Orientation selective.	One orientation (stationary or in motion) elicited a maximal response. There was no response, or inhibition, to other orientations.
Orientation biased.	One orientation (stationary or in motion) elicited a maximal response but all orientations elicited some response.
Non-oriented.	All orientations elicited equal responses.

*Direction*

Direction selective.	One direction elicited a maximal response there was no response (or inhibition) to the other direction.
Direction biased.	One direction elicited a maximal response but there was some response to the other direction.
Non-directional	Both directions of motion along the preferred axis of motion (if any) elicited equal responses.

*Length*

End stopped	Responded maximally to stimuli shorter than the receptive field and was inhibited by long stimuli.
Length summation	Responded maximally to stimuli longer than receptive field.
Not tuned	Responded well to stimuli of any length.

*Ocular dominance* (Hubel and Wiesel 1962)

1.	Contralateral eye only elicited a response.
2.	Response was dominated by contralateral eye.
3.	Response from contralateral eye was larger than that of ipsilateral.
4.	Both eyes elicited equal responses.
5.	Response from ipsilateral eye was larger than that of contralateral.
6.	Response was dominated by ipsilateral eye.
7.	Ipsilateral eye only elicited a response.

*Binocularity* (Zeki 1979)

I	Driven by ipsilateral eye only.
C	Driven by contralateral eye only.
ID	Driven by both eyes but dominated by the ipsilateral eye.
IC	Driven by both eyes but dominated by the contralateral eye.
B	Driven equally well by both eyes.
BO	Only driven by stimulation of both eyes simultaneously.

*Disparity* (Poggio and Fischer 1977)

TE*	Responded maximally to one disparity only.
TI†	Responded to all disparities except one.
Near	Responded to all disparities smaller than a particular disparity.
Far	Responded to all disparities larger than a particular disparity.
Flat	Responded to all disparities.

\*TE = Tuned Excitatory.

†TI = Tuned Inhibitory.

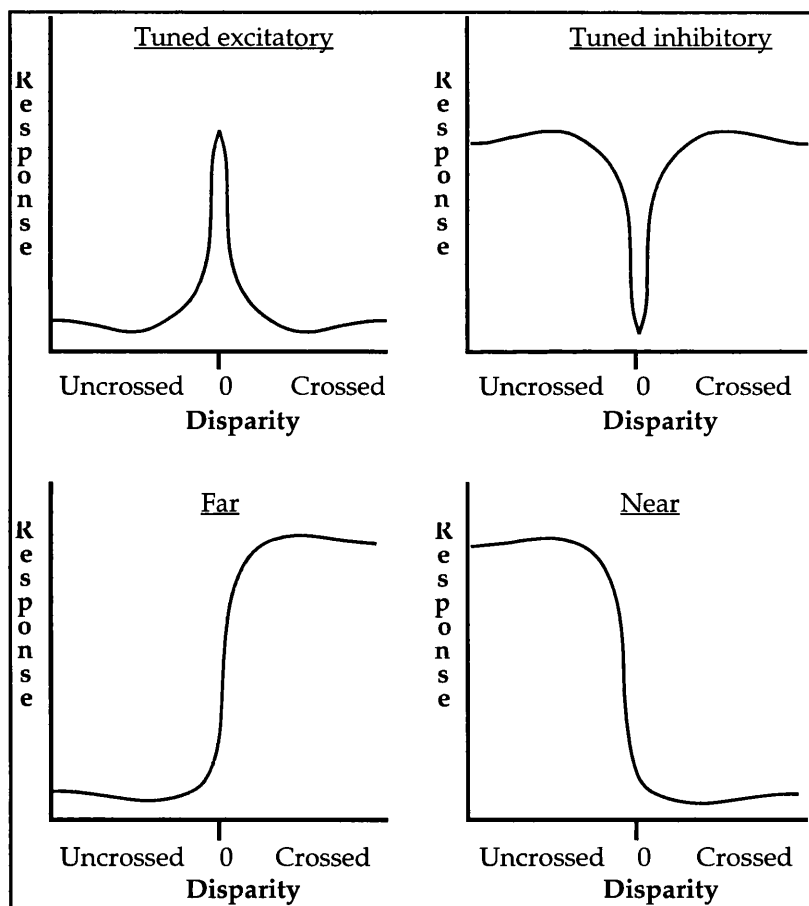


Figure 10.

An illustration of the disparity-response curves of the 4 types of disparity tuned cells defined by Poggio and Fischer (Poggio and Fischer 1977).

### The detection of cell grouping

Our principal concern here was to learn whether cells selective for different stimulus characteristics were clustered within the cortex of different visual areas. To this end, a statistical test called the One Sample runs test was used (Siegel 1956) to calculate the probability of obtaining the cell sequences that we did. This was done by assigning a 1 to the type of cell to be investigated and a 0 to all other cells. Each penetration then translated to a sequence of 0s and 1s. Within a series, a "run" was defined as an uninterrupted succession of 1s or 0s. For each of these series the total number of 1s and 0s (denoted as  $n_1$  and  $n_2$  respectively) and the number of runs ( $r$ ) were calculated. For example: in the series 11000100001101,  $n_1 = 6$ ,  $n_2 = 8$  and  $r = 7$ . For each  $n_1, n_2$  pair there was a range of expected values for  $r$ , if the distribution of 1s and 0s was random. The expected value of  $r$ , calculated assuming the distribution to be random, was denoted as  $R$ . If the distribution was not random, i.e. there was grouping,  $r$  will be smaller than its expected value  $R$ . Thus, for each  $n_1 n_2$  pair there exists a value  $R$  such that  $r \leq R$  has a probability of  $p = 0.025$ . Therefore  $p$  values less than 0.025 denote significant clustering of the cell type under scrutiny.

### Anatomical tracing and histological procedures

The connections of areas of the visual cortex were investigated by injection of the enzyme horseradish peroxidase (HRP) coupled to the lectin wheat germ agglutinin (WGA). This substance became bound to the neuronal cell membranes by means of the lectin constituent, thus limiting the extent of its diffusion away from the injection site, and ensuring a maximum uptake in the vicinity of the injection site, where it was taken inside the cell by the process of endocytosis (Trojanowski 1983). It was taken up by the soma or dendritic processes with which it made

contact, and transported to all other parts of the cell and it thus acted as a retrograde as well as an anterograde tracer. The effective transport time was 48 hours. The conjugate was then visualized by histochemical techniques which utilize its peroxidase enzymic activity, thus labelling those cell bodies with axons projecting to the site of the injection and producing a fine dust like deposit at the axon terminals of those cells lying within the injection site. The former is referred to as retrograde and the latter as anterograde labelling. There was also dense labelling around the injection site but only in about half of this region was there sufficient uptake of HRP to produce labelling in distant parts of the cortex, this smaller region being known as the "effective" injection site (Shook *et al.* 1984).

Animals were prepared for surgery as described above and, usually on the second or third day of recording, an injection of 0.06 to 0.3  $\mu\text{l}$  of a 4% solution of HRP-WGA (Sigma) made with a 1 $\mu\text{l}$  Hamilton microsyringe, with a glass micropipette of length up to 1.5 cm cemented to its tip. Areas on the surface of the brain were injected with reference to sulcal landmarks. Areas hidden within sulci (V3 and V3a) were located first with the recording electrode on the basis of their depth, white matter transitions, response properties and receptive field position and size, whereupon the recording electrode was withdrawn and replaced by the syringe at the same trajectory and depth in the cortex. The injection was made in small stages (0.05 $\mu\text{l}$  every 5 mins) to minimize pressure damage to the cortex which could have prevented uptake. After the injection the syringe was left in the cortex for a further 10 minutes to prevent the HRP from flowing up the syringe track and entering cortex not intended for injection. After the syringe was removed it was tested and, if found to be blocked, the procedure was repeated. Once injected, the hemisphere was

no longer recorded from, the chamber was packed with gelfoam ("Sterispon", Allen and Handbury's) and sealed with dental cement. The other hemisphere was then recorded from for a further 36 to 72 hours after which the monkey was killed with an overdose of anaesthetic. Not all monkeys received HRP injections, some were used for physiological recording only. However, if the quality of the physiological recording deteriorated, the monkey was killed prematurely (unless HRP had been injected). Factors that might cause the experiment to be drawn to a conclusion are: herniation of the cortex brought on by lack of oxygen to the brain which caused damage to the cortex by pushing it out through the exposure, and precluded both further recordings, and the reconstruction of electrode tracks. If the eyes became opaque due to drying of the corneas or bacterial infection visual responses were adversely affected. Clouding of the corneas could usually be prevented by regular irrigation and the application of antibiotic eye drops. In some cases it was not possible to get cells to respond to stimuli ("drive" cells) this could have been due to bleeding or damage caused by previous electrode penetrations inside the cortex. Sometimes a penetration or even an entire hemisphere yielded few drivable cells for no apparent reason; the cause of these unsuccessful experiments remains unknown.

### Histology

60  $\mu\text{m}$  horizontal sections were cut on a freezing microtome, every section was saved and separated into six sets, two of which were processed for HRP (Mesulam 1978; Mesulam 1982), one of which was cresyl-violet counter-stained so that cortical layers could be identified, thus enabling one to visualize the characteristic laminar patterns of the label. One can gain information regarding the type of projection from examination of the laminar pattern of HRP transport. Generally

throughout the cortex cells in different layers vary in their functions by playing different roles in the input-output relationships of an area. Forward projections for instance originate predominantly from the upper cortical layers and terminate in layer 4. They are invariably reciprocated by an asymmetrically organized backward projection that arises from both the upper and lower layers, but its termination avoids layer 4 to concentrate on layers 1 and 6 (Gilbert and Kelly 1975; Tigges *et al.* 1977; Rockland and Pandya 1979; Maunsell and Van Essen 1983b). Thus, the type of projection, as well as its target was elucidated by close examination of the HRP stained tissue. Usually two sets of sections were stained for cytochrome oxidase (Wong-Riley 1979). Cytochrome oxidase is a metabolic enzyme present in mitochondria and its distribution gives a picture of the metabolic architecture of the cortex, dark areas containing more of the enzyme than pale areas. The functional and anatomical significance of differently staining areas of the visual cortex for cytochrome oxidase will be discussed in the second section of the introduction.

The histochemical principles underlying the HRP and the cytochrome oxidase reactions are similar. In each case a benzidine derivative (tetramethyl benzidine, TMB for the HRP and diaminobenzidine, DAB, for the cytochrome oxidase) becomes oxidized by the tissue and forms a coloured insoluble polymeric deposit at its site of oxidation, thus staining the tissue. Molecular oxygen is the oxidising agent for the HRP reaction but a further enzyme, Cytochrome C, is required to couple the DAB into the redox reaction. The peroxidase is capable of reacting directly with the TMB, but requires the addition of hydrogen peroxide to do so. To prevent the HRP from showing up in the cytochrome oxidase stain and giving misleading patches of dense stain,

the hydrogen peroxide breakdown enzyme, catalase, is added to the cytochrome oxidase incubation medium. The rest of the sections were either stained with a routine cresyl-violet stain (for Nissl substance) and/or myelin stained by means of the Gallyas method (Gallyas 1979). The Nissl sections were generally best for finding and reconstructing the electrode tracks. The myelin stained sections were intended to be used for finding the borders of areas V3/V3a (Burkhalter *et al.* 1986) but in practice this was not possible because the subtle differences in myelo-architectural characteristics could not always be reliably seen.

The visual area V2 has a distinct architecture, when stained for cytochrome oxidase, stripes running tangential to the cortex become apparent. These stripes are of two types: thick and thin, and separating them are areas of pale staining tissue, so called interstripes. These compartments in V2 have been shown to contain cells with different functional properties as well as distinct projections (to be discussed later) so it was interesting to record from many stripes in succession to see how their cells' properties changed and to see how the visual field was represented within each stripe type. This was achieved by the use of tangential penetrations. For these penetrations it was necessary to "flat mount" the operculum so that the tissue could be cut in the plane of the electrode track, and that the stripes could be identified. Figure 11 shows the position of the operculum and the cuts necessary to remove it in one piece. The cortex and white matter at the fundi of the lunate sulcus, the inferior occipital sulcus and the calcarine sulcus were cut and the operculum carefully 'peeled' off. Once removed the operculum was mounted on the cutting stage, striate cortex facing upwards and cut in the plane parallel to the surface of the cortex. Thus the cutting plane is parallel to the electrode penetration. Flat mounted sections were usually

stained for cytochrome oxidase only so that the blobs in the striate cortex and the stripes in V2 could be visualized and reconstructed with respect to the electrode track.

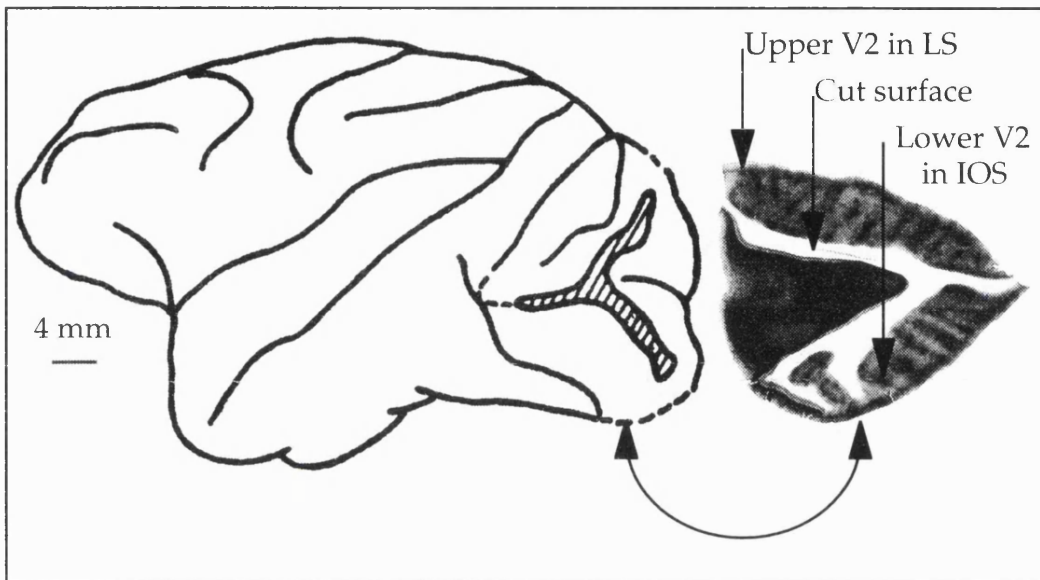


Figure 11.

The operculum shown removed and folded back to expose the banks of the lunate, calcarine and inferior occipital sulci. Once removed, it is sectioned in the plane of the paper.

### Cortical reconstructions

Once the histology was finished, the HRP sections were drawn at 30x magnification under a drawing tube attached to a cross polarising microscope (Zeiss). A contour line was drawn through layer 4 of each section, and the patches of HRP transport and injection site were marked on. The density of the transported HRP was given a value from 1 to 4. Since the quality of the stain and the amount of transport can vary significantly from injection to injection, these values were therefore dependent on the overall range of transport densities in a particular brain.

Figure 12 shows part of an horizontal HRP stained section of the fundus of the lunate sulcus seen under cross polarization microscopy. The cortex is seen as black, white matter is grey and HRP is seen as white patches of stained cells or terminals in the cortical layers. The section's corresponding drawing is shown below the photograph; the numbers 1 to 4 denote the HRP density and the larger numbers are the markers used to align sections, "Inj" is the injection site and "Dif" is the area of diffused HRP surrounding it. Note, that just the area of label, not the details of laminar distribution are shown.

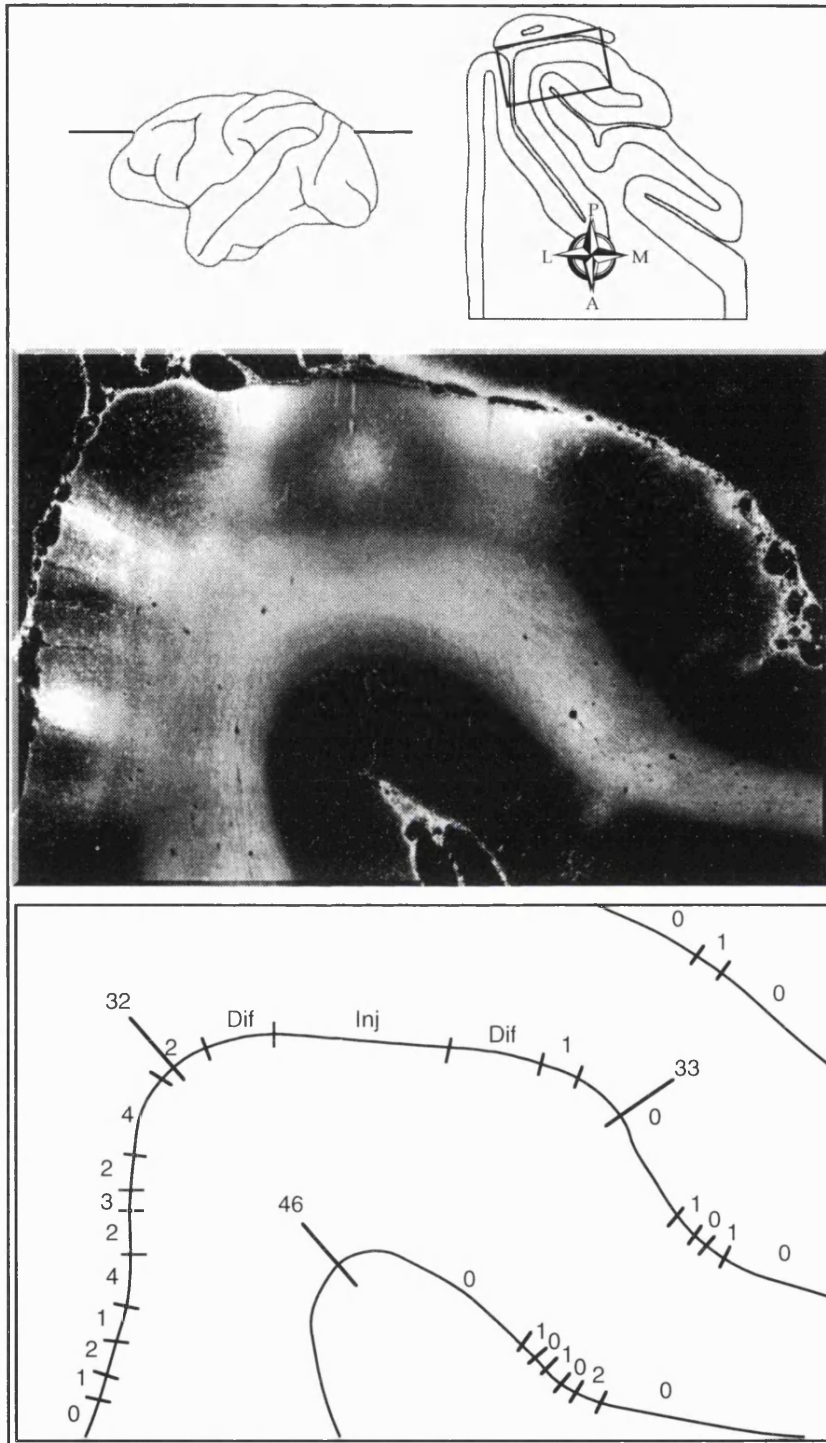


Figure 12.

A photograph of the part of a section shown as boxed in the single section diagram above. The photograph is taken with cross polarized light so that areas containing HRP injection and filled cells or terminals show up as lighter patches. Below the photograph is the drawing of the section made for reconstruction purposes. On the contour line that represents layer 4, the densities of HRP and the injection site are marked. Also shown are marker numbers, assigned to characteristic parts of the section.

The drawings had marker numbers added at particular points (fundi of sulci, crowns of gyri, etc.) and were digitized on a digitising palette and stored on the hard disk of a computer (Sun Spark work station). The computer program stacked all the sections and aligning them using their markers to form a complete three dimensional reconstruction of the brain with the HRP densities shown in a different colour (Romaya and Zeki 1985). The reconstruction could be rotated and resectioned in any plane to show the patches of HRP transport that would otherwise have been hidden within the sulci.

Figure 13 (overleaf) is an example of such a reconstruction with 2 coronal sections taken through the occipital lobe and 2 horizontal sections shown. The coronal sections are made up of a number of dots, each representing an intersection of the virtual cutting plane and a section outline.

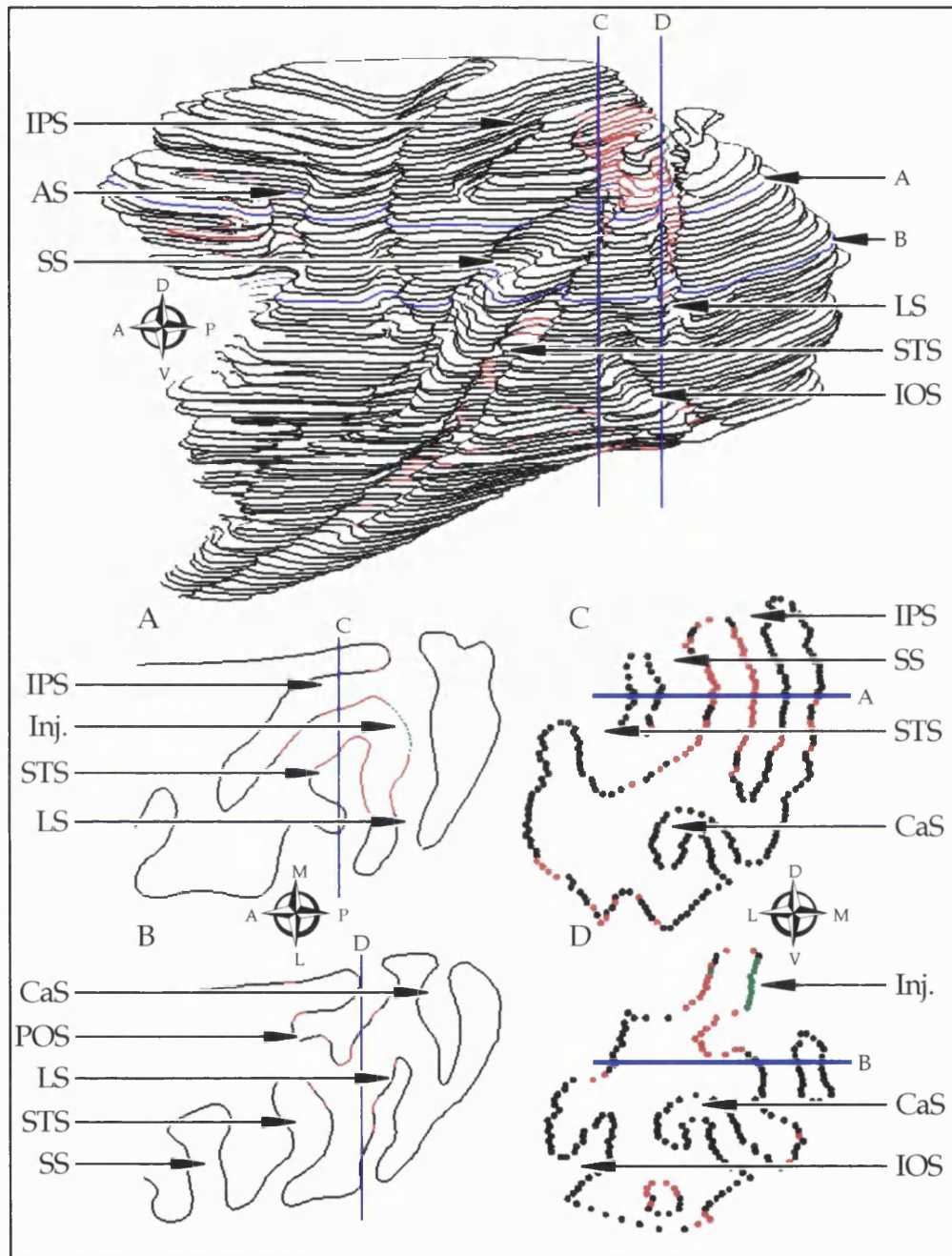


Figure 13.

A three dimensional reconstruction of the macaque brain made up of stacked drawings of many horizontal sections. Two horizontal sections (A and B) and two coronal sections (C and D) made from the reconstruction showing the areas of WGA-HRP transport are also shown.

Abbreviations are as follows:

AS = Arcuate sulcus. CaS = Calcarine sulcus. Inj. = Injection site. IOS = Inferior occipital sulcus. IPS = Intra parietal sulcus. LS = Lunate sulcus. OTS = Occipito temporal sulcus. POS = Posterior occipital sulcus. SS = Sylvian sulcus. STS = Superior temporal sulcus.

The injection site is shown in green and areas of transported WGA-HRP are shown in red. Blue lines represent the planes of sections.

Also using the Sun computer programmed to create these reconstructions it was possible to "flatten" an area of cortex, representing it in two dimensions by removing a part of each section and straightening the contour lines to expose areas hidden in the depths of sulci (Van Essen and Zeki 1978). These straight lines were then stacked and aligned with respect to one of the markers, e.g. the fundus of a particular sulcus. Since the markers represent features that are common to a number of sections, they were joined with dorso-ventral lines. The outlines of the sections were not shown on 2D reconstructions but the HRP transport was represented by dots of different density and the injection site by solid bars. Both 2D and 3D reconstructions are useful for displaying and examining the distribution of label in a brain. The process of flattening the cortex to produce a 2D reconstruction introduced a number of distortions: since it is not possible to transform a curved surface into a completely flat one, a degree of horizontal misalignment is introduced dependent upon the difference in curvature from one section outline to the next. Also, areas adjacent in the brain may appear separated in a 2D reconstruction. For example, the crowns of two adjacent gyri, when flattened, will have the entire area of the sulcus that divides them placed in-between one another. Although 3D reconstructions do not carry as many potentially misleading distortions as 2D reconstructions they do not show areas of the brain that are normally hidden from view, i.e. areas within sulci.

Figure 14 is an example of a 2D reconstruction of the superior temporal sulcus (STS), lunate sulcus (LS) and inferior occipital sulcus (IOS) of the left hemisphere of an HRP injected brain. HRP transport is represented by dots of varying density and the injection site is the black area on the anterior bank of the lunate sulcus. The shaded areas

represent cortex inside sulci and the white areas are on the surface of the brain. The lines are drawn through markers from many sections.

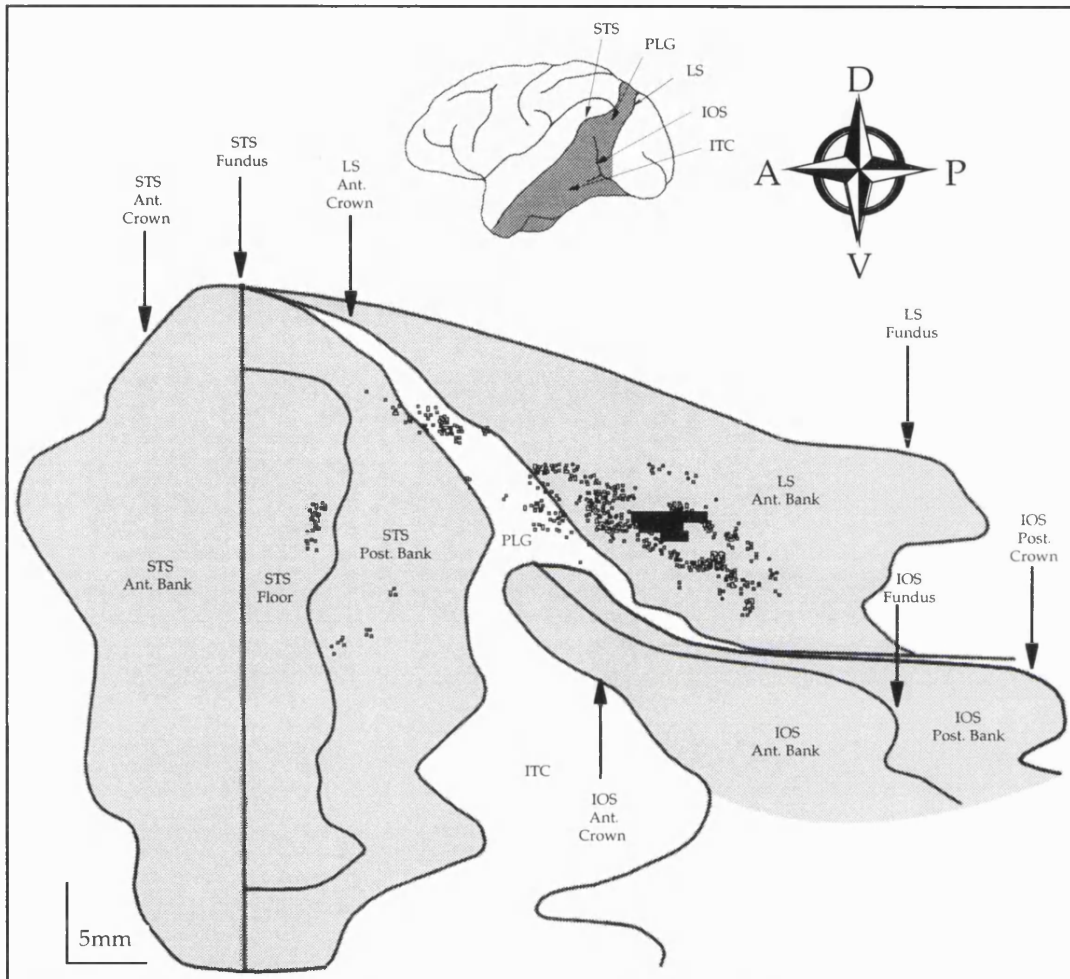


Figure 14.

A two dimensional reconstruction of part of the macaque visual cortex. The density of the dots represents the density of HRP transport, and the solid black area is the HRP injection site. Shaded areas are the banks of sulci and white areas are on the surface of the brain.

## **Results:**

The results are divided into two sections: the first deals with physiological recordings from prestriate areas, and the second with the results of anatomical tracing experiments following the injection of WGA-HRP into prestriate visual areas, including the V3 complex.

### **Section 1:**

#### **Electrophysiological data:**

The results presented here are from a total of 24 monkeys which had electrode penetrations made into one or more of the visual areas V1, V2, V3 and V3A. Those cells that were close to the V3-V3A border were classified as V3/A and included in the V3 complex population only. The total numbers of cells tested in V1, V2, V3 and V3A tested for disparity were 30, 226, 100 and 8 respectively, with 121 in the V3 complex and 76 whose visual area could not be classified. Both the properties of individual cells, and the functional architecture of their areas were investigated. The properties of single cells in a particular visual area are of significance because they show what attributes of the visual scene is emphasized in it, and therefore what visual modality it is specialized for. The functional organization of a particular area can be investigated by finding out how these single cell properties change with changing location within an area following careful reconstruction of the electrode track.

In the visual cortex there are many examples of functional organization, e.g. the ocular dominance columns and orientation columns in V1 (Hubel and Wiesel 1968; Hubel and Wiesel 1977) and the

stripes in V2 (Tootell *et al.* 1983; DeYoe and Van Essen 1985; Zeki and Shipp 1987). A common property of the visual system (and the entire brain) is the grouping of cells with similar properties into anatomical modules (Mountcastle 1957; Hubel and Wiesel 1977). One would expect such a grouping to have functional importance, whether it is for interaction between neighbouring cells with similar properties, or the clustering of functional properties for distribution to, or input from, other areas. In order to investigate both the properties of single cells and the functional organization of these properties within an area, recordings were made during long penetrations through the prestriate cortex.

#### Allocation of cells to visual areas

Before the results can be presented, it is important that the criteria used for identification of the various visual areas is shown. In previous studies, the boundaries of V3 and V3A have been demonstrated by callosal section and the placing of small lesions in the vertical meridian representation of V1 (Cragg 1969; Zeki 1969; Zeki 1970; Zeki and Sandeman 1976; Zeki 1978b) (see introduction for a more detailed description of these studies). When the electrode track is reconstructed and the positions of the sampled cells determined, their location within a visual area can usually be determined by comparison of the section with respect to the pattern of degenerating fibres following a corpus callosum transection or the degeneration following striate lesions, in a section taken at a similar level (see figure 15). This is true for cells that are well away from the boundaries. Cells that are close to, or lie on, boundaries between visual areas are harder to place in one area or another. The border between V1 and V2 is very clear in stained sections due to the stripe of Gennari, so cells can easily be classified as striate or prestriate. The border between V2 and V3 lies in the posterior bank of the lunate

sulcus and the horizontal meridian of both of these areas is represented at their border with each other (Zeki and Sandeman 1976; Zeki 1977b). Thus, cells located on the posterior bank of the lunate sulcus with their receptive fields at the horizontal meridian, were usually not used in the cell sample due to their ambiguous location. Cells' visual areas were not determined by examination of their response properties. Cells close to the V3/V3A boundary were classified as V3/A, and included in the V3 complex cell population but not V3 or V3A populations. Due to the electrode approach used in these experiments, no cells located at, or near to, the V3A/V4 border were recorded from.

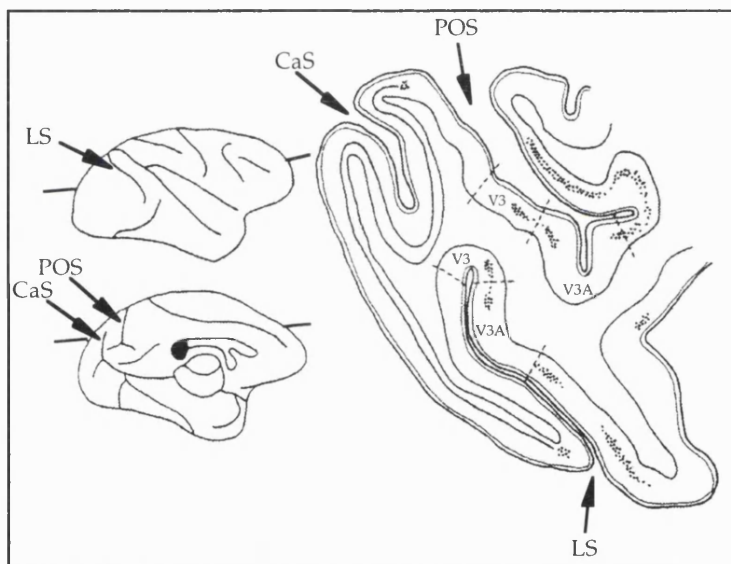


Figure 15.

Tracing of a horizontal section, taken at the level indicated on the surface drawings of the medial and lateral sides of the brain. The dots in the cortex represent the degeneration following transection of the splenium of the corpus callosum. Continuous line represents striate cortex (V1). The positions of V3 and V3A, in both the lunate and parieto-occipital sulci, are shown and their boundaries are drawn in interrupted lines. The two portions of each area are continuous across the annectant gyrus. CaS = calcarine sulcus, LS = lunate sulcus and POS = parieto-occipital sulcus. (Taken from Zeki, 1978a)

## The properties of cells in the V3 complex

### a) Orientation selectivity tuning

One of the most fundamental properties of cells in the visual cortex is their selectivity for the orientation of a stimulus. Their classification was originally done by using a hand held projector to pass a slit of light over the receptive field and the response was judged by the experimenter's auditory system (a highly sensitive apparatus). This method allowed cells to be qualitatively judged to be orientation selective or not, but did not give any quantitative measures of the preferred orientation, the extent or the tightness of tuning. Modern computer based stimulation and recording methods enable orientation tuning curves to be plotted by measuring responses during the in-field period, for the full range of stimulus orientations. Orientation tuning curves can then be plotted and analysed statistically to produce quantitative measures of orientation selectivity. The analysis that has been used in this study compares the orientation tuning curve to a number of mathematically defined models and gives the best fitting model with a measure of how similar that model is to the real data. The tuning characteristics that can be obtained by this analysis are half-width/half-height (*hw/hh*), preferred orientation, indices for orientation and direction tuning and the best fitting model of orientation/direction tuning. A detailed description of the statistical methods employed to analyse orientation and direction tuning curves can be found in appendix A.

A cell's preferred orientation is simply the angle of a luminance contrast bar or line that evokes the maximal response when presented to the cell's receptive field. The *hw/hh* can be calculated from a graph of

orientation versus response, and is a measure of the maximum response peak's width (in degrees) at half its height. The orientation tuning index (o.i.) is a value used to denote the extent of orientation tuning and is calculated by the formula 
$$o.i. = 1 - \frac{\{\text{Peak} - 90^\circ\} - \text{baseline}}{\text{Peak} - \text{baseline}}$$
 where "peak" is the response at the preferred orientation, "peak - 90°" is the response at an orientation 90° (perpendicular) to the preferred orientation and "baseline" is the background firing rate of the cell when no stimulus is present (DeYoe and Van Essen 1985; Burkhalter and Van Essen 1986; Felleman and Van Essen 1987). Orientation indices are useful because they provide a quantitative measure of the degree of tuning and are used to categorize cells into selective, biased or untuned categories. Cells with values of o.i. <0.5 are considered unselective, cells with values 0.5 and <0.7 will be labelled "biased" and cells whose indices are 0.7 will be considered "selective". Because this method of classification is based on a simple mathematical formula, it is prone to giving erroneous results when applied to cells with non-standard orientation response profiles. Not all cells in the visual cortex have tidy orientation tuning curves with two peaks 180° to each other; the calculation of o.i. assumes this to be the case. If a cell is inhibited by stimuli perpendicular to the preferred orientation, the o.i. will always be a number greater than 1 regardless of the cell's excitatory response to the preferred stimulus. These factors justify the use of care and judgement in applying these indices (including the analogous direction and colour indices) rather than their blind employment and reliance upon.

Figure 16 is the spike histogram and tuning curve derived from an orientation test on a single cell. The spike histogram is a plot of the number of spikes per second, displayed in 100 ms bins, as the stimulus passed over the monitor including the receptive field. The central shaded

portion of this histogram represents the period during which the stimulus occupied the receptive field of the cell. Thus, it is this portion of the histogram (the in-field period) from which the mean response is calculated. This cell is orientation selective for a moving vertical bar ( $0^\circ$  and  $180^\circ$ ) with a *hwhh* of  $24^\circ$ . The tuning curve is shown as a polar plot;  $\theta$  represents the angular orientation of the stimulus in degrees (a luminance contrast bar or line) and  $r$  represents the response to that stimulus measured in spikes per second.

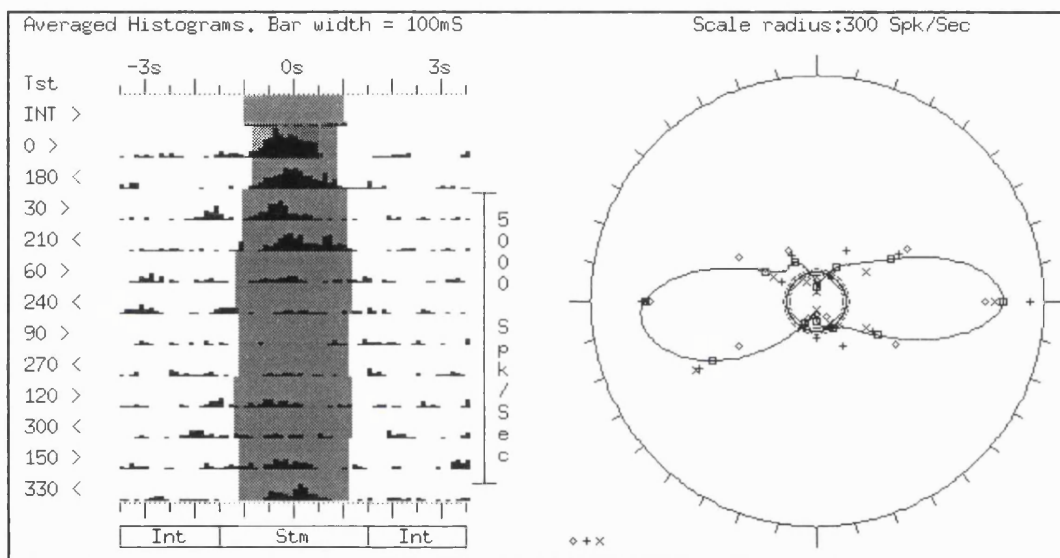


Figure 16.

Spike histogram and polar plot of the results of an orientation test on a single cell. Each row in the histogram represents the passage of a bar at the stated orientation. The response is shown as an histogram of spikes per second in 100 ms bins. The central shaded area is the in-field period. The polar plot illustrates response ( $r$ ) against bar orientation in degrees ( $\theta$ ). The central circle is the intertrial spike rate. The curve was produced by finding the mean (shown as squares) of 3 trials (shown as symbols:  $\square$ ,  $+$  and  $\times$ ).

The number of trials necessary to produce a record sufficiently devoid of noise depended on the response behaviour of the cell and its background discharge rate; some cells respond reliably every time a stimulus is presented but others behave more erratically, their responses varying across presentations. Usually three or four trials were sufficient, but with particularly noisy cells or those that gave inconsistent responses

as many as 10 trials were used, each consisting of a full set of orientation presentations.

In this study, out of all the cells recorded in the V3 complex, 80% were found to be orientation selective (as qualitatively judged by the experimenter). When this figure is compared to the percentage for V2 (72%) and previous studies of V4 in this laboratory (15% - classified with the same criteria) it can be seen that the V3 complex appears to be an area specialized for stimulus orientation. Different studies of the V3 complex have produced different values for the proportion of orientation selective cells, ranging from 33% (Baizer 1982) to 88% (Zeki 1978c). The reason for the discrepancy between studies is probably partly due to the criteria for classifying a cell as orientation selective or not. In order to reconcile this difference, the V3 complex cells from this study will be classified in a number of different ways, some of which have been used by other people, who have arrived at a variety of different proportions of orientation selective cells in that area.

#### *Quantitative methods:*

With use of the orientation index as a criteria for selectivity Felleman and Van Essen (1987), found that 76% (19/25) of V3 cells in the paralysed monkey were orientation selective.

Application of the o.i. 0.7 criteria to this study's population of V3 cells, produces a figure of 83% selective.

The use of the best model analysis as a criteria for orientation selectivity (present studies, see appendix A), Produces the proportions: 19%, 37%, 43%, 14% of C1 type cells (two equal peaks 180° apart) in the areas V1, V2, the V3 complex, and V4 respectively.

*Qualitative methods:*

"Cells were classified as orientation selective if, when tested with slits, bars and edges, they showed an orientation preference and did not respond to the orthogonal orientation." (Zeki 1978c). Zeki found that 88% (220/250) of V3 cells and 81.2% (203/250) of V3A cells in the paralysed monkey were orientation selective.

"Sensitivity to the orientation of a stationary elongated bar/slit" (Baizer 1982). Using this criteria, Baizer got the figure of 33% (25/75) for orientation selective V3 cells in the awake behaving monkey.

Most of the above criteria yield similar results for the proportions of orientation selective cells in the V3 complex. The exception to this is Baizer's study (1982), where a significantly smaller proportion of cells were found to be orientation selective. The reason for this is probably due to the less appropriate criteria used for classification, cells only being classified as orientation selective if they displayed orientation preferences in response to stationary stimuli. There is no reason to suppose that a cell is only orientation selective if it responds to stationary stimuli. Some cells respond to optimally oriented moving stimuli but they are not tuned to the direction of movement *par se*, but the orientation of the stimulus. Thus, these cells will respond equally to bars moving in directions 180° apart. A method of discriminating these cells from direction selective cells is to present them with textured bar stimuli moving on a textured background. This stimuli enables one to change the direction of the bar's motion while keeping its orientation constant. An orientation selective cell will respond to its optimal orientation irrespective of the direction of the textured elements that define the bar.

As mentioned previously, the half-width-half-height (*hwhh*) of a cell's orientation tuning curve provides a measure of its width of tuning, smaller *hwghs* denote tighter tuning. Figure 17 shows the population histograms of *hwgh* for cells in V2, the V3 complex and V4. These population distribution histograms show that V2 and the V3 complex contain more cells that are tightly tuned to orientation than area V4. There is little difference between the tightness of tuning of cells in V2 and the V3 complex. However, the V3 complex contains a higher proportion of orientation selective cells than V2.

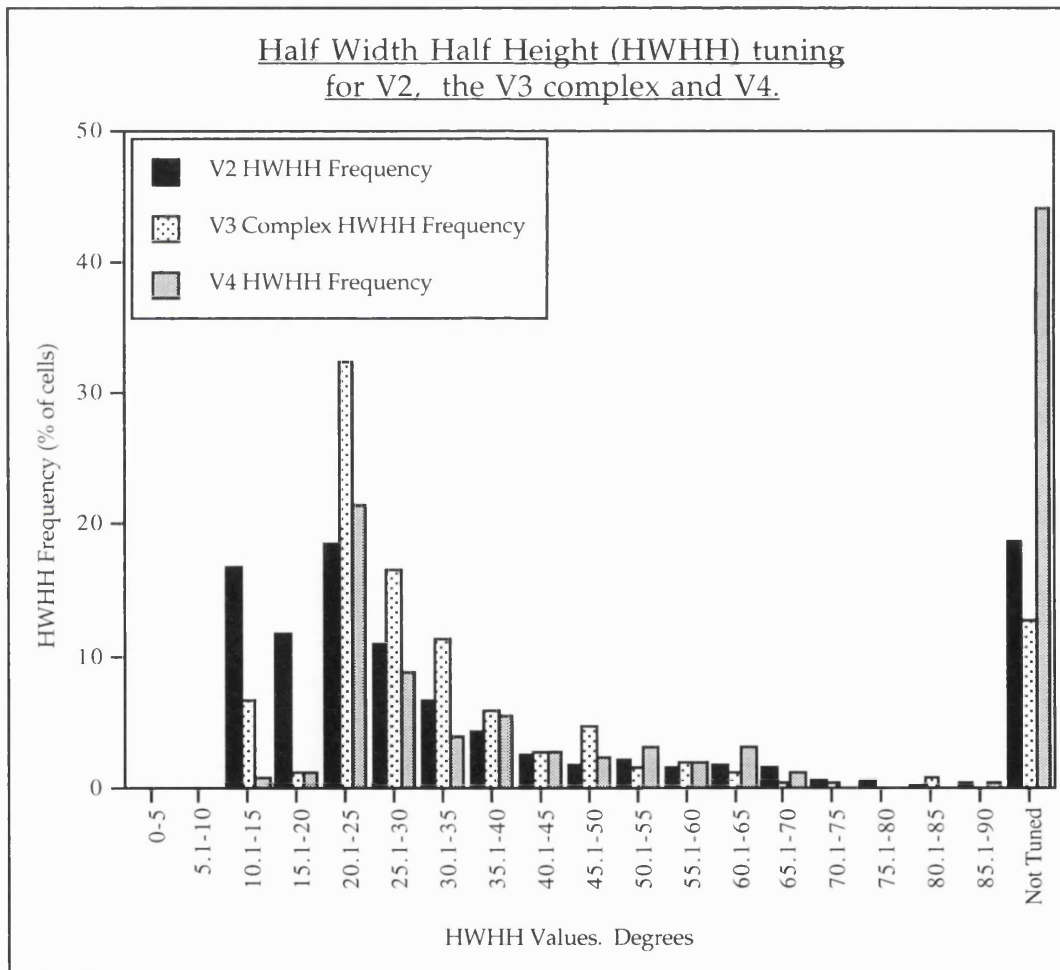


Figure 17.

Population histogram of half width half height (*hwgh*), in degrees, of orientation tuning, for cells in V2, the V3 complex (V3 and V3A) and V4.

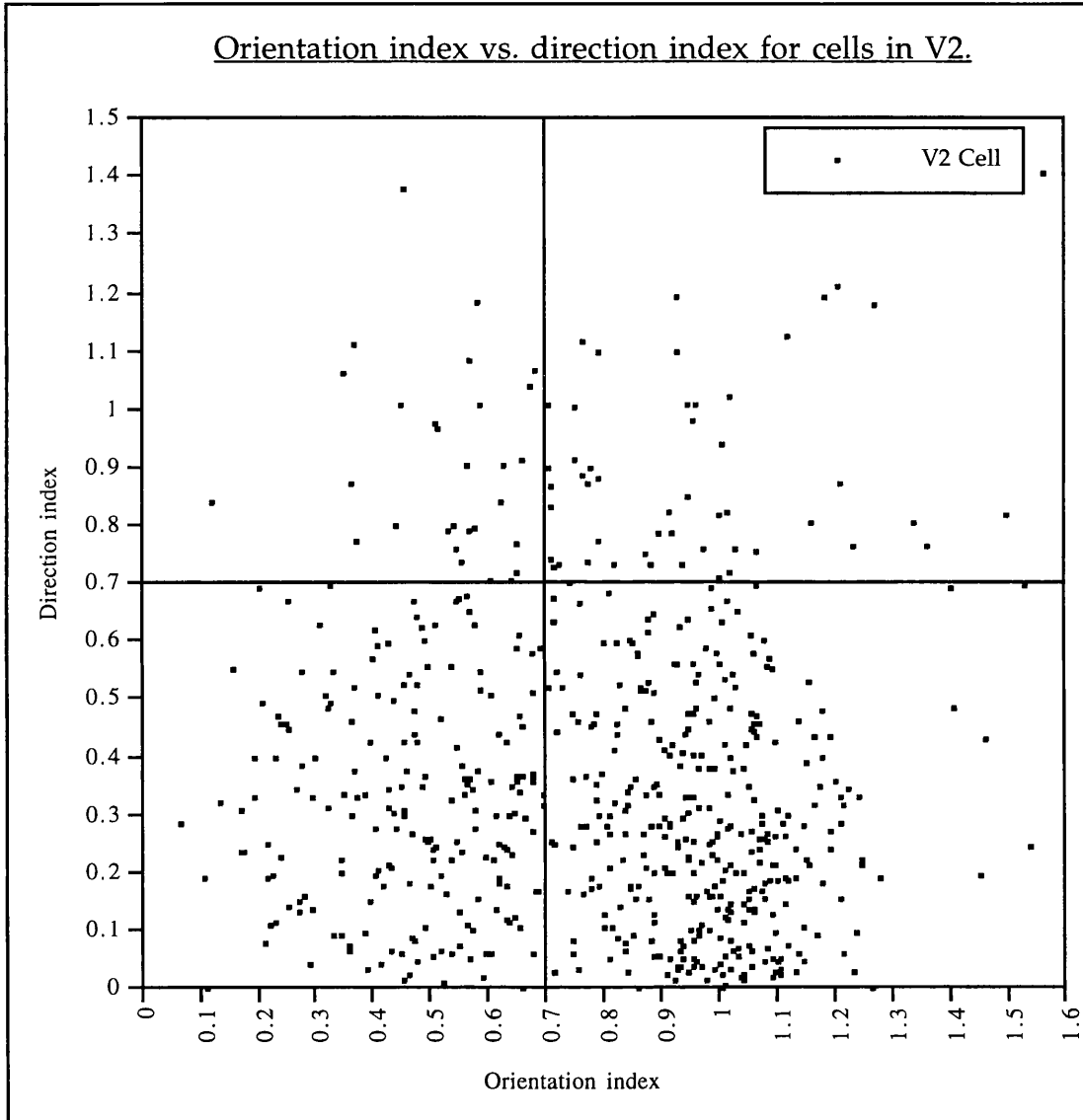
## b) Direction selectivity

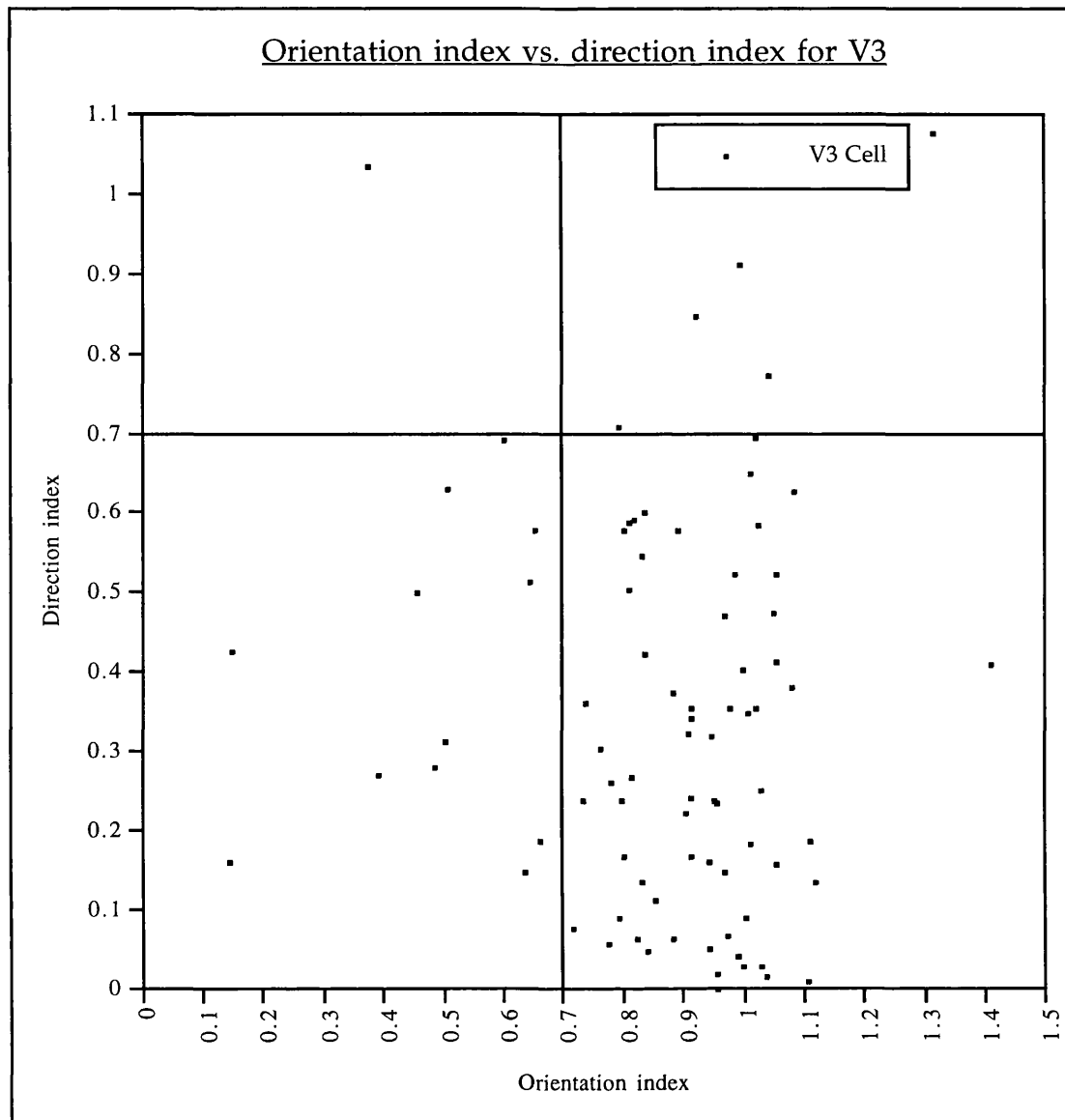
Direction selective cells are common in area V5 of the macaque, where they constitute the overwhelming majority of cells in that area (Zeki 1974b; Gattass and Gross 1981; Van Essen *et al.* 1981; Albright 1984). However, a smaller percentage of the V3 complex's cells are also direction selective or biased. Previous studies have found this proportion to range between 12% (Zeki 1978c) and 40% (Felleman and Van Essen 1987). The former study used qualitative criteria for the judgement of direction selectivity and the latter, the direction index, analogous to the previously mentioned orientation index. The formula for the direction index (d.i.) is  $d.i. = 1 - \frac{\{Best - 180^\circ\} - baseline}{Best - baseline}$  where "Best" is the response to the preferred direction, and "Best -180°" is the response to the direction orthogonal to the preferred direction. Cells with values of d.i. 0.5 and <0.7 will be considered "biased" and values 0.7 denote directional selectivity. Like the orientation index, the direction index is based on an arbitrary threshold and must be applied with caution. Figure 18 shows scatter graphs of d.i. plotted against o.i. This graph format allows one to see both the orientation and direction selectivity tuning of a population of cells. Graphs are shown for each of the areas V2, V3, V3A and V4.

Figure 18 a-d.

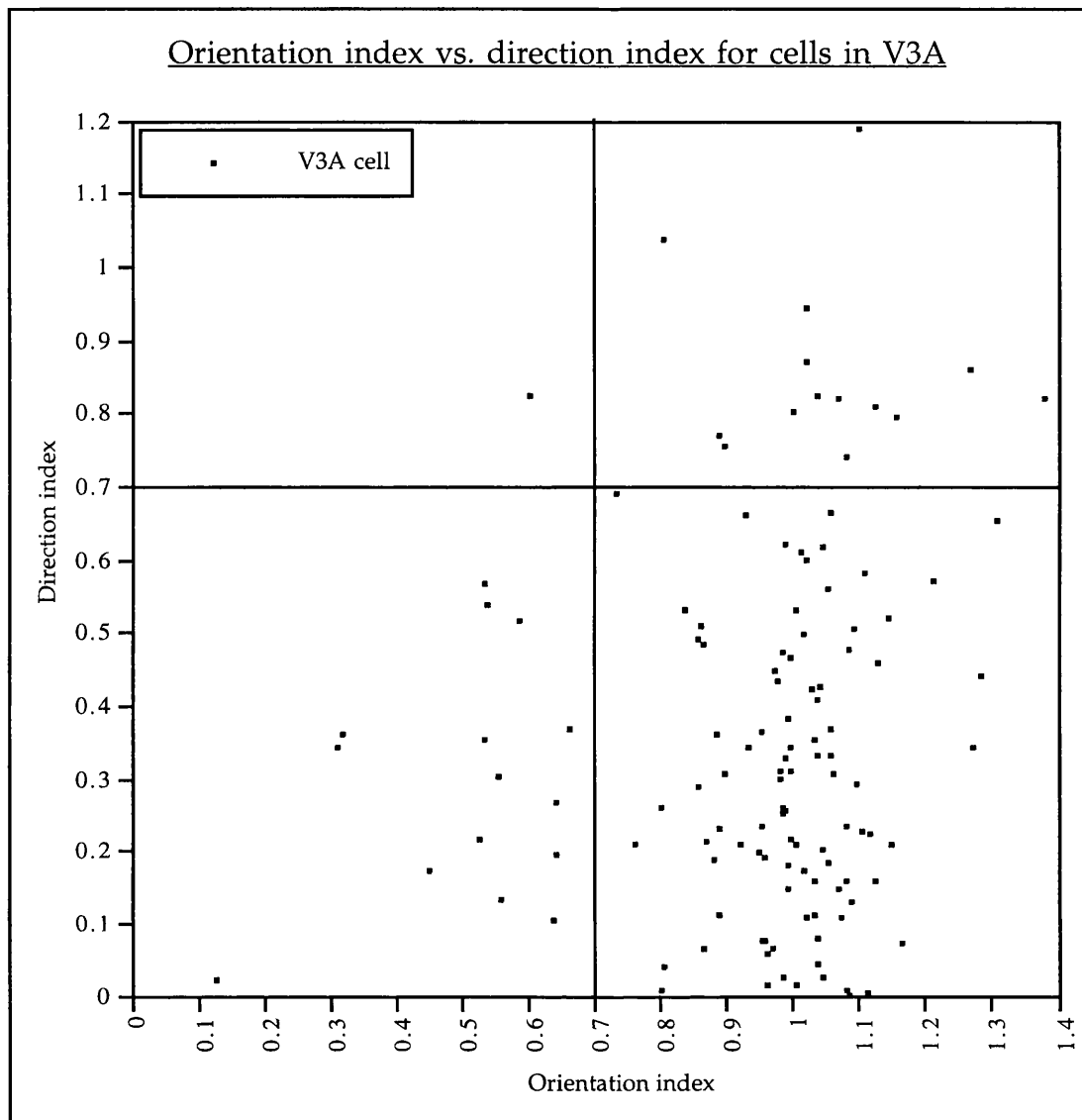
Scatter plots of Orientation index and direction index for cells in each of the areas V2, V3, V3A and V4. The lines drawn at an index value of 0.7 represent the point at which cells are said to be "selective". Thus, cells with index values above these lines are orientation selective, direction selective or both.

18a.

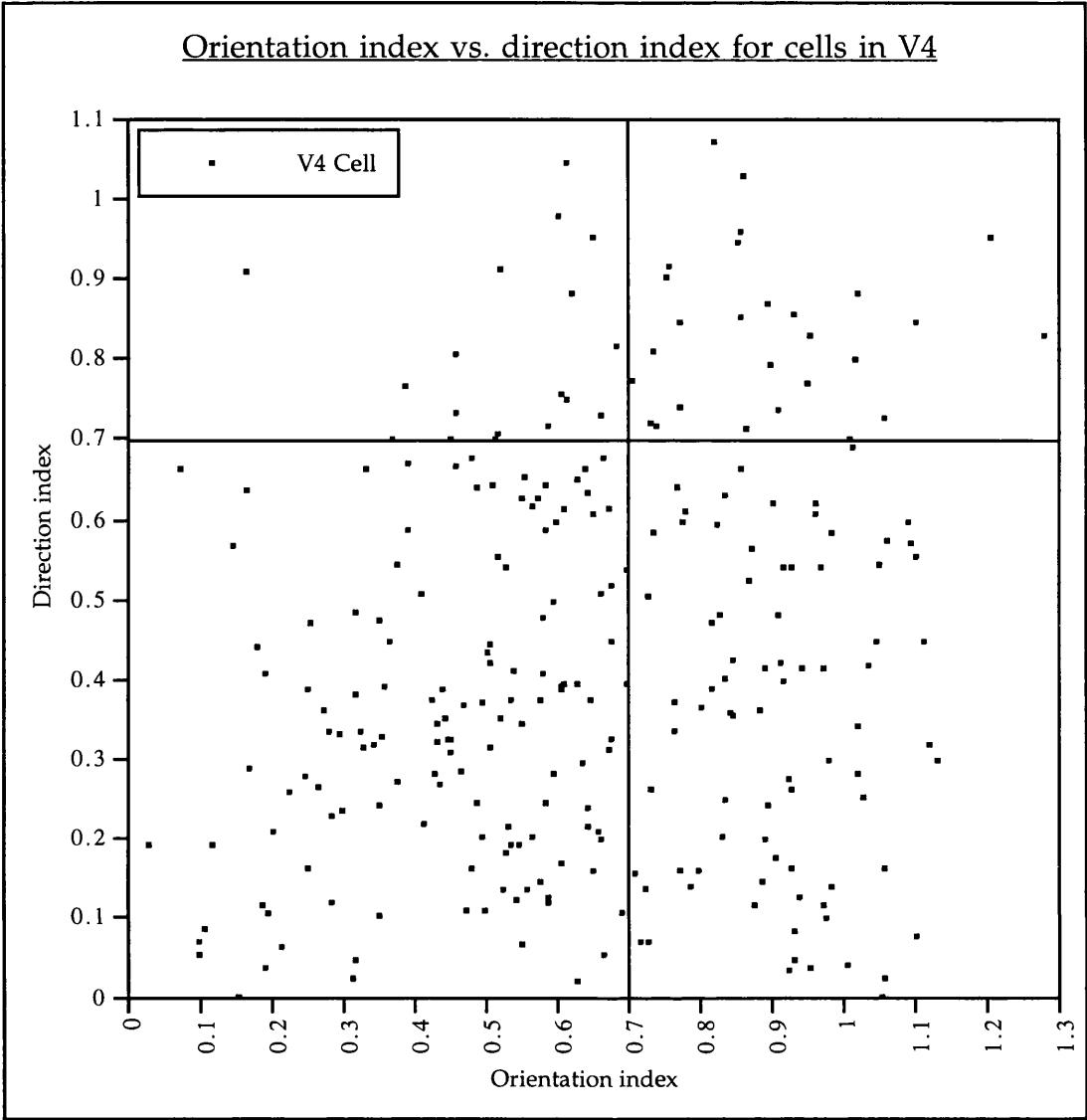




18c.



18d.

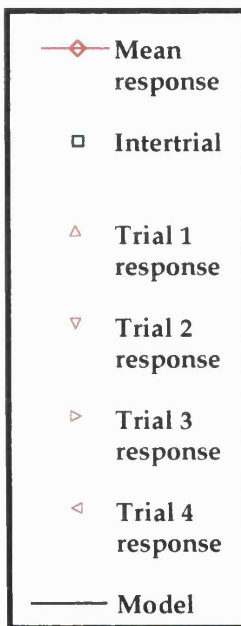


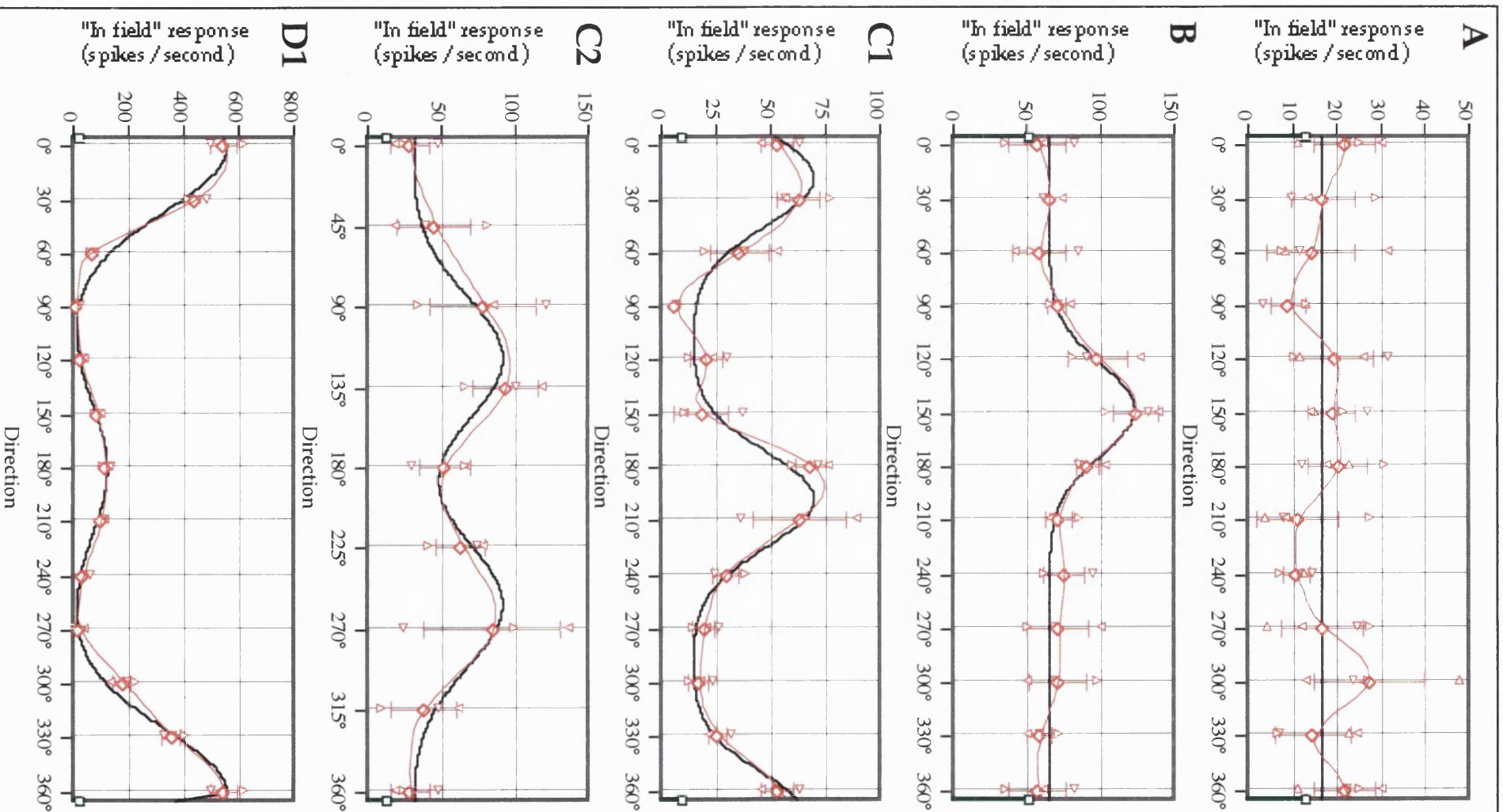
Another method of categorising the orientation and direction selectivity of cells is to compare the cells' orientation tuning curves with a number of binomial models. This method of analysis was developed by J. Romaya, working in this laboratory. A detailed description of the statistical method of this comparison may be found in appendix A. The comparison enables one to classify cells into one of 10 groups. The groups are outlined in figure 19 overleaf:

Figure 19.

Orientation tuning curves to illustrate the 10 models of types of orientation tuned cell. The model curves have been fitted to experimental data. The types of model are as follows:

- A. Flat distribution.
- B. One peak.
- C1. Two similar peaks  $180^\circ$  apart.
- C2. Two similar peaks not  $180^\circ$  apart.
- D1. Two peaks of unequal height, equal *hwhh* and  $180^\circ$  apart.
- D2. Two peaks of equal height, unequal *hwhh* and  $180^\circ$  apart.
- E1. Two peaks of unequal height, unequal *hwhh* and  $180^\circ$  apart.
- E2. Two peaks of equal height, unequal *hwhh* and not  $180^\circ$  apart.
- E3. Two peaks of unequal height, equal *hwhh* and not  $180^\circ$  apart.
- E4. Two peaks of unequal height, unequal *hwhh* and not  $180^\circ$  apart.





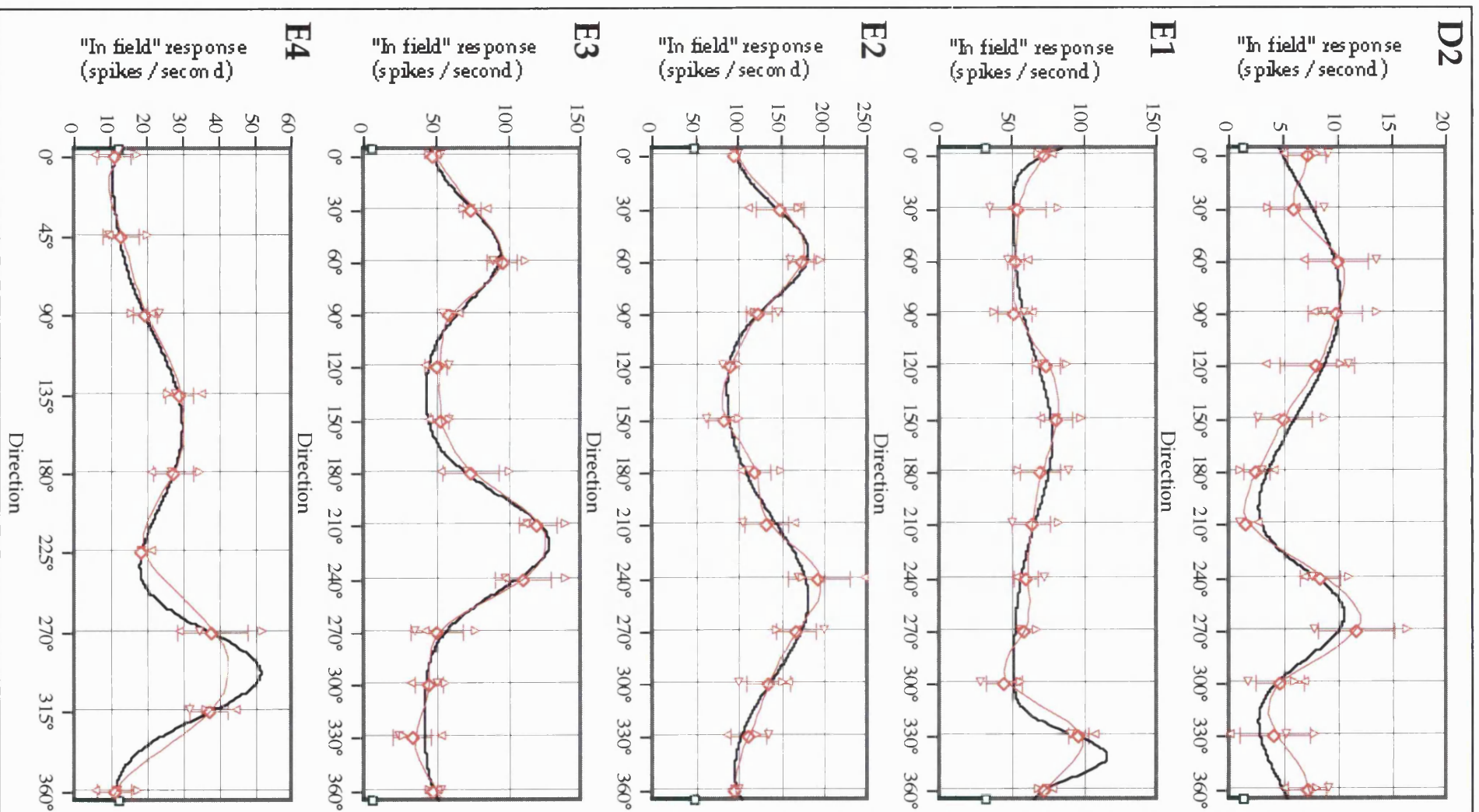


Figure 20 is a graph of the frequency of each of the 10 models for cells in V2, the V3 complex and V4.

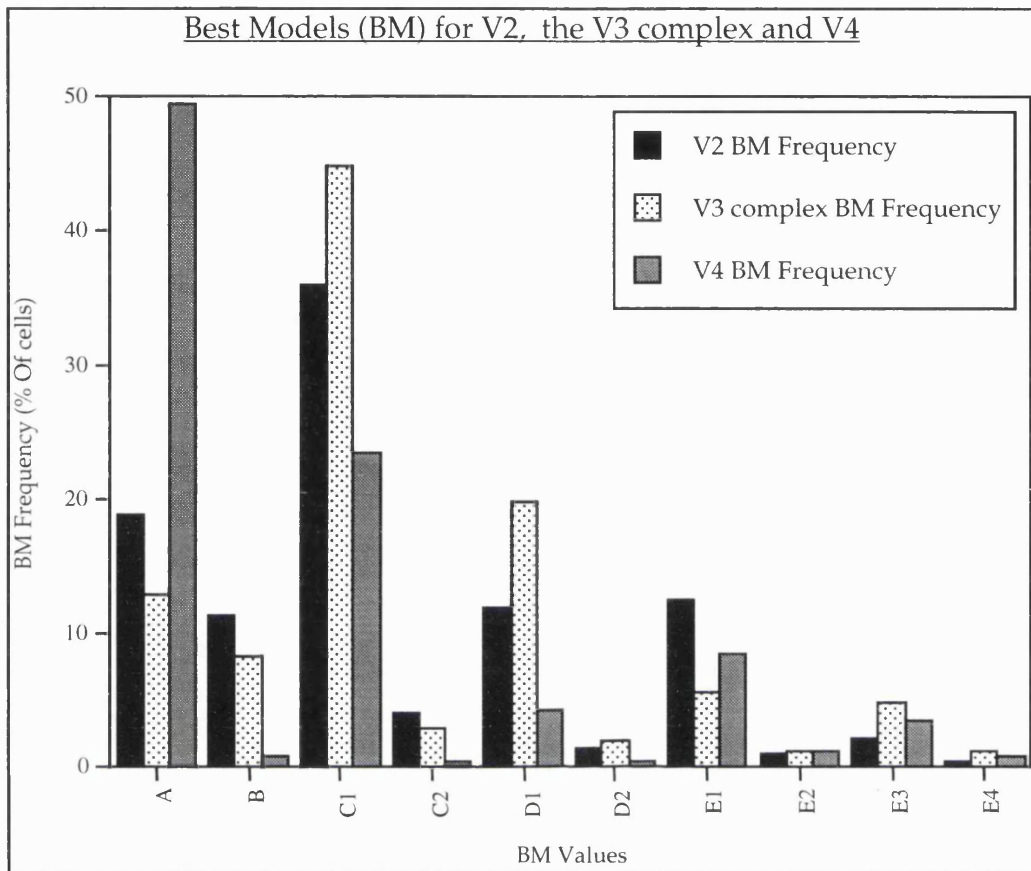


Figure 20.

Graph to show the relative frequencies of each of the 10 orientation/direction tuning models in the areas V2, the V3 complex and V4.

- A Flat distribution (Unselective).
- B One peak (direction selective).
- C1 Two similar peaks 180° apart (classical orientation selective).
- C2 Two similar peaks not 180° apart (bi-direction).
- D1 Two peaks of unequal height, equal *hw* and 180° apart (orientation selective with direction bias)
- D2 Two peaks of equal height, unequal *hw* and 180° apart (orientation selective, direction anomaly).
- E1 Two peaks of unequal height, unequal *hw* and 180° apart (orientation selective, direction anomaly).
- E2 Two peaks of equal height, unequal *hw* and not 180° apart (bi-direction).
- E3 Two peaks of unequal height, equal *hw* and not 180° apart (bi-direction).
- E4 Two peaks of unequal height, unequal *hw* and not 180° apart (bi-direction).

The use of these models to classify cells is advantageous because it allows one to take the shape of the whole orientation tuning curve into

account, rather than just the best and orthogonal responses (as used in the o.i. and d.i. indexes). The variety of models also introduces the idea that cells do not simply fall into one of three groups: Untuned, direction selective and orientation selective, but rather that there are a number of response profiles which cannot be immediately classified as direction or orientation selective. An example of this is a cell fitting model E1, i.e. a cell with two equal response peaks separated by  $180^\circ$  but not of similar *hwhh*. This type of cell must be able to differentiate between the two directions of the stimulus along an axis because it has an unequal tightness of tuning for each. However, it could not be classified as direction selective because the magnitude of both responses is similar.

### c) Wavelength selectivity

Most cells recorded from in the V3 complex were tested for wavelength selectivity by presentation of a number of roughly isoluminant bars over the receptive field at the cells preferred orientation. No examples of qualitatively judged wavelength selective cells were found in this study of the V3 complex. However, some cells were found that had wavelength preferences, i.e. their responses to different wavelengths were not identical but some wavelengths provoked a slightly better response than others. Previous studies are divided on the subject of wavelength selective cells' presence in the V3 complex, most have failed to find wavelength cells in V3 using qualitative criteria (Van Essen and Zeki 1978; Zeki 1978b; Baizer 1982; Zeki 1983). Others (Burkhalter *et al.* 1986; Felleman and Van Essen 1987) give a figure of about 20% wavelength selective cells in V3. These two studies used the colour index (c.i.) as criteria for assessing wavelength selectivity. This index, similar to the direction and orientation indices, compares the responses to the best and worst colours using the formula:

$c.i. = 1 - \frac{(\text{Response to least effective monochromatic wavelength} - \text{background})}{(\text{Response to most effective monochromatic wavelength} - \text{background})}$ . Like the

o.i. and d.i., cells with values greater than 0.7 are said to be selective and values between 0.5 and 0.7 denote a colour bias. It seems that when cells are judged qualitatively, wavelength selectivity is not assigned to V3 complex cells, but when examined quantitatively (using the colour index) a small but significant number of cells are judged to be wavelength selective. The observation that a cell produces a larger response to one wavelength over another does not necessarily denote that the cell is part of the colour processing system because many cells in the visual cortex get an unbalanced input from the different types of cone. In order to be qualitatively judged as wavelength selective, a cell should display an active colour opponency, either a centre surround opponency or a specific inhibition to some wavelengths with excitation by others. These are the properties that are associated with the colour processing machinery in the visual cortex. No cells have been found in the V3 complex that display this type of wavelength selectivity by any study, suggesting that the V3 complex is not actively involved in the processing of colour.

In order to assess the wavelength selectivities of V3 complex cells, the colour index (c.i.) was applied to the cells tested in this study. On initial inspection, about 15% of cells were found to have c.i. 0.7 and would be classified as wavelength selective by the index criteria. However, on closer examination, many of these cells were found to have very variable responses and/or high background firing rates. If the background firing rate is high, the difference between the best and worst response to the preferred and non-preferred wavelengths does not have to be very large for the cell to be assigned a high index. Since the

responses of cells in the cortex usually have a certain amount of variability when presented with identical stimuli, this can often happen if the index is applied without close examination of the responses.

Figure 21 is an example of one of the few wavelength selective cells found in V3. It was qualitatively judged "wavelength biased" and has a c.i. of 0.82. Although this cell is one of the most wavelength 'selective' found in the V3 complex, it responds to all colours (green best and red least) and its response to white is very similar to its best chromatic response. The wavelength selectivity of this cell (and most other V3 complex cells that displayed wavelength preferences) is characterized by a lack of response to a particular hue (in this case red), rather than the specificity for a particular wavelength. Use of the colour index does not take this type of observation into account.

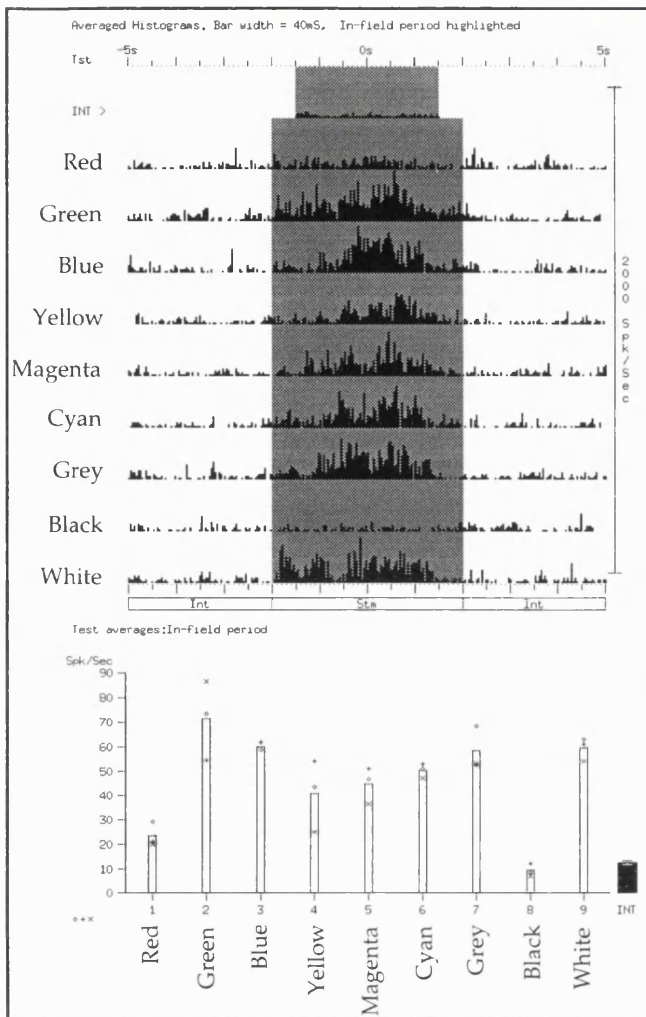


Figure 21.

Spike histogram and (below) average responses to different coloured isoluminant bars passed over the receptive field of a V3 cell. The shaded portion represents the period during which the bar occupied the receptive field; it is this portion that is used to plot the average responses to the different wavelengths.

#### d) Clustering of cells with similar properties

In order to present the types of clustering present in the V3 complex, electrode penetrations are shown, with the properties of cells marked onto them. The types of property that were examined for the characteristic of clustering in the V3 complex are (a) orientation selectivity and (b) direction selectivity.

As mentioned previously, the functional organization of an area can be elucidated by sampling from many cells in that area. If cells are organized into columns of functionally similar cells stretching from the surface of the cortex to the white matter boundary (for instance ocular

dominance columns), then penetrations that are normal to the cortical surface will encounter fewer different types of cell than those running parallel to the cortical surface. This is illustrated for the property of orientation tuning in the V3 complex. Figure 22 shows two penetrations through area V3A. Onto the lines representing the electrode tracks are placed symbols of the preferred orientation. When one makes a tangential penetration through areas V3A and records from successive cells 50-100 $\mu$ m apart, one finds that the orientation preferences of successive cells change gradually and in an orderly manner; a full cycle of orientations occupies about 1mm of cortex (figure 22a). By contrast, when a normal penetration is made through this area and successive cells are recorded from at the same separation, then most cells are found to respond to the same or similar orientations or directions (figure 22b).

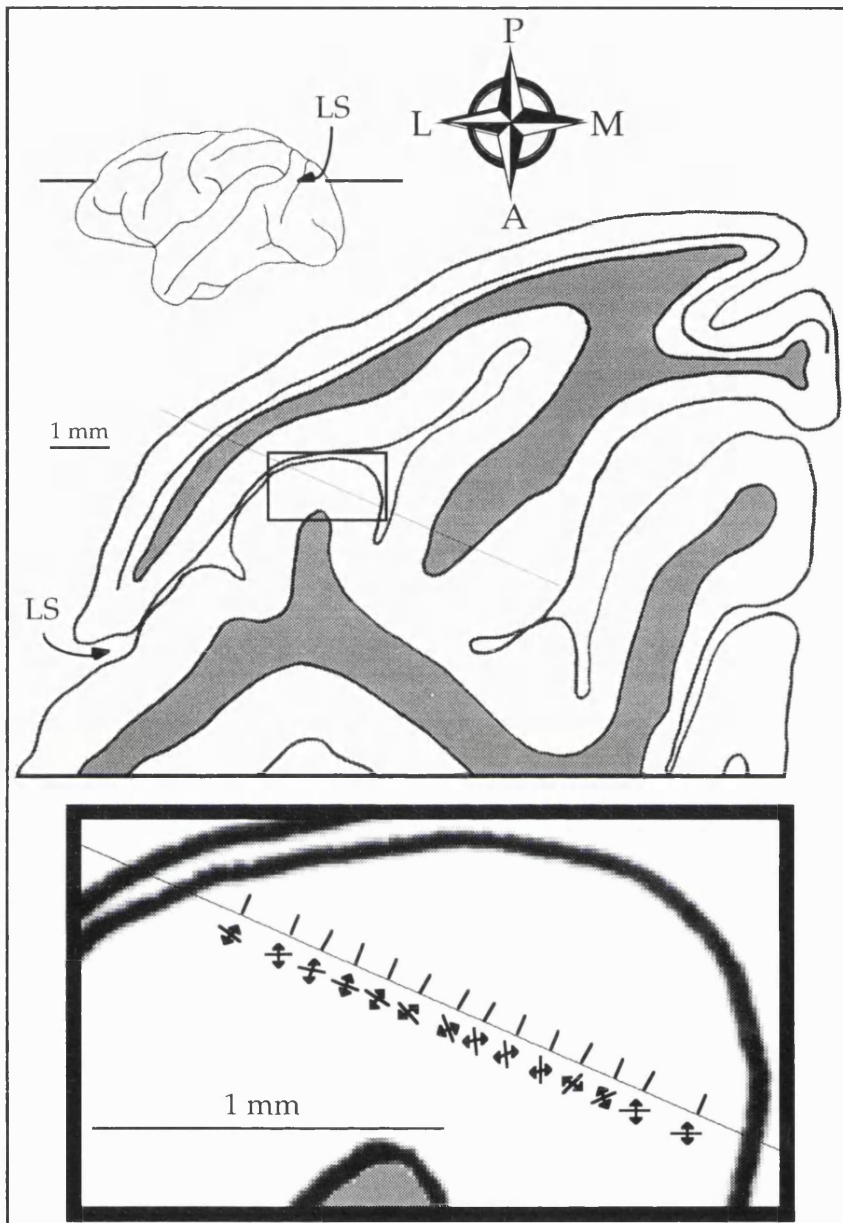


Figure 22a and b (Overleaf).

Electrode penetrations through the cortex at the level indicated in the whole brain pictures. The boxed areas on the horizontal sections are shown at greater magnification and the orientation preferences of the cells recorded from are shown next to the cells' positions. Figure 7a is a tangential penetration through V3A and figure 23b is a normal penetration through the same area.

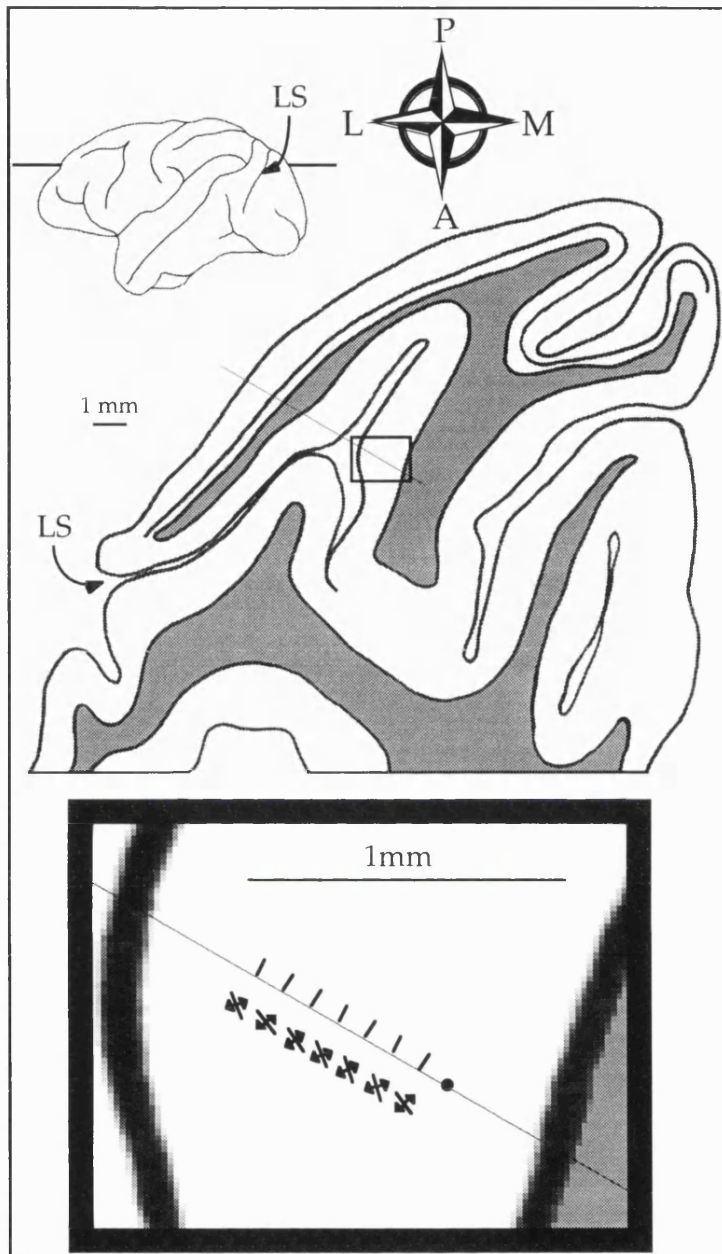


Figure 22b. (See legend to figure 22a.)

#### e) Binocular properties

When cells were first recorded from in the paralysed cat and monkey (Hubel and Wiesel 1959; Hubel and Wiesel 1962; Hubel and Wiesel 1965b; Hubel and Wiesel 1968) the two receptive fields of a binocular cell were often treated separately and not stimulated simultaneously. Thus, Hubel and Wiesel's idea of binocularity was a

comparison of the responses from each eye rather than a comparison of binocular versus monocular responses. Since they were recording from the striate cortex, where cells are organized into ocular dominance columns, this was of little importance at the time. All cells in the prestriate cortex are binocular and most have similar responses from each eye; therefore Hubel and Wiesel's classification of cells is inappropriate there, and a scheme of classification based on the responses of cells to binocular stimulation is more useful.

The binocular interaction histogram was first used by Zeki (1979) to assess the possible involvement of areas in stereoscopic depth analysis. It differs from the ocular dominance histogram of Hubel and Wiesel (1968) in that their histograms were produced by separate stimulation of each eye, whereas these are produced by simultaneous stimulation of both receptive fields. Thus, they reveal the ocular dominance of cells and also their ocular interaction, a property that cannot be assessed in any way other than binocular stimulation. The ocular interaction histogram for a particular visual area may show that an area is involved in binocular vision. For example, a binocular interaction histogram for V1 would show a large number of cells responding only to monocular stimulation whereas the same histogram for a prestriate area will show the majority of cells to be binocular, with differing degrees of binocular interaction. Figure 23 is a plot of the binocular interaction histograms for areas V1, V2, V3 and V3A.

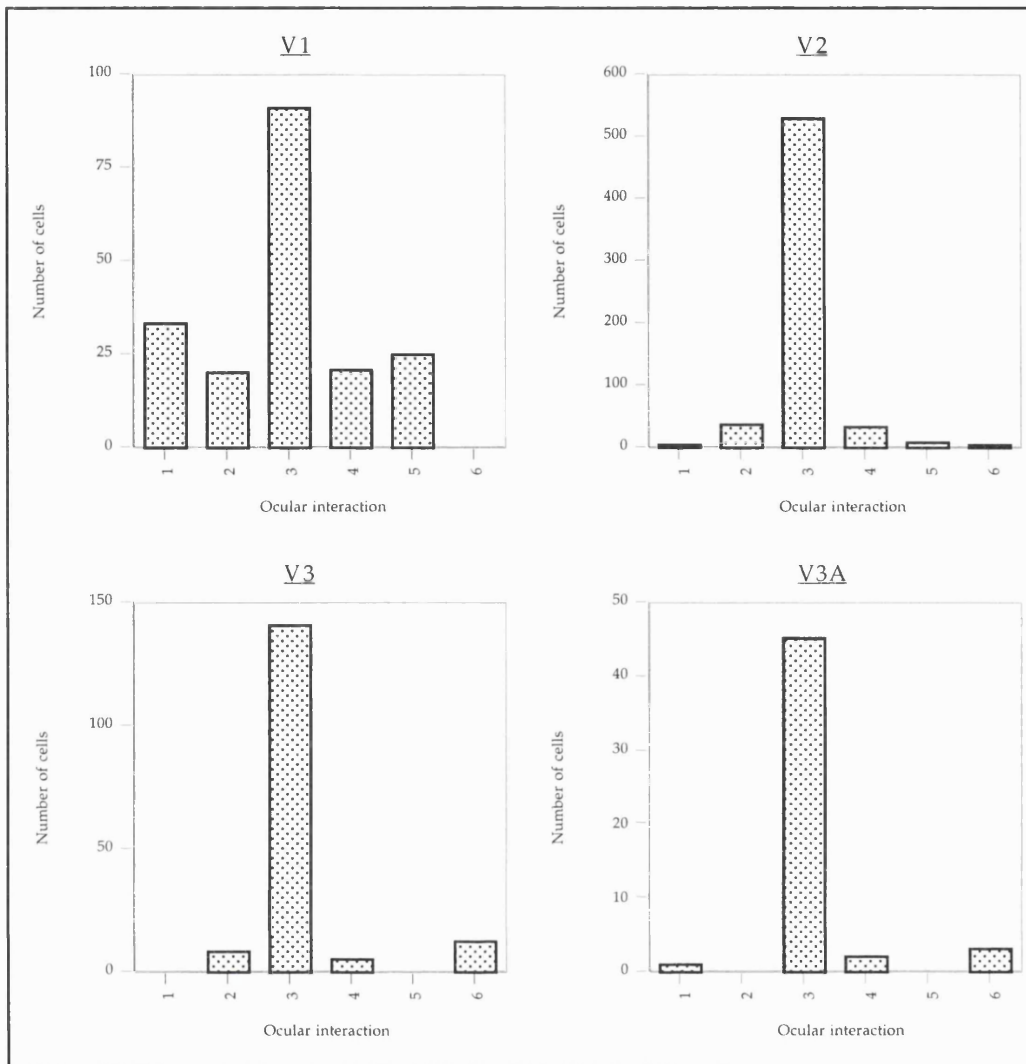


Figure 23.

Ocular interaction histograms for cells in V1, V2, V3 and V3A.

- 1 Cells driven by the ipsilateral eye only.
- 2 Cells dominated by the ipsilateral eye.
- 3 Binocularly driven cells.
- 4 Cells dominated by the contralateral eye.
- 5 Cells driven by the contralateral eye only.
- 6 Cells activated by binocular stimulation only.

The most distinct of these histograms is that of V1, an unsurprising result considering the high proportion of monocular cells in that area. The differences between the other histograms are more subtle. The V3 complex's histogram shows a higher proportion of cells in the category "BO" (binocular only) than V2. In this study, all "BO" type cells were found to be tightly disparity tuned. Another type of binocular

cell very often found to be disparity tuned is the binocularly facilitated ("B") cell. These are also found to be most common in the V3 complex. Ocular interaction histograms therefore suggest that all prestriate areas are involved in binocular vision and are therefore potential candidates for stereoscopic processes. This is not to say that V1 is excluded from binocular processes. Although Hubel and Wiesel failed to find binocular depth cells in V1, since then the presence of these cells has been demonstrated unequivocally (Poggio and Fischer 1977; Fischer and Poggio 1979; Poggio and Talbot 1981; Poggio *et al.* 1985), V1 cells have even been shown to be selective for absolute disparity, i.e. egocentric distance (Trotter *et al.* 1992). The downfall of studying an area with ocular interaction histograms is that the responses of disparity tuned cells are critically dependant on the disparity they are stimulated at, for instance a near cell would fit into the B category if stimulated at a near disparities, but would appear to exhibit monocular responses only, if stimulated at far disparities. It has been suggested that the eye dominance of a cell is a factor that is involved in the mechanism by which the cell is made to be disparity tuned. Poggio and Fischer (1977) found that asymmetric disparity tuned cells (near and far cells) in V1 had asymmetric responses to monocular stimulation, i.e. they would be characterized as ipsilateral eye dominant (group 6) or contralateral eye dominant (group 2) cells in Hubel and Wiesel's (1962) ocular dominance scheme. "Tuned" disparity cells (TE, TI) cells were found by Poggio and Fischer to exhibit equal responses from each eye (Hubel and Wiesel's ocular dominance group 4). This is a distinction that we have failed to confirm from cells in the V3 complex. Figure 24 is a histogram of different types of disparity tuned cells divided into two groups, tuned (including T0, TI, TN and TF) and asymmetric (near and far). These two categories are plotted against number of cells. The X axis is divided into the 7 ocular dominance

categories. Two histograms are shown, one for V2 and one for the V3 complex. The histograms show that, for the cells recorded from in this study, there is correlation between the type of disparity tuning and the ocular dominance characteristic of a cell; the vast majority of cells in V2 and the V3 complex, regardless of their disparity tuning category, fall into Hubel and Wiesel's group 4.

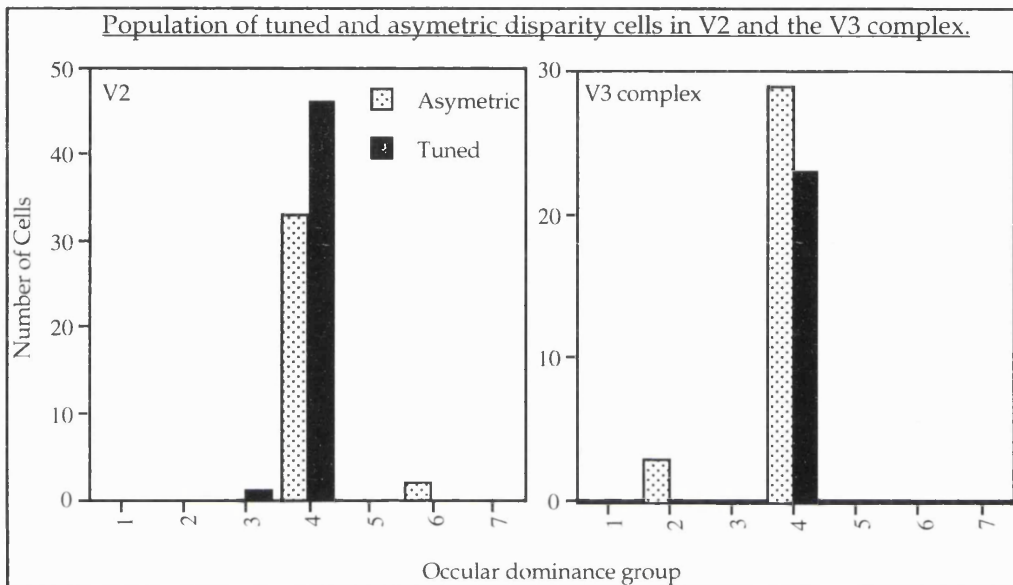


Figure 24.

Population histogram of the number of disparity tuned cells of the asymmetric and tuned types and their ocular dominance groups of Hubel and Wiesel. Histograms for V2 and the V3 complex are shown.

#### f) Disparity tuning

When looking at the disparity tuning profile of a cell, a useful way of presenting the result of a stimulus trial is to plot disparity against response. As previously mentioned, the disparity represents the stereoscopic depth the stimulus was presented at relative to the horopter. In these data, the exact position of the horopter is unknown because the animal's eyes were not converged on the same point on the stimulus screen. Therefore, the disparities shown here are the distance in degrees between the two stimuli. Since this distance is dependant on the distance

between the two receptive fields, and is arbitrary, the numbers on the X axes of these disparity tuning curves show the magnitude of disparity only and not disparity relative to the fixation plane. However, the shape of the curve is what signifies the degree and type of disparity tuning present. The disparity cell type can be judged by normal observation of the shape of the curve and the extent of tuning can be calculated by measurement of the half width half height (*hwhh*) of the peak response. The measurement of *hwhh* is useful only for the "Tuned" type of disparity cell (TE, TI, TN or TF) because only these cells have a peak in their response profile. Figures 25a-c are the spike histogram, disparity tuning curve and orientation tuning polar plot for a single disparity tuned cell.

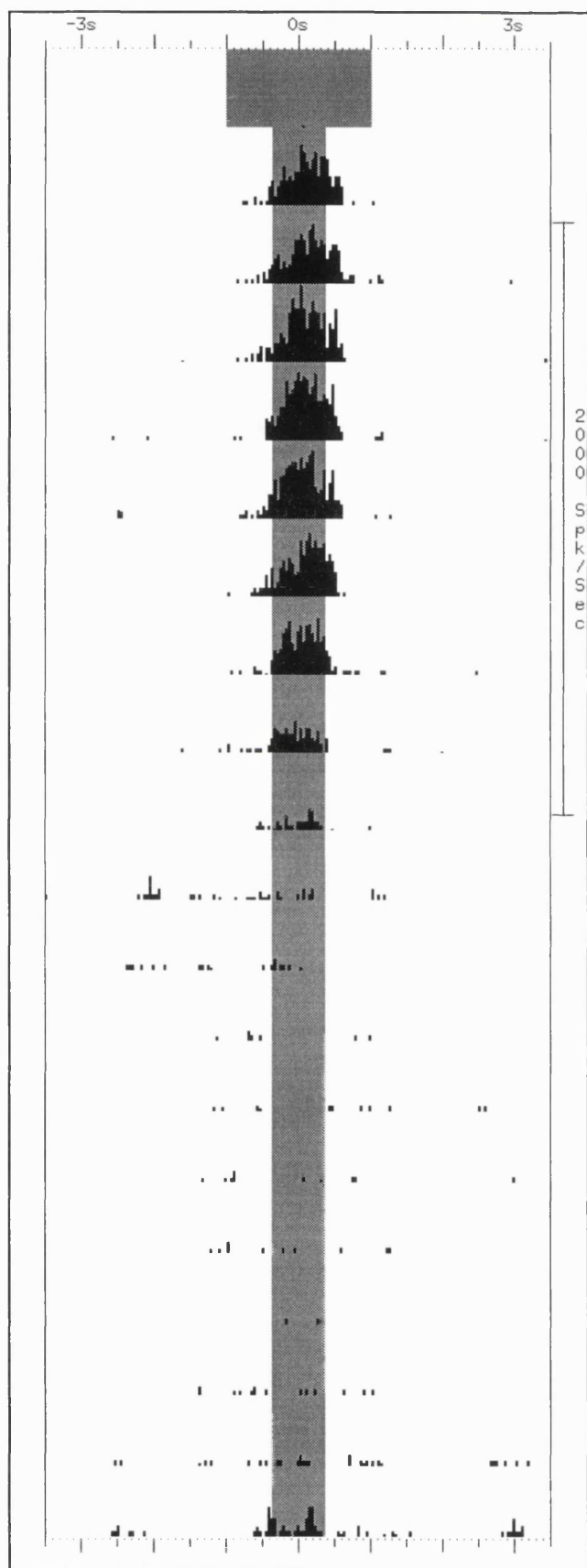


Figure 25a.

Spike histogram for a disparity tuning test. Bin width = 40ms.

The first row is the mean of all the intertrials. From top to bottom the relative disparities for each trial (in degrees) are:

- |     |      |
|-----|------|
| 1)  | 0.46 |
| 2)  | 0.58 |
| 3)  | 0.7  |
| 4)  | 0.81 |
| 5)  | 0.93 |
| 6)  | 1.05 |
| 7)  | 1.17 |
| 8)  | 1.4  |
| 9)  | 1.52 |
| 10) | 1.64 |
| 11) | 1.75 |
| 12) | 1.87 |
| 13) | 1.98 |
| 14) | 2.11 |
| 15) | 2.22 |
| 16) | 2.34 |
| 17) | 2.45 |
| 18) | 2.57 |
| 19) | 2.69 |

These numbers correspond to the stimulus bar separation. The central shaded area is the in-field period for the left bar. Each trial was repeated 4 times and the mean responses are shown here. Since this cell responded only to disparities smaller than a threshold (in this case about  $1.4^\circ$ ) it was classified as a near cell.

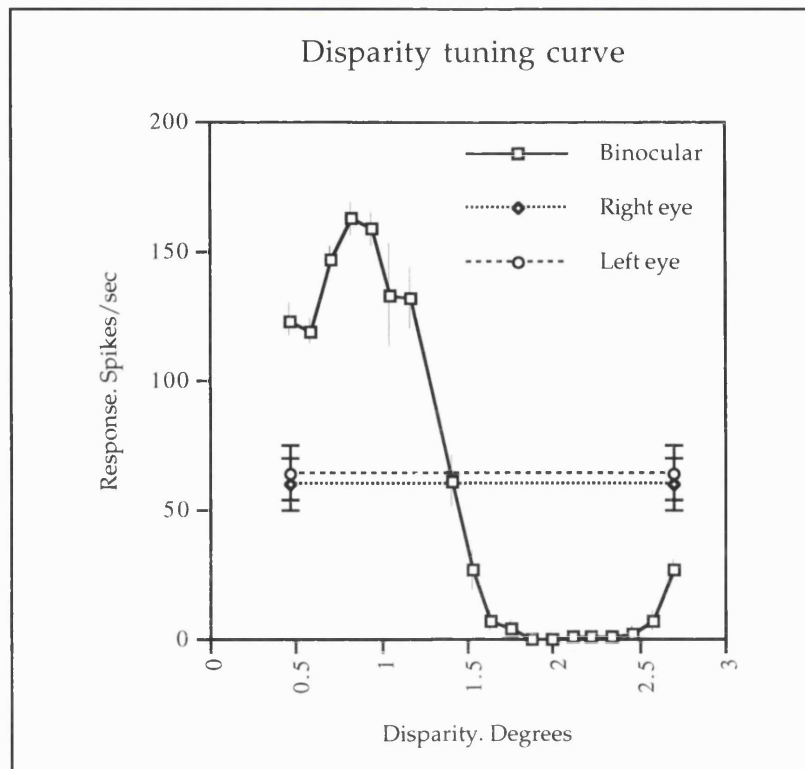


Figure 25b.

The disparity tuning curve plotted from the data shown in histogram form in figure 25a on the previous page. The error bars are the standard errors of the mean responses from 4 trials. The monocular responses for each eye are shown as horizontal lines. The shape of this disparity tuning curve characterizes this cell as a near cell.

Previous studies on the disparity tuning of V3 complex cells have shown that a large proportion are stereoscopic depth cells. Felleman and Van Essen's (1987) study on the paralysed monkey found that 43% (20/46) of the cells tested were selective for disparity. 28% (13/46) of cells tested were of the tuned excitatory (TE) type and 15% (7/46) were asymmetric (near/far). Felleman *et al.* did not distinguish between TE cells and TN/TF cells, classifying them all as TE. Another study using the awake behaving monkey (Poggio *et al.* 1988) found 80% (51/64) of V3 complex cells were tuned to positional disparity. Of these roughly half (26/51) were of the "tuned" variety, nearly all of which were TN or TF, the rest being of the asymmetric (near/far) type. The classification of disparity tuning was assessed qualitatively in both of these studies.

Of the cells tested for disparity in this study, a large proportion were found to be orientation selective. Figure 25c shows the orientation tuning curve for the same cell as figures 25a and b. The shape of the disparity tuning curve shows that this cell is a near cell which is very tightly tuned, i.e. the transition from response to near disparity to that of inhibition to far disparities is very steep. The binocularity of this cells can be assessed from the monocular properties plotted as horizontal lines on the disparity tuning curve. This cell falls into group 4 of Hubel and Wiesel's classification of binocularity, i.e. the left and right monocular responses are similar in magnitude. The orientation selectivity of the cell is shown in figure 25c; the polar plot shows that the cell is tuned to  $150^\circ/330^\circ$ , it has a *hwhh* of  $32.8^\circ$ .

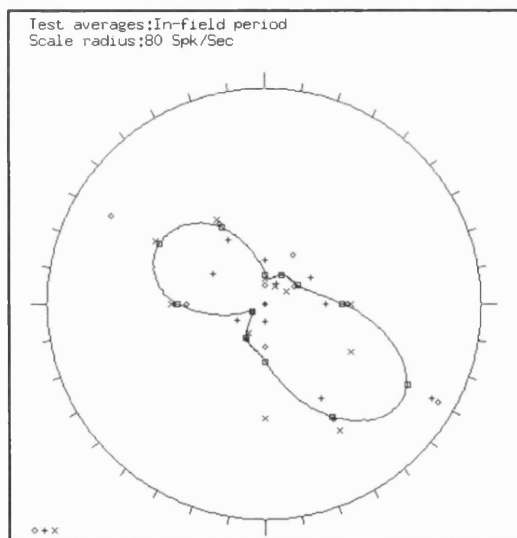


Figure 25c.

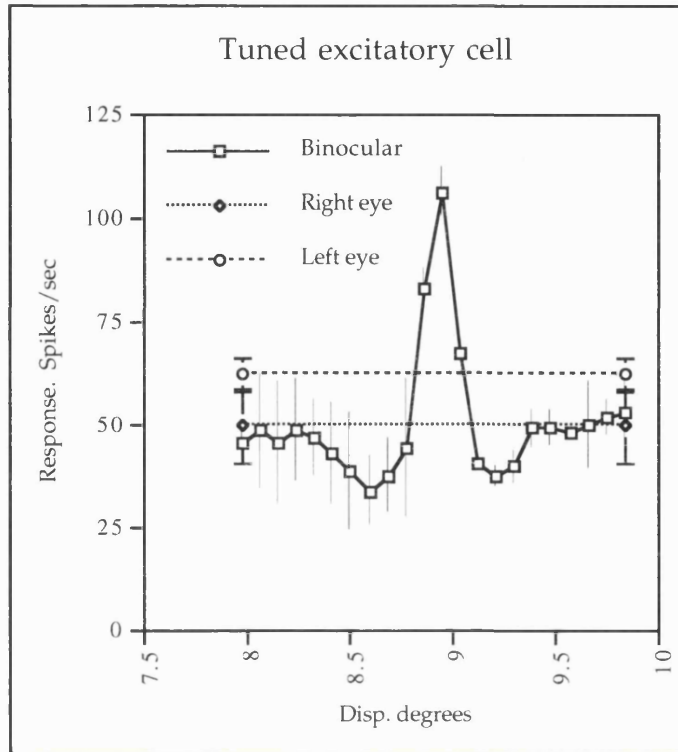
Orientation polar plot for the same cell that's disparity tuning curve is shown in figure 10b.

Figure 26a-e are examples of each of the types of disparity tuned cells found in this study: TE, TI, near, far, and TN.

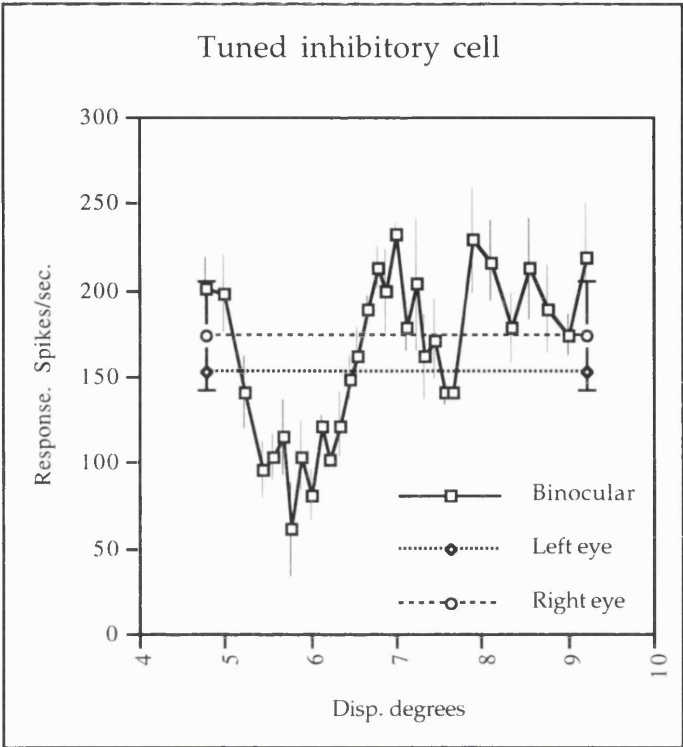
Figure 26.

Examples of the types of disparity tuned cells found in this study.

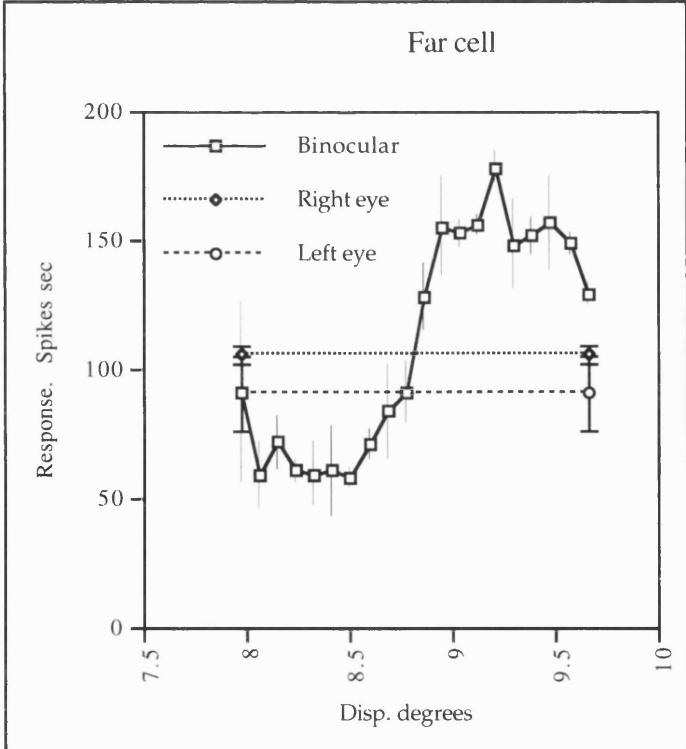
a) Tuned 0 excitatory cell.



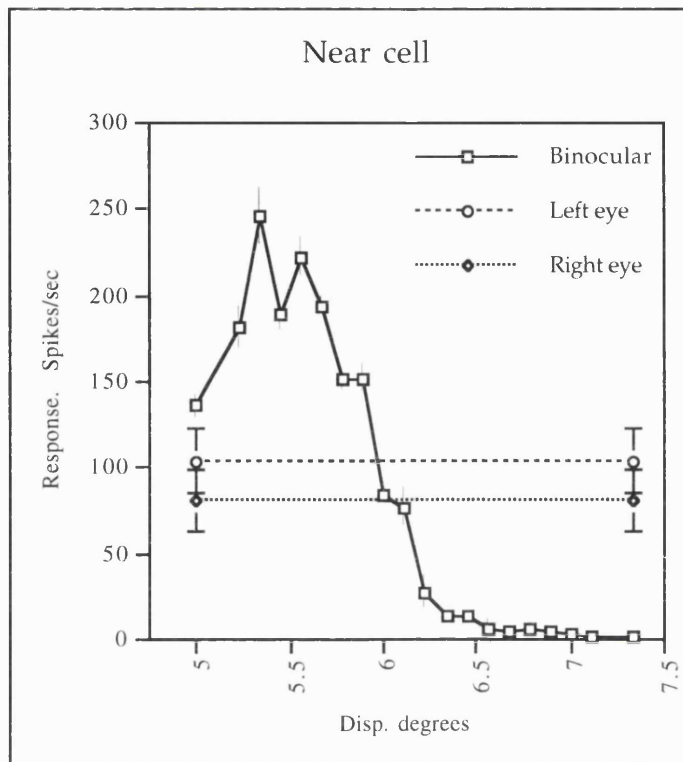
b) Tuned inhibitory cell.



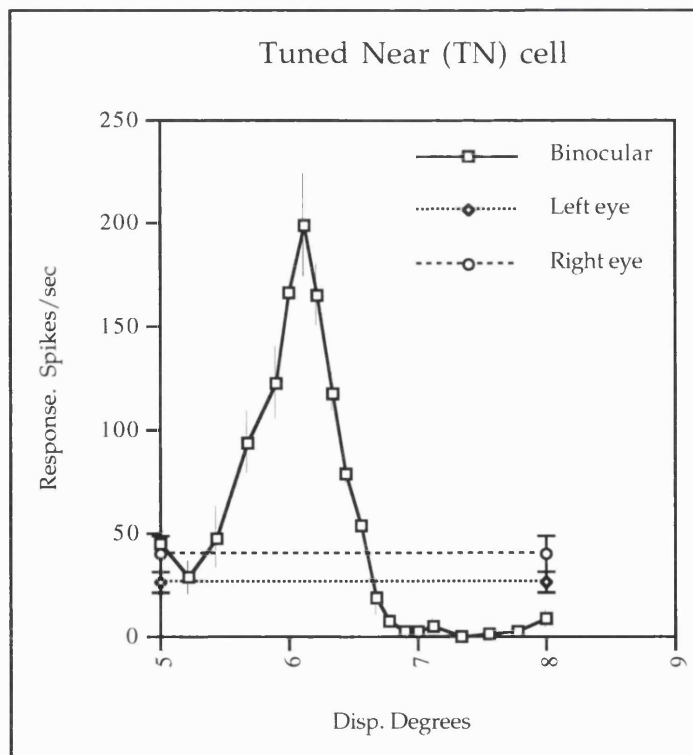
c) Far cell.



d) Near cell.



e) Tuned near cell.



The classification of cells into one of the disparity tuned categories is assessed qualitatively and is not always a clear cut determination. The cells were judged on a number of criteria: the shape of their disparity tuning curves, the position and extent of regions of excitation and/or inhibition compared to the monocular responses and the position of the curve with respect to an estimate of zero disparity based on the receptive field disparity and the positions of TE cell peaks from neighbouring cells. Perhaps the most subjective distinction was that of tuned near/far cells over near/far cells. When classifying these cells, a single peak with *hwhh* less than  $0.5^\circ$  was considered tuned and a multiple peak, or *hwhh* greater than  $0.5^\circ$  was classified as near/far. Since the exact position of zero disparity is not obtainable, the receptive field disparity was used to help classify the types of disparity tuned cell. Although the receptive field disparity is not an accurate measure of zero disparity because of the inherent inaccuracies in receptive field plotting and possibility of receptive field disparities, it at least provides a rough guide. A more accurate method of obtaining the point of zero disparity is to examine the shapes of consecutive cells' disparity tuning curves. Since it is well established that the peaks of TE cells' disparity tuning curves do not vary from zero disparity by more than  $\pm 1^\circ$  (Poggio and Fischer 1977; Poggio *et al.* 1988), an average value for a number of TE cells will give a reasonable locus for zero disparity.

We found that the disparity tuning curves of TE cells and those of TN and TF cells differ, the latter having a long asymmetric inhibitory area that extends towards zero disparity whereas TE cells often exhibit small inhibitory regions either side of the peak response. Thus, TN and TF cells can usually be easily distinguished from TE cells. This distinguishing feature of TE and TN/TF cells can be seen in Figure 27.

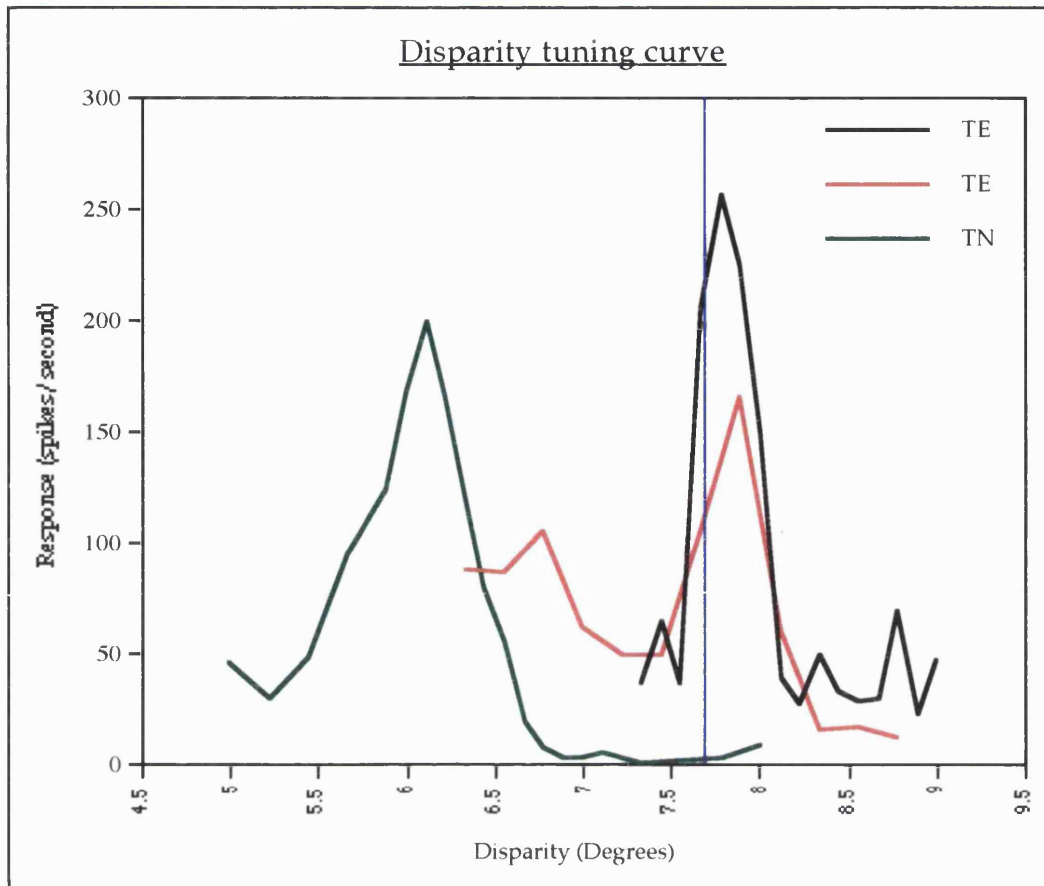


Figure 27.

An example of the distinguishing features between a group of TE cells and a TN cell. Note that the TE cells' peaks are aligned (presumably at zero disparity), whereas the TN cell's peak occurs at a nearer disparity and is followed by a region of asymmetric inhibition that passes through zero disparity. The vertical blue line represents the average receptive field disparity for all cells in the penetration.

### .c2.Proportions of disparity cells

The proportions of these different types of disparity tuned cells were calculated in the areas V1, V2, V3, and V3A (see table 2).

%	Near	Far	T0	TN	TF	TI	U	# Tested
V1	2	0	6	0	0	1	21	30
V2	19	14	32	11	3	1	146	226
V3	21	9	12	2	5	1	50	100
V3A	0	1	0	0	0	0	10	11
V3C	22	11	15	2	5	1	63	119

Table 2.

The proportions of the different types of disparity tuned cells in the areas V1, V2, V3, V3A and the V3 complex (V3C = V3 + V3A + V3/A). T0=Tuned Zero. TI = Tuned Inhibitory. TN = Tuned near. TF = Tuned far. Tuned = Total tuned. # Tested = Total number of cells tested. Values are percentages of # tested for disparity in that area.

Overall, the most common type of cell is the T0 cell, whereas in V3, the near cell is the most prolific. Only one disparity tuned cell was found in V3A but, due to the small population of cells sampled in this area, it is not possible to draw any concrete conclusions from this.

#### Properties of disparity tuned cells

The properties of disparity tuned cells, i.e. their orientation selectivity, direction selectivity, binocular properties, colour selectivities and eccentricities, are important to ascertain because it is these properties that will presumably be co-processed with disparity. For example, it has been shown psychophysically that the efficacy of the stereoscopic depth system is compromised by presentation of random dot stimuli at isoluminance (Lu and Fender 1972). For this reason it seems unlikely that one would find a high proportion of disparity tuned cells that are also colour selective.

The following histogram (Figure 28) shows the percentage of disparity tuned cells in the V3 complex and V2 that are:

- (a) Orientation selective.
- (b) Direction selective.
- (c) Wavelength selective.
- (c) Length tuned.

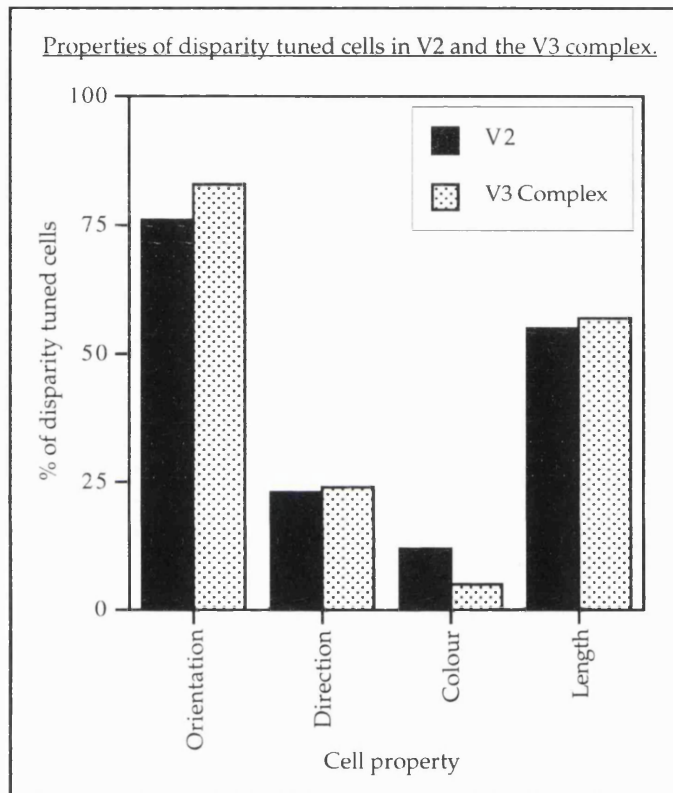


Figure 28.

Histogram of the percentages of disparity tuned cells in the areas V2 and the V3 complex that are also tuned to: orientation, direction, wavelength and stimulus length.

It is clear from this graph that the great majority of disparity selective cells are also orientation selective, some are direction selective, of these some have length preferences, but few are wavelength selective. A previous study on V2 cells suggested that V2 may contain cells that are polymodal, some of which are tuned for disparity and wavelength (Gegenfurtner *et al.* 1996). However, close examination of the criteria

Gegenfurtner *et al.* used to classify their cells as colour selective shows that the colour index system used in their study was not stringent enough to exclude the normal variation in response that occurs during physiological recording. When the wavelength selective cells that make up the small proportion shown on figure 28 were closely examined, it was found that these cells tend to be broadly biased, usually having a smaller response to one wavelength only, these cells were not tightly tuned to a particular wavelength such as those that might be found in V4. For an example see the section on wavelength selectivity.

#### Orientation and direction tuning

In order to discover whether disparity and orientation are co-processed, we performed a  $\chi^2$  test:

$\chi^2$ Test	Ori. Tuned	Ori. Untuned	Tot. Disp.
Disp. Tuned	O=119 E=101.17	O=0 E=17.83	119
Disp. Untuned	O=176 E=193.83	O=52 E=34.17	228
Tot. Ori.	295	52	347

Degrees of freedom =1.

$$\chi^2 = 31.91$$

The critical value for significance at  $p < 0.001$  with 1 degree of freedom =10.83. Therefore disparity tuned cells are significantly different in their orientation tuning properties than non-disparity tuned cells. Disparity and orientation are attributes that are co-processed in the visual areas studied here (V1, V2 and the V3 complex).

Direction selectivity is not an uncommon property of cells in V2 or the V3 complex. The fact that some direction selective cells are also

disparity selective is unsurprising. In the sample of cells found to be selective for disparity in this study, 23% were found to be direction selective in V2 and 24% in the V3 complex. The proportions of the different types of disparity tuned cells were found to be similar for both direction and orientation selective cells. Figure 29 is a histogram of the number of disparity tuned cells fitting the models for orientation/direction tuning.

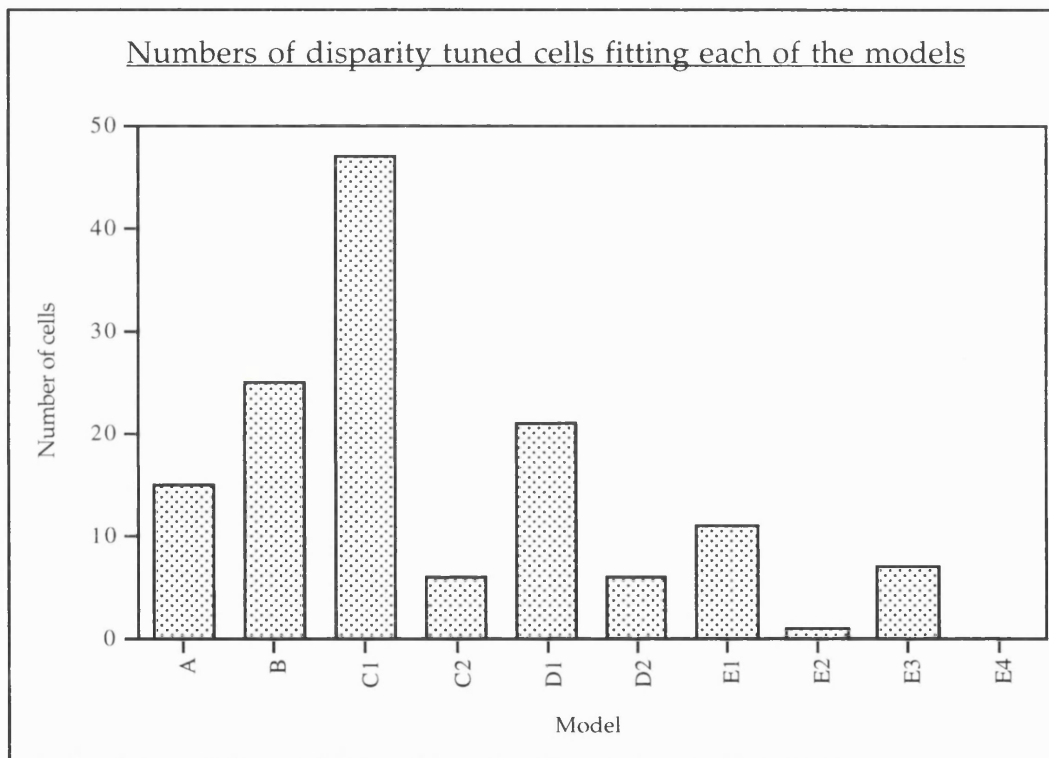


Figure 29.

Histogram of numbers of all disparity tuned cells fitting the orientation/direction models.

- A Flat distribution (Unselective).
- B One peak (direction selective).
- C1 Two similar peaks 180° apart (classical orientation selective).
- C2 Two similar peaks not 180° apart (bi-direction).
- D1 Two peaks of unequal height, equal *hwhh* and 180° apart (orientation selective with direction bias)
- D2 Two peaks of equal height, unequal *hwhh* and 180° apart (orientation selective, direction anomaly).
- E1 Two peaks of unequal height, unequal *hwhh* and 180° apart (orientation selective, direction anomaly).
- E2 Two peaks of equal height, unequal *hwhh* and not 180° apart (bi-direction).
- E3 Two peaks of unequal height, equal *hwhh* and not 180° apart (bi-direction).
- E4 Two peaks of unequal height, unequal *hwhh* and not 180° apart (bi-direction).

### Length tuning

Disparity selective cells were monocularly tested for length preferences and many of these cells were found to exhibit this property. Both end-stopped, length facilitated and length tuned cells were found. End-stopped cells were often also direction selective and length facilitated cells were often orientation selective. Closer examination of the disparity tuned cells selective for vertical axis directions shows them to be a subset of cells that are also end-stopped. These cells will only respond to very short bars, the vertical borders of which can be used for the detection of horizontal disparity.

### Receptive field eccentricity

In order to discover if there is a correlation between the eccentricity of cells' receptive fields and its disparity tuning characteristics, the receptive field positions of disparity tuned cells were plotted for the areas V2 and the V3 complex. These figures (30a and 30b) are shown below. The cells are clustered into groups because cells in an individual penetration, cells tend to have receptive field positions that are very close, each cluster therefore represents a single penetration. All types of disparity tuned cells were found at all eccentricities in both V2 and the V3 complex.

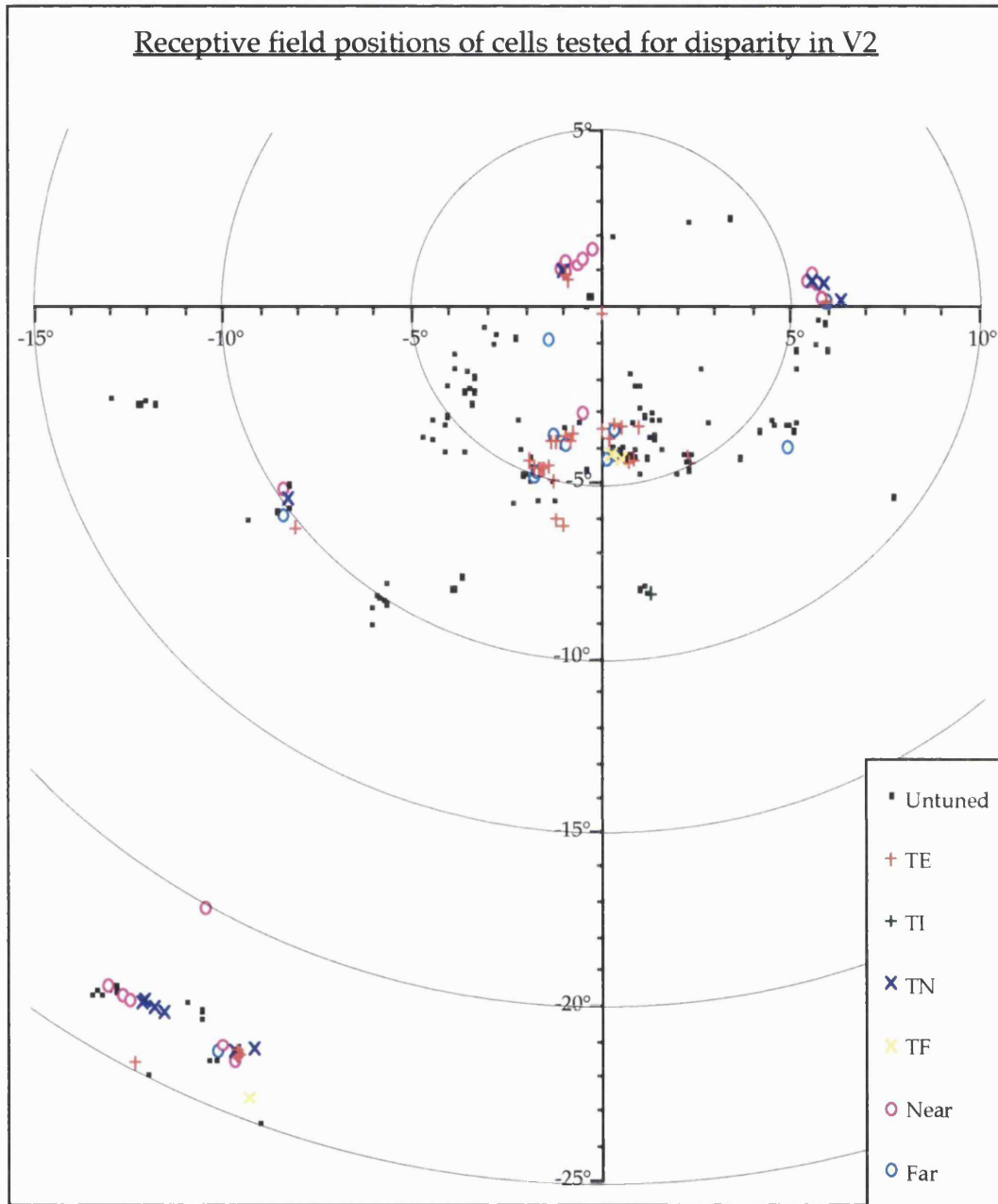


Figure 30a.

Plot of the receptive field positions of cells in the area V2. Each symbol represents the mean position of the centres of both receptive fields of a single cell. The different symbols show the type of disparity tuning of the cell. The axes show eccentricity from the fovea in degrees.

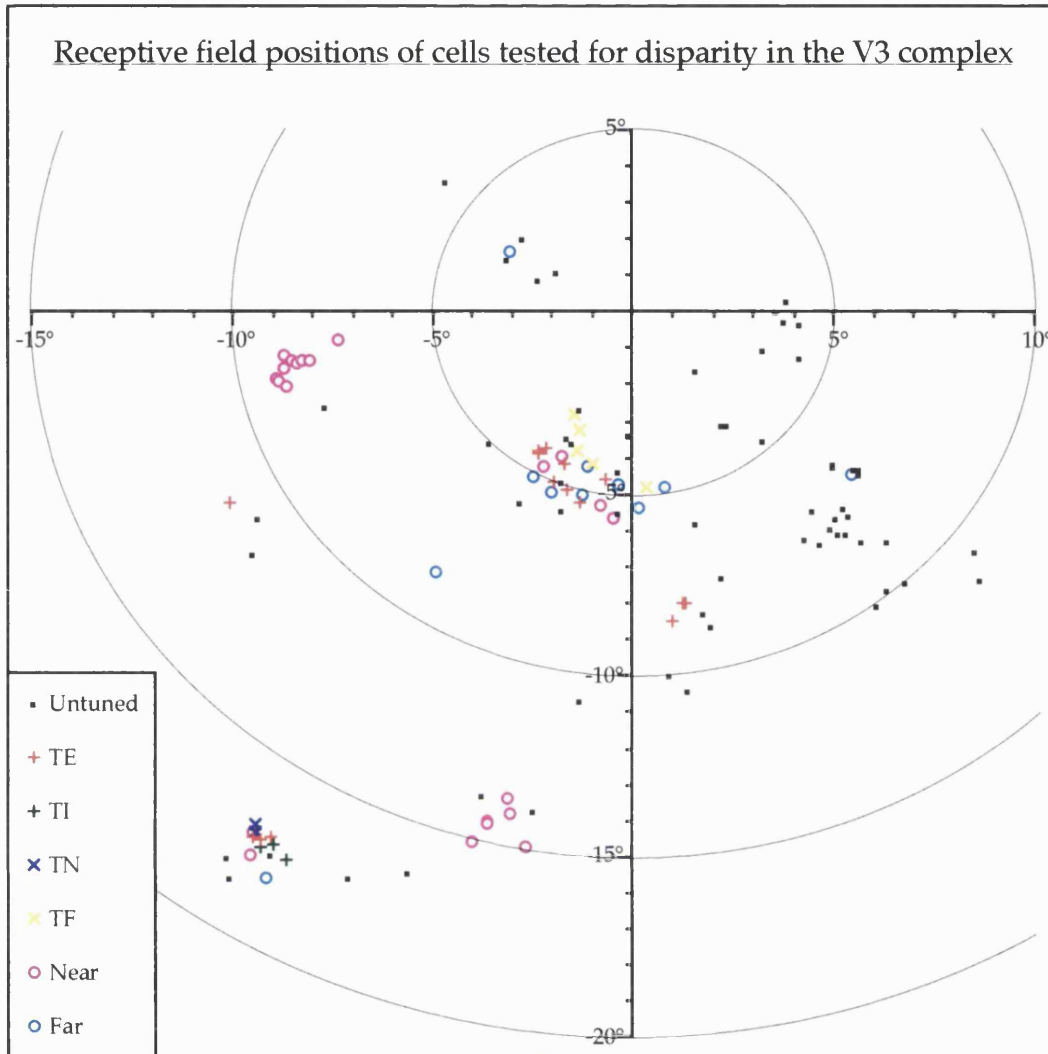


Figure 30b

Plot of the receptive field positions of cells in the V3 complex. Each symbol represents the mean position of the centres of both receptive fields of a single cell. The different symbols show the type of disparity tuning of the cell. The axes show eccentricity from the fovea in degrees.

### .c2. Vertical disparity

A sample of 34 cells were tested for vertical disparity, 19 in V2 and 15 in the V3 complex. Only cells with an horizontal (or near horizontal) orientation preference, or end-stopped cells were tested, since only these cells will respond to a stimulus whose vertical disparity could be varied. All the cells found to have a vertical disparity preference were also tuned to horizontal disparity. Figure 31 shows horizontal (a) and vertical (b)

disparity tuning curves for a V3 cell found to be selective for horizontal and vertical disparity. The shape of the cell's horizontal disparity tuning curve, shows it to be a far cell. This cell could be stimulated at different horizontal and vertical disparities because it was end-stopped. The vertical disparity tuning curve was produced by presenting small spots at a preferred horizontal disparity ( $9^\circ$ ) and varying their vertical disparity. The result is a narrow peak in the response profile centred about the cell's vertical receptive field separation. A minority of cells were found that displayed this property but there were no subdivisions of the type of vertical disparity tuning present, i.e. there were no analogies of asymmetric cells that are found for horizontal disparity tuned cells. Of the small number of cells found to be tuned to vertical disparity (5/34), some exhibited "asymmetric" and some "tuned" horizontal disparity responses. The majority of cells tested for vertical disparity were not tuned.

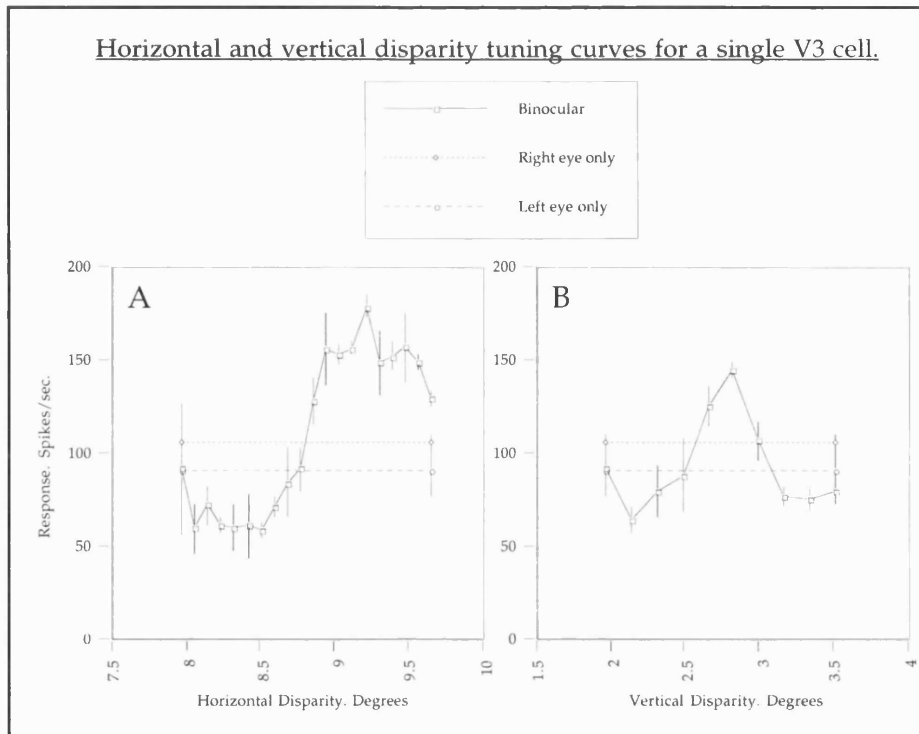


Figure 31.

Horizontal (a) and vertical (b) disparity tuning curves for a cell in V3. This cell is of the "far" type. Vertical disparity was varied at a constant excitatory horizontal disparity. The horizontal lines represent the monocular responses. Error bars are standard errors of mean responses taken over 4 trials for each disparity.

A previous electrophysiological study of vertical disparity tuning using random dot stereograms found that 30% of V1 and 41% of V2 cells are tuned to both horizontal and vertical disparity (Gonzalez *et al.* 1993). They found that all cells in these areas that were tuned to horizontal disparity were also tuned to vertical disparity. Both TE and TI response profiles were found for vertical disparity. These cells have been proposed to be the neural mechanism responsible for the calculation of the horizontal gradient of vertical disparity and the scaling of horizontal disparities for fixation distance (Longuet-Higgins 1981; Longuet-Higgins 1982a; Bishop 1989).

### Functional organization of disparity tuned cells

The aim of recording from cells in V2 and the V3 complex was to determine the presence or absence of a functional organization for disparity tuned cells in these areas. To this end, penetrations were made in these areas at as many different angles as possible. Thus, any differences in the disparity tuning of cells could be correlated with the position of the cells in the cortex. This assessment was done on the V3 complex and V2.

In order to elucidate the functional organization of disparity, the penetrations were examined and the clustering of different cell types was investigated. If columns of cells with similar properties are present in the cortex, one would expect to find regions of homogenous cell types. The length of penetration containing a homogenous type of disparity cell does not necessarily have to be constant. The width of cortex containing one type of cell will only be constant if the columns are stripes, and all the penetrations traverse all the stripes at a similar angle. If the columns are any other shape (e.g. circular), then the length of electrode track containing an homogenous cell type will vary within individual penetrations.

The clustering of cells types was investigated by application of the One Sample Runs Test (see methods) (Siegel 1956). This statistical test calculates the probability of obtaining different sequences of tuned and untuned cells, for example, cells are classified as TE or non-TE and the test is used to see if the order is "random". Since many of the penetrations contained few cells, all the penetrations from a particular visual area (V2 or the V3 complex) were made into one long series of cells and the One Sample Runs test performed as if all the cells were from one

penetration. Penetrations were grouped in this way because many contained too few cells to perform the test on individually. Grouping penetrations in this way is more likely to "de-cluster" the data than increase clustering and the penetrations were put together in the order that they were made. There are 226 cells in the V2 population (31 penetrations from 15 animals) and 121 cells in the V3 complex population (16 penetrations from 8 animals). The clustering of tuned and untuned cells as well as the clustering of each of the different types of disparity tuned cells were investigated and a  $p$  score calculated for each. The  $p$  score is a measure of how probable it is that the sequence of cells occurred by chance in a random sequence. Table 3 is a summary of the cells tested in this way. All types of disparity tuned cell in V2 and the V3 complex showed highly significant clustering with  $p$  scores below the cut-off value of 0.025.

	Tuned	Near	Far	TE	TI	TN	TF
V2 $p$	0.0000	0.0000	0.0001	0.0000	-	0.0000	0.0000
V3C $p$	0.0000	0.0000	0.0248	0.0000	0.0000	0.0000	0.0000

Table 3.

$p$  scores for the One Sample Runs test applied to the whole population of cells in V2 and the V3 complex (V3C). Each of the different types of disparity tuned cell was tested for clustering in this way and each was found to display highly significant clustering in both areas V2 and the V3 complex. Since only one TI cell was found in V2, it was not possible to perform the test. TE = Tuned excitatory; TI = Tuned inhibitory; TN = Tuned near; TF = Tuned far.

Since there is significant clustering of disparity tuned cells in areas V2 and the V3 complex, we set out to discover the pattern of this clustering. Cells could be clustered into columns, layers or a patchwork within the cortical sheet; we investigated the pattern of clustering (functional organization) by the examination of electrode penetrations

that traversed the cortical sheet at different angles. Three examples of electrode tracks have been used to illustrate the functional organization of the V3 complex. The first is a penetration that traverses the cortex in a radial direction, the second passes more tangentially through the cortex and the third passes through a fold in the cortex in such a way that it starts radial, becomes tangential and then goes back to radial before entering white matter again. Three penetrations will be presented here, these being the ones that illustrate the functional organization best. However, the organization is evident in all penetrations through the V3 complex.

Figure 32 (VG37) is an electrode penetration through the anterior bank of the lunate sulcus. The angle of the penetration in this brain is quite close to normal, therefore the electrode passed through the cortical lamellae in a near perpendicular direction.

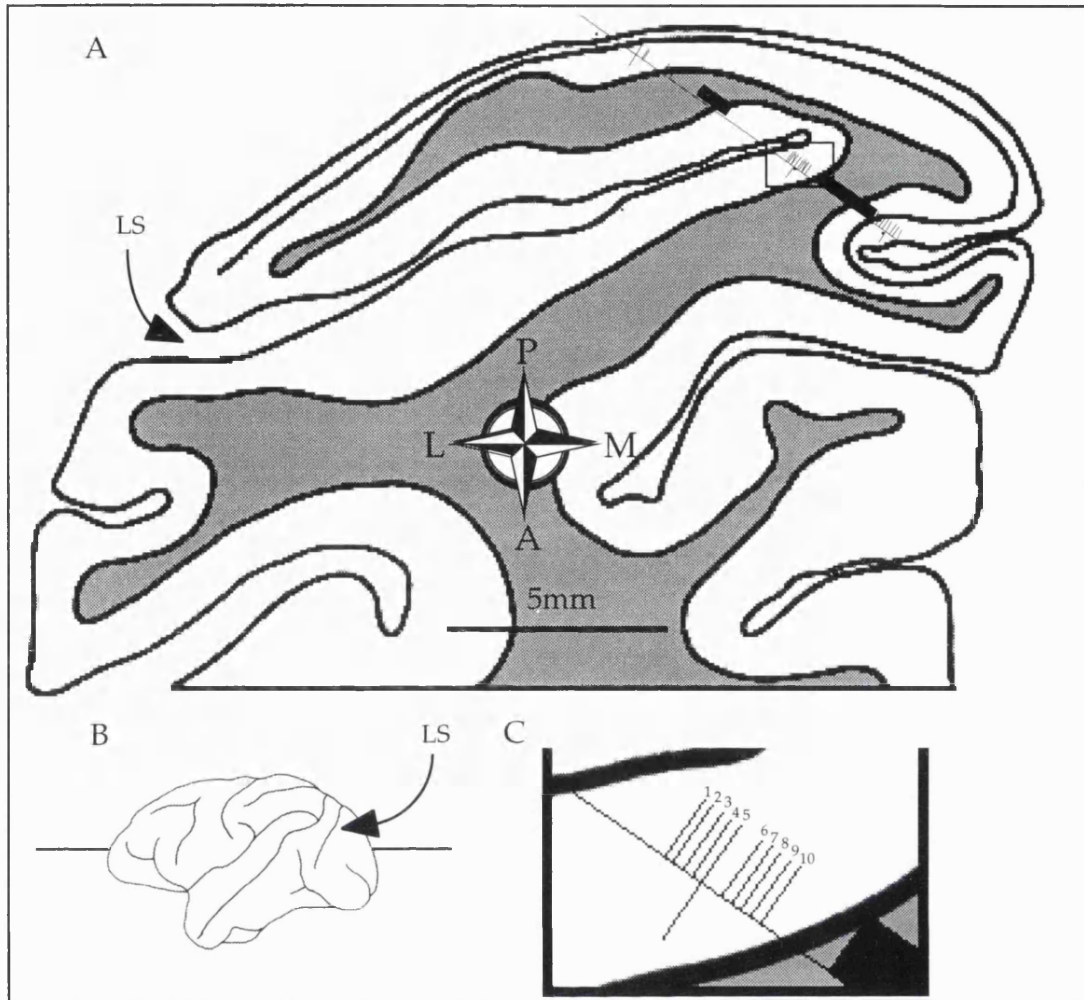
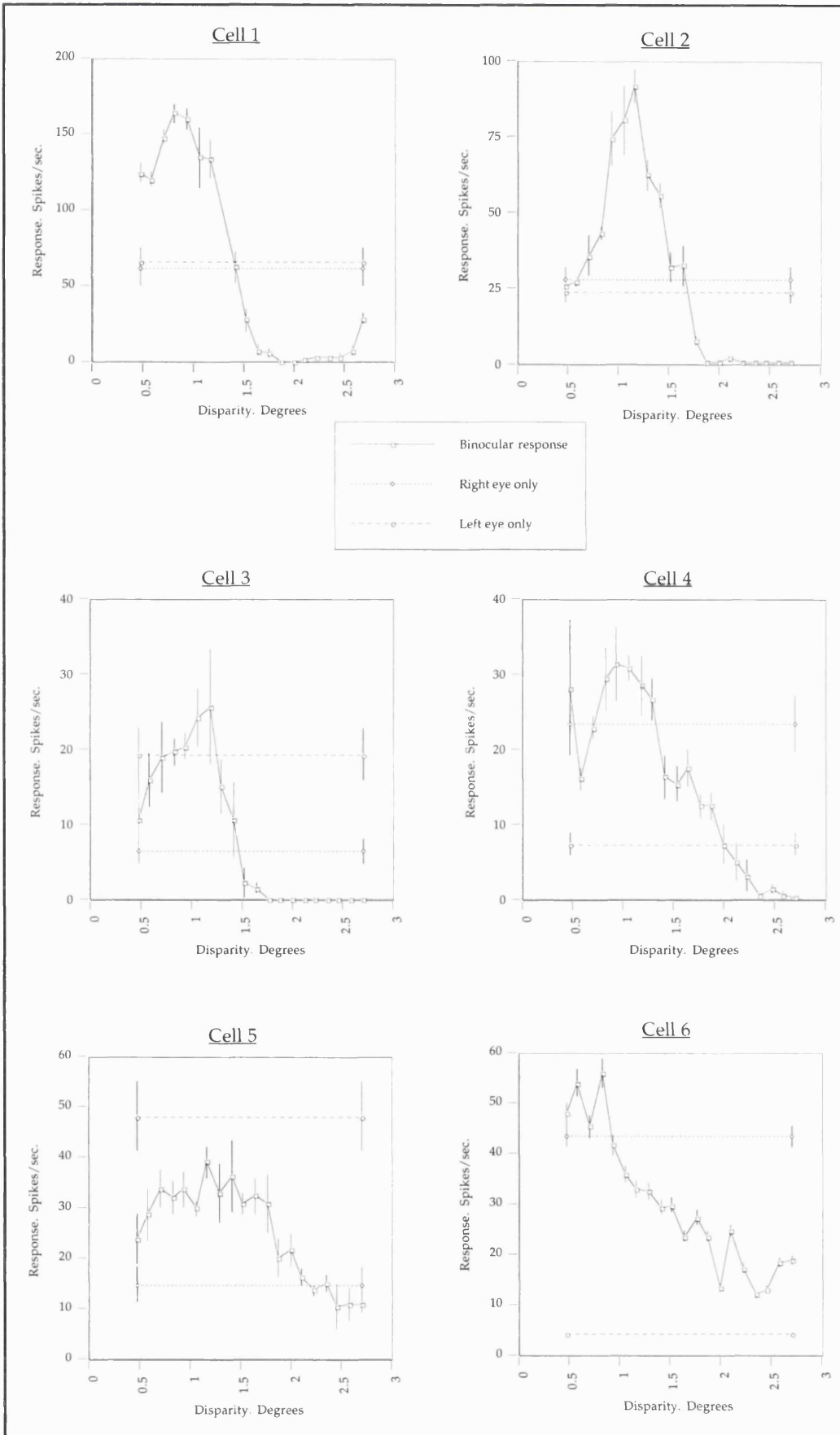
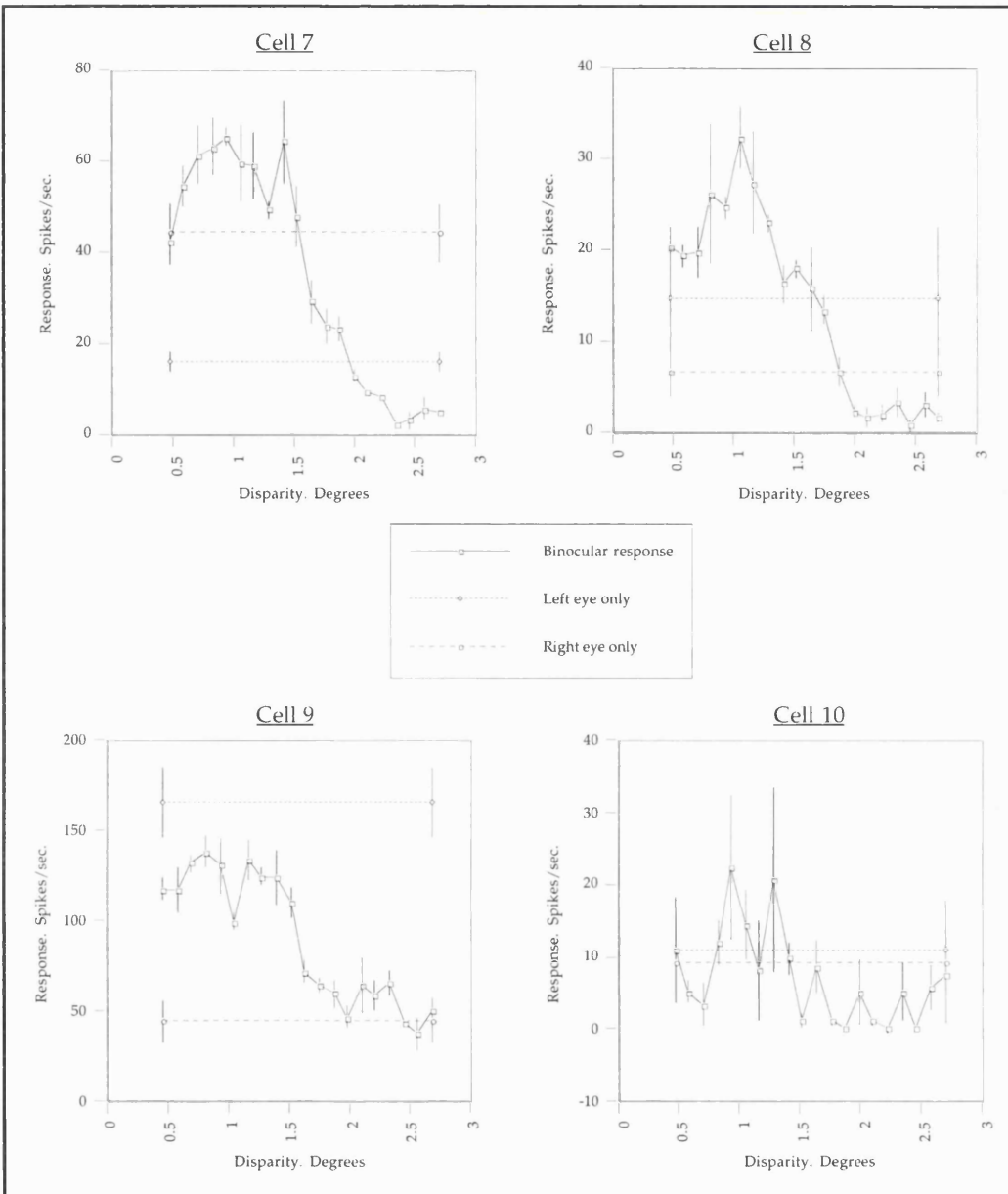


Figure 32.

Reconstruction of an electrode track in the right hemisphere of a brain. The track is drawn onto an horizontal section. Layer 4C in the striate cortex is shown and white matter is represented in grey. The track runs in an horizontal plane at the dorso-ventral level shown in 31b. The part of the track in the anterior bank of the lunate sulcus has been boxed and expanded to show the individual cells recorded from in that area.

The disparity tuning curves and orientation polar plots for the cells recorded from in the anterior bank of the lunate sulcus of brain VG37 are shown in figure 33 (overleaf).





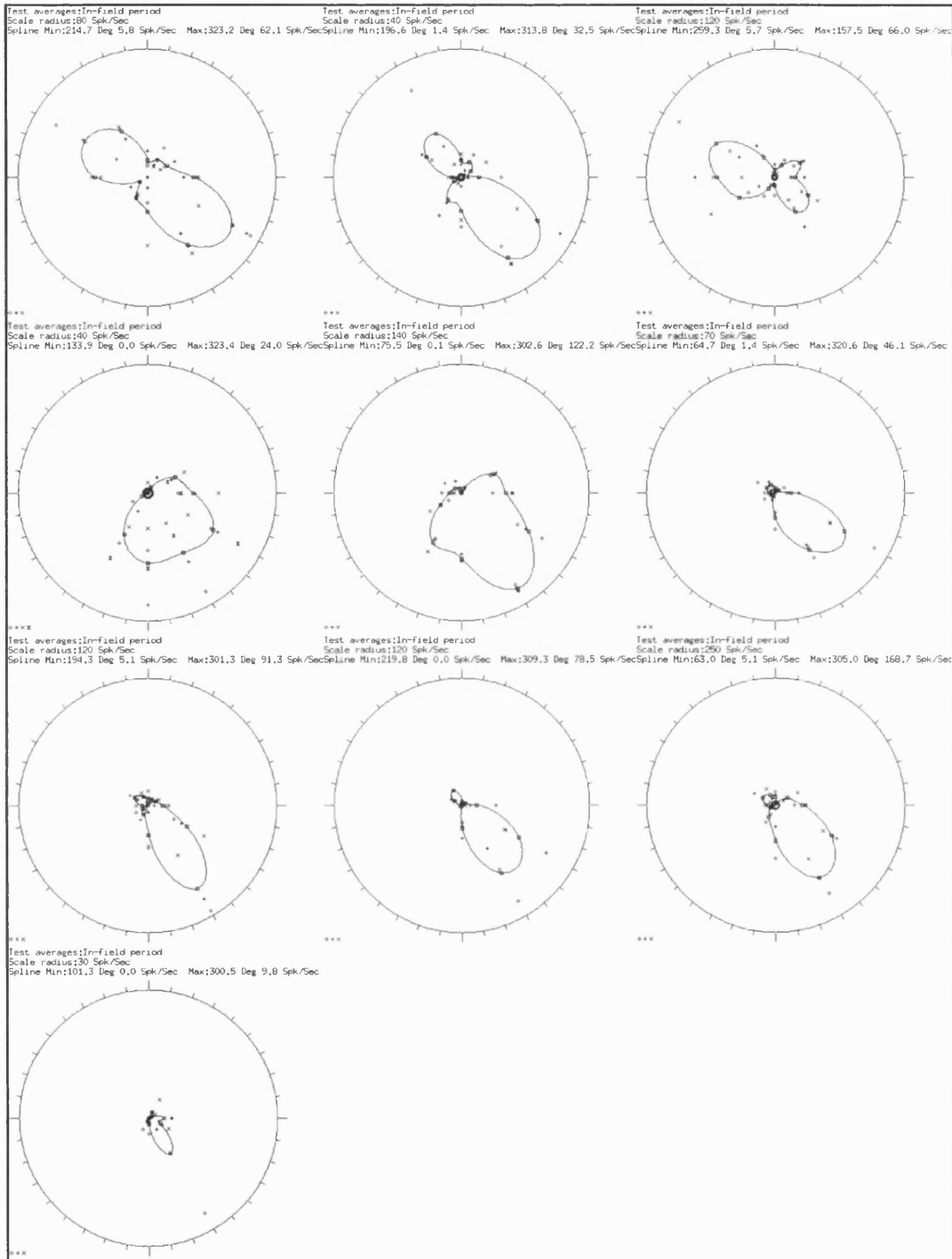


Figure 33b.

Polar plots of orientation tuning for the 10 cells in V3A of brain VG37.  $\theta$  represents the angle at which the stimulus was moving, and  $r$  the response to that stimuli in spikes per second.

Figure 34 is a summary diagram of the cells in VG37, the electrode track in the anterior bank of the lunate sulcus is shown with the cells in their correct position with their orientation preference and disparity tuning category shown. The majority of the cells are of the near type, and their orientation properties change from orientation selective to direction selective, however, the orientations and directions remains constant. The single change in cellular properties from orientation selective to direction selective might be expected because the penetration is not perfectly radial.

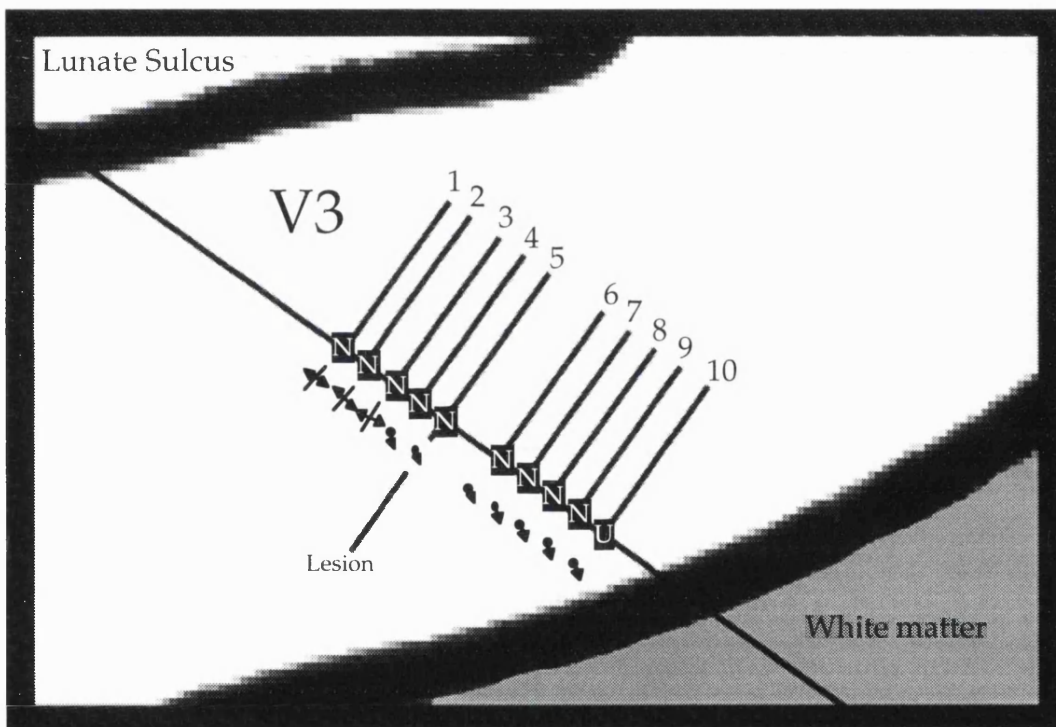


Figure 34.

Part of the anterior bank of the lunate sulcus of the brain represented in figure 32. The positions of cells are represented by lines perpendicular to the electrode track and their orientation selectivity is represented by lines or spots at the appropriate orientation with arrows to denote their direction selectivity (a double headed arrow represents no directional bias). The cells' disparity tuning categories are also shown: N = near, and U = Untuned.

The brain illustrated in figure 35 (VG45) also had an electrode penetration through cortex considered to be part of the V3 complex. Although the electrode passed radially to the cortex in the horizontal plane, the angle of the cortex was not perpendicular to the angle of the electrode in the vertical plane. This is reflected by the apparent thickening of the cortex due to that part of the cortical sheet having been cut in a more tangential plane than the previous brain. Thus, the penetration in this brain (VG45) is closer to a tangential angle than that of the previous brain (VG37).

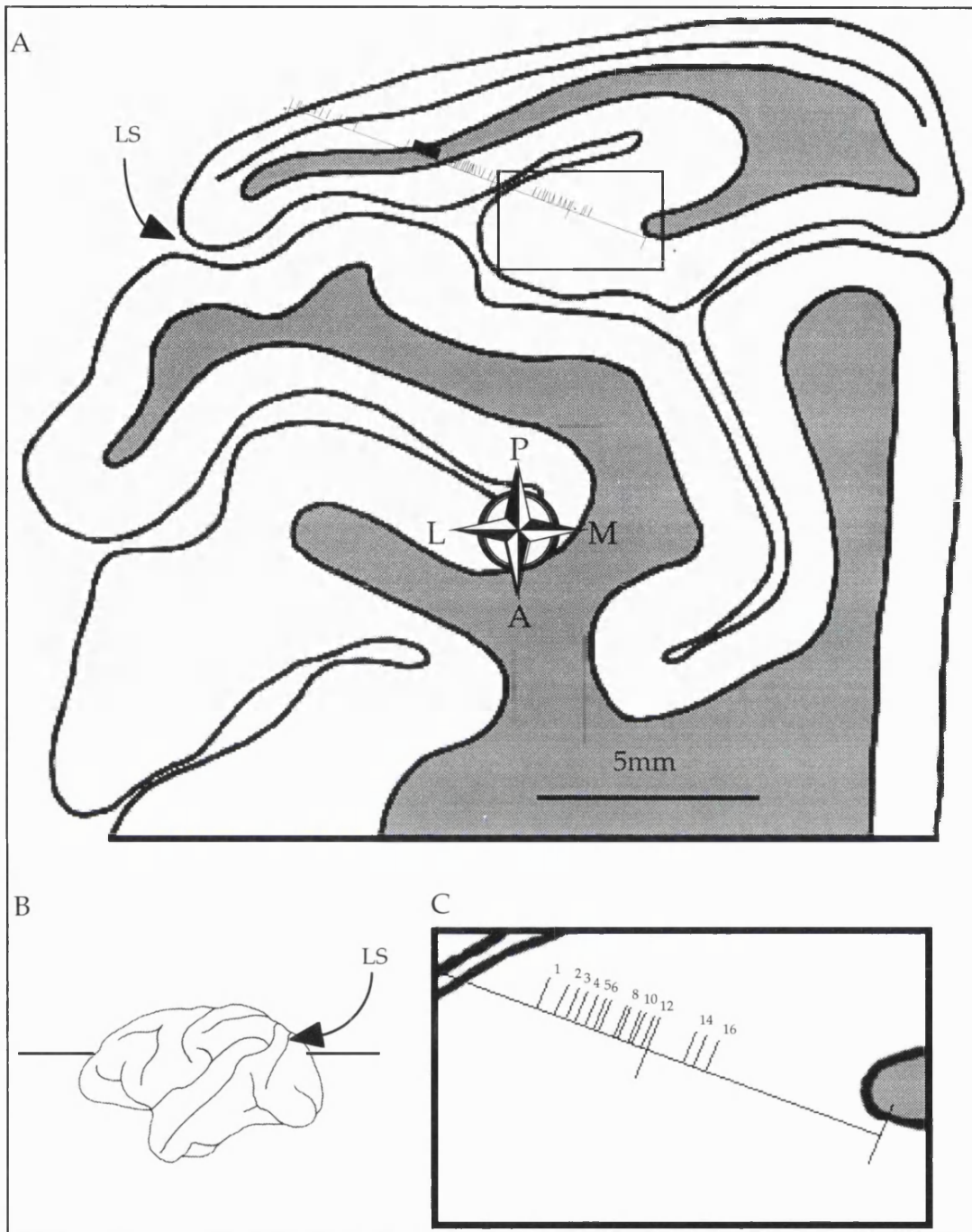
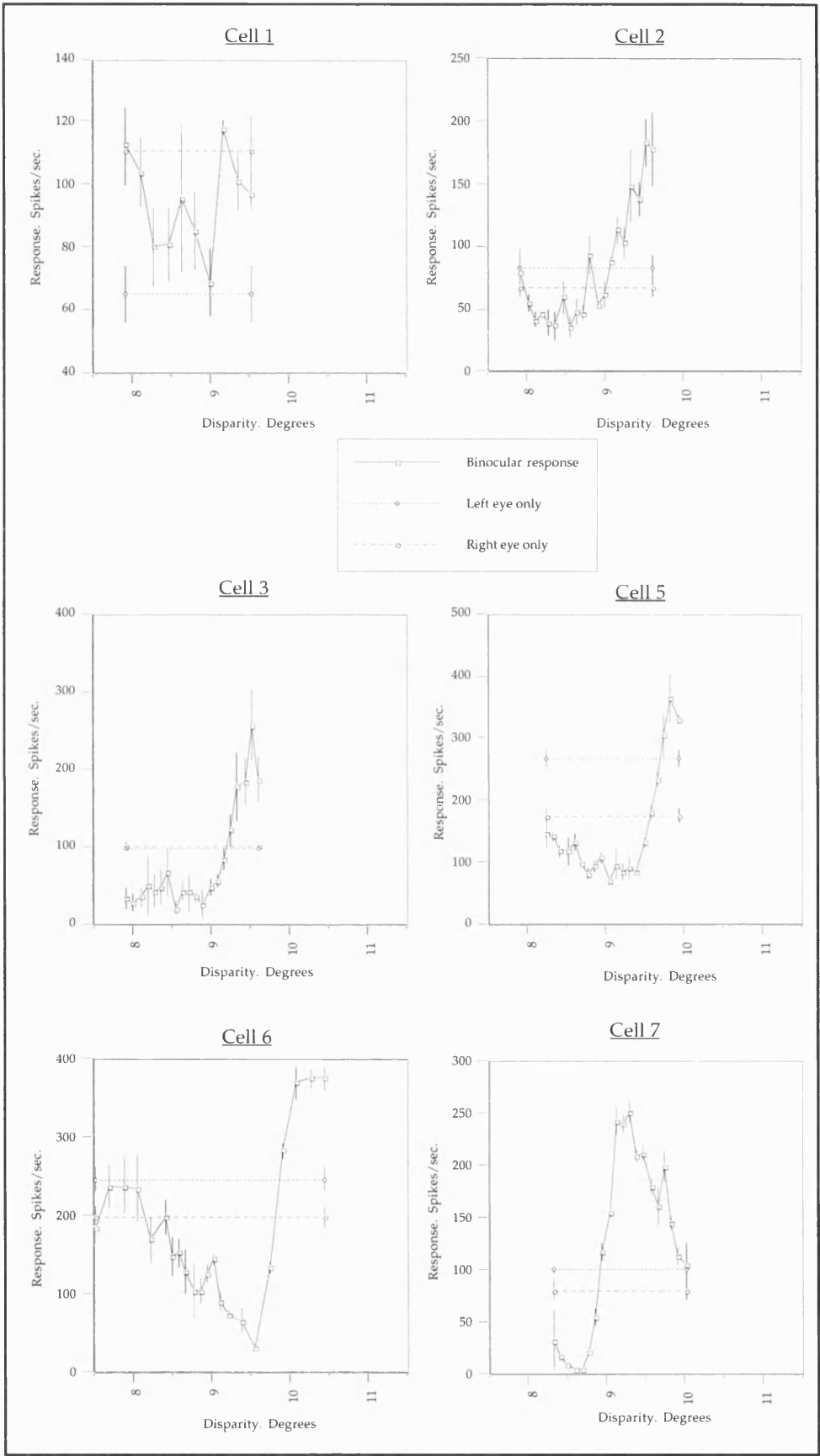
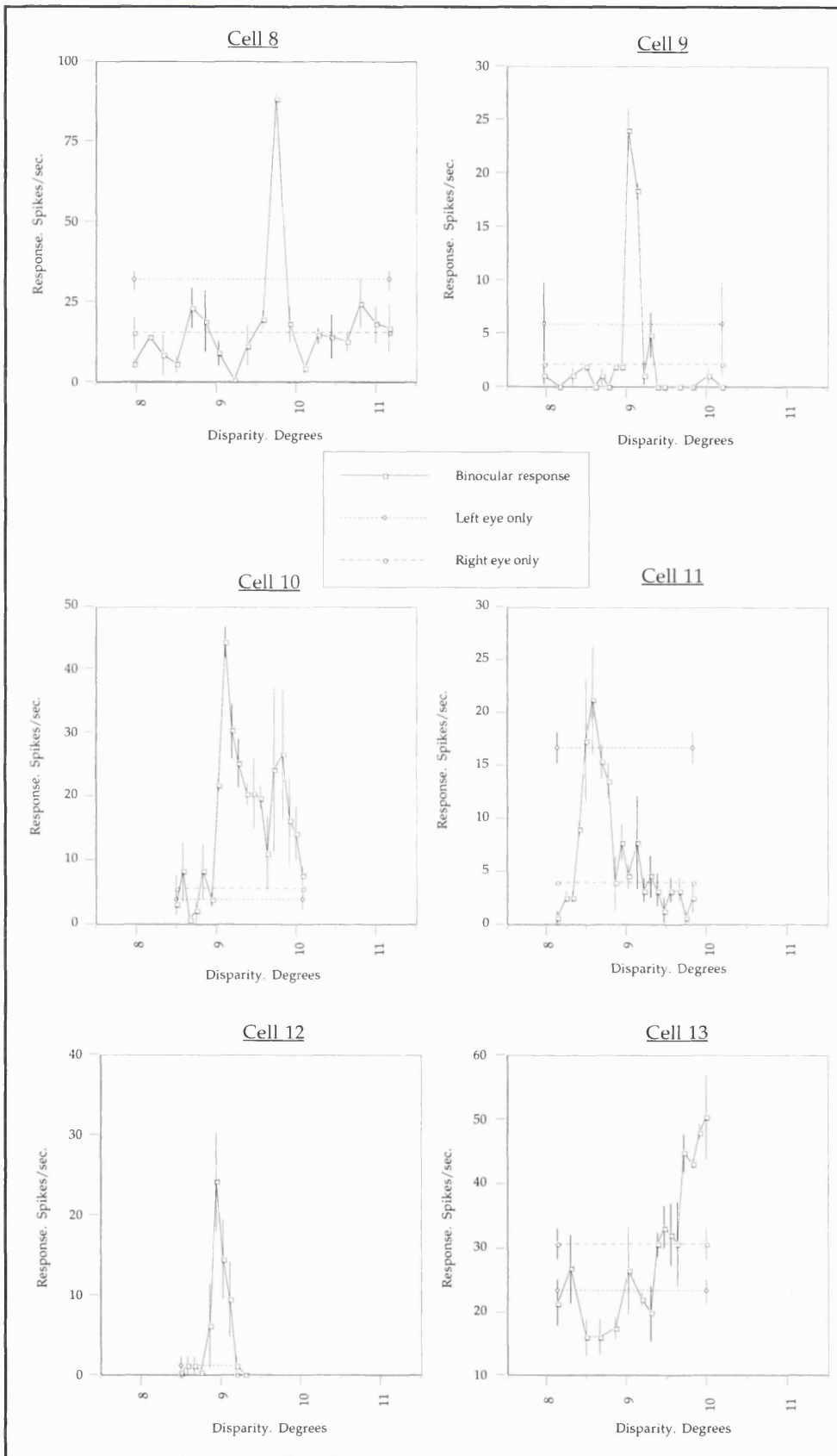


Figure 35.

Reconstruction of an electrode track in the right hemisphere of a brain. The track is drawn onto an horizontal section. Layer 4C in the striate cortex is shown and white matter is represented in grey. The track runs in an horizontal plane at the dorso-ventral level shown in 34b. The part of the track in the anterior bank of the lunate sulcus has been boxed and expanded to show the individual cells recorded from in that area (34c).

The disparity tuning curves and orientation tuning polar plots are shown for the above brain in figure 36a-b.





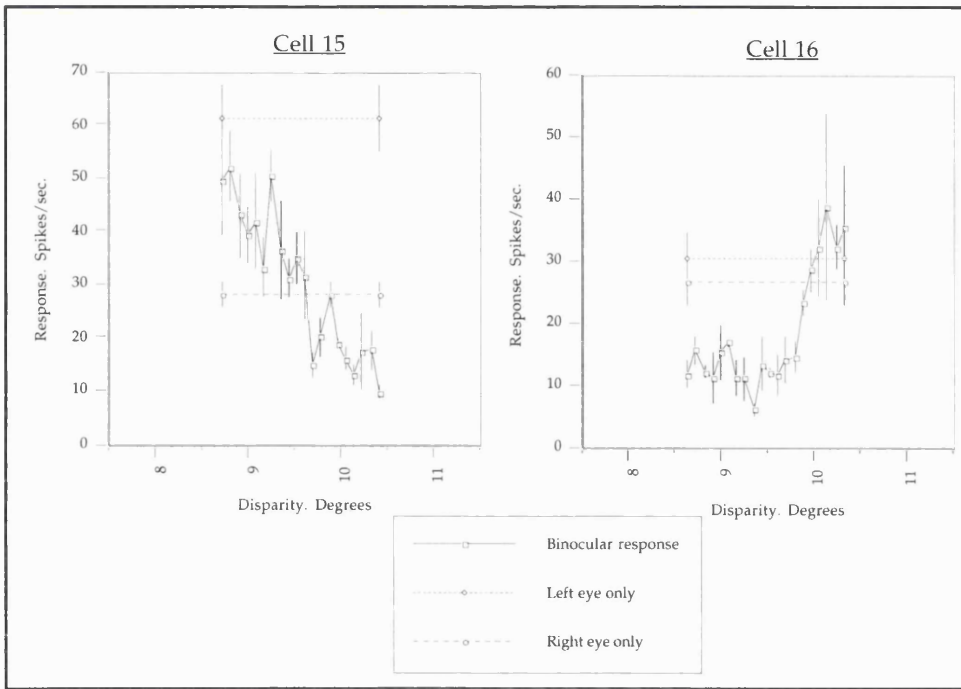


Figure 36a (above and previous pages).  
Disparity tuning curves for the V3 cells of brain VG45.

Figure 36b (overleaf).

Polar plots of orientation response curves for cells in the brain VG45. Plots 9 and 11 did not cover the whole range of orientations because they were presented stationary at  $10^\circ$  steps over a range of  $90^\circ$ .

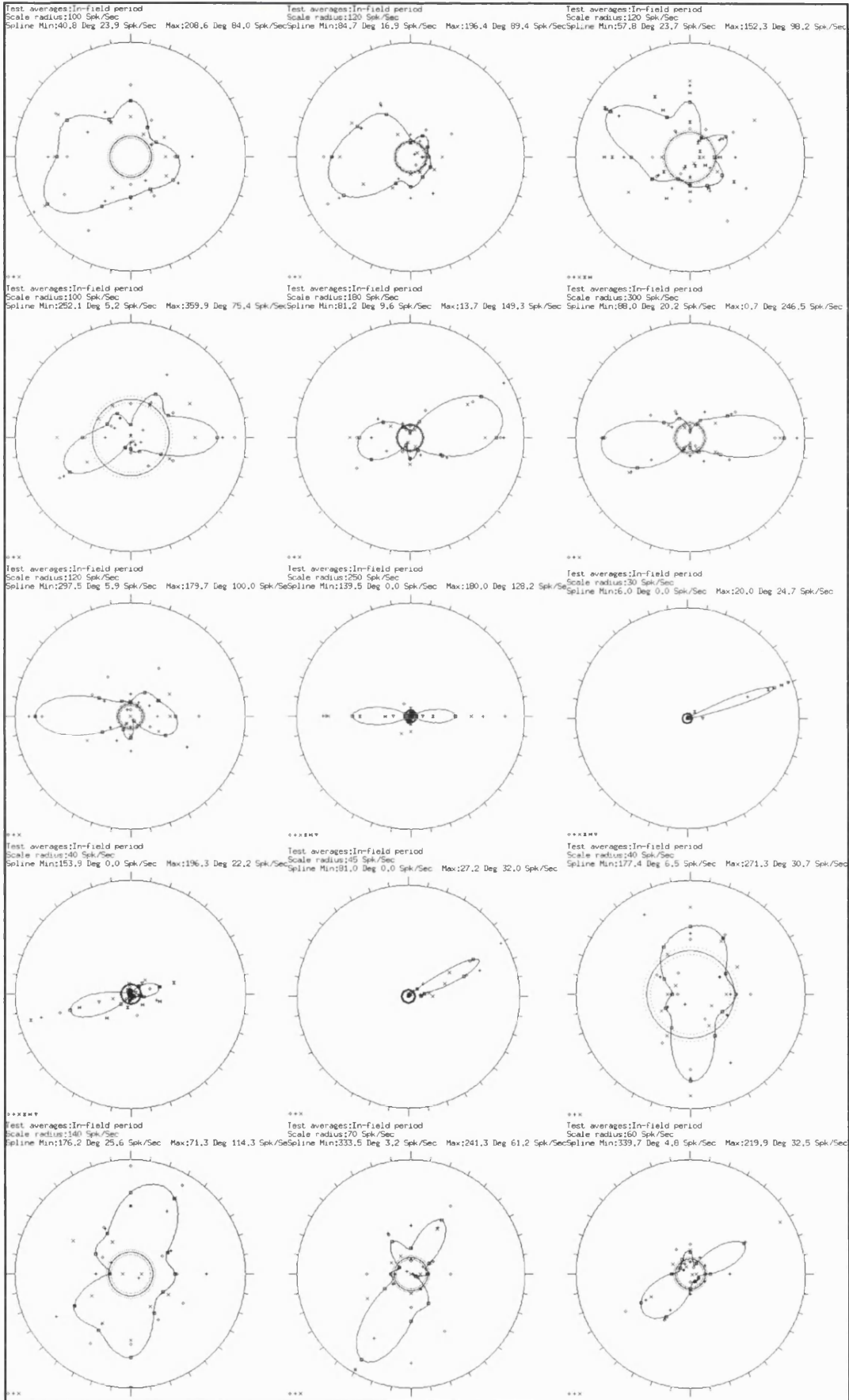


Figure 37 is a drawing of the part of the section illustrated in figure 35 with the selectivities (orientation and disparity) of the cells marked on as in the previous brain. The sequence of disparity tuning categories and orientation preferences changes frequently throughout the penetration.

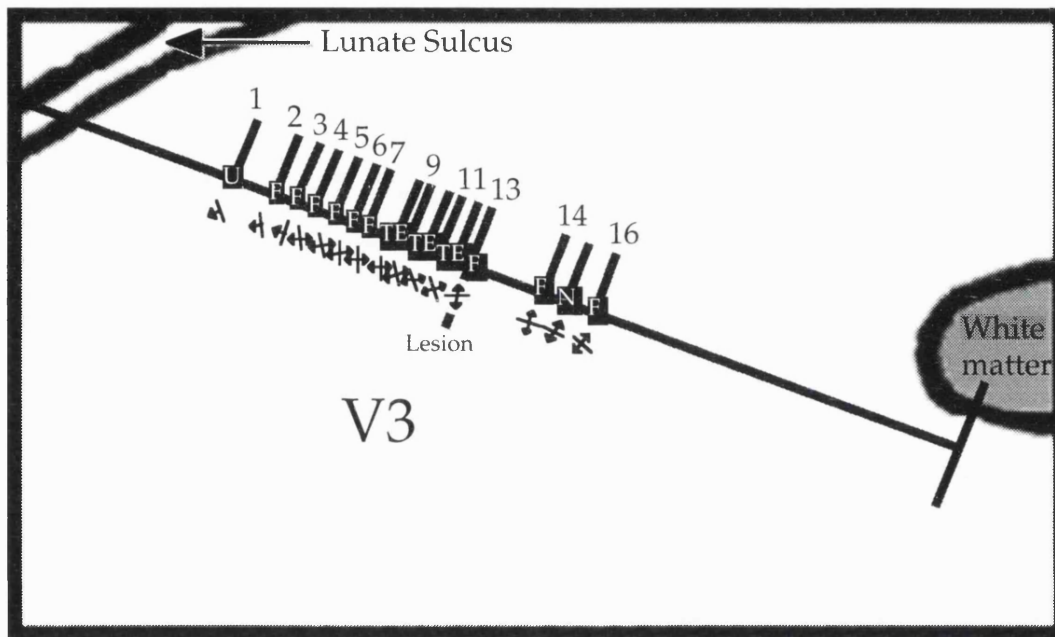


Figure 37.

Part of the anterior bank of the lunate sulcus of the brain represented in figure 36. The positions of cells are represented by lines perpendicular to the electrode track and their orientation selectivity is represented by lines or spots at the appropriate orientation with arrows to denote their direction selectivity (a double headed arrow represents no directional bias). The cells' disparity tuning categories are also shown: TE = Tuned excitatory, F = far and U = Untuned.

Usually, electrode penetrations pass through cortex at a constant angle. However, the penetration illustrated in figure 38 traversed the cortex at the fundus of the lunate sulcus and so the angle at which the electrode passed through the cortical lamella changed with changing electrode depth.

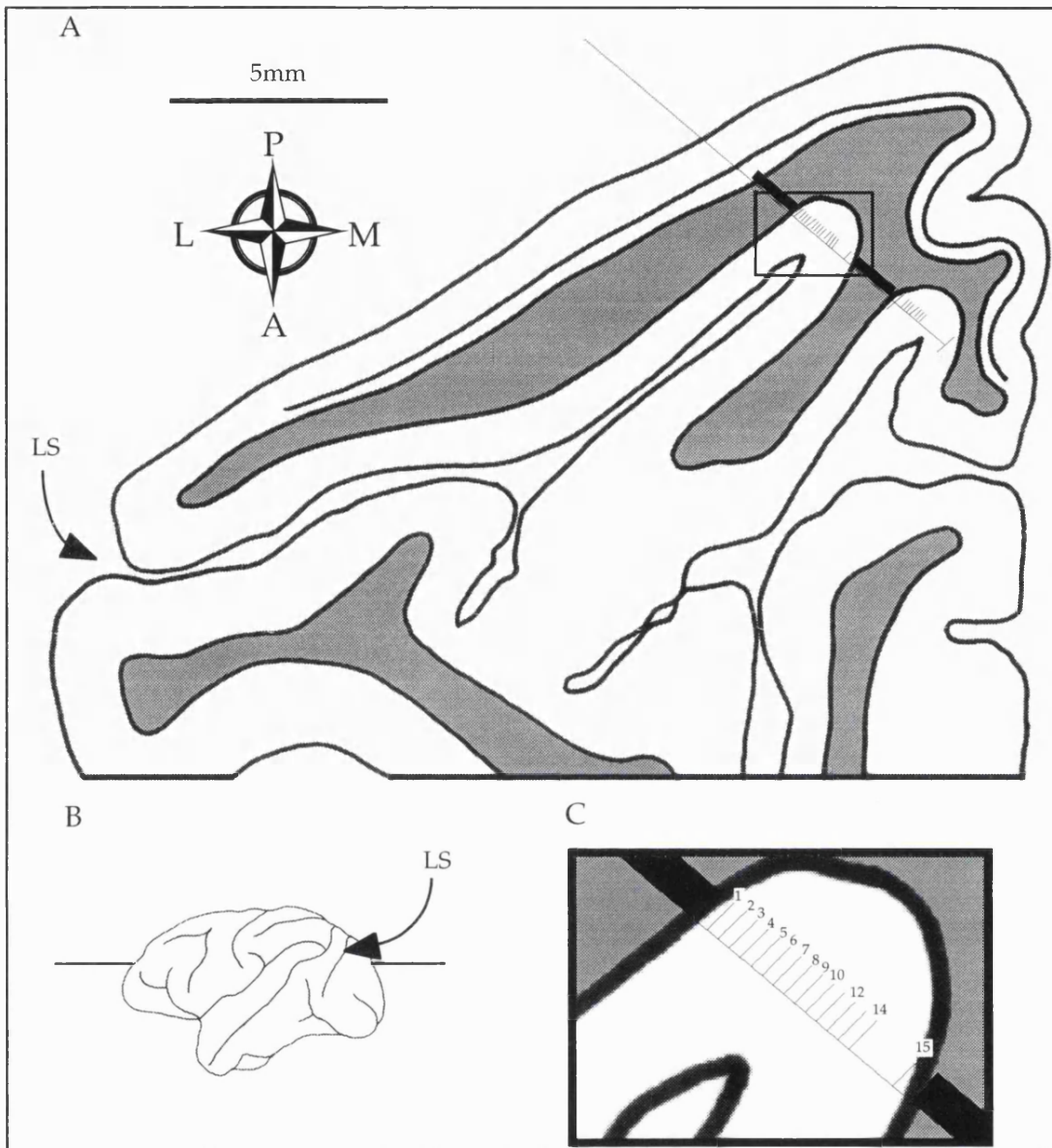
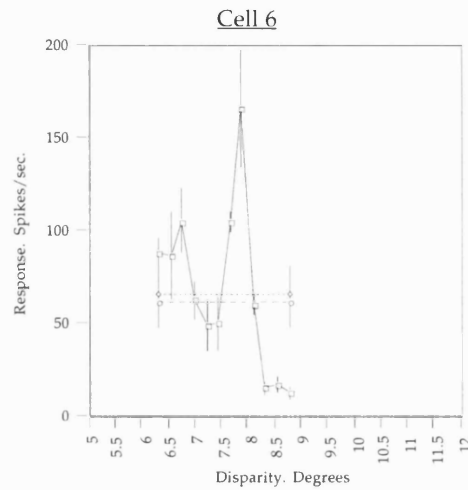
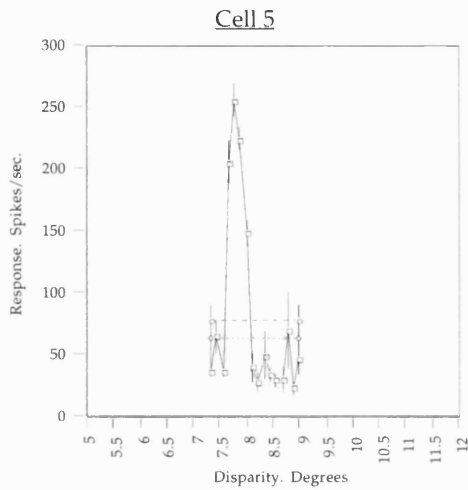
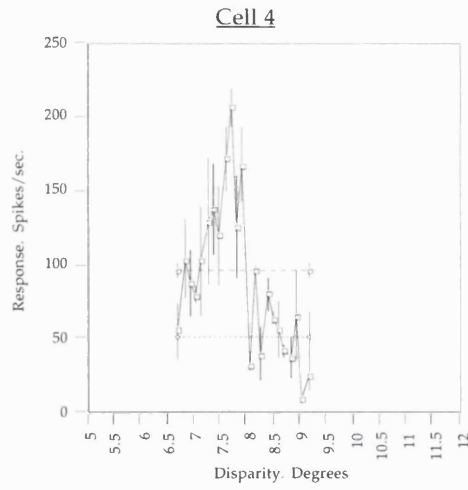
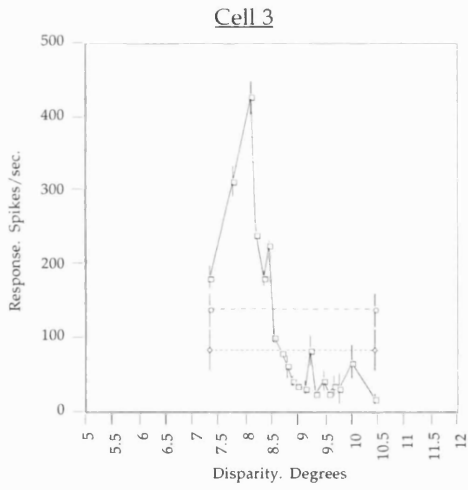
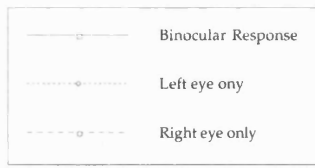
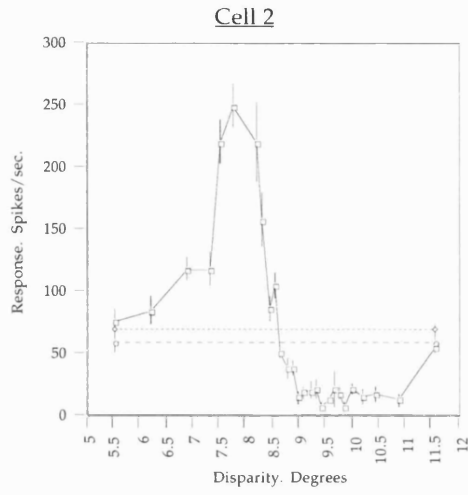
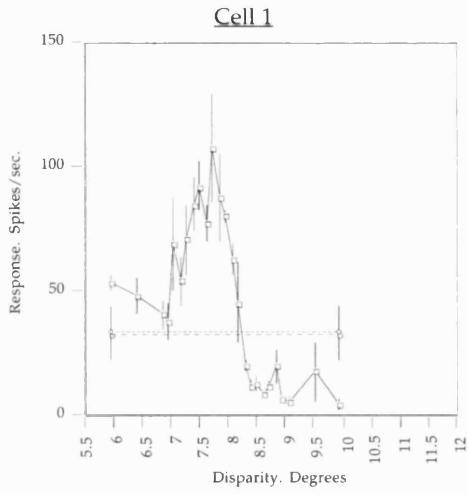


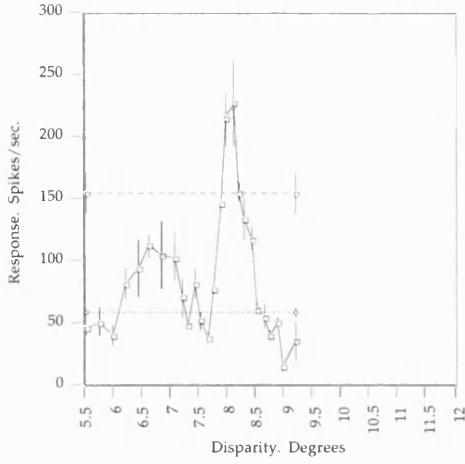
Figure 38.

Reconstruction of an electrode track in the right hemisphere of a brain (VG52). The track is drawn onto an horizontal section. Layer 4C in the striate cortex is shown and white matter is represented in grey. The track runs in an horizontal plane at the dorso-ventral level shown in 37b. The part of the track in the fundus of the lunate sulcus has been boxed and expanded to show the individual cells recorded from in that area.

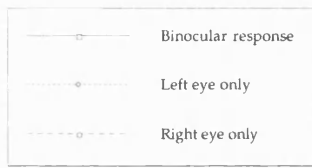
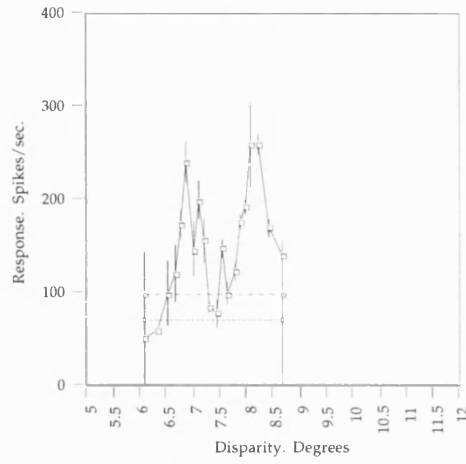
At the start of the penetration the angle is nearly normal and at the centre of the cortex it is travelling tangentially. As the electrode reaches the white matter its angle becomes more normal again. The cells recorded from in this part of the cortex have been numbered from 1 to 15 and their disparity tuning curves and orientation tuning polar plots are shown on the following pages.



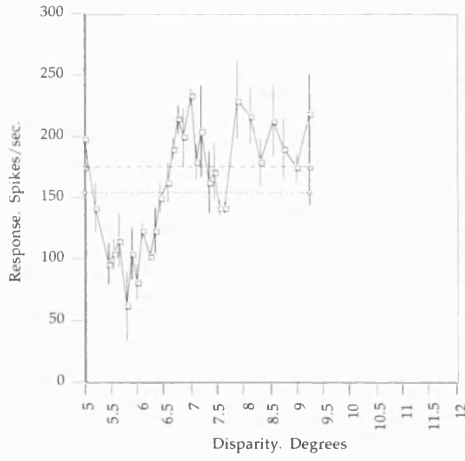
Cell 7



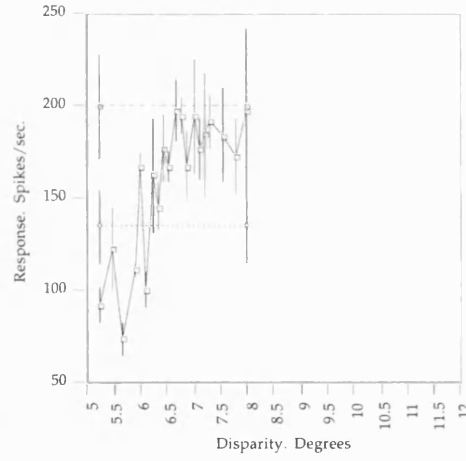
Cell 8



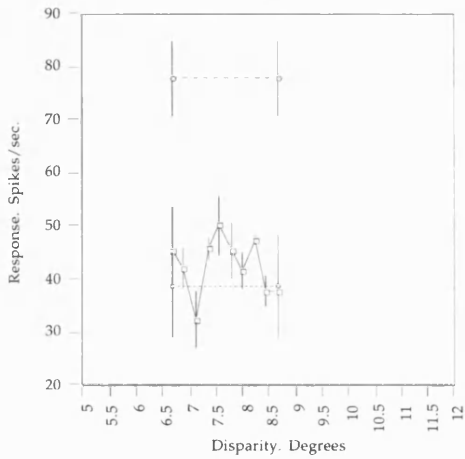
Cell 9



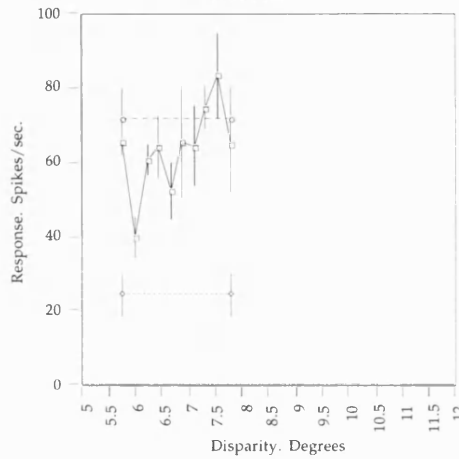
Cell 10



Cell 13



Cell 14



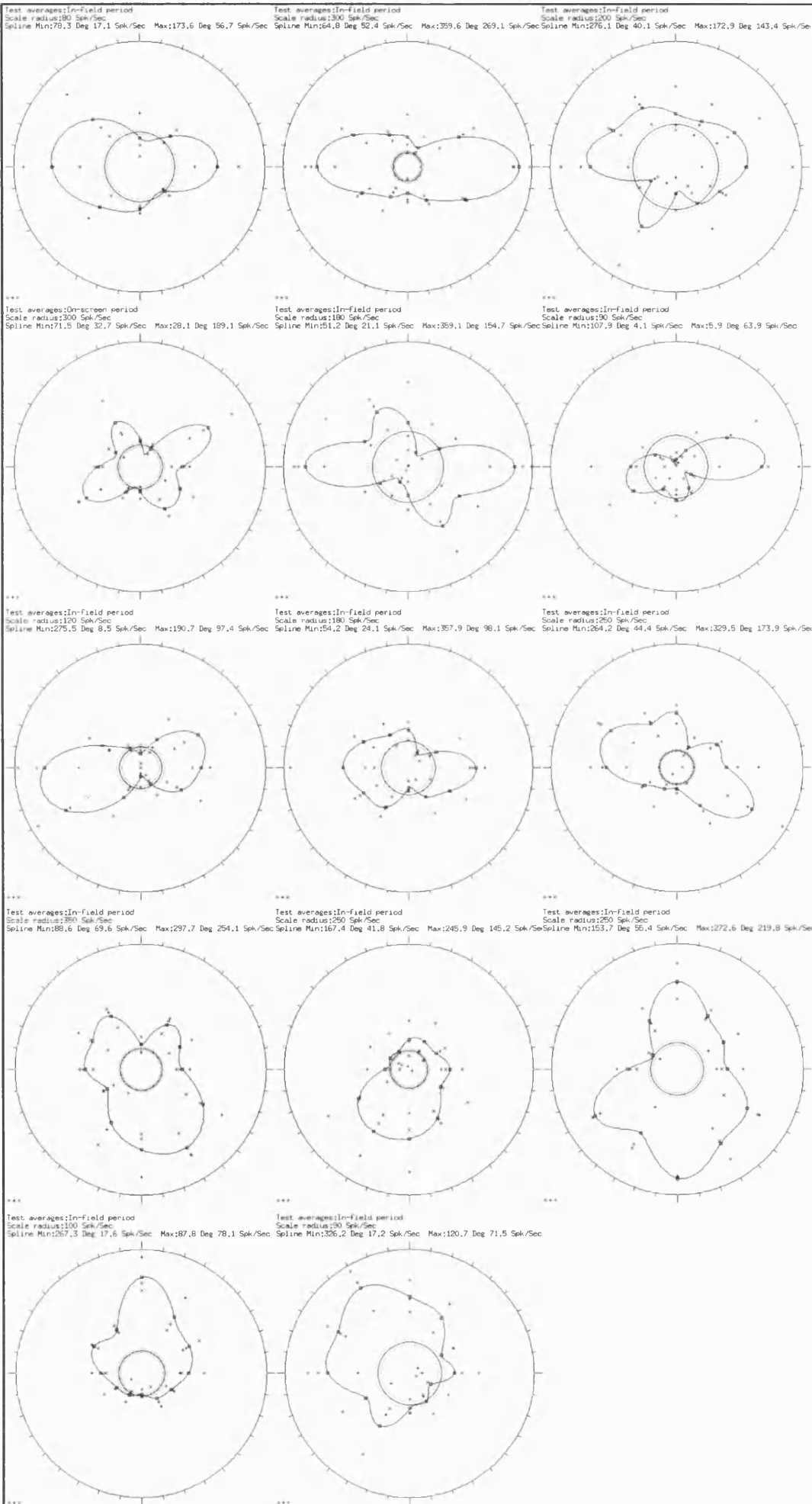


Figure 39 (previous page)

Polar plots of orientation tuning for cells in V3 of the brain VG52. Each plot is from a consecutive cell as shown in figure 38.

This sequence is represented in figure 40 which is an illustration of the area in question with the electrode track drawn on, the cells are shown at their correct positions and are represented by symbols to denote their orientation preference and disparity tuning category. The preferred orientation of the cells changes the most from cell to cell at the apex of the fold in cortex in accordance with previous studies. The disparity tuning category of the cells changes the most in the same location suggesting that this property has a similar functional organization to that of orientation tuning.

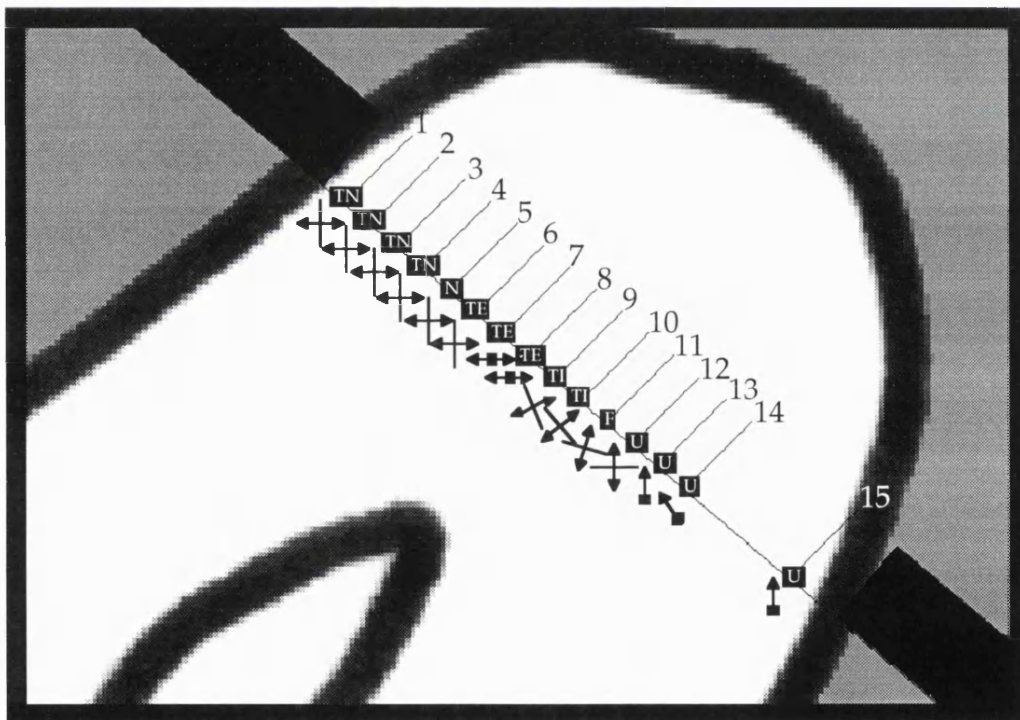


Figure 40.

The fundus of the lunule sulcus of the brain represented in figure 38. The positions of cells are represented by lines perpendicular to the electrode track and their orientation selectivity is represented by lines or spots at the appropriate orientation with arrows to denote their direction selectivity (a double headed arrow represents no directional bias). The cells' disparity tuning categories are also shown: TN = Tuned near, N = near, TE = Tuned excitatory, F = far and U = Untuned.

The disparity tuning profiles of cells 6, 7 and 8 appear to have two peaks; it is possible that is a novel type of disparity tuned cell which will be discussed later (see discussion). Also, the orientation tuning curves of cells 4 and 5 have two peaks, this type of cells has been found in previous studies (see discussion).

### Comparison with V2

A similar analysis of electrode tracks was done on the area V2. Since the proportion of disparity tuned cells is much smaller in V2 than in the V3 complex, there are fewer electrode tracks containing disparity tuned cells. Previous studies have shown that disparity tuned cells are present mostly in V2's thick cytochrome oxidase stripes (Burkhalter and Van Essen 1982; Burkhalter and Van Essen 1986; Livingstone and Hubel 1988) so much so, that Livingstone *et al.* called them "disparity stripes". Disparity selective cells have also been found in thin stripes but here they are in the minority. Figure 41 shows a long electrode penetration through V2 which passes serially through a number of cytochrome oxidase stripes.

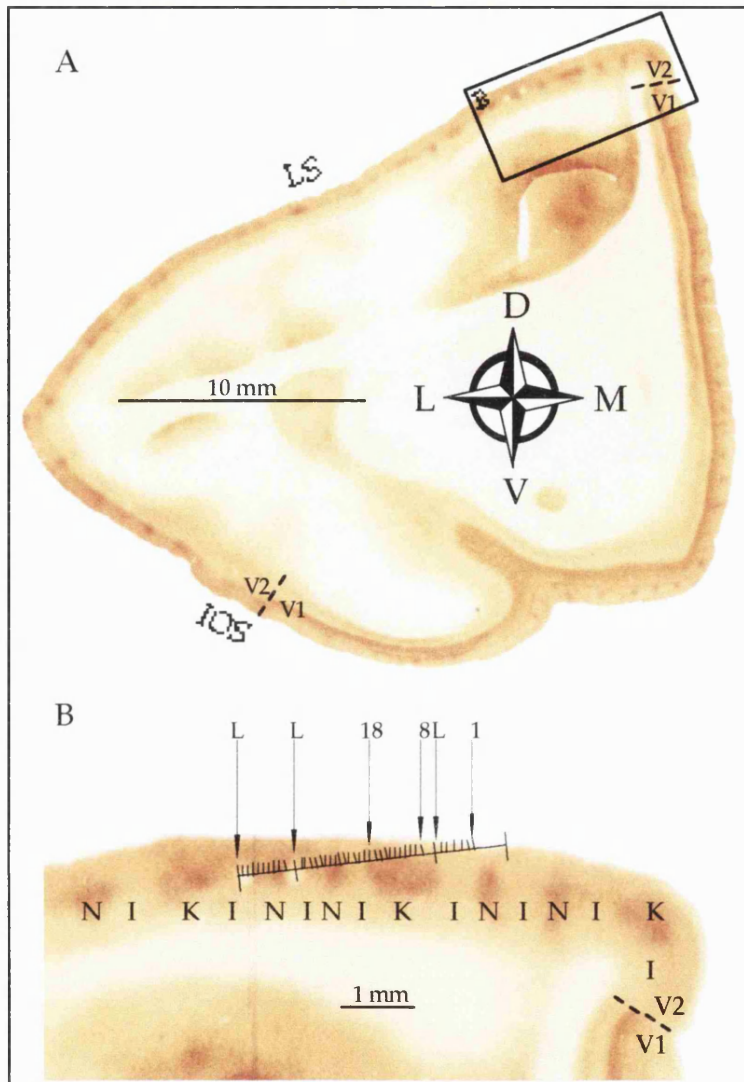


Figure 41.

A) A flat mounted section through the operculum of a left hemisphere stained for the enzyme cytochrome oxidase to reveal the stripes in V2 and the darkly stained layer 4C and blobs in V1.

B) The part of the section shown boxed in (A). The line represents the passage of an electrode with the short lines denoting the positions of cells recorded from. Longer lines (labelled "L") show the positions of electrolytic lesions, two of which can be seen on the section as light circular marks. The electrode passed serially through a number of stripes. N = Thin stripe, I = Interstripe and K = Thick stripe. Cells 8-18 fall within a thick stripe and are disparity tuned (see figure 42 for their disparity tuning curves.)

The extent of disparity tuned cells (cells 8-18) coincide with the boundaries of a thick cytochrome oxidase stripe. Figure 42 shows the disparity tuning curves for cells 8-18: the only disparity tuned cells found in this penetration.

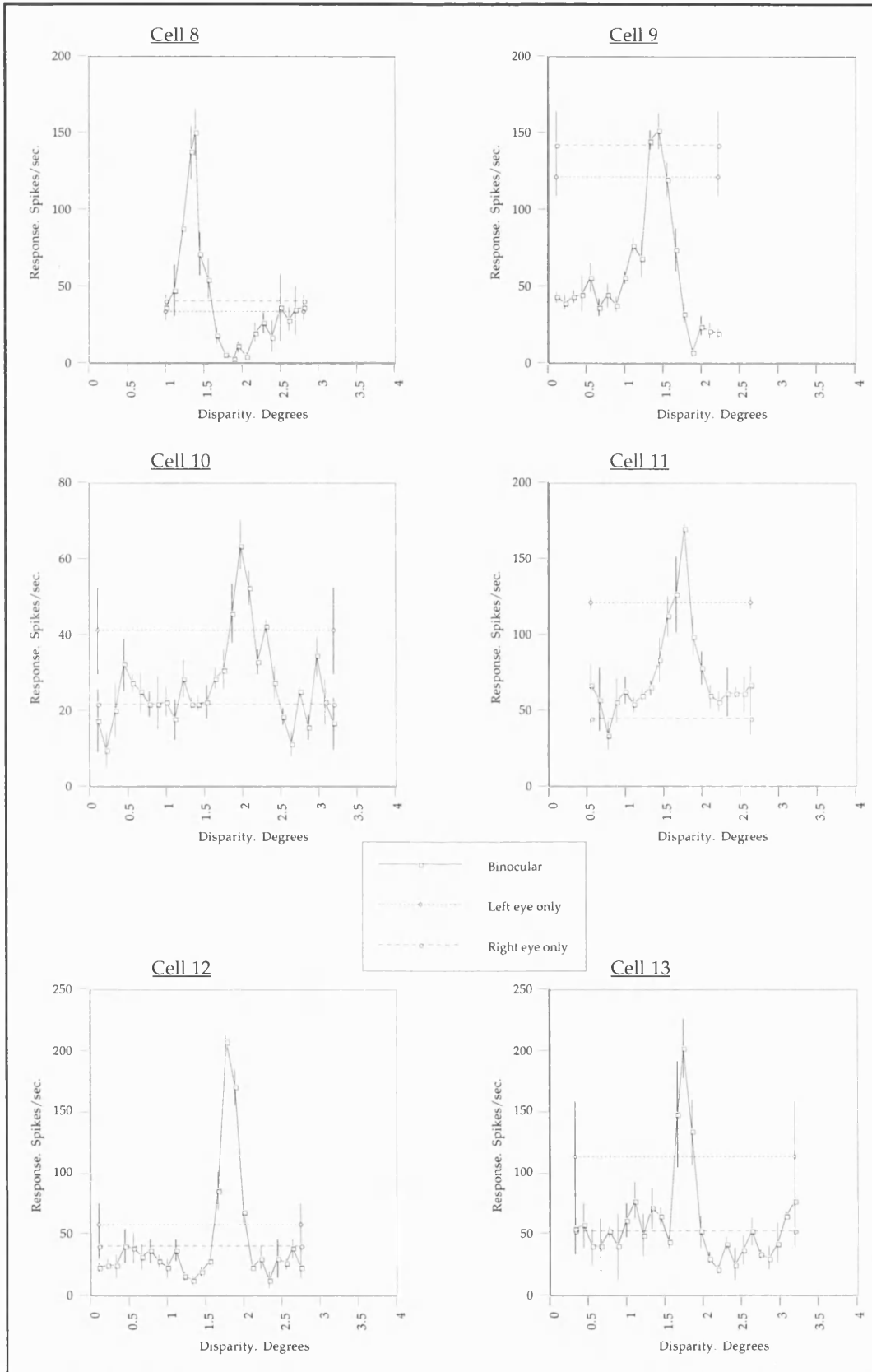


Figure 42 (continued overleaf.)

Disparity tuning curves for the cells in a thick stripe of V2 shown in figure 41. Error bars are standard errors. Average response to a monocularly presented stimuli are shown as horizontal lines.

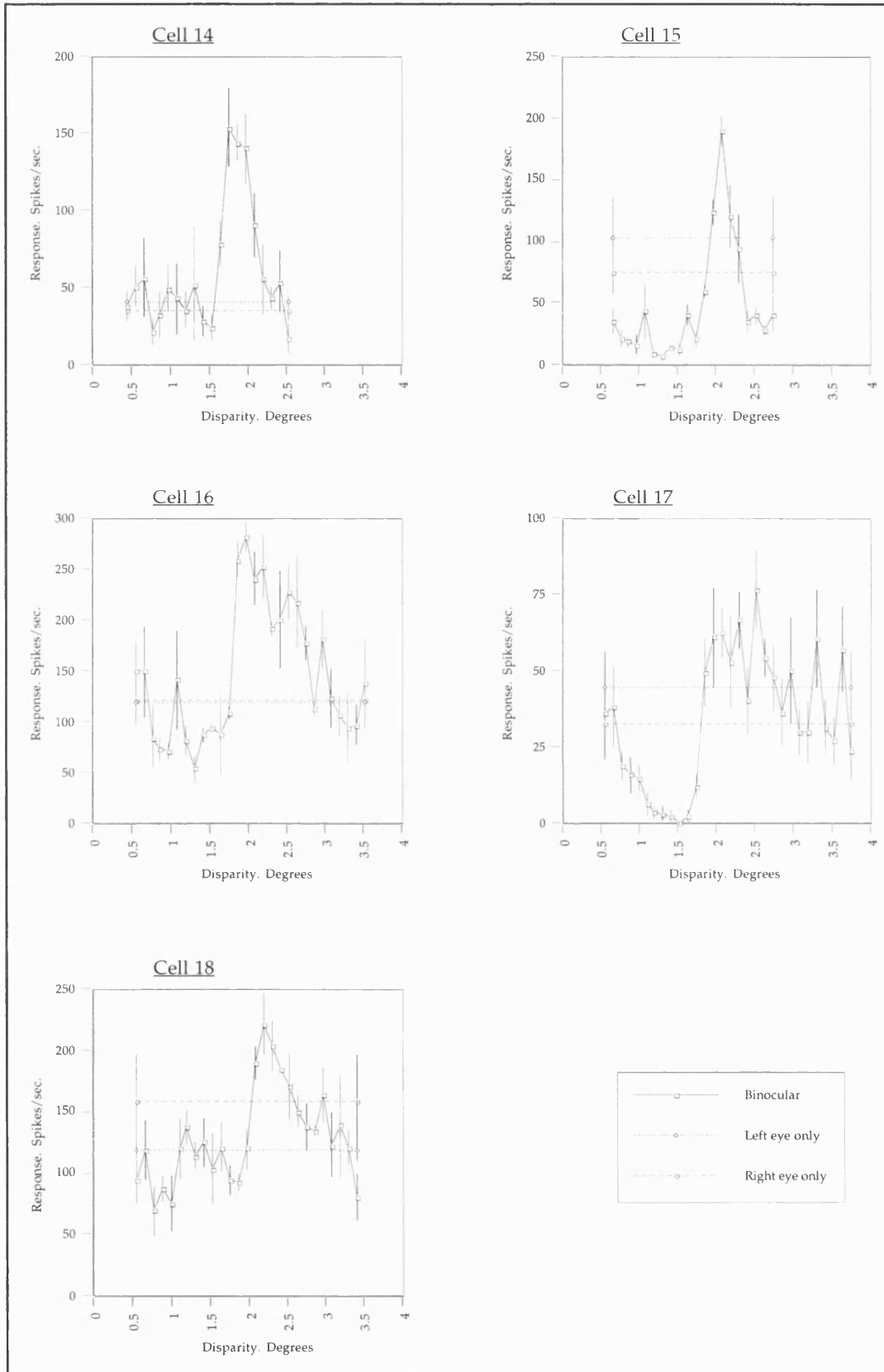


Figure 42

The sequence of disparity tuned cells in this V2 penetration runs as follows:

Cells 8-9 TN.

Cells 10-15 TE.

Cells 16-18 Far.

It appears that in V2 similar disparity tuned cells are clustered within the thick stripes, however, not enough penetrations were made in this study to discover whether these clusters form cortical columns in V2 as they do in the V3 complex.

## **Section 2:**

### **Anatomical Data:**

#### **Introduction**

The V3 complex's most prominent functional feature is the predominance of orientation selectivity (Zeki 1978b; Burkhalter *et al.* 1986). Given that orientation selectivity is also a dominant feature in other visual areas, it becomes naturally interesting to ask how the output of the cells in V3 and V3A differs from the output of cells in other areas with similar functional properties. The first step in such an analysis, and the simplest, is to trace the anatomical outputs from these areas.

This section will be subdivided, each division describing the projections from a particular area that has been injected. Here I shall describe the location of transported WGA-HRP to various predefined brain areas. I shall describe the functional properties and significance of the projections to these areas in the discussion section. The anatomical study is based on a total of 6 monkeys, 1 of which received an injection into V3, 3 into V3a (1 medial and 2 lateral), 2 into the dorsal prelunate area (DP). The aim of tracing the cortical connections of these areas was to elucidate the circuitry that connects the V3 complex to parietal and temporal "higher" areas, where the form and disparity information, processed in the V3 complex, may be further analysed and representations of three dimensional space produced so that depth information can be made use of by perceptual and motor systems.

### Description of the visual areas

The locations of the visual areas of the macaque monkey visual cortex have been determined by a number of techniques including receptive field mapping (Zeki 1969; Van Essen and Zeki 1978), callosal connections (Zeki and Sandeman 1976; Van Essen and Zeki 1978; Van Essen *et al.* 1982) myelin staining (Von Bonin *et al.* 1942; Van Essen *et al.* 1981; Desimone and Ungerleider 1986) cytochrome oxidase staining and single unit recording (Zeki 1978a). Thus, a number of maps have been produced by different investigators. Although some of these maps differ in fine detail and terminology, the major divisions of the visual cortex are quite well agreed upon. An individual brain area can generally be defined as one which has a distinct function, such as vision or audition, or a distinct architecture, and preferably both. More specifically, a single visual area can be considered autonomous if it contains a representation of the visual hemifield (with a fine or coarse topography) and its cells have a common functionality. In addition, some areas, for example V5, have a particular myelo- cyto- or cytochrome oxidase architecture. However, exceptions to this definition exist, archetypally V1 and V2, which contain subdivisions which together could themselves be defined as individual areas. For instance, in V2 all the different types of cytochrome oxidase stripe each contain a separate map of the visual field (Zeki and Shipp, personal communication) and cells which differ in their functional properties (Zeki and Shipp 1987; Livingstone and Hubel 1988), yet V2 is considered a single area.

The principle plane of section in these studies was horizontal. However, the use of computer brain reconstructions allows one to show sections in any plane by placing "virtual" cutting planes through 3D reconstructions. Thus, whole 3D brain reconstructions are presented,

along with coronal and horizontal sections, all showing the density of transported tracing agents to areas of interest. The same computerized technique allows the production of 2D reconstructions that present the cortex as if it had been unfolded, these reconstructions are of particular use for examining the tangential distribution of label hidden within sulci.

### Injection sites

The sites of injection of WGA-HRP are represented in figure 43. This figure shows a cut-away view of the anterior bank of the lunate sulcus. The injection sites are drawn on with reference to the 3D reconstructions of each injected brain. The two most dorsal sites shown in red and green are those of the brains MP2 and MP3 respectively, and are on the dorsal part of the prelunate gyrus (DP). The yellow, cyan and magenta injections sites are those of brains SP14, SP15 and SP28 respectively and lie within the borders of V3A on the anterior bank of the lunate sulcus. The site shown in blue is that of brain SP44 and, being located at the fundus of the lunate sulcus, lies within area V3 proper.

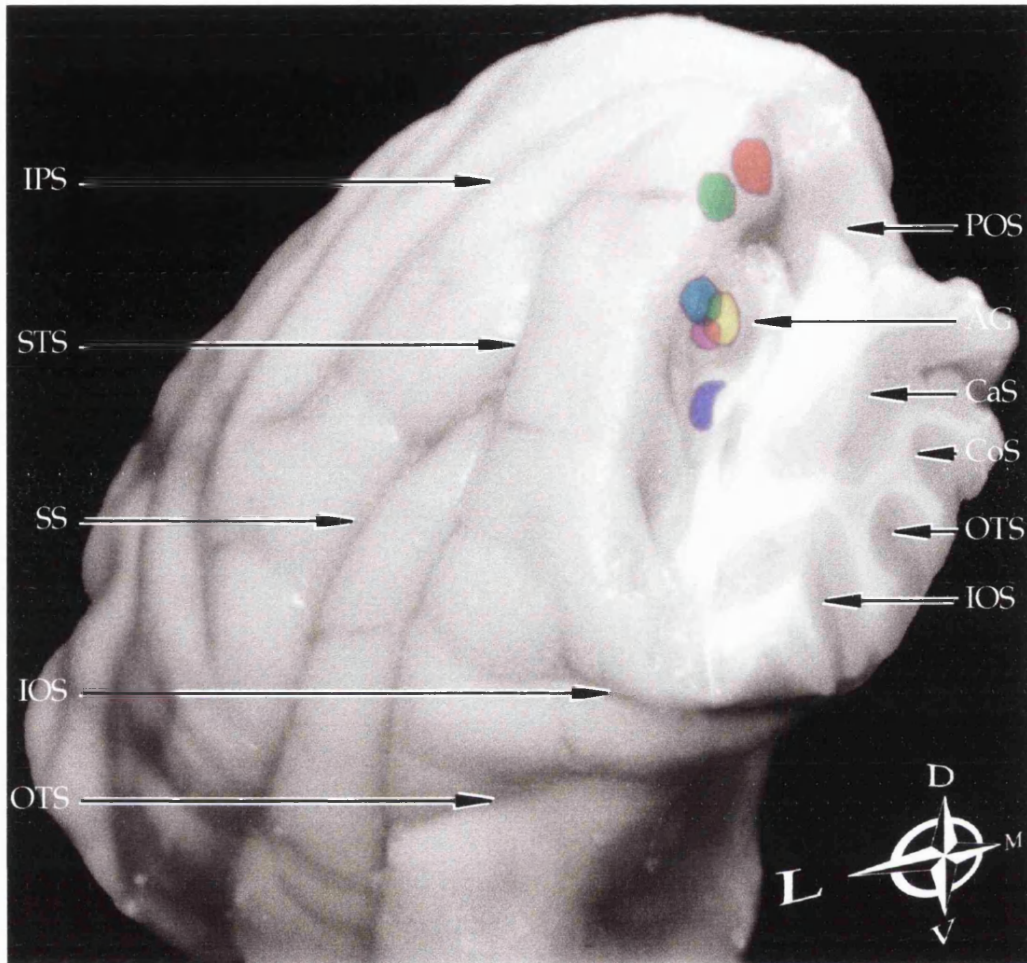


Figure 43.

A photograph of a macaque monkey's left hemisphere with the cortex posterior to the lunate sulcus removed to expose its anterior bank. The positions of the six injections used in this study are shown as coloured patches superimposed onto the brain.

Red = MP2  
 Green = MP3  
 Yellow = SP14  
 Cyan = SP15  
 Magenta = SP28  
 Blue = SP44

AG = Annectant gyrus; CaS = Calcarine sulcus; CoS = Collateral sulcus; IOS = Inferior occipital sulcus; IPS = Intra-parietal sulcus; OTS = Occipito-temporal sulcus; POS = Parieto-occipital sulcus; SS = Sylvian sulcus; STS = Superior temporal sulcus.

### .c2.Cortical projections of V3.

I shall begin with a description of a brain with an injection into area V3 at the fundus of the lunate sulcus (SP44). The operculum of this brain was removed prior to sectioning so that the distribution of label within the subdivisions of V2 and V1 could be analysed. In order to make comparisons between all of the brains to be described here,

standard 2D and 3D reconstructions have been made for each. The 2D reconstruction is shown in figure 44 for this brain. The area represented in the reconstruction is shown shaded in the whole brain drawing and includes the entire superior temporal sulcus (STS), the lunate sulcus (LS), the inferior occipital sulcus (IOS) and the cortex between these sulci: prelunate gyrus (PLG) and inferior temporal cortex (ITC). On the 2D reconstruction, shaded areas are those hidden within the depths of sulci and unshaded areas represent cortex on the surface of the brain. The dot density represents the density of transported WGA-HRP, the solid black area represents the injection site. The 3D reconstruction of this brain is shown in figure 45. This reconstruction was prepared by stacking the drawn out-lines of the cortical layer 4. Horizontal and coronal sections have been taken from the reconstruction to show the location of the injection site and patches of transported label. Since the operculum of this brain was removed prior to sectioning, the coronal section "D" of figure 44 is not complete.

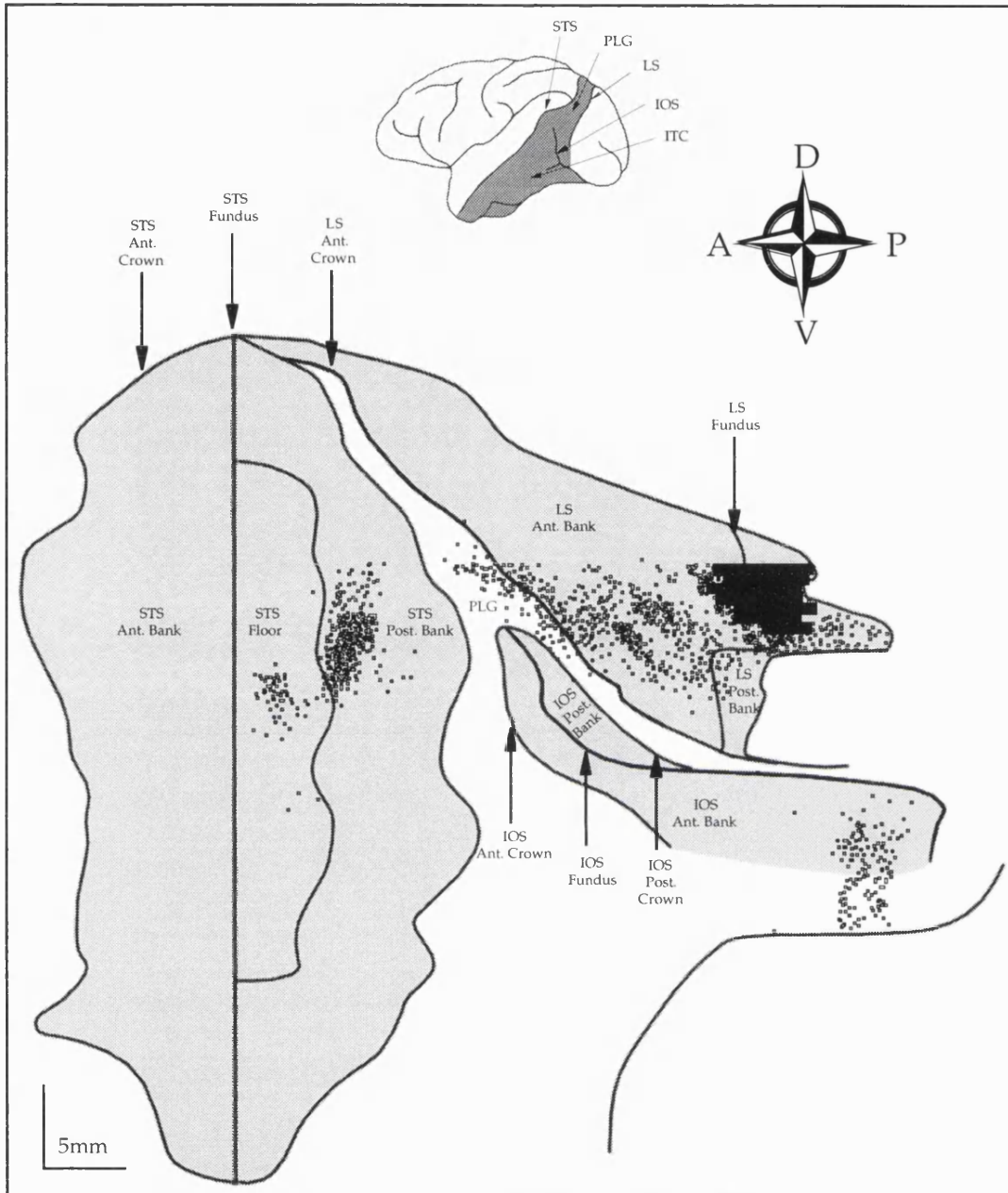


Figure 44.(SP44)

2D reconstruction of the prestriate area shaded on the whole brain drawing. The superior temporal, lunate and inferior temporal sulci (STS, LS and IOS) have been opened and their banks are shown shaded. The HRP-WGA injection site is shown as solid black bars and its transport as small open squares. PLG = prelunate gyrus; ITC = inferior temporal cortex.

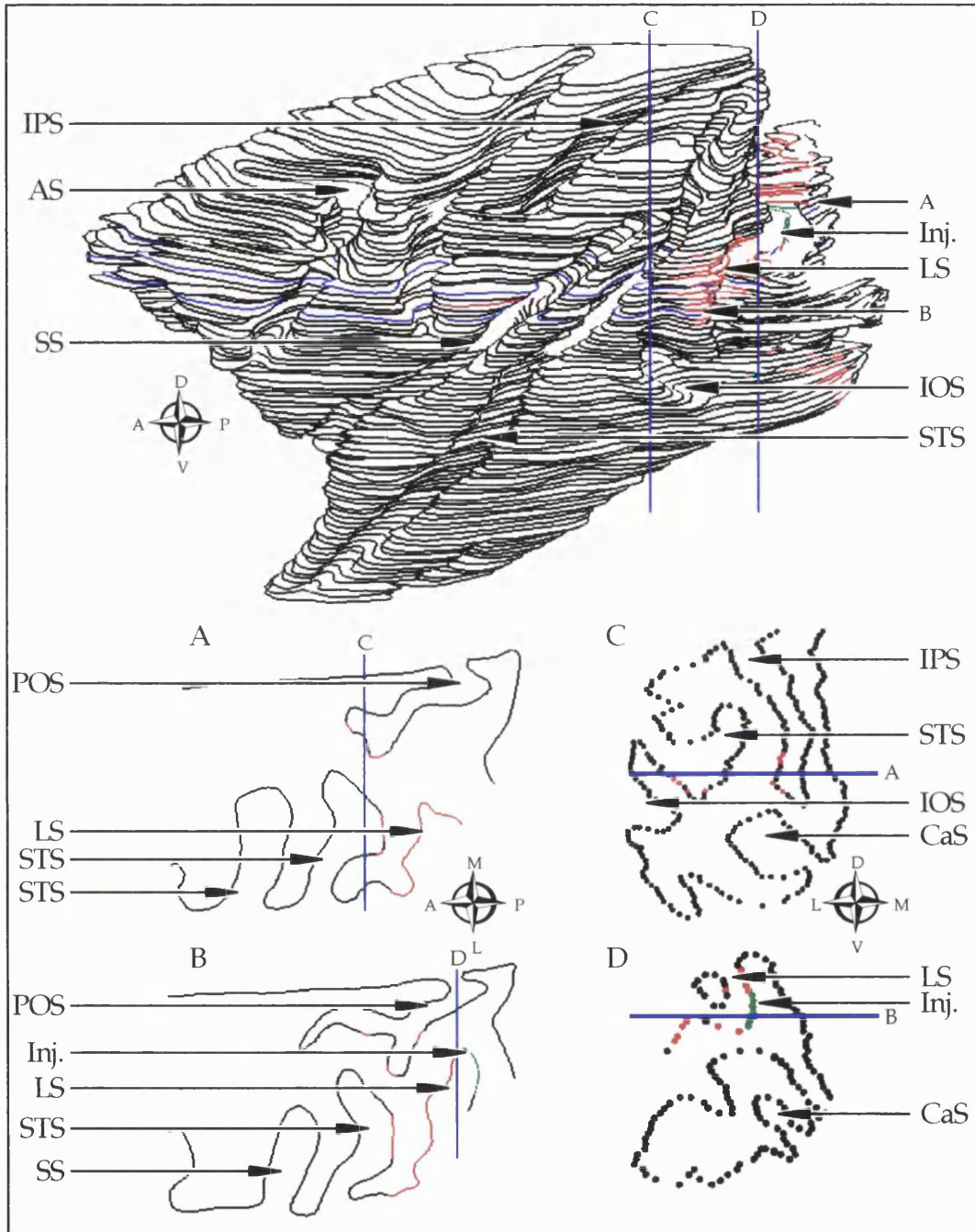


Figure 45. (SP44)

3D reconstruction of a brain injected with WGA-HRP into V3 at the fundus of the lunate sulcus. The whole brain reconstruction is shown with the levels of two horizontal sections (A and B) and two coronal sections (C and D). Abbreviations are as follows: AS = Arcuate sulcus. CaS = Calcarine sulcus. Inj. = Injection site. IOS = Inferior occipital sulcus. IPS = Intra parietal sulcus. LS = Lunate sulcus. OTS = Occipito temporal sulcus. POS = Posterior occipital sulcus. SS = Sylvian sulcus. STS = Superior temporal sulcus. The injection site is shown in green and areas of transported WGA-HRP are shown in red. Blue lines represent the planes of section

The locations of patches of label lying on the surface of the brain can be more easily located in the 3D reconstruction of the whole brain. The area of label that lies on the crown of the LS can be seen as well as the patch in the POS. Horizontal and coronal sections through the injection site are shown to illustrate its location and the location of the patches of transport in the dorsal prelunate gyrus (PLG) and inferior temporal cortex (ITC).

Examination of these reconstructions reveal a number of distinct patches of transport:

a) V3 complex.

There are two islands of dense transport in the anterior bank of the lunate sulcus (LS) these falling within an almost continuous spread of label at the same dorso-ventral level (but separated from) the injection site. This spread of label in the anterior bank of the LS culminates in a denser dorso-ventral stripe of label at the crown of the LS. Label in the anterior bank of the LS lies within V3A. Transport was also observed in the parieto-occipital sulcus (POS) and comprises two parallel dorso-ventral stripes running from the depths of the posterior bank of the POS to terminate on the surface of the brain ventral to the POS. These patches of transport are within parts of the POS where the lower field representations of V3 and V3A are located (Zeki 1977b; Zeki 1978b).

b) V4.

Label in the prelunate gyrus was restricted to a considerable ventral patch that formed a continuous spread into the lunate sulcus to the injection site, visible in the 2D and 3D reconstructions of SP44. The portion of this label that lies on the surface (the prelunate gyrus) is well

within cortex defined as V4 (Zeki 1977a), an area closely associated with colour vision (Zeki 1973; Zeki 1978a). No label was observed in more dorsal parts of the prelunate gyrus (DP).

c) V5 complex.

In the superior temporal sulcus (STS) there are patches of label that can be subjectively divided into three areas, two in the floor of the sulcus and one (larger and more dense) in the posterior bank. The latter patch is well within cortex defined as area V5 and the smaller two patches are in areas that correspond to V5A (MST) and FST.

d) Intraparietal sulcus.

Label was found in the lateral bank of the intraparietal sulcus, visible in coronal section C and horizontal section B of the 3D reconstruction of SP44. This portion of the IPS is posterior to area LIP (Andersen *et al.* 1985). Recently, this part of the IPS was found to contain axis orientation selective (AOS) cells (Kusunoki *et al.* 1993) and surface orientation selective (SOS) cells (Shikata *et al.* 1996). A smaller patch of label was also seen nearer the fundus of the IPS, which appears to be too far posterior to be within the area VIP (Colby *et al.* 1993).

e) V2.

Figure 46 shows the distribution of labelled cells in V2. Figure 46a is the whole operculum stained for cytochrome oxidase so that the stripes can be visualized. The part of V2 corresponding to the projection zone from the V3 injection is shown larger in 46b. Figure 46c is a dark field photograph a neighbouring section stained for WGA-HRP; stained cells appear as white patches in the cortex. The stripes are superimposed onto the section stained for WGA-HRP from those stained for cytochrome

oxidase so that the distribution of label within the different stripe compartments of V2 could be elucidated. This shows that the majority of labelled cells fall within the thick cytochrome oxidase stripes of V2. However, the injection is within the part of V3 where upper visual field is represented (Zeki 1977b; Zeki 1978b) and this patch of transport is within V2's Lower field representation in the LS (Zeki and Sandeman 1976; Gattass *et al.* 1981). This patch of labelled cells provides evidence for a lower or mixed field representation within lateral V3.

Figure 46. (Overleaf)

A) A flat mounted operculum section stained for the enzyme cytochrome oxidase so that V2's stripes and V1's blobs can be visualized.

B) Part of the section of A which projects to the V3 injection site.

C) The same part of the section shown in B, stained for HRP. The positions of the cytochrome oxidase stripes have been superimposed. K (Red) = Thick stripe. N (Green) = Thin stripe. I = Interstripe. LS = Lunate sulcus. IOS = Inferior occipital sulcus. CaS = Calcarine sulcus.

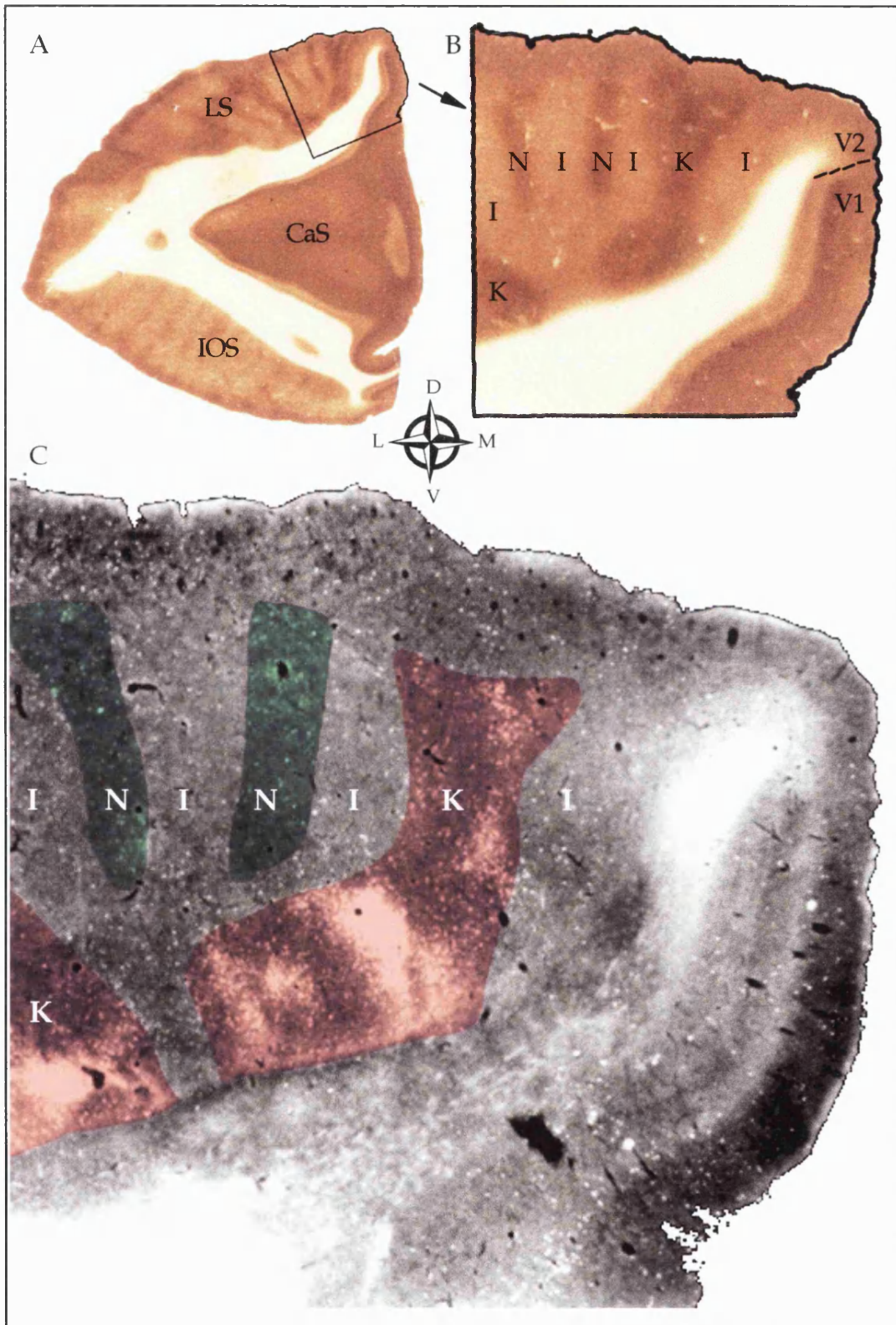


Figure 46. (See previous page for legend.)

### The projections of V3A

Here I shall describe the pattern of transport following injection of WGA-HRP into the anterior bank of the lunate sulcus starting with brain SP28. The 2D and 3D reconstructions for this brain are shown below.

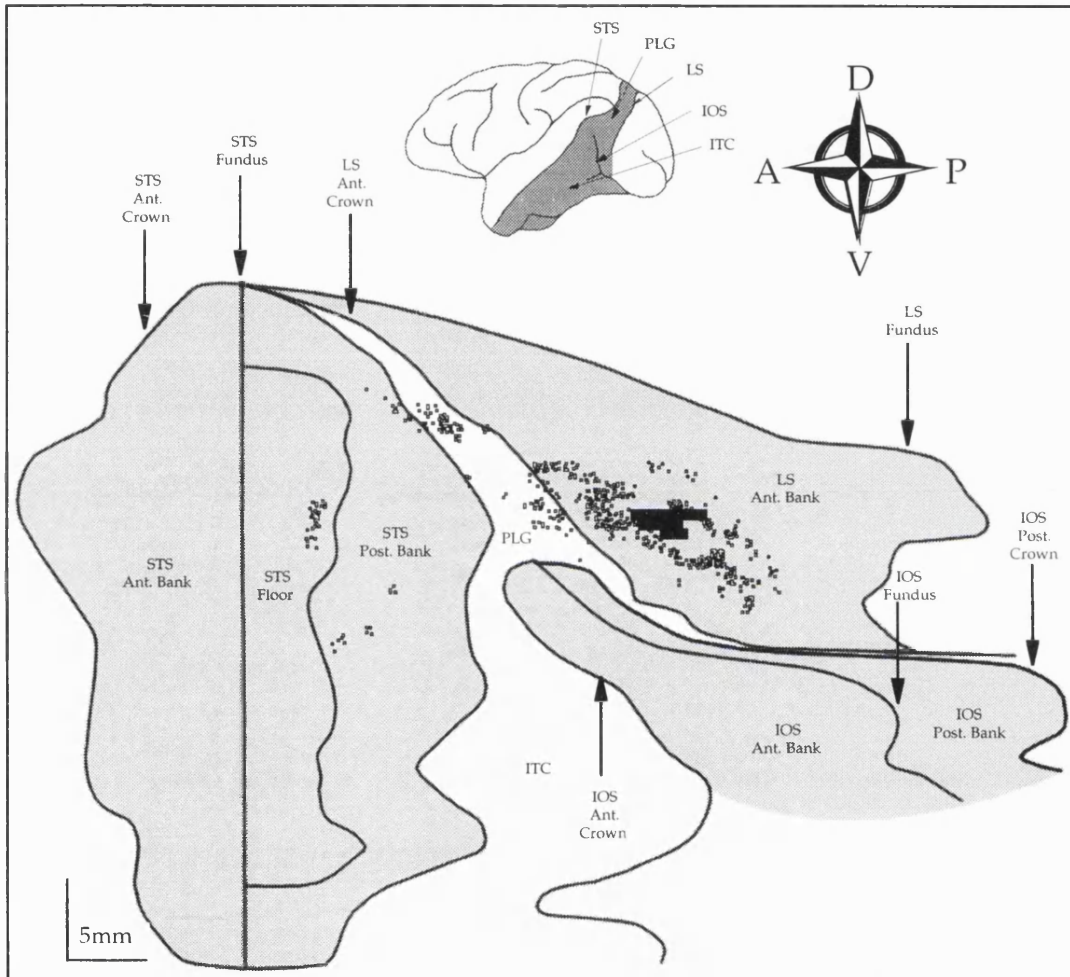


Figure 47. (SP28)

2D reconstruction of the prestriate area shaded on the whole brain drawing. The superior temporal, lunate and inferior temporal sulci (STS, LS and IOS) have been opened and their banks are shown shaded. The HRP-WGA injection site is shown as solid black bars and its transport as small open squares. PLG = prelunate gyrus; ITC = inferior temporal cortex.

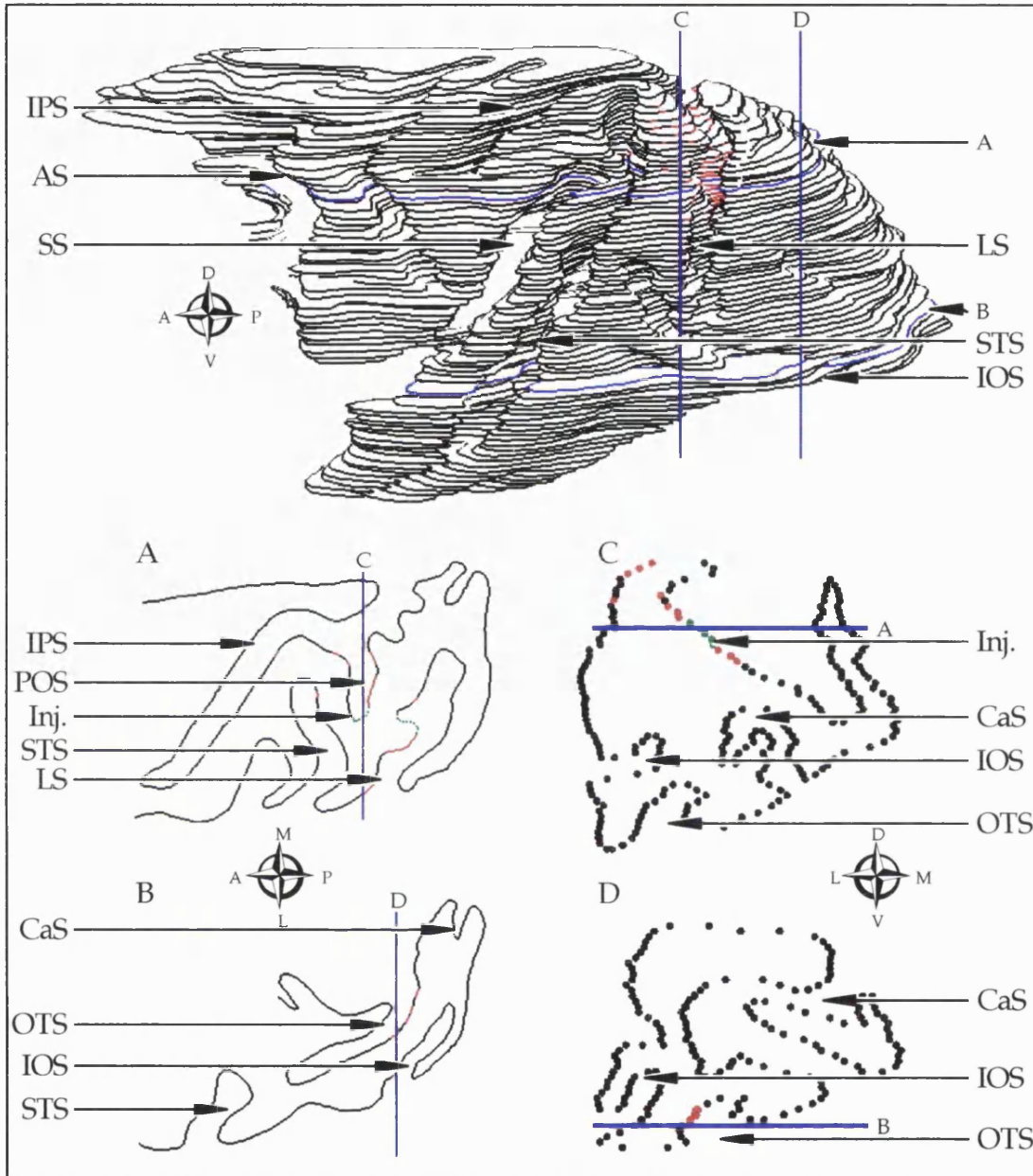


Figure 48. (SP28)

3D reconstruction of a brain injected with WGA-HRP into the anterior bank of the lunate sulcus at the level of the annectant gyrus spreading across white matter and into the posterior bank of the POS. The whole brain reconstruction is shown with the levels of two horizontal sections (A and B) and two coronal sections (C and D). Abbreviations are as follows: AS = Arcuate sulcus. CaS = Calcarine sulcus. Inj. = Injection site. IOS = Inferior occipital sulcus. IPS = Intra parietal sulcus. LS = Lunate sulcus. OTS = Occipito temporal sulcus. POS = Posterior occipital sulcus. SS = Sylvian sulcus. STS = Superior temporal sulcus.

The injection site is shown in green and areas of transported WGA-HRP are shown in red. Blue lines represent the planes of section.

The injection site was located within the annectant gyrus so that it involved the anterior bank of the lunate sulcus, the annectant gyrus and the posterior bank of the parieto-occipital sulcus, cortical zones which fall wholly within V3A although V3A extends beyond these limits, (Van Essen and Zeki 1978; Zeki 1978b). The injection occupied 2.66 mm<sup>2</sup> of cortex within V3A.

a) V2.

Label was seen in the posterior bank of the lunate sulcus. This was limited to the most dorsal sections and the more medial of the two patches there was within the lower field representation in V2, at the V1-V2 border. This corresponds to transport from the lower field representation within medial V3A which received part of the injection. There was an extensive band of label in the posterior bank of the occipito-temporal sulcus visible in sections B and D of the 3D reconstruction. This consists of several independent patches and lies within the upper field representation of V2. Since the injection was within upper and lower field representations of V3A, it is unsurprising that V2's label also encroaches on both upper and lower field representations.

b) V3 complex.

On the anterior bank of the lunate sulcus, label was seen spreading away from the injection site to form several 'fingers' of transport visible in the 2D reconstruction. These patches of transport lie within area V3A. Within the medial part of the V3 complex, label was seen on parts of the posterior bank of the POS corresponding to V3A and V3 proper, these patches can be seen in sections A and C of the 3D reconstruction.

## c) V4.

More ventrally on the prelunate gyrus there is another island of label measuring 2.5 mm<sup>2</sup>. This falls largely on the exposed surface of the prelunate gyrus and, like the more dorsal island, it is separated from the central large patch of label surrounding the injection site. This more ventral patch is most likely located within V4.

## d) The V5 complex.

Label appeared both in the posterior bank and the floor of the superior temporal sulcus, as is shown in the 2D reconstruction. The patches on the posterior bank and the floor of the STS correspond to similarly located patches in the previous brain (SP44) and although myelin stained sections were not available to verify that the patch on the posterior bank is within V5, the chances that this is so are high. The patch on the floor of the STS is most probably located within V5A (MST) or FST.

## e) DP.

At the most dorsal level there was label on the crown of the prelunate gyrus, visible in the 2D reconstruction. The 2D reconstruction shows this to be an island measuring 3.8mm<sup>2</sup> and separated from other zones of label. This is a zone corresponding to the area DP, which were injected in the brains MP2 and MP3 (see below).

f) The intraparietal sulcus

The small patch of transport visible in section A of the 3D reconstruction lies on the posterior part of the lateral bank of the IPS, within the area containing AOS and SOS cells (Kusunoki *et al.* 1993; Shikata *et al.* 1996) This area lies posterior to LIP on the lateral bank of caudal IPS (cIPS).

In another brain whose 2D and 3D reconstructions are illustrated in figures 49 and 50 (SP15), an injection had also been made into area V3A, though this was of smaller dimensions. In addition, it was restricted to the part of V3A located within the lunate sulcus on the lateral side of the brain and did not extend to the medial extension of V3A, as had the injection in brain SP28.

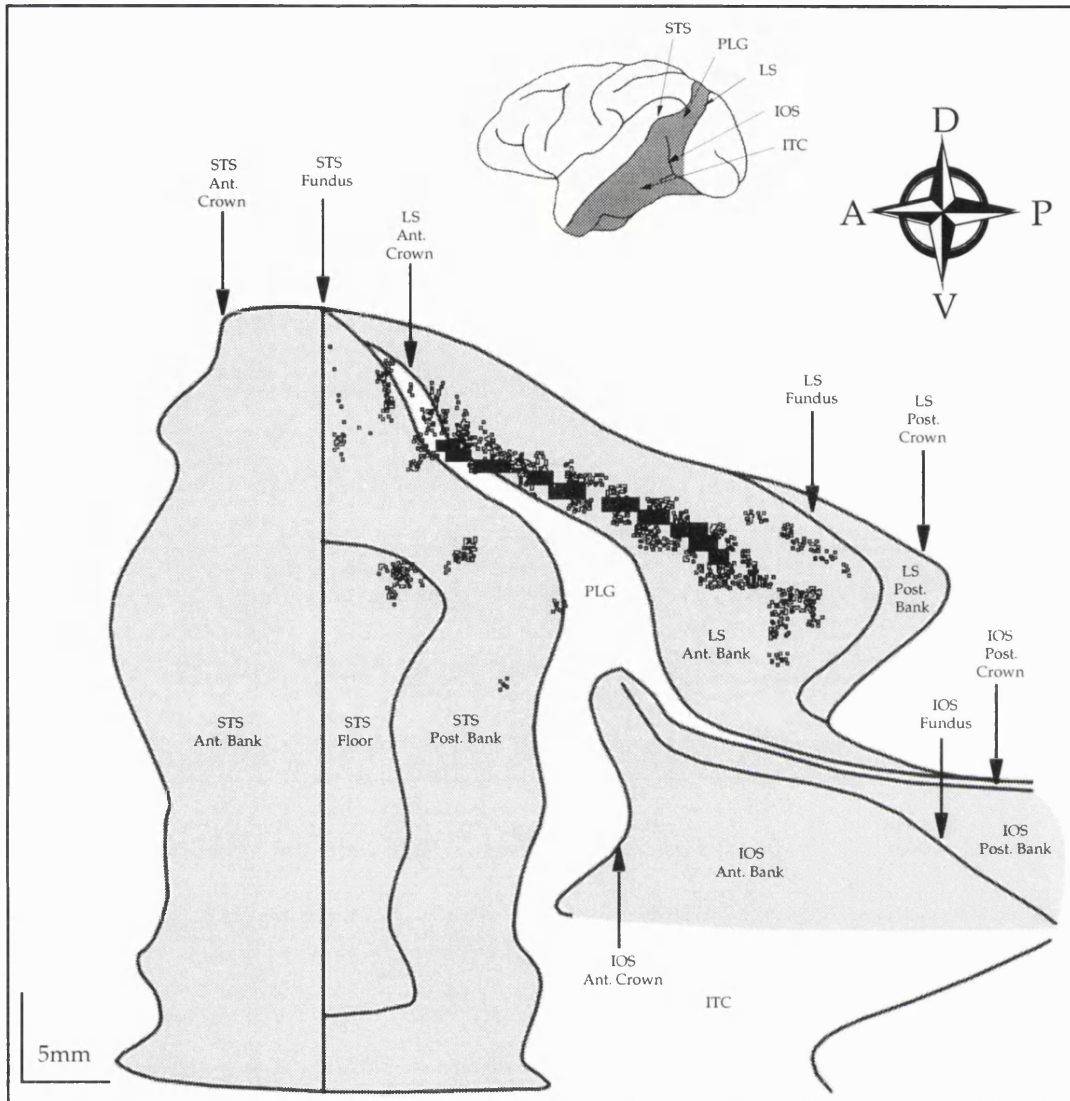


Figure 49. (SP15)

2D reconstruction of the prestriate area shaded on the whole brain drawing. The superior temporal, lunate and inferior temporal sulci (STS, LS and IOS) have been opened and their banks are shown shaded. The HRP-WGA injection site is shown as solid black bars and its transport as small open squares. PLG = prelunate gyrus; ITC = inferior temporal cortex.

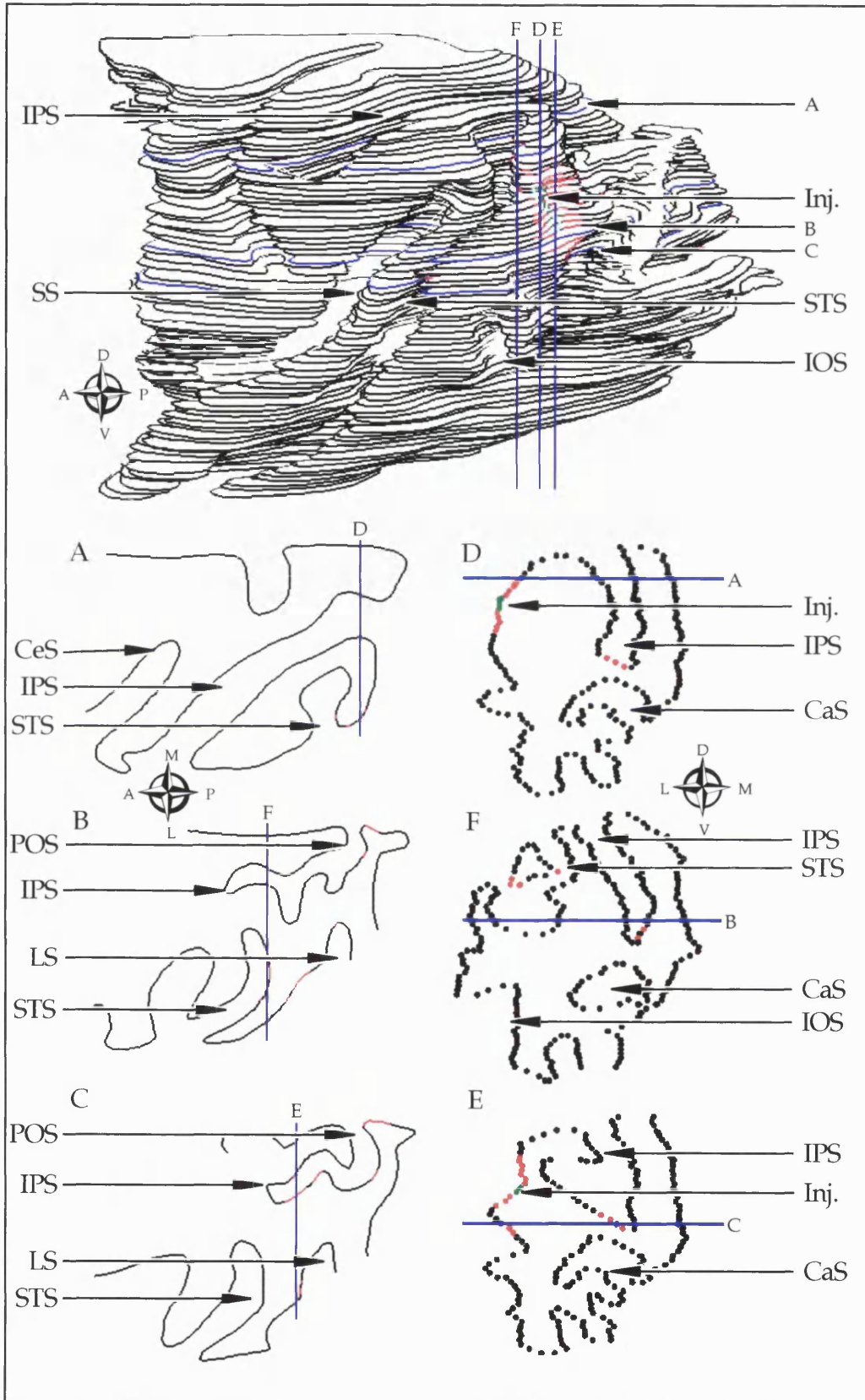


Figure 50. (SP15) (Previous page)

3D reconstruction of a brain injected with WGA-HRP into the anterior bank of the lunate sulcus at the level of the annectant gyrus. The whole brain reconstruction is shown with the levels of three horizontal sections (A, B and C) and three coronal sections (C, D and F). Abbreviations are as follows:

CaS Calcarine sulcus  
 Inj. Injection site  
 IOS Inferior occipital sulcus  
 IPS Intra parietal sulcus  
 LS Lunate sulcus  
 OTS Occipito temporal sulcus  
 POS Posterior occipital sulcus  
 SS Sylvian sulcus  
 STS Superior temporal sulcus

The injection site is shown in green and areas of transported WGA-HRP are shown in red. Blue lines represent the planes of section.

The pattern of label resulting from this injection showed striking similarities and differences to that seen following the more extensive injection, described above. Among the similarities were: the presence of label in V2 in the posterior bank of the lunate sulcus, in the anterior bank of the lunate sulcus (including area V3), in the dorsal part of the prelunate gyrus (DP), but not extending as ventrally as V4, in the intraparietal sulcus and in the superior temporal sulcus (V5). The most significant difference between the two brains was the absence of label in the occipito-temporal sulcus ventrally (upper field V2). This brain also had a much more widely distributed pattern of label within the STS.

a) V3 complex.

Label was widely distributed throughout the anterior and posterior banks and within the fundus. In the anterior bank, the zones of label seemed to form dorso-ventral stripes of label, running ventrally from the injection site towards the fundus. The label here therefore certainly involved both V3A and V3.

## b) DP.

As in the previous brain (SP28), there was a patch of label in the dorsal part of the prelunate gyrus visible in section A of the 3D reconstruction. Although slightly more anterior than SP28's patch, we suppose this label to be located with area DP.

## c) The intraparietal sulcus.

Label was seen at the fundus of the IPS, visible in sections D and E of the 3D reconstruction, but not in either the lateral or medial banks. Area VIP has been proposed to be at the fundus of the IPS (Colby *et al.* 1993), but this patch appears to be too far posterior to be within area VIP. It is more likely that this patch of transport is within the zone shown to contain axis orientation and surface orientation selective cells (Kusunoki *et al.* 1993; Shikata *et al.* 1996), referred to as cIPS.

## d) V5 complex.

Label in the STS was widely distributed and encroached on both areas seen in the injections of V3 and V3A in the brain SP44 and SP28 (V5 and V5A/FST). In addition a large zone of label was seen in far dorsal and ventral regions of the STS visible in the 2D reconstruction. The former spread over anterior and posterior banks, but the latter was restricted to the posterior bank. Thus label fell within V5, V5A (MST) and FST. Using Seltzer and Pandya's (1978) subdivisions, we assigned the label in rostral STS to areas TPO, PGa, and IPa. TPO and PGa are contained within the superior temporal polysensory area (STP).

A third brain (SP14) receiving an injection into the anterior bank of the lunate sulcus is shown in the 2D and 3D reconstructions of figures 51 and 52 overleaf.

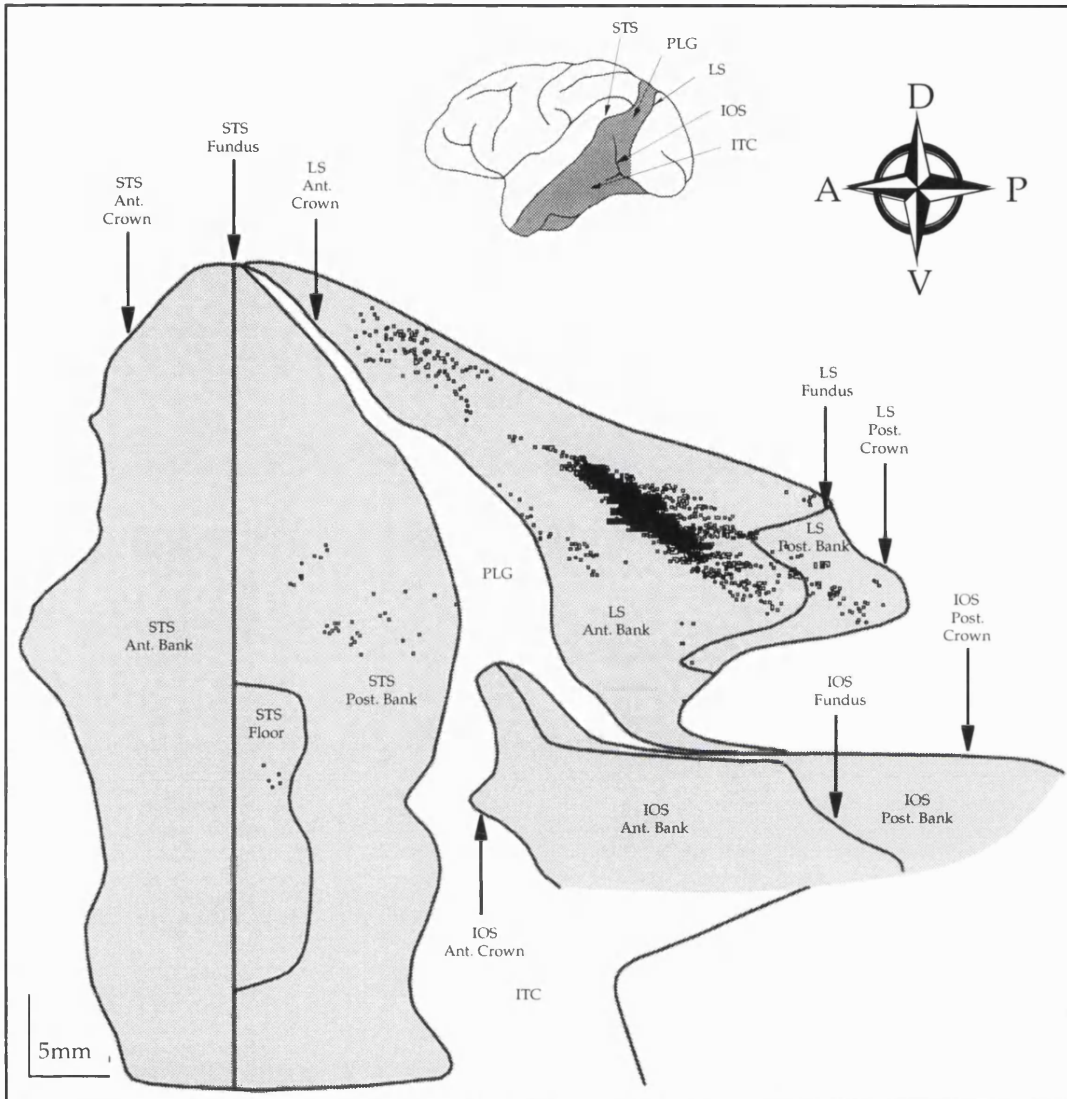


Figure 51. (sp14)

2D reconstruction of the prestriate area shaded on the whole brain drawing. The superior temporal, lunate and inferior temporal sulci (STS, LS and IOS) have been opened and their banks are shown shaded. The HRP-WGA injection site is shown as solid black bars and its transport as small open squares. PLG = preunate gyrus; ITC = inferior temporal cortex.

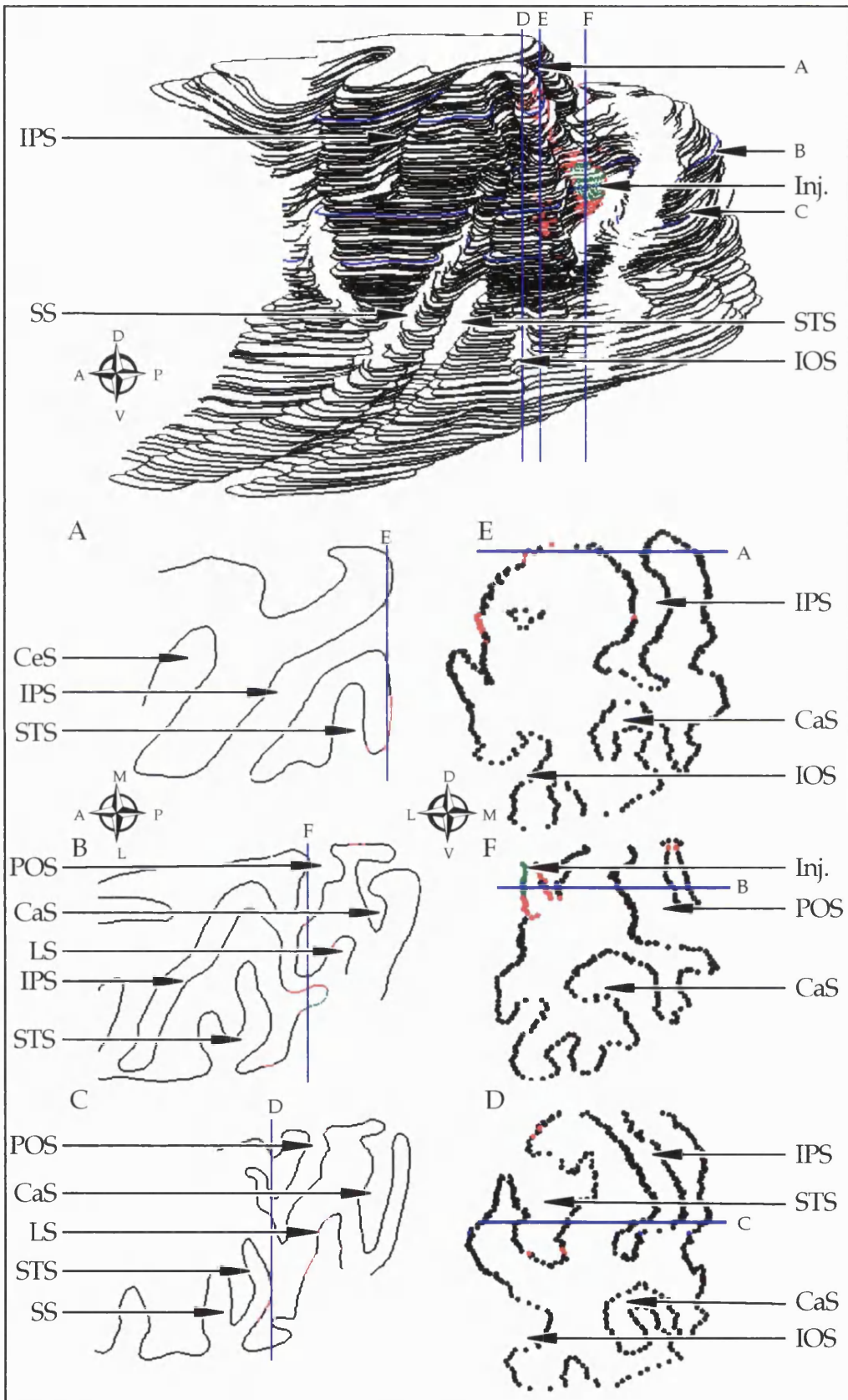


Figure 52. (SP14) (Previous page)

3D reconstruction of a brain injected with WGA-HRP into the anterior bank of the lunate sulcus at the level of the annectant gyrus. The whole brain reconstruction is shown with the levels of three horizontal sections (A, B and C) and three coronal sections (D, E and F). Abbreviations are as follows:

AS	Arcuate sulcus
CaS	Calcarine sulcus
CeS	Central sulcus
Inj.	Injection site
IOS	Inferior occipital sulcus
IPS	Intra parietal sulcus
LS	Lunate sulcus
OTS	Occipito temporal sulcus
POS	Posterior occipital sulcus
SS	Sylvian sulcus
STS	Superior temporal sulcus

The injection site is shown in green and areas of transported WGA-HRP are shown in red. Blue lines represent the planes of section.

The pattern of transport in this brain (SP14) is similar to that of SP28 except that this injection did not involve the part of V3A within the POS.

a) V2.

Patches of label appeared in the posterior bank of the lunate sulcus, coinciding with lower field representation in V2.

b) V3 complex.

Label was seen in the anterior bank and fundus of the LS, as well as in the posterior bank of the POS, all zones corresponding with V3 or V3A.

c) V4

A more ventral patch was also present close to the crown of the prelunate gyrus at the same dorso-ventral level as (and therefore within) V4.

d) DP.

A patch of label appeared on the dorsal extent of the prelunate gyrus, visible in the 2D reconstruction and in section A of the 3D reconstruction, although more posterior than that of SP28, we propose that this patch lies within area DP.

e) V5 complex

Label was found in the STS, on the posterior bank and (more ventrally) the floor. The patch on the bank is most probably within V5 and that on the floor in V5A or FST.

c) The intraparietal sulcus

A small patch of label was observed on the lateral bank of the IPS, in a similar zone to the previous injections, which lies posterior to area LIP. No label was observed at the fundus or on the medial bank of the IPS, and therefore the injected area did not project to the proposed areas VIP or MIP (Colby *et al.* 1993).

#### Comparison of V3 and V3A.

Comparison of the pattern of label distribution in brain SP14, SP15 and SP28 with that in brain SP44 allows one to discern the differences and similarities between the projections of areas V3 and V3A. We found a connection with V1 (layer 4b) only in the V3 brain and not the V3A brains. Two of the V3A brains had connections to lower field V2 (SP14 and SP15) the other showed transport to upper field V2 (SP28), consistent with the injections to V3A's lower and upper field representations respectively. The V3 brain's projection to V2 was to the thick cytochrome oxidase stripes in the lower field representation of V2. Both V3 and V3A brains showed patches of transport in the depths of the POS and the

anterior bank and fundus of the LS showing that V3 and V3A project to one another in both their medial and lateral aspects. The projection to V4 was strong in the V3 brain, but less dense, and only present in 2 of the 3 V3A brains. Like the V3A brains, the V3 brain also had label in the posterior bank of the STS, almost certainly within the territory of area V5. This latter label was denser and less fractionated in the brain with the V3 injection than in the one with the V3A injection. In the V3A brains there is a discontinuity between the label appearing on the crown of the prelunate gyrus and that appearing within the anterior bank of the lunate sulcus and continuous with the injection, whereas the V3 brain showed no transport to dorsal prelunate gyrus. This suggests that V3A projects to the separate area DP, located on the dorsal crown of the prelunate gyrus, whereas V3 proper does not. There was label in the lateral bank of the caudal IPS in the V3A brains but not the V3 brain. The location of this label is similar to the location of SOS and AOS cells of Sakata *et al.* (Kusunoki *et al.* 1993; Shikata *et al.* 1996).

#### The projections of DP.

After examination of the V3 and V3A injection brains we decided to examine 2 brains with injections into the dorsal part of the parietal cortex that received ascending projections from V3A. The area in question is the dorsal prelunate area (DP). We examined 2 monkeys with the intention of elucidating the cortical connections of this area and therefore the destination of the signals provided to it by V3A. Previous studies (Maguire and Baizer 1984; Andersen *et al.* 1990a) have suggested that the area DP is not purely visual but contains cells that respond to motor signals and it has been suggested that DP along with neighbouring areas such as 7a, PM and AL have a function in visual motor integration.

Figure 53 is the standard 2D reconstruction of MP2, a brain injected with WGA-HRP into the superior part of the dorsal prelunate gyrus known as DP.

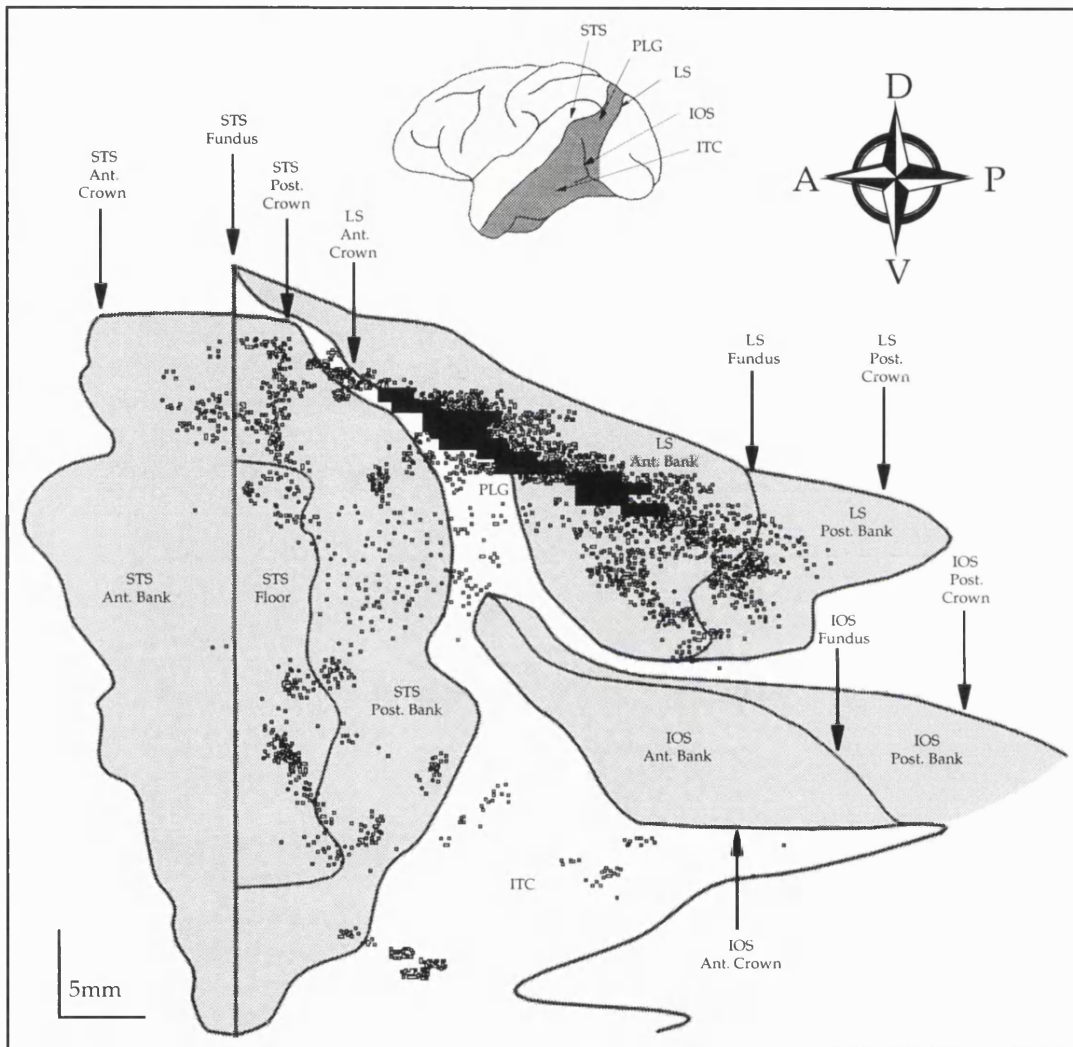


Figure 53. (MP2)

2D reconstruction of the prestriate area shaded on the whole brain drawing. The superior temporal, lunate and inferior temporal sulci (STS, LS and IOS) have been opened and their banks are shown shaded. The HRP-WGA injection site is shown as solid black bars and its transport as small open squares. PLG = prelunate gyrus; ITC = inferior temporal cortex.

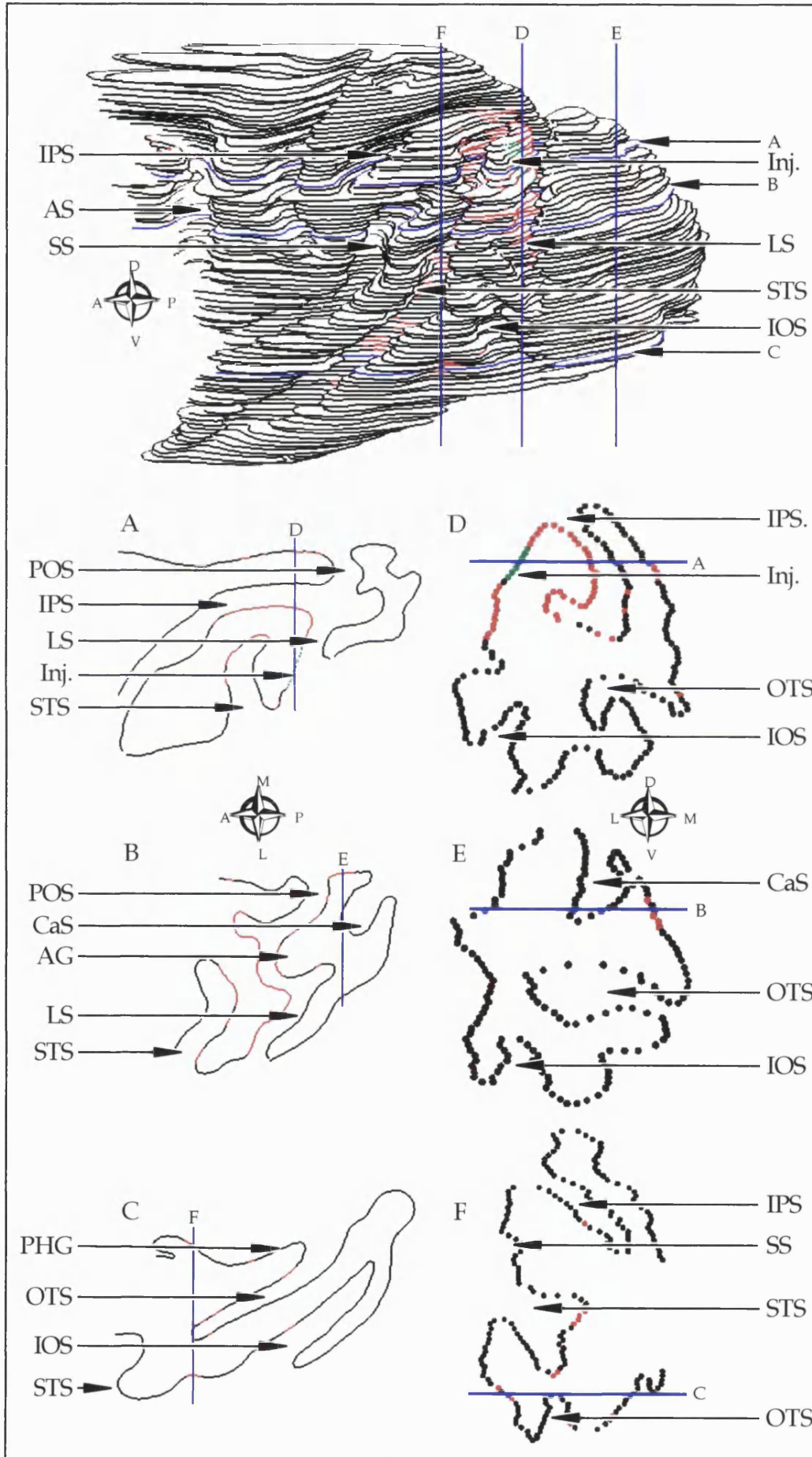


Figure 54. (MP2) (Previous page)

3D reconstruction of a brain injected with WGA-HRP into the dorsal part of the prelunate gyrus (DP). The whole brain reconstruction is shown with the levels of two horizontal sections (A and B) and two coronal sections (C and D). Abbreviations are as follows:

AS Arcuate sulcus  
 CaS Calcarine sulcus  
 CeS Central sulcus  
 Inj. Injection site  
 IOS Inferior occipital sulcus  
 IPS Intra parietal sulcus  
 LS Lunate sulcus  
 OTS Occipito temporal sulcus  
 PHG Para-hippocampal gyrus  
 POS Posterior occipital sulcus  
 SS Sylvian sulcus  
 STS Superior temporal sulcus

The injection site is shown in green and areas of transported WGA-HRP are shown in red. Blue lines represent the planes of section

The other DP injection brain (MP3) shown below, had a very similar distribution of label to the above but the injection was not in an identical position, being displaced medially, more inside the LS.

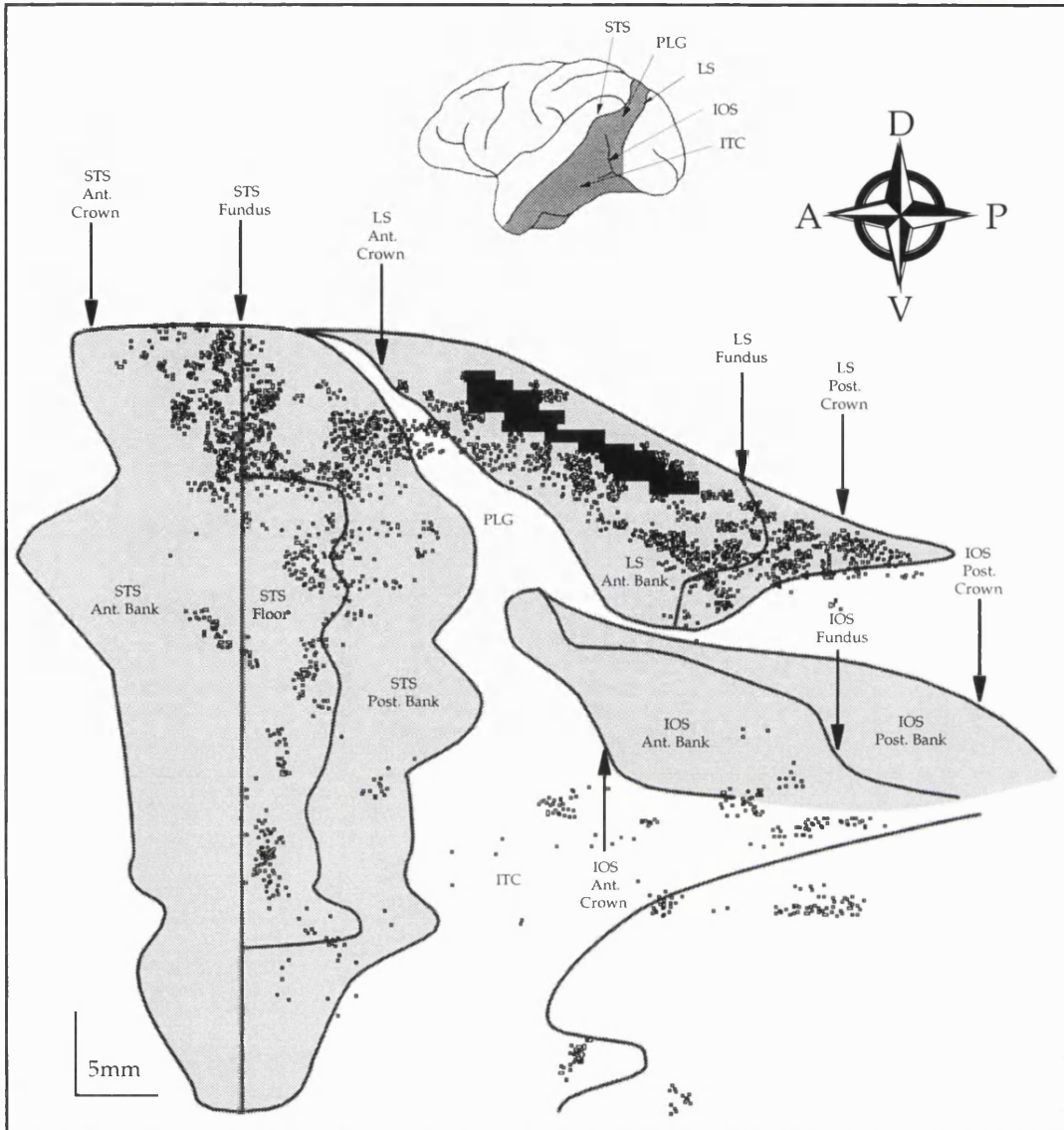


Figure 55. (MP3)

2D reconstruction of the prestriate area shaded on the whole brain drawing. The superior temporal, lunate and inferior temporal sulci (STS, LS and IOS) have been opened and their banks are shown shaded. The HRP-WGA injection site is shown as solid black bars and its transport as small open squares. PLG = prelunate gyrus. ITC = inferior temporal cortex.

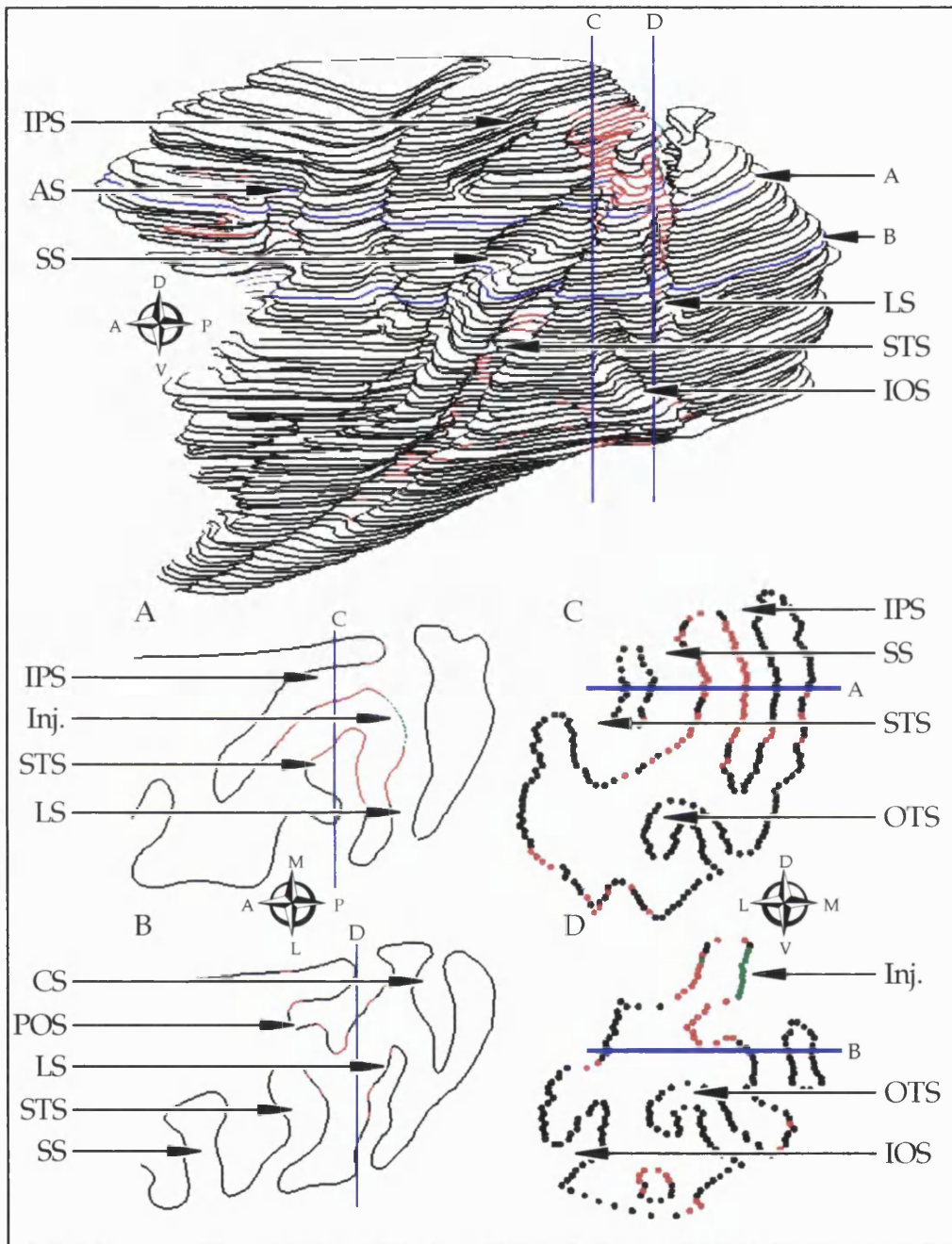


Figure 56. (MP3)

3D reconstruction of a brain injected with WGA-HRP into the dorsal part of the prelunate gyrus (DP). The whole brain reconstruction is shown with the levels of two horizontal sections (A and B) and two coronal sections (C and D). Abbreviations are as follows: AS = Arcuate sulcus. CaS = Calcarine sulcus. Inj. = Injection site. IOS = Inferior occipital sulcus. IPS = Intra parietal sulcus. LS = Lunate sulcus. OTS = Occipito temporal sulcus. POS = Posterior occipital sulcus. SS = Sylvian sulcus. STS = Superior temporal sulcus. The injection site is shown in green and areas of transported WGA-HRP are shown in red. Blue lines represent the planes of section.

## a) V1.

Neither brain showed connections with any part of V1.

## b) V2.

MP2 had a small patch of transport on the medial representation of lower field V2 at about 15-20° eccentricity (Gattass *et al.* 1981). MP3 did not show any connections with V2.

## c) V3 complex

Injections into DP produce areas of transport in the lunate sulcus. Label appeared in both the posterior banks and at the fundus which can be seen in section B of the 3D reconstruction of figure 56. In both DP injection brains the lunate sulcus appears to have continuous bands of label spreading from the injection site in a postero-ventral direction to the posterior bank of the lunate sulcus. These bands are more pronounced in MP2 and spread through cortex within areas V3 and V3A.

## d) V4.

Both of the two DP injection brains contained label in the IOS, this appearing as a light distribution on the medio-ventral anterior bank. It is possible that this part of the cortex may fall within the confines of V4. The brain MP2 also received a projection to V4 on the prelunate gyrus visible in the 2D reconstruction.

## e) V5 complex.

Both of the brains injected in the dorsal part of the prelunate gyrus have a wide distribution of label in the STS. The label falls on both anterior and posterior banks at the dorsal end of the STS but is more restricted to the posterior bank at the ventral part of the STS. Patches of

label on the floor and posterior bank of the STS are almost certainly within area V5 although this cannot be confirmed by histological means. Label was also seen in the anterior bank of the STS, possibly within V5A (MST) and FST.

f) V6.

Both DP injection brains showed connections with the medial bank of the POS, visible in section A and D of figure 54 and section A and B of figure 56. This cortical zone lies within the borders of area V6 (Covey *et al.* 1982; Zeki 1986; Battaglini *et al.* 1990).

f) Temporal lobe.

Both brains have a sparse distribution of label on the lateral surface of the temporal lobe marked ITC in the reconstruction. These patches of transport fall within the borders of area TEO (Iwai and Mishkin 1969; Kikuchi and Iwai 1980).

g) Intraparietal sulcus.

Both brains had considerable projections to the IPS, with patches of transport in the lateral bank, fundus and smaller patches in the medial bank. In agreement with previous studies (Maguire and Baizer 1984; Andersen *et al.* 1990a; Tanaka *et al.* 1990) these patches represent connections with the intraparietal areas LIP (Andersen *et al.* 1985; Colby *et al.* 1988), VIP (Maunsell and Van Essen 1983b; Colby *et al.* 1993) and MIP (Colby *et al.* 1988), as well as a physiologically defined area posterior to LIP (cIPS) (Kusunoki *et al.* 1993; Shikata *et al.* 1996), that also received a projection in the V3A injection brains.

h) Frontal eye fields.

In agreement with previous studies of the connections of DP (Andersen *et al.* 1990a), both DP injection brains showed a heavy projection to cortex within the arcuate sulcus, a cortical zone occupied by the frontal eye fields.

## Summary

The following is a table summarising the connection of V3, V3A and DP. The strength of the projection is represented by the number of +s.

Area	ID.	V1	V2	V3	V3A	V4	V5	V5A	V6	DP	LIP	MIP	VIP	cIPS*	TEO	FEF
V3	SP44	+++	+++		+++	+++	+++	++			+		+			
V3A	SP14		++	+++		++	++	++		+++						
V3A	SP15		++	+++		+	++	++		+++				++		
V3A	SP28		++	+++		++	++	++		++				++		
DP	MP2		++	+++	+++	++	+++	+++	++		++	+	+	+	+++	+++
DP	MP3		++	+++	+++		+++	+++	++		++	++		++	+++	+++

\*cIPS refers to the lateral bank of caudal IPS where SOS and AOS cells were found by Sakata's group (Kusunoki *et al.* 1993; Shikata *et al.* 1996; Sakata *et al.* 1997).

## Discussion:

### Section 1:

#### Physiology:

##### Introduction

The main objective of this study was to discover whether the V3 complex has a special role in the processing of disparity. To this end, many cells were recorded from in V2 and the V3 complex. This enabled a detailed comparison of the physiological properties of cells in these areas with particular reference to their selectivity for disparity. Previous studies have characterized cells in both areas according to their selectivities for a vast collection of visual attributes. This study concentrated on the properties of orientation, direction and disparity and led to a picture of a functional organization of cells in the V3 complex.

Previous studies have show that V2 is a polymodal area containing cells selective for (among others) orientation, direction, colour and disparity (DeYoe and Van Essen 1985; Hubel and Livingstone 1985; Shipp and Zeki 1985; Hubel and Livingstone 1987). Studies of V3 have shown the majority of cells there to be orientation selective with some direction selectivity (Zeki 1978b; Baizer 1982; Felleman *et al.* 1984; Felleman and Van Essen 1987). The present study has demonstrated that some V2 cells and a very large proportion of V3 complex cells are, in addition to being orientation selective, selective for horizontal disparity, these cells falling into the classification regime of Poggio and Fischer (1977; 1988).

### Orientation and direction

I used a novel method of classifying orientation and direction selective cells based on the shape of their whole tuning curve produced by bar stimuli moving at 12 orientations separated by 30°. Many cells recorded from in area V2 and the V3 complex were orientation selective. These cells display a symmetrical orientation tuning curve with two similar peaks 180° apart and were found to be organized into columns of similar orientation preference in the V3 complex. Direction selective cells were also found, the orientation profiles of these cells show a single response peak to one direction. These cells are also clustered together into columns.

### Non-classical orientation/direction cells

Types of cell that do not appear to fit the classical profiles of orientation or direction selective cells were also found in area V2 and the V3A complex. Some of these cells are sensitive to the direction of a moving bar, but do not modulate their response magnitude; instead they exhibit a more tightly tuned response to one stimulus direction than the other. It is difficult to imagine why these cells might be useful to the visual system. Cells were also found that responded to two non-180° opposed directions. Rarely, cells were found that have more than 2 peaks in their orientation/direction tuning curve. Multi-peaked orientation/direction cells have been reported in previous studies of macaque V1 (DeValois *et al.* 1982). V3 (Felleman and Van Essen 1987) and V5 (Albright 1984), where it has been suggested that they have a function in higher-order form and/or motion analysis. However, their extreme rarity in all the areas in which they have been encountered casts doubts on their functional significance.

Two types of direction selective cell were found in this study, one of which (also called direction biased) has an optimum response in one direction, and a smaller response in the opposite direction. The other type has an optimum response in one direction and is inhibited by stimuli moving in the opposite direction (direction selective). Direction biased cells pose a dilemma; since the spike rate of cells varies considerably from cell to cell in the visual cortex, how does the system distinguish a weak response to a stimulus moving in a direction opposite to the cells preferred direction, from a strong response to a preferred direction in a cell which exhibits a much smaller spike rate? Both of these responses from direction biased cells (or one biased and one selective) would be similar in magnitude, but they could be from cells with opposite direction preferences. In order to resolve this problem the cells that these two cells project to would have to "take into account" the spike rate capabilities of their presynaptic cells. One must assume this to be the case; perhaps cells with lower spike rates synapse on parts of the post synaptic cell that produce larger postsynaptic effects, for instance more proximal parts of the dendritic tree, producing similar effects to cells with larger spike rates. Although an interesting question, this dilemma cannot be resolved within the confines of this type of experiment.

#### Comparison of V2 and the V3 complex

Since both orientation and direction selective cells were found in areas V2 and the V3 complex, I thought it would be interesting to see if there were any differences in the characteristics of these cells between the two areas. Intuitively, one would expect there to be a difference, otherwise the V3 complex would seem obsolete. I compared the *hwhh* tuning of orientation selective cells in both areas and discovered that

there was little difference between them. If anything, V2 contained a greater proportion of orientation selective cells that were more tightly tuned to orientation. However, the proportion of orientation selective cells over unoriented cells in the V3 complex is greater. This characteristic of the V3 complex (and its predominantly "M" derived input) has given it the label of an area specialized for dynamic form (Zeki 1978b; Zeki 1992). However, orientation selective cells exist in most, if not all, visual areas, so a question arises; "What are V3 complex orientation selective cells doing that can not be done by the myriad of other orientation selective cells in the visual cortex?"

The functional organization of orientation selective cells in the V3 complex has been studied in the past and in this study, and an architecture of orientation selective columns has been found, radially neighbouring cells having similar orientation preferences, and tangentially neighbouring cells having progressively changing orientation preferences (Zeki 1978b). This organization within the V3 complex has been verified in the present study, and is a feature of the V3 complex that adds evidence for its specialization as an area involved in form vision. The purpose of the V3 complex's organization with respect to orientation is unknown, but such a columnar organization of function (or at least a clustering of functionally similar cells) is a common principle in many areas. In V1, both ocular dominance and orientation are organized into columns. Ocular dominance columns form "slabs" that run parallel to each other and orthogonal to the V1/V2 border (Hubel and Wiesel 1969; 1972). Hubel and Wiesel thought it would be interesting to know whether the two sets of stripes in V1 were parallel or orthogonal, or if they had any fixed relationship. This carries functional significance because a binocular orientation tuned cell in V1 must receive

an input from two monocular (layer 4) cells in adjacent ocular dominance columns but the same orientation column. The connectivity would be greatly simplified if the two sets of stripes ran orthogonal to each other (Hubel and Wiesel 1972). At the time, the shape of the orientation columns in V1 was not known, but subsequent studies using the 2DG technique (Hubel *et al.* 1978) and optical imaging (Blasdel and Salama 1986; Blasdel *et al.* 1995) have revealed orientation columns to be considerably more complex than the ocular dominance stripes and although the orientation columns are not strictly orthogonal to ocular dominance columns, neither are they parallel. Apparently random intersection is enough to guarantee that the two sets of stripes intersect frequently. Thus, the organization of functionally similar cells into columns and the way coexisting sets of columns are arranged in a particular area is an important feature of the striate cortex. Presumably, this statement also applies to columns of orientation and coexisting properties (e.g. disparity) in prestriate cortex.

Previous studies of the V3 complex in the awake behaving monkey have found that, in addition to orientation selectivity, the cells are able to modulate their responses with eye position so as to produce "real motion" and "gaze-dependent" cells (Aicardi *et al.* 1987a; Aicardi *et al.* 1987b; Galletti and Battaglini 1989; Galletti *et al.* 1990). Real motion cells are not uniquely found in the V3 complex; they have also been found in both V1 and V2 (Galletti *et al.* 1984; Galletti *et al.* 1988). These types of cell would be useful to the visual system to construct a map of real (as opposed to retinotopic) space. Although both V3 and V3A are retinotopically organized areas, their content of gaze-dependent cells could be forming a coexisting map of egocentric space by only becoming responsive at particular gaze angles. In this way, maps of real and

retinotopic space would be compatible within a single area. Galletti and Battaglini (1989) stated that they found gaze-dependent cells clustered together within V3A. It would be interesting to discover the functional organization of gaze-dependent and non-gaze-dependent cells in V3A, two maps may be present there, one retinotopic and one egocentric (made up of gaze-dependent cells). These two maps could be represented in two sets of columns, similar to the double representation of retinotopic fields in V1's ocular dominance columns.

### Orientation and disparity

All disparity tuned cells found in this study were, in addition, orientation or direction selective. Since this is true of many previous studies in both cat and monkey (Nikara *et al.* 1968; Pettigrew *et al.* 1968; Hubel and Wiesel 1970; Joshua and Bishop 1970; Hubel and Wiesel 1973; Poggio and Fischer 1977), one must assume that orientation or direction selectivity is a required feature for a cell to be disparity tuned. This seems to be a reasonable criterion because, in order to detect disparity, a cell must detect a feature of the stimulus that appears at that disparity. This result is also supported by some psychophysical evidence which shows that the masking of stereopsis is orientation dependent (Mansfield and Parker 1993). Furthermore, the potential value of orientation information in the stereoscopic appreciation of surface slant (orientation disparity) (Blakemore *et al.* 1972; Rogers and Cagenello 1989) suggests that orientation tuned units might play an important role in the generation of the 3D stereoscopic percept. Psychophysical experiments that show that stereopsis is primarily masked by spatial frequency tuned elements (Julesz and Miller 1975; Yang and Blake 1991) and the demonstration that disparities presented at very different spatial frequencies may be perceived

simultaneously at different depths (Mayhew and Frisby 1977), suggest that spatial frequency tuning also has an important role in stereopsis.

### Topography of the V3 complex

Since both V3 and V3A are retinotopically organized areas, one must assume that every part of the visual field in each area must contain a full complement of orientation selective cells, representing the full range of orientations. The most intuitive method of making such an organization would be to change the orientation preferences of cells in one cortical direction (radially) and retinotopy in the other (tangentially). The fact that this does not happen in any part of the visual cortex suggests a number of possibilities:

- 1) That each representation of a small area of space requires a large population of orientation cells with the same (or very similar) orientation preferences.
- 2) Assuming the redundancy of orientation selective cells is not a required feature of the visual system, it is reasonable to suggest that each cell with a similar orientation preference representing a similar retinotopic part of the visual field may have an additional property that makes it more unique.
- 3) I have shown that disparity tuning is a common feature of cells in the V3 complex. Therefore, it is possible that cells with similar orientation preferences representing the same part of retinotopic space may differ in their responses to stereoscopic depths.
- 4) I have shown that cells tuned to near, far and zero disparities are arranged in columns of about 300 $\mu$ m in width, parallel to (but smaller than) a full cycle of orientation columns whose width is in the order of 1mm (see results).

5) Therefore, disparity is also multiply represented for a particular retinotopic space, but the fact that disparity is represented in the same cortical dimension as orientation reduces the redundancy of orientation selective cells.

On the basis of the above statements, I propose an organization of the V3 complex with respect to its function.

Both V3 and V3A are retinotopically organized areas (Cragg 1969; Zeki 1978b). For each area to represent the whole visual field, each must contain many cells with different orientation preferences (covering the whole range) but representing the same retinotopic portion of space. This is achieved with radial columns of similarly tuned orientation selective cells, presumably because the laminar dimension is reserved for another function. One property that is organized in a laminar fashion in the V3 complex, as it is in other areas, is the input/output "wiring" of the cortex. Anatomical tracing experiments (Rockland and Pandya 1979; Shipp and Zeki 1988) have shown that different layers contain cells that either receive input from other areas or project to other (or the same) areas.

I have shown that disparity is also functionally organized in a similar way to orientation; cells are organized into columns of the same disparity tuning profile (near, far, TE, TI, TN and TF). Figure 57 is an illustration of this organization.

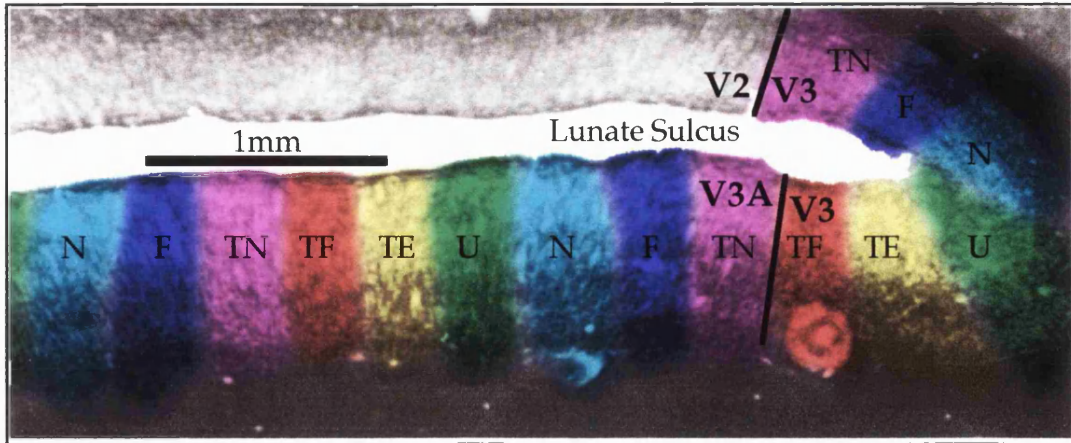


Figure 57.

Representation of the functional organization of disparity tuned cells in the V3 complex. Columns of different types of disparity tuned cell, e.g. Near, Far, TE, TN, TF and Untuned, are represented as different coloured stripes.

Given that disparity tuned cells are present in at least the central  $20^\circ$  of the visual field (see results) these columns must cover the majority, if not all, of the V3 complex. Thus, there are functional units within the V3 complex which contain a full complement of orientation selective cells and single or multiple columns of each of the different types of disparity tuned cell; each of these units will contain millions of cells with many overlapping receptive fields so that the whole visual field may be represented by all orientations and all disparity cell types. Thus, two coexisting sets of columns exist in the V3 complex, one for orientation and one for disparity. Since both disparity columns and orientation columns appear to be roughly circular (rather than stripes) and the diameter of disparity columns is smaller than that of orientation columns ( $\sim 300\mu$  compared with  $\sim 1\text{mm}$ ), ample opportunity is allowed for local interaction between these two column sets. This organization of orientation and disparity leads us to propose that the V3 complex has a special role in the processing of stereoscopic depth. I propose that the stereo-scotomas of Richards *et al.* (1973) could be due to inadequate

coverage of the visual field by disparity tuned cells in the normal population, thus leaving spots which are blind to either stereomotion, near, or far disparities.

#### Disparity selective cells in the prestriate areas.

The disparity selective cells encountered in this study were of the types first described by Poggio *et al.* (1977; 1988). They proposed functions for these different types of disparity cell. Near and far cells signal "in front of" or "behind" the fixation plane, and would therefore be useful for coarse stereopsis and the control of vergence eye movements. I propose that near cells could also have a specialized function in the control of visually guided grasping movements because they would respond to the presence of a hand while it is in front of the fixated object and stop responding when the hand had reached the object to be grasped. Tuned cells (TE, TI, TN, TF) have been proposed to signal fine stereopsis about a distance in depth very close to the horopter (Poggio and Fischer 1977; Poggio 1979). Therefore the range of disparities that tuned cells prefer (typically  $\pm 1.0^\circ$ ) corresponds to the neural correlate of Panum's fusional area. If so, and there is a different (and quite diverse) function for asymmetric (i.e. near and far cells) and tuned disparity cells, one might expect them to be separated in the cortex and to have different projection targets, the asymmetric cells projecting to areas involved with the control of eye movements and fine reaching and grasping limb movements while tuned type cells project to areas specialized for functions requiring fine stereoscopic acuity, e.g. 3D form vision. The connections of the V3 complex to areas that could be fulfilling these functions are discussed in the next section.

The anatomical separation of asymmetric and tuned cells in the V3 complex has been demonstrated in this study. One might ask "why do the cells need to be separated into columns?" Functional segregation is a common attribute in the visual system and brain in general, one can only hypothesize that the division of cells into clusters, each of a similar property, simplifies their projections to other areas and enables the cells to communicate easily and extract further information by "pooling" information. In the case of "tuned" disparity selective cells, two types of information could be obtained by the integration of responses from many cells: motion in depth and three dimensional form and structure. Selectivity for motion in depth is a property of cells in V5 (Zeki 1974a; Maunsell and Van Essen 1983a), an area shown here to receive a strong projection from the V3 complex and the V3A projection zone on the dorsal part of the prelunate sulcus (DP). Cortical areas containing cells selective for 3D form and structure include posterior parietal association cortex, where 3D surface orientation selective neurones have been found that are selective for particular orientations of flat surfaces defined by random dot stereograms (Shikata *et al.* 1996). I propose that the projection from V3A to posterior parietal cortex provides at least some of the stereoscopic information necessary for the generation of this property. Cells in inferotemporal cortex (IT) have been shown to be selective for complex 3D shapes, and some cells there respond independent to the spatial orientation of the stimuli (Logothetis *et al.* 1995). Although the responses of these cells has not definitively been shown to employ stereoscopic cues, the chances that this is so are likely because stereopsis is a powerful method of defining 3D orientation; indeed disparity tuned cells have been found that respond specifically to 3D axis orientation of objects (Ohtsuka *et al.* 1995; Sakata, H. personal communication). I propose that the projection shown here, from the dorsal part of the

prelunate gyrus to temporal cortex, carries the stereoscopic depth information necessary for the generation of complex object selective cells found there. This information would be primarily derived from "tuned" rather than "asymmetric" disparity selective cells.

### Proportions of disparity tuned cell types

As well as the proportions of disparity tuned cells varying in different prestriate areas, the types of disparity tuned cells have also been found to have a different distribution across the prestriate cortex.

The results presented here have shown that there is a difference in the proportions of different types of disparity tuned cell between V2 and the V3 complex. The most common in V2 is the tuned zero (tuned excitatory) cell (40%), whereas in the V3 complex the near cell is most common (39%). Previous studies (Maunsell and Van Essen 1983a; Poggio *et al.* 1988; Gnadt and Mays 1991; Roy *et al.* 1992; Trotter *et al.* 1992; Trotter 1995) have shown that the proportion of asymmetric cells increases from V1 to V2 to the V3 complex to V5 and to LIP and MST. This progression suggests functionality along this pathway. A higher proportion of asymmetric cells would suggest that an area is more concerned with coarse rather than fine disparity. It seems reasonable that such an area may also be more concerned with the generation of motor signals rather than fine stereoacuity.

The predominance of near cells in the V3 complex may have a functional significance. Near cells are stimulated by objects that fall closer to the animal than the fixation plane. During the manual manipulation of objects this space is occupied by the hands and is therefore of more importance to the brain than space further away from the animal than

the fixation plane. For this reason one would expect to find more near cells than far cells in an area that is involved with visuo-motor coordination. Previous studies have found an increase in the proportions of asymmetric cells as one goes higher up the dorsal stream (Trotter 1995). It would be interesting to see if there is an increase in the proportions of near cells too. Area V5 (MT) contains 23% near cells and 13% far cells (Maunsell and Van Essen 1983a) and area V5A (MSTd) contains 46% near cells and 38% far cells (Roy *et al.* 1992). Although not remarked upon by these authors, the consistently larger proportion of near versus far cells in these areas as well as the V3 complex suggests their involvement in vergence eye movements and/or the visual guidance of reaching movements.

#### Vertical disparity selectivity

Viewed binocularly, vertical lines and edges give rise to horizontal disparities along their whole length, whereas it is only at their ends that horizontal lines and edges can have vertical disparities. Cells with a preferred line orientation that is vertical will therefore be specifically sensitive to horizontal disparities and end of line disparities arising from horizontal lines and edges will not provide an effective stimulus for the cell. The reverse is true for cells whose orientation preference is horizontal. End stopped cells do not suffer this limitation. A strongly end-stopped cell can signal horizontal disparity even when its preferred axis of movement is vertical; if the cell was not end-stopped it would not be able to "see" the vertical edges that define the disparity. Thus, cells were tested for vertical disparity if they had a non-vertical orientation preference or were selective for spots rather than bars. Cells with a vertical orientation preference could not be tested for vertical disparity because changing vertical disparity in these cells has no effect on the

stimulus within the cell's receptive field. Cells tested for vertical disparity were first tested for horizontal disparity and the optimal horizontal disparity used for all vertical disparity trials. On the whole, few V3 cells were found that were tightly tuned to vertical disparity. Some modulated their response with changing vertical disparity but the disparity tuning curves of these cells showed that this modulation was not as tight as that found for horizontal disparity. Previous studies have found many cells tightly tuned to horizontal and vertical disparity in the cat's striate cortex (Maske *et al.* 1984; Maske *et al.* 1986a; Maske *et al.* 1986b) and in V1 and V2 of the monkey (Gonzalez *et al.* 1993).

To calculate the distance between two objects in a three-dimensional space from horizontal disparities, it is necessary to know the fixation distance. It has been suggested that the horizontal gradient of vertical disparity contains information to estimate the fixation distance and therefore to scale horizontal disparities (Longuet-Higgins 1982b). It has also been suggested that the cells sensitive to horizontal and vertical disparities represent a neural mechanism that provides information to the visual system in order to achieve correct eye alignment and depth perception (Bishop 1989). In a previous study (Gonzalez *et al.* 1993), random dot stereogram stimuli were used to find cells tuned to vertical disparity. These stimuli can present vertical disparity to cells irrespective of their orientation preference, allowing less limited testing for this stimulus parameter. However, random dot stereograms were not used in this study due to the misalignment of the receptive fields causing difficulties in aligning the texture elements of the RDS onto corresponding points of each retina. Had it been possible to use stereograms rather than bars in this study, more cells tuned to vertical disparity may have been found.

Whether cells would have shown their vertical disparity tuning if RDS stimuli were used in this study remains unknown. If vertical disparity tuning were a common property of V3 cells one would expect to find more examples using bar stimuli, especially since cells tuned to vertical disparity were found in the cat using these stimuli (Maske *et al.* 1984; Maske *et al.* 1986a; Maske *et al.* 1986b). Interestingly, previous (and the present) studies show an important difference between cells tuned to horizontal and those tuned to vertical disparities, i.e. cells tuned for vertical disparity are only of the tuned type (vertical TE and TI) (Gonzalez *et al.* 1993), there are no equivalent asymmetric cells in the vertical disparity domain. The lack of vertical asymmetric disparity cells provides evidence for asymmetric cells' involvement in vergence and visuomotor control because there is no "vertical vergence" mechanism and vertical disparity does not encode depth directly.

#### Unorthodox disparity cells

The great majority of disparity tuned cells encountered in this study were of the types defined by Poggio *et al.* (1977; 1988). However, a few had multiple peaks in their disparity tuning curves and were therefore not classifiable with respect to this scheme. Figure 58 shows two examples of this type of cell.

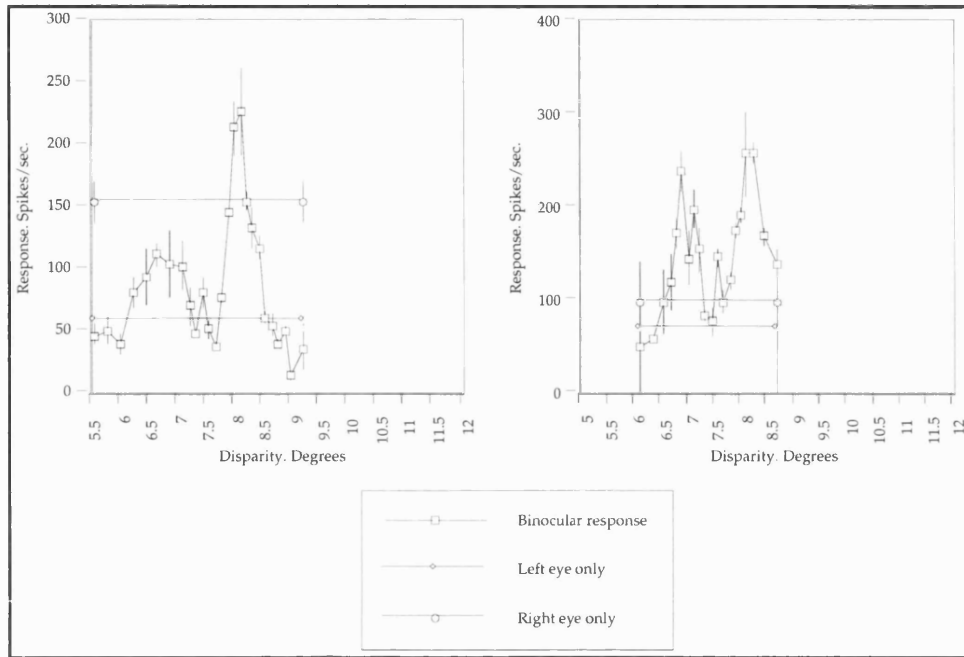


Figure 58.

Disparity tuning curves for two cells which do not fit into any of the groups defined by Poggio *et al* (1988).

These cells have two narrow peaks in their disparity tuning curves. It is possible that these cells are tuned inhibitory cells, the point of zero disparity falling between the two peaks. However, the spike rate at the point of maximum "inhibition" is about the same as the monocular response firing rate of the cells. The two larger peaks either side of this point would enable the cells to respond maximally when a stimulus was just in front, or just behind the fixation plane. It is feasible that this type of cell may be useful to drive searching micro-vergence eye movements, such as those that occur during fusion because it would produce a large response when the stimulus appeared with a small non-zero disparity. However, the fact that only a small number of these cells was found (in V3) casts doubt on their importance.

### Quantitative depth selectivities

The present study has focused on the qualitative categories of disparity selective cells in the cortex. Another feature of disparity selective cells is the particular point in depth they are tuned to. The reason this study is not the most powerful way of examining this feature of disparity selectivity is the problem of eye movements. In order to make non ambiguous conclusions regarding the relative depths cells are tuned to, one first needs to know what stimulus separation corresponds to zero disparity. In this study it was not possible to get an accurate measure of this disparity because the eyes were arbitrarily diverged. Secondly, one has to ensure that no eye movements take place during the course of recording from a single cell. The measurement of eye movements (eye drift and larger movements due to routine cleaning of the eyes) was attempted by means of the reversible ophthalmoscope but this technique is not accurate enough to eliminate the possibility of small movements going unnoticed. These small movements can be falsely interpreted as physiological differences between the depth selectivities of consecutive cells. The advantage of studying the properties of cells in the anaesthetized monkey is that in long penetrations, sampling from many cells is easily achieved and therefore the investigation of functional architecture is more powerful. Thus, there is a trade-off of advantages between the anaesthetized and awake monkey preparations. Previous studies using the awake behaving macaque have shown that cells are tuned to within  $\pm 1^\circ$  of zero disparity (Poggio and Fischer 1977) but the functional organization (if any) of this physiological property has not been investigated. This may be an important area of future research because if, for example, cells with particular depth selectivities are clustered together and ordered within an area, it would suggest that different parts of the cortex within a particular area are representing

different positions in depth. This type of organization would be the first step in the building of a map of three dimensional space superimposed onto the cortex, a "3D retinotopy".

### Motor and sensory systems

A distinction can be made between the mechanisms required for the control of motor events (for example a vergence eye movement) and visual analysis of 3D objects at the fixation plane. However, this distinction is by no means easy to make when recording from visually responsive cells because it is impossible to tell whether the response they are producing is used by one or both of the sensory or motor systems. Previous studies of disparity selective cells have suggested that the types of disparity selective cells may be divided into two groups: those that are of use to the ocular motor system and those used for fine stereoscopic judgements of depth at the fixation plane. This hypothesis is based on the response profiles of disparity tuned cells; asymmetric cells would be useful to drive vergence eye movements, bringing the stimulus into the horopter, and tuned cells, with their tight tuning profiles near to the horopter, would be useful for fine discrimination of depth within Panum's fusional area. In this study I have shown that the different types of disparity tuned cells are separated into columns within V3, assuming the above distinction is true one would expect the two groups of disparity selective cells to have different projection zones; the asymmetric cells projecting to areas involved in the control of eye movements and the tuned cells projecting to higher visual areas. Injections of V3 (to be discussed in detail in the next section) have shown that there are indeed connections to both sensory motor areas (dorsal parietal cortex) and higher visual areas (V4, V5, IT). An interesting study for the future would be to make small injections into columns of either asymmetric or

tuned cells in V3 and compare their projection zones. This was not possible in this study because the WGA-HRP injections were too large to be restricted within a single V3 disparity column.

### Form vision

Since their discovery, orientation tuned cells have been equated with form vision. This is not an unreasonable assumption, since these are the cells which will respond when one is presented with lines and edges that constitute the shapes of objects. The activation of orientation tuned cells will impress an activity map of an object onto topographically organized cortex. However, form is more than a collection of outlines that define a shape. To possess form vision one has to distinguish between objects, assigning the different parts of an object to the whole. The concept of form is notoriously difficult to define because it spans a number of cognitive levels: In its simplest context, form can be a single oriented line, or a number of lines that comprise a simple shape. This simple idea of form naturally progresses to more complex shapes and objects in 3 dimensions. Therefore depth is also an important constituent of form, real objects are always seen in three dimensions, and their particular form is dependent on the 3D position from which they are viewed. 3D line and surface orientation must therefore also be important constituents of form vision. Once an object is represented in the cortex by a population of orientation and disparity tuned cells one could say that its shape in three dimensions has been completely described, yet is this all that is necessary for form vision? One could hypothesize that further processing (in the same or "higher" areas) is necessary for an object's recognition and cognitive compartmentalization, but how this is achieved, and what the responses of cells that are undertaking these

operations would look like remains a considerable and very interesting problem.

## Section 2:

### Anatomy:

#### Introduction

Among the many known visual areas in the prestriate cortex of the monkey, perhaps the least studied is area V3 and its associated area V3A. This is surprising since area V3 was among the very first prestriate visual areas to be identified (Cragg 1969; Zeki 1969). Its most prominent functional feature is the predominance of orientation selectivity (Zeki 1978b; Burkhalter *et al.* 1986). Given that orientation selectivity is also a dominant feature in other visual areas, it becomes naturally interesting to ask how the output of the cells in V3 and V3A differs from the output of cells in other areas with similar functional properties. The first step in such an analysis, and the simplest, is to trace the anatomical outputs from these areas.

#### Pathways in the visual cortex

In order to evaluate the role the V3 complex plays in the parallel processing of visual information it is useful to first summarise the various pathways present from the LGN onwards, their anatomy and physiological properties.

Beginning in the retina with the large and relatively rare P $\alpha$  cells, the magnocellular ("M") pathway projects, via the magnocellular LGN layers, to layer 4C $\alpha$  and then to layer 4B of V1. The magnocellular outputs from V1 go to the thick stripes of V2, to V3 and to V5. From here, magnocellular information is directed towards parts of the parietal lobe including V5A (or the medial superior temporal area, MST) and the ventral intraparietal area (VIP). The parvocellular pathway begins with

P $\beta$  retinal ganglion cells which terminate on the parvocellular layers of the LGN. Geniculate "P" cells project to 4C $\beta$  and 4A of V1 and then to the superficial layers of V1, probably to both cytochrome oxidase divisions of that area, the blobs and interblobs. Blobs project to thin cytochrome oxidase stripes in V2 and interblobs project to V2's interstripes. From here the "P" pathway projects via V4 to a variety of inferotemporal cortical regions. The cortical autonomy of these two pathways has been disputed and several "cross talk" pathways have been found that throw the "M" and "P" classification into disarray (at least in cortical terms). In particular, a modest "M" input has been found from striate layer 4B to V1's blobs (Blasdel *et al.* 1985), and striate layers 4C $\alpha$ / $\beta$  to interblobs (Fitzpatrick *et al.* 1985). Within V2 horizontal connections exist that are capable of providing cross-talk between all stripe types (Rockland 1985). Projections have been found between V3/V3A and V4 (Felleman and Van Essen 1983), and between V5 and V4 (Maunsell and Van Essen 1983b; Ungerleider and Desimone 1986). These connections are of the lateral variety (Shipp and Zeki 1988). Both V4 and V5 project to areas of the temporal lobe, but these projection fields are largely non-overlapping (Desimone *et al.* 1980; Maunsell and Van Essen 1983b; Ungerleider and Desimone 1986; Shipp and Zeki 1995). Hence the "M" pathway is relatively pure but the "P" pathway is mixed.

The physiological differences between the "M" and the "P" pathway from the retina to the LGN are striking. The "M" pathway is characterized by a lack of wavelength sensitivity, transient responses to flashed stimuli, fast conduction velocity, relatively large receptive fields and activation by low contrast stimuli (Wiesel and Hubel 1966; Dreher *et al.* 1976; Kaplan and Shapley 1982; Derrington *et al.* 1984; Derrington and Lennie 1984). In addition, the majority of cells in layer 4B of V1 are

direction selective (Dow 1974; Hawken *et al.* 1988) and it is these cells that project to V5 (Movshon and Newsome 1984). In contrast, cells in the "P" pathway are characterized by a high incidence of wavelength selectivity, sustained responses to flashed stimuli, slower conduction velocities, relatively small receptive fields and poor responses to low contrast stimuli (Wiesel and Hubel 1966; Dreher *et al.* 1976; Kaplan and Shapley 1982; Derrington *et al.* 1984; Derrington and Lennie 1984). The properties of orientation selectivity and disparity selectivity have been found to be common to both "M" and "P" divisions of V1 (Hubel and Wiesel 1968; Poggio and Fischer 1977; Malpeli *et al.* 1981). Within V2, disparity tuned cells have been found in all stripe compartments (Peterhans and Von der Heydt 1993), although Hubel and Livingstone (1987) reported that they were restricted to the thick stripes, and De Yoe and Van Essen (1988) found them only in thick and inter-stripes. Disparity tuned cells are also present in V3 (Felleman and Van Essen 1987; Poggio *et al.* 1988; present study), V3A (present study), V4 (Felleman and Van Essen 1987) and V5 (Maunsell and Van Essen 1983a).

Information derived from disparity can be used for spatial and object vision and confuses the distinction between these two divisions of vision. Disparity information tells one where an object is in relation to the observer but also what shape the object is in 3D. Disparity derived depth information is also critically important in the accurate control of reaching arm movements and vergence eye movements. A recent study (Servos *et al.* 1992) compared reaching and grasping movements in normal humans under monocular and binocular conditions, and found that grasping movements made under monocular conditions showed longer movement times, lower peak velocities, proportionally longer deceleration phases and smaller grip apertures than movements made

under binocular viewing. For this reason one would expect information derived from disparity to be routed to areas involved with spatial processing and those thought to be involved in the recognition of objects as well as sensory motor areas. A 3D representation of objects is necessary for the control of their manipulation. Goodale and Milner (1992) proposed that the dorsal cortical visual pathways, including the parietal cortex, are concerned with the visual information processing for "how to manipulate objects." In order to reach and grasp an object under visual guidance, the visual system is required to provide information concerning the real position, real size, real orientation and 3D shape of the object in space.

In earlier studies, Zeki (1978b) found the majority of neurons in the V3 complex are strongly binocular. Galletti *et al.* (1989) found the visual responses of most of V3A neurons are dependent on gaze direction. More recently, Galletti *et al.* (1993) found some of the neurons of area V6 (PO) of the parietal cortex adjacent to V3A encode the egocentric position of the stimulus, independent of the direction of gaze, suggesting that this pathway is concerned with the perception of position of objects in real space. Here I have found projections from the V3A to DP and from DP to V6. In addition these findings suggest the possibility that the target areas of the V3 complex are concerned not only with the spatial location but also with the spatial orientation and 3D shape of objects.

### Connections of the V3 complex

It is well established that the visual cortical pathways are segregated into several separate pathways to process different aspects of visual information (DeYoe and Van Essen 1988; Zeki and Shipp 1988; Felleman

and Van Essen 1991). In general, the dorsal stream, leading to the parietal cortex, is related to spatial vision with motion and depth, and the ventral stream, leading to the temporal cortex, is related to object identification with colour and form (Mishkin *et al.* 1983). In the dorsal stream, the pathway through the V3 complex is known to mediate binocular disparity signals as well as motion signals from the magnocellular system.

Most previous studies of the connectivity of the V3 complex have concentrated on its projections from areas V1 and V2 (Cragg 1969; Lund *et al.* 1975; Zeki 1975; Zeki 1978b; Zeki 1980a; Felleman and Van Essen 1983; Burkhalter *et al.* 1986; Van Essen *et al.* 1986). In this study we were more interested in the projections from the V3 complex to "higher" cortical areas and those shown to be concerned with aspects of 3D vision.

A consistent projection of V3A was to the dorsal prelunate area (DP) (Maguire and Baizer 1984). This area contains visual and visual-motor responsive cells, the visual-motor units respond to "gaze-fields", i.e. they respond when the monkey shifts its gaze to a particular part of the visual field. The input to most of these cells was found to be from an extra-retinal source because their properties persist in total darkness (Andersen *et al.* 1990a). Saccade related activity has also been found in area DP, cells there fire post-saccadically, with a latency of about 80ms (Andersen *et al.* 1990a). The high incidence of eye movement and position related activity in DP makes it a likely candidate for an area involved in the mapping of egocentric space, and its connection with V3A suggests that its cells may require orientation and disparity information to undertake this operation. A possible function that would require both extraretinally derived eye position and disparity tuned cells

is the scaling of retinal disparity for fixation distance with the objective of building a 3D representation of objects in real space. The eye position properties of cells in posterior parietal cortex would also be required to produce V3A's "gaze-dependent" cells (Galletti and Battaglini 1989) by modulating their excitability with eye position. The connection between these two areas demonstrated here could be subserving this function.

### "What" and "Where" pathways

The previously discussed "What" and "Where" dichotomy of cortical pathways can be divided into 3 independent classification criteria:

- 1) "M" versus "P" input.
- 2) Dorsal versus ventral pathways.
- 3) "Where" (spatial) function versus "What" (object) function.

Each of these can be challenged:

- 1) As mentioned above, "M" information is known to contribute to the "Where" pathway ("M" input to V1's blobs, V4 etc.)
- 2) The strong projection to TEO from DP, and an input to DP from V3A found in this study represents spatial information from the dorsal stream finding its way to the ventral stream in the temporal lobe (TEO) (Ungerleider and Mishkin 1982). This pathway could represent another source of interaction between the two streams, the area DP being placed in between the dorsal and ventral streams. This "cross-over" of connections is an example showing that there are not 2 independent and unconnected networks.
- 3) The functional dichotomy of "What" and "Where" pathways is a vast oversimplification. Disparity information would be useful to both dorsal and ventral streams because it can provide both spatial and object related

information, telling the system either where an object is (in depth) or describing the shape of an object in 3D. The projection of disparity information to the temporal and parietal cortices could also be divided into signals of use to the motor system, for example asymmetric cell output, and output from tuned cells which would be of use to a fine stereoscopic "form from depth" mechanism.

Although parietal areas have been shown to contain a predominance of asymmetric cells, the ventral system has not been investigated with respect to disparity. It would be very interesting if ventral stream areas were found to contain a predominance of the "tuned" type of disparity cells.

We also found a projection from V3 and V3A to area V6 (Covey *et al.* 1982; Zeki 1986; Galletti *et al.* 1996). The cells of this area have been shown to have interesting spatial properties, some are "gaze locked", and some having the property of encoding real position in egocentric space (Battaglini *et al.* 1990; Galletti *et al.* 1993). V6's cells are also mostly orientation selective, so they are encoding "what" (orientation or 'form' vision) and "where" egocentric position. and as such are another example of the false dichotomy of the what and where pathways expounded by Ungerleider *et al.* (1982).

### Oculomotor systems

If disparity tuned cells are to be of use to the oculomotor system, a pathway should exist between areas containing such cells and the brainstem nuclei that have been shown (by single unit recording) to control vergence, i.e. the oculomotor nucleus (Judge and Cumming 1986) and the nucleus reticularis tegmenti pontis (NRTP) (Gamlin and Clarke

1995; Gamlin *et al.* 1996). Such a pathway does exist; NRTP receives a projection from the frontal eye fields (Stanton *et al.* 1988) and projects to the posterior interposed (IP) and fastigial nuclei of the cerebellum (Gamlin *et al.* 1996). In this study I have shown that area DP receives a projection from V3A and itself projects to the frontal eye fields, which have also been shown to contain cells with activity that is modulated by vergence (Gamlin *et al.* 1996). Thus, the frontal eye fields, NRTP and IP form part of a cerebro-ponto-cerebellar pathway modulating or controlling vergence and ocular accommodation that probably receives at least some of its stereoscopic information from disparity tuned cells in the V3 complex.

#### Parietal connections

We found a projection from V3A to the lateral bank of the intraparietal sulcus. This region has been divided into a number of areas on the basis of its anatomy and physiology. Seltzer and Pandya's (1980) architectonic study revealed the presence of a distinct cortical belt (area POa) in the lateral bank of the IPS that could be further subdivided on the basis of myeloarchitecture, into two rostro-caudal ribbons: POa-i, lying ventrally and POa-e being positioned dorsally and parallel to POa-i (Seltzer and Pandya 1980). Anatomical studies by the same authors revealed two specialized inputs to area POa: visual information from the contralateral peripheral field, by way of the middle portion of the prelunate gyrus and kinaesthetic information from the contralateral head and neck, via the rostral inferior parietal lobule (area PF). They thus assigned POa with the function of integrating visual and somatosensory information to relate the position of the head and neck to the visual environment. Electrophysiological studies of the lateral bank of the IPS (LIP) have revealed some cells that exhibit "gaze-field" behaviour, i.e.

they respond when the eyes are directed towards a particular portion of the visual field (Andersen *et al.* 1990a; Andersen *et al.* 1990b). Presaccadic activity was also recorded from some cells in area LIP; these cells fire about 80ms before the onset of a saccadic eye movement (Andersen *et al.* 1990a; Andersen *et al.* 1990b). Andersen *et al.* also found LIP cells that responded to flashes of light, but the exact stimulus characteristics required to maximally stimulate cells were not further investigated. A more detailed electrophysiological study of the selectivities of cells in the caudal part of the lateral IPS (cIPS) was done more recently (Kusunoki *et al.* 1993; Ohtsuka *et al.* 1995; Shikata *et al.* 1996; Sakata *et al.* 1997), and some cells were found that were (a) disparity tuned and (b) respond maximally to a 3D shape whose long axis is oriented in the cell's preferred 3D axis. These "axis orientation selective" (AOS) cells have been proposed to have a function in the visual guidance of grasping hand movements, orienting the hand to the correct position to hold an object. Indeed, the area cIPS projects to the anterior intraparietal area (AIP) (Sakata *et al.* 1995) which is reciprocally connected to ventral premotor (F5) area (Rizzolatti *et al.* 1988) and plays an essential role in matching hand orientation and shape with 3D objects for manipulation (Sakata *et al.* 1997). Sakata's group (Shikata *et al.* 1996) also found disparity tuned cells in the cIPS that responded preferentially to a flat stimulus at a particular 3D orientation. These "surface orientation selective" (SOS) cells extract surface orientation signals from binocular disparity. The positions of SOS and AOS cells was posterior to area LIP of Andersen *et al.* (1990), where saccade and eye movement cells are found. In the current study, projections from V3A to the lateral bank of the IPS were restricted to the caudal extent of this zone, the same area where disparity tuned AOS and SOS cells were found. I propose that at least some of the stereoscopic and orientation information required to generate these

higher order 3D-structure selective cells, important for the manipulation of 3D objects, comes from disparity tuned cells in the V3 complex.

### Patchiness of connections

Many projections in the visual cortex can be described as being "patchy". This is perhaps unsurprising given the common feature of clustering of cells with similar response properties. Assuming that cells with different physiological properties have different projection zones, one would expect this patchiness to represent the input to or output from functional divisions included in the injection site. Following this hypothesis, the patches of transport in V3 following a DP injection could coincide with the columns of V3 containing particular types of cell.

In order to investigate this hypothesis further, the sizes of HRP patches in V3 following a DP injection were compared to the sizes of disparity columns found from recording in that area. A rough average size estimate of patches of HRP transport in V3 following a DP injection is about 1 mm. Unfortunately, it was not possible to make a long tangential penetration through the V3 complex that passed through many disparity columns so the exact width of a disparity column could not be measured. However, evidence from the penetrations that were made suggest that the width of a disparity column must be roughly 300 $\mu$ m. It is possible that the patches of HRP observed in the V3 complex following a DP injection correspond to a group of "asymmetric" or "tuned" disparity columns. A combined recording/injection technique would be necessary to verify this hypothesis, injecting DP with WGA-HRP and plotting the disparity selectivities of cells in relation to patches of HRP transport in that area. Unfortunately this was not achieved in this study.

### General conclusions

This study has attempted to discover the role of the V3 complex in the processing of disparity information and to trace the pathway along which this information is further processed. To this end, a high proportion of orientation and stereotuned cells with their own columnar functional organization was found in this area. The connections of the V3 complex, and a nearby area, DP, to which the V3 complex projects, were investigated with the assumption that form and depth information present in the V3 complex would be further analysed and combined with further information within this pathway. The combination of form and depth information with eye position would be useful in building the internal representations of three dimensional space and the perception of space and 3D form.

From the results of this study, there emerges the idea of a disparity processing system, starting in V1 and becoming more prevalent in the V3 complex, where the visual responses of cells become integrated with other sensory information, like the positions and movement of the eyes. From V3A, it is sent to ventral area TEO (via DP) where it is presumably used for the 3D form analysis necessary for object vision, and to cIPS where the disparity information would be useful for the generation of AOS and SOS cells. The parietal areas (cIPS and AIP) that V3A supplies with stereoscopic information, play an essential role in matching hand orientation and shape with 3D objects for manipulation. Another projection of V3A (via DP) to V6, may have a role in the generation of spatial, egocentric maps of the visual field that are modulated by eye movements.

## Appendix A:

The following is a description of the analysis developed in this laboratory by John Romaya, which I have used to classify cells into functional groups depending on their orientation/direction tuning curves. The analysis also enables values of half width at half height (*hwhh*) to be calculated for tuned cells.

Woergoetter and Eysel (1991) presented a modelling method based on Fourier analysis to represent cell responses to oriented or moving stimuli. We have chosen a different approach because a precise measure of tuning width is required. The Fourier analysis essentially provides models which have fixed tuning widths.

### General model of cell response to different stimulus directions:

The processed data from the experiment take the form of a two column table, a column of directions with an accompanying column of cell responses for each of those directions. The modelling process attempts to fit a number of proposed models to describe the data and then to select a particular model based on statistical criteria.

The general (most complex) model describes the data as two peaks a variable distance apart above a baseline. The peaks have a characteristic peak height and a characteristic half width at half height (Figure n.n). There are ten variations of this model which either omit certain elements (e.g. a model with only one peak), or force certain values to have a fixed relationship with other elements (e.g. the two peaks have equal gains).

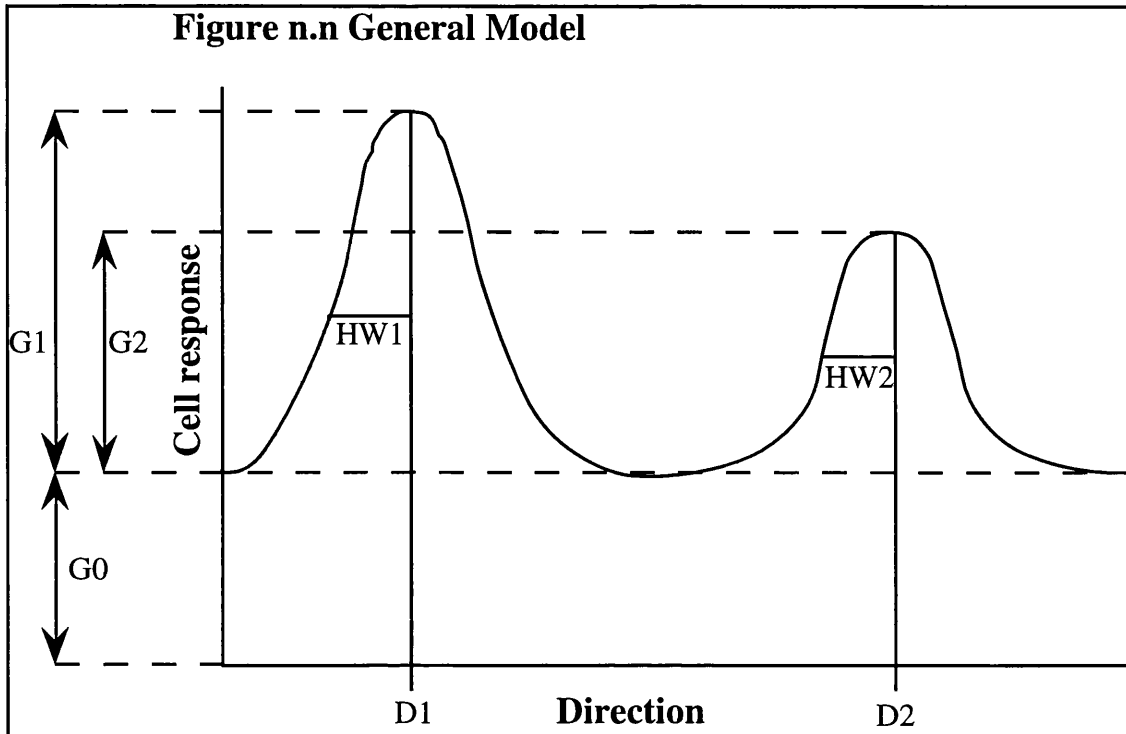


Figure n.n.

An illustration of the general model for orientation/direction tuned cell's responses to a bar stimuli moving in the full range of directions.

$G_0$  = Baseline gain (spike/sec)

$D_1$  = Primary direction (Bearing 0 to 360 degrees)

$HW_1$  = Half width for primary direction (degrees)

$G_1$  = Extra gain at primary direction (spike/sec)

$D_2$  = Secondary direction (Bearing 0 to 360 degrees)

$HW_2$  = Half width for secondary direction (degrees)

$G_2$  = Extra gain at secondary direction (spike/sec)

### Description of the models

There are ten variations on the general model.

- 1/ A flat line distribution with  $G_1$  and  $G_2 = 0$ .
- 2/ A single peak with  $G_2 = 0$ .
- 3/ Two similar peaks, 180 degrees apart,  $G_2 = G_1$ ,  $HW_2 = HW_1$ .
- 4/ Two similar peaks, variable separation,  $G_2 = G_1$ ,  $HW_2 = HW_1$ .
- 5/ Two peaks 180 degrees apart,  $G_2 < G_1$ ,  $HW_2 = HW_1$ .
- 6/ Two peaks 180 degrees apart,  $G_2 = G_1$ ,  $HW_2 < HW_1$ .
- 7/ Two peaks 180 degrees apart,  $G_2 < G_1$ ,  $HW_2 < HW_1$ .
- 8/ Two peaks, variable separation,  $G_2 = G_1$ ,  $HW_2 < HW_1$ .

9/ Two peaks, variable separation,  $G_2 = G_1$ ,  $HW_2 = HW_1$ .

10/ Two peaks, variable separation,  $G_2 = G_1$ ,  $HW_2 \neq HW_1$ .

An extra constraint which may be put on the models is that  $G_1 + G_2 \geq 0$ . This is done to stop models being selected with negative gains which signify inhibition. This occurs in some ambiguous cases when the cell response has wide peaks and there is little to distinguish between a small  $G_0$  with positive  $G_1$  and  $G_2$  or a large  $G_0$  with negative  $G_1$  and  $G_2$ .

Another constraint which may be put on the models is that  $G_0 \geq 0$ ; a negative baseline gain makes little sense.

### Model optimisation

Each model must be optimised so that it fits the actual cell responses as closely as possible; the actual criterion used is to minimise the residual sum of squares of differences between the actual cell response and that predicted by the model.  $G_0$ ,  $G_1$  and  $G_2$  can be optimised by an analytical solution as described below for the general model.

Let the actual cell response for each direction  $\theta$  be  $Act(\theta)$ .

Let the cell response for each direction  $\theta$  as predicted by the model be  $Prd(\theta)$ , given by the following formula:

Eq. 1.0

$$Prd(\theta) = G_0 + G_1.f_1(\theta) + G_2.f_2(\theta)$$

Where:

$f_1(\theta)$  = a function of  $\theta$ ,  $D_1$ ,  $HW_1$  for the primary direction.

$f_2(\theta)$  = a function of  $\theta$ ,  $D_2$ ,  $HW_2$  for the secondary direction.

$f(\theta)$  is a function which returns a value ranging from 0 to 1 and two such functions are available in this study; a simple normal distribution and a wrapped normal distribution (Mardia 1972).

For each angle there is a residual difference between the actual and predicted cell responses  $Res(\theta)$  and the squared residual  $Res^2(\theta)$ .

Eq. 2.1.0

$$Res(\theta) = G_0 + G_1.f_1(\theta) + G_2.f_2(\theta) - Act(\theta)$$

Eq. 2.1.1

$$\begin{aligned} Res^2(\theta) = & G_0^2 + G_1^2.f_1(\theta) + G_2^2.f_2(\theta) + Act^2(\theta) \\ & + 2.G_0.G_1.f_1(\theta) + 2.G_0.G_2.f_2(\theta) - 2.G_0.Act(\theta) \\ & + 2.G_1.G_2.f_1(\theta).f_2(\theta) \\ & - 2.G_1.f_1(\theta).Act(\theta) - 2.G_2.f_2(\theta).Act(\theta) \end{aligned}$$

Then summing over all 'n' cell responses let:

$$\begin{aligned} q &= \sum \{f_1(\theta)\} & r &= \sum \{f_2(\theta)\} & s &= \sum \{f_1^2(\theta)\} \\ t &= \sum \{f_1(\theta).f_2(\theta)\} & u &= \sum \{f_2^2(\theta)\} & v &= \sum \{Act^2(\theta)\} \\ a &= \sum \{Act(\theta)\} & b &= \sum \{Act(\theta).f_1(\theta)\} & c &= \sum \{Act(\theta).f_2(\theta)\} \end{aligned}$$

N.B. Values 'a' and 'v' above are independent of the model used.

Eq. 3.0

$$\begin{aligned} \sum Res^2 = & v + n.G_0^2 + s.G_1^2 + u.G_2^2 \\ & + 2q.G_0.G_1 + 2r.G_0.G_2 + 2t.G_1.G_2 \\ & - 2a.G_0 - 2b.G_1 - 2c.G_2 \end{aligned}$$

To find the minimum value for the residual sum of squares we differentiate and equate to zero for  $G_0$ ,  $G_1$  and  $G_2$ . Solving as three

simultaneous linear equations results in formulae for the optimal values for  $G_0$ ,  $G_1$  and  $G_2$  for any given  $D_1$ ,  $HW_1$ ,  $D_2$  and  $HW_2$ .

Eq. 4.0.0

$$G_0 = \frac{a(t^2 - su) + b(qu - rt) + c(rs - qt)}{nt^2 + uq^2 + sr^2 - nsu - 2qrt}$$

Eq. 4.1.0

$$G_1 = \frac{a(qu - rt) + b(r^2 - nu) + c(nt - qr)}{nt^2 + uq^2 + sr^2 - nsu - 2qrt}$$

Eq. 4.2.0

$$G_2 = \frac{a(rs - qt) + b(nt - qr) + c(q^2 - ns)}{nt^2 + uq^2 + sr^2 - nsu - 2qrt}$$

Eq. 5.0

$$\sum \text{Re } s^2(\theta) = v - (a.G_0 + b.G_1 + c.G_2)$$

Variations on the above formulae 4.0.1 - 4.2.1 are used for some models as listed below, but in each case Eq. 5.0 is still valid.

If there are no peaks ( $G_1 = 0$ ,  $G_2 = 0$ ):

Eq. 6.0.0

$$G_0 = \frac{a}{n}$$

If there is only one peak ( $G_2=0$ ):

Eq. 6.1.0

$$G_0 = \frac{(bq - as)}{q^2 - ns}$$

Eq. 6.1.2

$$G1 = \frac{(aq - bn)}{(q^2 - ns)}$$

If there are two peaks with equal gains ( $G2 = G1$ ):

Eq. 6.2.0

$$G0 = \frac{a(s+u+2t) - (b+c)(q+r)}{n(s+u+2t) - (q+r)^2}$$

Eq. 6,2,1

$$G1 = \frac{n(b+c) - a(q+r)}{n(s+u+2t) - (q+r)^2}$$

If  $G0$  is forced to be zero and there is only one peak ( $G0 = 0$ ,  $G2 = 0$ ):

Eq. 6.3.0

$$G1 = \frac{b}{s}$$

If  $G0$  is forced to be zero and there are two peaks with equal gains ( $G0 = 0$ ,  $G2 = G1$ ):

Eq. 6.4.0

$$G1 = \frac{b+c}{(s+u+2t)}$$

If  $G0$  is forced to be zero and there are two peaks ( $G0 = 0$ ):

Eq. 6.5.0

$$G1 = \frac{(ct - bu)}{(t^2 - su)}$$

Eq. 6.5.1

$$G2 = \frac{(bt - cs)}{t^2 - su}$$

An analytical solution has not been derived for optimising parameters D1, HW1, D2 and HW2. An iterative method is used instead which uses Eq. 5.0 to calculate derivatives and second derivatives of  $\text{Res}^2(\theta)$  with respect to each of the four parameters by introducing small increments in each one. New estimates are calculated for each parameter from these derivatives.

### Statistical analysis of models

Consider a set of data, directions and accompanying cell responses and a model which approximates the accompanying cell responses. For each direction there is an actual cell response and a cell response predicted from the model. The difference between these values is squared and summated over the whole set of data to give a measure of the error for the model, the residual sum of squares.

For a particular direction of stimulus there are a number of repeated trials resulting in a set of cell responses to that stimulus. These repeated trials are used to partition the residual sum of squares into two parts: pure error, which is a measure of variability in repeated trials and lack of fit, which is a measure of how well the experimental cell responses fit a particular model (Draper and Smith 1981).

Three tests were applied to choose between competing models:

1/ For a particular model the lack of fit sum of squares is compared to the pure error sum of squares using an F test. If the outcome of this test is

that the two error components exhibit no statistically significant difference at a pre-determined confidence level then it can be said that the model adequately describes the data within the limits of experimental error and there is no need to proceed to a more complex model to describe the data.

2/ When choosing between models with different degrees of freedom the F test is again used to decide whether the more complex model results in a reduction of lack of fit which is significant at a pre-determined confidence level.

3/ When choosing between different models with the same degrees of freedom the model with the smallest lack of fit is automatically selected.

For this study the confidence levels were set at 50% for test 1 above and at 10% for test 2. These values were chosen because they resulted in model selections which corresponded most closely to selections made by a skilled human judge.

## References

Aicardi, G., P.P. Battaglini and C. Galletti (1987a). The angle of gaze affects the response to visual stimulation of cells in the V3 complex of macaque monkey visual cortex. Journal of Physiology, London **390**: 270.

Aicardi, G., P.P. Battaglini and C. Galletti (1987b). Retinal eye-motion input affects real-motion cell activity in the V3-complex of behaving macaque monkeys. Journal of Physiology, London **388**: 470.

Albright, T.D. (1984). Direction and orientation selectivity of neurons in visual area MT of the macaque. Journal of Neurophysiology **52**: 1106-30.

Alhazen, I. (1989). Book of optics, Warburg institute, University of London.

Andersen, R.A., A. Asanuma and W.M. Cowan (1985). Callosal and prefrontal associational projecting cell populations in area 7A of the macaque monkey: a study using retrogradely transported fluorescent dyes. Journal of Comparative Neurology **232**: 443-55.

Andersen, R.A., A. Asanuma, G. Essick and R.M. Siegel (1990a). Corticocortical connections of anatomically and physiologically defined subdivisions within the inferior parietal lobule. Journal of Comparative Neurology **296**: 65-113.

Andersen, R.A., R.M. Bracewell, S. Barash, J.W. Gnadt and L. Fogassi (1990b). Eye position effects on visual, memory, and saccade-related activity in areas LIP and 7a of macaque. Journal of Neuroscience **10**: 1176-96.

Andersen, R.A. and V.B. Mountcastle (1983). The influence of the angle of gaze upon the excitability of the light-sensitive neurons of the posterior parietal cortex. Journal of Neuroscience **3**: 532-48.

Anstis, S. and P. Cavanagh (1983). A minimum motion technique for judging equiluminance. Colour Vision, Physiology and Psychophysics. J.D. Mollon and L.T. Sharpe. London, Academic press: 155-66.

Baizer, J.S. (1982). Receptive field properties of V3 neurones in monkey. Investigative Ophthalmology and Visual Science **23**: 87-95.

Baker, F.H., P. Grigg and G.K. von Noorden (1974). Effects of visual deprivation and strabismus on the response of visual neurons in the visual cortex of the monkey, including studies on the striate and prestriate cortex in the normal animal. Brain Research **66**: 185-208.

Barlow, H.B., C. Blakemore and J.D. Pettigrew (1967). The neural mechanism of binocular depth discrimination. Journal of Physiology, London **193**: 327-42.

Battaglini, P.P., P. Fattori, C. Galletti and S. Zeki (1990). The physiology of area V6 in the awake, behaving monkey. Journal of Physiology, London **423**: 100P.

Bishop, P.O. (1989). Vertical disparity, egocentric distance and stereoscopic depth constancy: a new interpretation. Proceedings of the Royal Society (London) B **237**: 445-69.

Bishop, P.O., G.H. Henry and C.J. Smith (1971). Binocular interaction fields of single units in the cat striate cortex. Journal of Physiology, London **216**: 39-68.

Bizzi, E. (1968). Discharge of frontal eye field neurons during saccadic and following eye movements in unanesthetized monkeys. Experimental Brain Research **6**: 69-80.

Blakemore, C. (1970). A new type of stereoscopic vision. Vision Research **10**: 1181-99.

Blakemore, C. (1976). The conditions required for maintenance of binocularity in the kitten's visual cortex. Journal of Physiology, London **261**: 423-44.

Blakemore, C., A. Fiorentini and L. Maffei (1972). A second neural mechanism of stereoscopic depth discrimination. Journal of Physiology, London **226**: 725-49.

Blakemore, C. and R.C. Van Sluyters (1975). Innate and environmental factors in the development of the kittens visual cortex. Journal of Physiology, London **482**: 663-716.

Blasdel, G., K. Obermayer and L. Kiorpes (1995). Organization of ocular dominance and orientation columns in the striate cortex of neonatal macaque monkeys. Visual Neuroscience **12**: 589-603.

Blasdel, G.G., J.S. Lund and D. Fitzpatrick (1985). Intrinsic connections of macaque striate cortex: axonal projections of cells outside lamina 4C. Journal of Neuroscience **5**: 3350-69.

Blasdel, G.G. and G. Salama (1986). Voltage-sensitive dyes reveal a modular organization in monkey striate cortex. Nature (London) **321**: 579-85.

Braddick, O.J. (1979). Binocular single vision and perceptual processing. Proceedings of the Royal Society of London. B **204**: 503-12.

Buisseret, P. and L. Maffei (1977). Extraocular proprioceptive projections to the visual cortex. Experimental Brain Research **28**: 421-5.

Burkhalter, A., D.J. Felleman, W.T. Newsome and D.C. Van Essen (1986). Anatomical and physiological asymmetries related to visual areas V3 and VP in macaque extrastriate cortex. Vision Research **26**: 63-80.

Burkhalter, A. and D.C. Van Essen (1982). Processing of color, form and disparity in visual areas V2 and VP of ventral extrastriate cortex in the macaque. Society of Neuroscience Abstracts **8**: 811.

Burkhalter, A. and D.C. Van Essen (1986). Processing of color, form and disparity information in visual areas VP and V2 of ventral extrastriate cortex in the macaque monkey. Journal of Neuroscience **6**: 2327-51.

Colby, C.L., J.R. Duhamel and M.E. Goldberg (1993). Ventral intraparietal area of the macaque: anatomic location and visual response properties. Journal of Neurophysiology **69**: 902-14.

Colby, C.L., R. Gattass, C.R. Olson and C.G. Gross (1988). Topographical organisation of cortical afferents to extrastriate visual area PO in the macaque monkey. Journal of Comparative Neurology **269**: 392-413.

Comerford, J.P. (1974). Stereopsis with chromatic contours. Vision Research **14**: 975-892.

Courville, J. and J.A. Saint Cyr (1978). Modification of the horseradish peroxidase method avoiding fixation. Brain Research **142**: 551-8.

Covey, E., R. Gattass and C.G. Gross (1982). A new visual area in the parieto-occipital sulcus of the macaque. Society for Neuroscience Abstracts **8**: 681.

Cowey, A. (1985). Disturbances of stereopsis by brain damage. Brain mechanisms and spatial vision. D.J. Ingle, M. Jeannerod and N. Lee. Dordrecht, Nijhoff: 259-78.

Cowey, A. and J. Porter (1979). Brain damage and global stereopsis. Proceedings of the Royal Society of London. B **204**: 399-407.

Cragg, B.G. (1969). The topography of the afferent projections in circumstriate visual cortex studied by the Nauta method. Vision Research **9**: 733-47.

Crawford, M.L.J. and G.K. von Noorden (1979). Concomitant strabismus and cortical eye dominance in young rhesus monkeys. Transaction of the Ophthalmology Society, U.K. **99**: 369-74.

Cumming, B.G. (1995). The relationship between stereoacuity and stereomotion thresholds. Perception (London) **24**: 105-14.

Cumming, B.G., E.B. Johnston and A.J. Parker (1991). Vertical disparities and perception of three-dimensional shape. Nature (London) **349**: 411-3.

Cynader, M. and D. Regan (1978). Neurones in cat parastriate cortex sensitive to the direction of motion in three-dimensional space. Journal of Physiology, London **274**: 549-69.

Danta, G., R.C. Hilton and D.J. O'Boyle (1978). Hemisphere function and binocular depth perception. Brain **101**: 569-89.

De Monasterio, F.M. (1983). Color selectivity of V4 cells and induced spectral properties. Society of Neuroscience Abstracts **9**: 153.

De Monasterio, F.M. and S.J. Schein (1982). Spectral bandwidths of color-opponent cells of geniculocortical pathway of macaque monkeys. Journal of Neurophysiology **47**: 214-24.

Derrington, A.M., J. Krauskopf and P. Lennie (1984). Chromatic mechanisms in lateral geniculate nucleus of macaque. Journal of Physiology, London **357**: 241-65.

Derrington, A.M. and P. Lennie (1984). Spatial and temporal contrast sensitivities of neurones in lateral geniculate nucleus of macaque. Journal of Physiology, London **357**: 219-40.

Desimone, R., J. Fleming and C.G. Gross (1980). Prestriate afferents to inferior temporal cortex: An HRP study. Brain Research **184**: 41-55.

Desimone, R. and L.G. Ungerleider (1986). Multiple visual areas in the caudal superior temporal sulcus of the macaque. Journal of Comparative Neurology **248**: 164-89.

DeValois, R., E.W. Yund and N. Helper (1982). The orientation and direction selectivity of cells in macaque visual cortex. Vision Research **22**: 531-44.

DeValois, R.L. (1991). Orientation and spatial frequency selectivity. From pigments to perception. A. Valberg and B.B. Lee. New York, Plenum Press: 261-7.

DeValois, R.L. and K.K. DeValois (1988). Spatial vision. New York, Oxford University Press.

DeYoe, E.A. and D.C. Van Essen (1985). Segregation of efferent connections and receptive field properties in visual area 2 of the macaque. Nature (London) **317**: 58-61.

DeYoe, E.A. and D.C. Van Essen (1988). Concurrent processing streams in the monkey visual cortex. Trends in Neuroscience **11**: 219-26.

Dow, B.M. (1974). Functional classes of cells and their laminar distribution in monkey visual cortex. Journal of Neurophysiology 37: 927-46.

Draper, N. and H. Smith (1981). Applied Regression Analysis, John Wiley & Sons.

Dreher, B., Y. Fukada and R.W. Rodieck (1976). Identification, classification and anatomical segregation of cells with X-like and Y-like properties in the lateral geniculate nucleus of Old-World primates. Journal of Physiology, London 258: 433-52.

Enright, J.T. (1987). Art and the oculomotor system: Perspective illustrations evoke vergence changes. Perception (London) 16: 731-46.

Felleman, D.J., G.J. Carman and D.C. Van Essen (1984). Evidence for a functional distinction between areas V3 and VP of macaque extrastriate cortex. Investigative Ophthalmology and Visual Science, Supplement 23: 278.

Felleman, D.J. and D.C. Van Essen (1983). Cortical connections of area V3 in macaque extrastriate cortex. Society of Neuroscience Abstracts 10: 933.

Felleman, D.J. and D.C. Van Essen (1987). Receptive field properties of neurons in area V3 of macaque monkey extrastriate cortex. Journal of Neurophysiology 57: 889-920.

Felleman, D.J. and D.C. Van Essen (1991). Distributed hierarchical processing in the primate cerebral cortex. Cerebral Cortex 1: 1-47.

Fink, R.P. and L. Heimer (1967). Two methods for selective silver impregnation of degenerating axons and their synaptic endings in the central nervous system. Brain Research 4: 369-74.

Fiorentini, A., L. Maffei, M.C. Cenni and A. Tacchi (1985). Deafferentation of oculomotor proprioception affects depth discrimination in adult cats. Experimental Brain Research 59: 296-301.

Fischer, B. and G.F. Poggio (1979). Depth sensitivity of binocular cortical neurones of behaving monkeys. Proceedings of the Royal Society of London. B 204: 409-14.

Fitzpatrick, D., J.S. Lund and G.G. Blasdel (1985). Intrinsic connections of macaque striate cortex: afferent and efferent connections of lamina 4C. Journal of Neuroscience 5: 3329-49.

Frisby, J.P. and B. Julesz (1975a). Depth reduction effects in random line stereograms. Perception (London) 4: 151-8.

Frisby, J.P. and B. Julesz (1975b). The effect of orientation differences on stereopsis as a function of line length. Perception (London) 4: 179-86.

Galen, C. (175). De usa partium corporis humani. Ithaca, NY, Cornell University Press.

Galletti, C. and P.P. Battaglini (1989). Gaze-dependant visual neurones in area V3a of monkey prestriate cortex. Journal of Neuroscience 9: 1112-25.

Galletti, C., P.P. Battaglini and G. Aicardi (1988). 'Real-motion' cells in visual area V2 of behaving macaque monkeys. Experimental Brain Research **69**: 279-88.

Galletti, C., P.P. Battaglini and P. Fattori (1990). 'Real-motion' cells in area V3A of macaque visual cortex. Experimental Brain Research **82**: 67-76.

Galletti, C., P.P. Battaglini and P. Fattori (1993). Parietal neurons encoding spatial locations in craniotopic coordinates. Experimental Brain Research: 1-9.

Galletti, C., P. Fattori, P.P. Battaglini, S. Shipp and S. Zeki (1996). Functional demarcation of a border between areas V6 and V6A in the superior parietal gyrus of the macaque monkey. European Journal of Neuroscience **8**: 30-52.

Galletti, C., S. Squatrito, P.P. Battaglini and M.G. Maioli (1984). 'Real-motion' cells in the primary visual cortex of macaque monkeys. Brain Research **301**: 95-110.

Gallyas, F. (1979). Silver staining of myelin by means of physical development. Neurological Research **1**: 203-9.

Gamlin, P.D. and R.J. Clarke (1995). Single-unit activity in the primate nucleus reticularis tegmenti pontis related to vergence and ocular accommodation. Journal of Neurophysiology **73**: 2115-9.

Gamlin, P.D., K. Yoon and H. Zhang (1996). The role of cerebro-ponto-cerebellar pathways in the control of vergence eye movements. Eye **10**: 167-71.

Gattass, R. and C.G. Gross (1981). Visual topography of striate projection zone (MT) in posterior superior temporal sulcus of the macaque. Journal of Neurophysiology **46**: 621-38.

Gattass, R., C.G. Gross and J.H. Sandell (1981). Visual topography of V2 in the macaque. Journal of Comparative Neurology **201**: 519-39.

Gegenfurtner, K.R., D.C. Kiper and S.B. Fenstemaker (1995). Integration of color information in macaque area V2. Max-Planck Institut fur biologische kybernetic. Technical report **10**: 1-14.

Gegenfurtner, K.R., D.C. Kiper and S.B. Fenstemaker (1996). Processing of color, form, and motion in macaque area V2. Visual Neuroscience **13**: 161-72.

Gilbert, C.D. and J.P. Kelly (1975). The projections of cells in different layers of the cat's visual cortex. Journal of Comparative Neurology **163**: 81-105.

Gnadt, J.W. and L.E. Mays (1991). Depth-tuning in area LIP by disparity and accommodative cues. Society of Neuroscience Abstracts **17**: 443-511.

Gonzalez, F., J.L. Relova, R. Perez, C. Acuna and J.M. Alonso (1993). Cell responses to vertical and horizontal retinal disparities in the monkey visual cortex. Neuroscience Letters **160**: 167-70.

Goodale, M.A. and A.D. Milner (1992). Separate visual pathways for perception and action. Trends in Neuroscience **15**: 20-5.

Grafstein, B. and R. Laurenco (1973). Transport of radioactivity from eye to visual cortex in the mouse. Experimental Neurology **39**: 44-57.

Graves, A.L., Y. Trotter and Y. Frégnac (1987). Role of extraocular muscle proprioception in the development of depth perception in cats. Journal of Neurophysiology **58**: 816-31.

Gregory, R.L. (1979). Stereo vision and isoluminance. Proceedings of the Royal Society of London. B **204**: 467-76.

Guillery, R.W. (1971). Patterns of synaptic interconnections in the dorsal lateral geniculate nucleus of cat and monkey: a brief review. Vision Research **3**: 211-27.

Hanny, P., R. Von der Heydt and G.F. Poggio (1980). Binocular neurone responses to tilt in depth in the monkey visual cortex. Evidence for orientation disparity processing. Experimental Brain Research **41**: 26.

Hawken, M.J., A.J. Parker and J.S. Lund (1988). Laminar organization and contrast selectivity of direction selective cells in the striate cortex of the Old-World monkey. Journal of Neuroscience **8**: 3541-8.

Hebb, D.O. (1949). The Organization of Behavior: A Neuropsychological Theory. New York, Wiley.

Hein, A. and R. Diamond (1983). Contributions of eye movement to the representation of space. Spatially oriented behavior. M. Jeannerod. Berlin, Springer: 119-33.

Helmholtz, H.v. (1893). Popular lectures on scientific subjects. London, Longmans Green.

Helmholtz, H.v. (1909). Physiological Optics. New York, Dover.

Henry, G.H., P.O. Bishop and J.S. Coombs (1969). Inhibitory and subliminal excitatory receptive fields of simple units in cat striate cortex. Vision Research 9: 1289-96.

Hillebrand, F. (1893). Die Stabilität der Raumwerte auf der Netzhaut. Zeitschrift für Psychologie und Physiologie der Sinnesorgane 5: 1-60.

Hong, X. and D. Regan (1989). Visual field defects for unidirectional and oscillatory motion in depth. Vision Research 29: 809-19.

Horton, J.C. (1984). Cytochrome oxidase patches: a new cytoarchitectonic feature of monkey visual cortex. Philosophical Transactions of the Royal Society of London, B 304: 199-253.

Horton, J.C. and D.H. Hubel (1981). Regular patchy distribution of cytochrome oxidase staining in primary visual cortex of macaque monkey. Nature (London) 292: 762-4.

Hubel, D.H. and M.S. Livingstone (1985). Complex-unoriented cells in a subregion of primate area 18. Nature (London) 315: 325-7.

Hubel, D.H. and M.S. Livingstone (1987). Segregation of form, color, and stereopsis in primate area 18. Journal of Neuroscience 7: 3378-415.

Hubel, D.H. and T.N. Wiesel (1959). Receptive fields of single neurones in the cat's striate cortex. Journal of Physiology, London 148: 574-91.

Hubel, D.H. and T.N. Wiesel (1962). Receptive fields, binocular interaction and functional architecture in the cat's visual cortex. Journal of Physiology, London 160: 106-54.

Hubel, D.H. and T.N. Wiesel (1965a). Binocular interaction in striate cortex of kittens reared with artificial squint. Journal of Neurophysiology 28: 1041-59.

Hubel, D.H. and T.N. Wiesel (1965b). Receptive fields and functional architecture in two non-striate visual areas (18 and 19) in the cat. Journal of Neurophysiology 28: 229-89.

Hubel, D.H. and T.N. Wiesel (1968). Receptive fields and functional architecture of monkey striate cortex. Journal of Physiology, London 195: 215-43.

Hubel, D.H. and T.N. Wiesel (1969). Anatomical demonstration of columns in the monkey striate cortex. Nature (London) 221: 747-50.

Hubel, D.H. and T.N. Wiesel (1970). Cells sensitive to binocular depth in area 18 of the macaque monkey. Nature (London) 225: 41-2.

Hubel, D.H. and T.N. Wiesel (1972). Laminar and columnar distribution of geniculate-cortical fibers in the macaque monkey. Journal of Comparative Neurology 146: 421-50.

Hubel, D.H. and T.N. Wiesel (1973). A re-examination of stereoscopic mechanisms in area 17 of the cat. Journal of Physiology, London 232 P: 29-30.

Hubel, D.H. and T.N. Wiesel (1977). The Ferrier Lecture: Functional architecture of macaque monkey visual cortex. Proceedings of the Royal Society (London) B 198: 1-59.

Hubel, D.H., T.N. Wiesel and M.P. Stryker (1978). Anatomical demonstration of orientation columns in macaque monkey. Journal of Comparative Neurology 177: 361-79.

Iwai, E. and M. Mishkin (1969). Further evidence on the locus of the visual area in the temporal lobe of the monkey. Experimental Neurology 25: 585-94.

Jansen, G.F., M. Kedaria and W.W. Zuurmond (1990). Total intravenous anaesthesia during intracranial surgery. Continuous Propofol infusion in combination with either Fentanyl or Sufentanil. Canadian Journal of Anaesthesia 37: S128.

Joshua, D.E. and P.O. Bishop (1970). Binocular single vision and depth discrimination. Receptive field disparities for central and peripheral vision and binocular interaction on peripheral single units in cat striate cortex. Experimental Brain Research 10: 389-416.

Judge, S.J. and B.G. Cumming (1986). Neurons in the monkey midbrain with activity related to vergence eye movement and accommodation. Journal of Neurophysiology 55: 915-30.

Judson, J.R. and C. van de Velde (1978). part XXI; book illustrations and title-pages. London, Philadelphia, Harvey Miller-Heyden and son.

Julesz, B. (1960). Binocular depth perception of computer generated patterns. Bell Systems Technical Journal 39: 1125-62.

Julesz, B. (1971). Foundations of cyclopean perception. Chicago, Univ. of Chicago press.

Julesz, B. and J.E. Miller (1975). Independent spatial frequency tuned channels in binocular fusion and rivalry. Perception (London) 4: 125-43.

Julesz, B. and H.P. Oswald (1978). Binocular utilization of monocular cues that are undetectable monocularly. Perception (London) 7: 315-22.

Kaplan, E. and R.M. Shapley (1982). X and Y cells in the lateral geniculate nucleus of macaque monkeys. Journal of Physiology, London 330: 125-43.

Kaye, M., D.E. Mitchell and M. Cynader (1982). Depth perception, eye alignment and cortical ocular dominance of dark reared cats. Developmental Brain Research 2: 37-53.

Keele, K.D. (1955). Leonardo da Vinci on vision. Proceedings of the Royal Society of Medicine 48: 384-90.

Kikuchi, R. and E. Iwai (1980). The locus of the posterior subdivision of the inferotemporal visual learning area in the monkey. Brain Research **198**: 347-60.

Kolmel, H.W. (1988). Pure homonymous hemiachromatopsia: findings with neuro-ophthalmologic examination and imaging procedures. European Archives of Psychiatry and Neurological sciences **237**: 237-43.

Kusunoki, M., Y. Tanaka, K. Ohtsuka and H. Sakata (1993). Selectivity of the parietal visual neurons in the axis orientation of objects in space. Society for Neuroscience Abstracts **19**: 770.

LeVay, S., M. Connolly, J. Houde and D.C. Van Essen (1985). The complete pattern of ocular dominance stripes in the striate cortex and visual field of the macaque monkey. Journal of Neuroscience **5**: 486-501.

LeVay, S. and T. Voigt (1988). Ocular dominance and disparity coding in cat visual cortex. Visual Neuroscience **1**: 395-414.

Lippincott, J.A. (1889). On the binocular metamorphosis produced by correcting glasses. Archives of Ophthalmology **18**: 18-30.

Livingstone, M.S. and D.H. Hubel (1982). Thalamic inputs to cytochrome oxidase-rich regions in monkey visual cortex. Proceedings of the National Academy of Sciences of the USA **79**: 6098-101.

Livingstone, M.S. and D.H. Hubel (1984). Anatomy and physiology of a color system in the primate visual cortex. Journal of Neuroscience **4**: 309-56.

Livingstone, M.S. and D.H. Hubel (1987a). Connections between layer 4B of area 17 and the thick cytochrome oxidase stripes of area 18 in the squirrel monkey. Journal of Neuroscience 7: 3371-7.

Livingstone, M.S. and D.H. Hubel (1987b). Psychophysical evidence for separate channels for the perception of form, color, movement, and depth. Journal of Neuroscience 7: 3416-68.

Livingstone, M.S. and D.H. Hubel (1988). Segregation of form, color, movement, and depth: anatomy, physiology, and perception. Science (New York) 240: 740-9.

Livingstone, M.S., S. Nori, D.C. Freeman and D.H. Hubel (1995). Stereopsis and binocularity in the squirrel monkey. Vision Research 35: 345-54.

Logothetis, N.K., J. Pauls and T. Poggio (1995). Shape representation in the inferior temporal cortex of monkeys. Current Biology 5: 552-63.

Logothetis, N.K., P.H. Schiller, E.R. Charles and A.C. Hurl Bert (1990). Perceptual deficits and the activity of the color-opponent and broad-band pathways at isoluminance. Science (New York) 247: 214-7.

Longuet-Higgins, H.C. (1981). A computer algorithm for reconstructing a scene from two projections. Nature (London) 293: 133-5.

Longuet-Higgins, H.C. (1982a). Appendix to paper by John Mayhew entitled: "The interpretation of stereo-disparity information: The computation of surface orientation and depth.". Perception (London) **11**: 405-7.

Longuet-Higgins, H.C. (1982b). The role of the vertical dimension in stereoscopic vision. Perception (London) **11**: 377-86.

Lu, C. and D.H. Fender (1972). The interaction of colour and luminance in stereoscopic vision. Investigative Ophthalmology and Visual Science **2**: 482-9.

Lund, J.S., R.D. Lund, A.E. Hendrickson, A.M. Bunt and A.F. Fuchs (1975). The origin of efferent pathways from the primary visual cortex, (area 17), of the macaque monkey as shown by retrograde transport of horseradish peroxidase. Journal of Comparative Neurology **164**: 287-304.

Maguire, W.M. and J.S. Baizer (1984). Visuotopic organization of the prelunate gyrus in rhesus monkey. Journal of Neuroscience **4**: 1690-704.

Malpeli, J.G., P.H. Schiller and C.L. Colby (1981). Response properties of single cells in monkey striate cortex during reversible inactivation of individual lateral geniculate laminae. Journal of Neurophysiology **46**: 1102.

Mansfield, J.S. and A.J. Parker (1993). An orientation-tuned component in the contrast masking of stereopsis. Vision Research **33**: 1535-44.

Mardia, K.V. (1972). Statistics of directional data, Academic Press: 48-69.

Maske, R., S. Yamane and P.O. Bishop (1984). Binocular simple cells for local stereopsis: comparison of receptive field organizations for the two eyes. Vision Research **23**: 1921-9.

Maske, R., S. Yamane and P.O. Bishop (1986a). End stopped cells and binocular depth discrimination in the striate cortex of cats. Proceedings of the Royal Society of London. B **229**: 257-76.

Maske, R., S. Yamane and P.O. Bishop (1986b). Stereoscopic mechanisms: binocular responses of the striate cells of cats to moving light and dark bars. Proceedings of the Royal Society of London. B **229**: 227-56.

Maunsell, J.H. and D.C. Van Essen (1983a). Functional properties of neurons in middle temporal visual area of the macaque monkey. II. Binocular interactions and sensitivity to binocular disparity. Journal of Neurophysiology **49**: 1148-67.

Maunsell, J.H.R. and D.C. Van Essen (1983b). The connections of the middle temporal visual area (MT) and their relationship to a cortical hierarchy in the macaque monkey. Journal of Neuroscience **3**: 2563-86.

Mayhew, J. (1982). The interpretation of stereo-disparity information: The computation of surface orientation and depth. Perception (London) **11**: 387-403.

Mayhew, J.E. and H.C. Longuet-Higgins (1982). A computational model of binocular depth perception. Nature (London) **297**: 376-8.

Mayhew, J.E.W. and J.P. Frisby (1977). Global processes in stereopsis: Some comments on Ramachandran and Nelson (1976). Perception (London) **6**: 195-206.

Merrill, E.G. and A. Ainsworth (1972). Glass coated platinum-plated tungsten microelectrodes. Medical, Electrical and Biological Engineering **10**: 662-72.

Mesulam, M.M. (1978). Tetramethyl benzidine for horseradish peroxidase neurohistochemistry: a non-carcinogenic blue reaction product with superior sensitivity for visualizing neural afferents and efferents. Journal of Histochemistry and Cytochemistry **26**: 106-17.

Mesulam, M.M. (1982). Tracing neural connections with horseradish peroxidase. New York, Wiley.

Michael, C.R. (1978a). Color vision mechanisms in monkey striate cortex: simple cells with dual opponent-color receptive fields. Journal of Neurophysiology **46**: 1233-49.

Michael, C.R. (1978b). Color-sensitive complex cells in monkey striate cortex. Journal of Neurophysiology **41**: 1250-66.

Mishkin, M., L.G. Ungerleider and K.A. Macko (1983). Object vision and spatial vision: two cortical pathways. Trends in Neuroscience **6**: 414-7.

Mountcastle, V.B. (1957). Modality and topographic properties of cat's somatic sensory cortex. Journal of Neurophysiology **20**: 408-34.

Movshon, J.A. and W.T. Newsome (1984). Striate cortical neurons projecting to MT in the macaque monkey. Perception (London) **13**: A24.

Müller, J. (1826). Zur Vergleichenden Physiologie des Gesichtssinnes des Menschen und der Thiere. Leipzig, Cnobloch.

Nauta, W.J.H. and Gyax (1954). Silver impregnation of degenerating axons in the central nervous system. Stain Technology **29**: 91-3.

Nelson, J.I., H. Kato and P.O. Bishop (1977). Discrimination of orientation and position disparities by binocularly activated neurones in cat striate cortex. Journal of Neurophysiology **40**: 260-83.

Nikara, T., P.O. Bishop and J.D. Pettigrew (1968). Analysis of retinal correspondence by studying receptive fields of binocular single units in cat striate cortex. Experimental Brain Research **6**: 353-72.

Ogle, K.N. (1962). The optical space sense. The eye. H. Davson. New York, Academic press. **4**, part 2: 211-407.

Ogle, K.N. (1964). Binocular vision. New York, Hafner.

Ohtsuka, H., Y. Tanaka, M. Kusunoki and H. Sakata (1995). [Neurons in monkey parietal association cortex sensitive to axis orientation]. Nippon Ganka Gakkai Zasshi **99**: 59-67.

Ono, H. and J. Comerford (1977). Stereoscopic depth constancy. Stability and constancy in visual perception. W. Epstein. New York, Wiley. **1**: 91-128.

Over, R., N. Long and W. Lovegrove (1973). Absence of binocular interaction between spatial and color attributes of visual stimuli. Perception and Psychophysics **13**: 534-40.

Pandya, D.P. and L.A. Vignolo (1968). Interhemispheric neocortical projections of somatosensory areas I and II in the rhesus monkey. Brain Research **7**.

Panum, P.L. (1858). Physiologische Untersuchungen über das Sehen mit zwei Augen. Keil, Schwes.

Papert, S. (1961). Centrally produced geometrical illusions. Nature (London) **191**: 733.

Peterhans, E. and R. Von der Heydt (1993). Functional organisation of area V2 in the alert macaque. European Journal of Neuroscience **5**: 509-24.

Pettigrew, J.D. (1973). Binocular neurones which signal change of disparity in area 18 of cat visual cortex. Nature (London) **241**: 123-4.

Pettigrew, J.D., T. Nikara and P.O. Bishop (1968). Binocular interaction on single units in cat striate cortex: Simultaneous stimulation by single moving slit with receptive fields in correspondence. Experimental Brain Research **6**: 391-410.

Poggio, G.F. (1979). Mechanisms of stereopsis in monkey visual cortex. Trends in Neuroscience: 199-201.

Poggio, G.F., F.H. Baker, R.J.W. Mansfield, A. Silito and P. Grigg (1975). Spatial and chromatic properties of neurons subserving foveal and parafoveal vision in rhesus monkey. Brain Research **100**: 25-59.

Poggio, G.F. and B. Fischer (1977). Binocular interaction and depth sensitivity in striate and prestriate cortex of behaving rhesus monkey. Journal of Neurophysiology **40**: 1392-405.

Poggio, G.F., F. Gonzalez and F. Krause (1988). Stereoscopic mechanisms in monkey visual cortex: binocular correlation and disparity selectivity. Journal of Neuroscience **8**: 4531-50.

Poggio, G.F., B.C. Motter, S. Squatrito and Y. Trotter (1985). Responses of neurons in visual cortex (V1 and V2) of the alert macaque to dynamic random-dot stereograms. Vision Research **25**: 397-406.

Poggio, G.F. and W.H. Talbot (1981). Mechanisms of static and dynamic stereopsis in foveal cortex of the rhesus monkey. Journal of Physiology, London **315**: 469-92.

Pohl, W. (1973). Dissociation of spatial discrimination deficits following frontal and parietal lesions in monkeys. Journal of Comparative Physiology and Psychology **82**: 227-39.

Prévost, A. (1843). Essai sur la theorie de la vision binoculaire. Geneva, Ramboz.

Ptito, M., F. Lepore and J.P. Guillemot (1992). Loss of stereopsis following lesions of cortical areas 17 - 18 in the cat. Experimental Brain Research **89**: 521-30.

Ramachandran, V.S. and S. Sriram (1972). Stereopsis generated with Julesz patterns in spite of rivalry imposed by colour filters. Nature (London) **237**: 347-8.

Ramón y Cajal, S. (1911). Histologie du system nerveux de l'homme et des vertébrés. Paris, A. Maloine.

Regan, D. and K.I. Beverley (1973). Electrophysiological evidence for existence of neurones sensitive to direction of depth movement. Nature (London) **246**: 504-6.

Richards, W. (1968). Spatial remapping in the primate visual system. Kybernetik **4**: 146-56.

Richards, W. (1970). Stereopsis and stereoblindness. Experimental Brain Research **10**: 380-8.

Richards, W. (1973). Reversal in stereo discrimination by contrast reversal. American Journal of Optometry and Archives of American Academy of Optometry **50**: 853-62.

Richards, W. and D. Regan (1973). A stereo field map with implications for disparity processing. Investigative Ophthalmology and Visual Science **12**: 904-9.

Riddoch, G. (1917). Dissociation of visual perceptions due to occipital injuries, with especial reference to the appreciation of movement. Brain **40**: 15-57.

Ritter, M. (1977). Effect of disparity and viewing distance on perceived depth. Perception and Psychophysics **22**: 400-7.

Rizzolatti, G., R. Camarda, L. Fogassi, M. Gentilucci, G. Luppino and M. Matelli (1988). Functional organization of inferior area 6 in the macaque monkey. II. Area F5 and the control of distal movements. Experimental Brain Research **71**: 491-507.

Rockland, K.S. (1985). A reticular pattern of intrinsic connections in primate area V2 (area 18). Journal of Comparative Neurology **235**: 467-78.

Rockland, K.S. and D.N. Pandya (1979). Laminar origins and terminations of cortical connections of the occipital lobe in the rhesus monkey. Brain Research **179**: 3-20.

Rodieck, R.W. (1971). Central nervous system: afferent mechanisms. Annual reviews of physiology **33**: 203-40.

Rogers, B.J. and R. Cagenello (1989). Disparity curvature and the perception of three-dimensional surfaces. Nature (London) **339**: 135-7.

Romaya, J. and S. Zeki (1985). Rotatable three-dimensional reconstructions of the macaque monkey brain. Journal of Physiology, London **371**: 25P.

Rosene, D.L. and M.M. Mesulam (1978). Fixation variables in horseradish peroxidase neurohistochemistry. I. The effect of fixation time and perfusion procedures upon enzyme activity. Journal of Histochemistry and Cytochemistry **26**: 28-39.

Rouse, M.W., J.S. Tittle and M.L. Braunstein (1989). Stereoscopic depth perception by static stereo-deficient observers in dynamic displays with constant and changing disparity. Optometry and Vision Science **66**: 355-62.

Roy, J.P., H. Komatsu and R. Wurtz (1992). Disparity sensitivity of neurons in monkey extrastriate area MST. Journal of Neuroscience **12**: 2478-92.

Sakata, H., H. Shibutani and K. Kawano (1980). Spatial properties of visual fixation neurones in posterior parietal association cortex of the monkey. Journal of Neurophysiology **43**: 1654-72.

Sakata, H., M. Taira, M. Kusunoki, A. Murata and Y. Tanaka (1997). The TINS Lecture: The parietal association cortex in depth perception and visual control of hand action. Trends in Neuroscience **20**: 350-7.

Sakata, H., M. Taira, A. Murata and S. Mine (1995). Neural mechanisms of visual guidance of hand action in the parietal cortex of the monkey. Cerebral Cortex **5**: 429-38.

Schiller, P.H. and N.K. Logothetis (1990). The color-opponent and broad-band channels of the primate visual system. Trends in Neuroscience **13**: 392-8.

Schiller, P.H., N.K. Logothetis and E.R. Charles (1990). Functions of the colour-opponent and broad-band channels of the visual system. Nature (London) **343**: 68-70.

Schlag-Rey, M. and J. Schlag (1984). Visuomotor functions of central thalamus in monkey. I. Unit activity related to spontaneous eye movements. Journal of Neurophysiology **51**: 1149-74.

Seltzer, B. and D.N. Pandya (1978). Afferent cortical connections and architectonics of the superior temporal sulcus and surrounding cortex in the rhesus monkey. Brain Research **149**: 1-24.

Seltzer, B. and D.N. Pandya (1980). Converging visual and somatic sensory cortical input to the intraparietal sulcus of the rhesus monkey. Brain Research **192**: 339-51.

Servos, P., M.A. Goodale and J. L.S. (1992). The role of binocular vision in prehension: a kinematic analysis. Vision Research **32**: 1513-21.

Shikata, E., Y. Tanaka, H. Nakamura, M. Taira and H. Sakata (1996). Selectivity of the parietal visual neurones in 3D orientation of surface of stereoscopic stimuli. Neuroreport **7**: 2389-94.

Shipp, S. and S. Zeki (1995). Segregation and convergence of specialised pathways in macaque monkey visual cortex. Journal of Anatomy **187**: 547-62.

Shipp, S.D. and S.M. Zeki (1985). Segregation of pathways leading from area V2 to areas V4 and V5 of macaque visual cortex. Nature (London) **315**: 322-5.

Shipp, S.D. and S.M. Zeki (1988). The functional logic of cortical connections. Nature (London) **335**: 311-7.

Shipp, S.D. and S.M. Zeki (1989). The organization of connections between areas V5 and V2 in macaque monkey visual cortex. European Journal of Neuroscience **1**: 333-54.

Shook, B.L., B.P. Abramson and L.M. Chalupa (1984). An analysis of the transport of HRP-WGA in the cat's visual system. Journal of Neuroscience Methods **11**: 65-77.

Siegel, S. (1956). Nonparametric statistics for the Behavioral sciences. Tokyo, McGraw-Hill Kobakusha.

Silva, P.S. (1956). Some anatomical and physiological aspects of the lateral geniculate body. Journal of Comparative Neurology **106**: 463-86.

Smith, E. and Holmes, G. (1916). A case of bilateral motor apraxia with disturbance of visual orientation. British Medical Journal **March 25**: 437.

Smith, E.L., M.J. Bennett, R.S. Harwerth and M.L.J. Crawford (1979). Binocularity in kittens reared with optically induced squint. Science (New York) **204**: 875-7.

Sokoloff, L. (1977). Relation between physiological function and energy metabolism in the central nervous system. Journal of Neurochemistry **29**: 13-26.

Sparks, D.L. (1986). Translation of sensory signals into commands for control of saccadic eye movements: role of primate superior colliculus. Physiological Reviews **66**: 118-71.

Stanton, G.B., M.E. Goldberg and C.J. Bruce (1988). Frontal eye field efferents in the macaque monkey: II. Topography of terminal fields in midbrain and pons. Journal of Comparative Neurology **271**: 493-506.

Strong, D.S. (1979). Leonardo on the eye. New York, Garland.

Tanaka, M., E. Lindsley, S. Lausmann and O.D. Creutzfeldt (1990). Afferent connections of the prelunate visual association cortex (areas V4 and DP). Anatomy and Embryology (Berlin) **181**: 19-30.

Tieman, D.G., N. Tumosa and S.B. Tieman (1983). Behavioral and physiological effects of monocular deprivation: A comparison of rearing with diffusion and occlusion. Brain Research **280**: 41-50.

Tigges, J., M. Tigges and A.A. Perachio (1977). Complementary laminar terminations of afferents to area 17 originating in area 18 and in the lateral geniculate nucleus in squirrel monkey. Journal of Comparative Neurology **176**: 87-100.

Tootell, R.B.H. and S.L. Hamilton (1989). Functional anatomy of the second visual area (V2) in the macaque. Journal of Neuroscience 9: 2620-44.

Tootell, R.B.H., S.L. Hamilton, M.S. Silverman and E. Switkes (1988a). Functional anatomy of macaque striate cortex. I. Ocular dominance, binocular interactions, and baseline conditions. Journal of Neuroscience 8: 1500-30.

Tootell, R.B.H., M.S. Silverman, R.L. DeValois and G.H. Jacobs (1983). Functional organization of the second visual cortical area in primates. Science (New York) 220: 737-9.

Tootell, R.B.H., M.S. Silverman, S.L. Hamilton, E. Switkes and R.L. DeValois (1988b). Functional anatomy of macaque striate cortex. Journal of Neuroscience 8: 1500-624.

Tootell, R.B.H., M.S. Silverman, S.L. Hamilton, E. Switkes and R.L. DeValois (1988c). Functional anatomy of macaque striate cortex. V. Spatial frequency. Journal of Neuroscience 8: 1610-24.

Trojanowski, J.Q. (1983). Native and derivated lectins for in vivo studies of neuronal connectivity and neuronal cell biology. Journal of Neuroscience Methods 9: 185-204.

Trotter, Y. (1995). Cortical representation of visual three-dimensional space. Perception (London) 24: 287-98.

Trotter, Y., S. Celebrini, J.C. Beaux, B. Grandjean and M. Imbert (1993). Long-term dysfunctions of neural stereoscopic mechanisms after unilateral extraocular muscle proprioceptive deafferentation. Journal of Neurophysiology **69**: 1513-29.

Trotter, Y., S. Celebrini, B. Stricanne, S. Thorpe and M. Imbert (1992). Modulation of neural stereoscopic processing in primate area V1 by the viewing distance. Science (New York) **257**: 1279-81.

Trusk, T.C., W.S. Kaboord and M.T.T. Wong-Riley (1990). Effects of monocular enucleation, tetrodotoxin and lid suture on cytochrome-oxidase reactivity in supragranular puffs of adult macaque striate cortex. Visual Neuroscience **4**: 185-204.

Ungerleider, L.G. and R. Desimone (1986). Cortical connections of visual area MT in the macaque. Journal of Comparative Neurology **248**: 190-222.

Ungerleider, L.G. and M. Mishkin (1982). Two cortical visual systems. Analysis of Visual Behaviour. D.J. Ingle, M.A. Goodale and R.J.W. Mansfield. Cambridge, MA, MIT Press: 549-86.

Van Essen, D.C., J.H.R. Maunsell and J.L. Bixby (1981). The middle temporal visual area in the macaque: myeloarchitecture, connections, functional properties and topographic organization. Journal of Comparative Neurology **199**: 293-326.

Van Essen, D.C., W.T. Newsome and J.L. Bixby (1982). The pattern of interhemispheric connections and its relationship to extrastriate visual areas in the macaque monkey. Journal of Neuroscience **2**: 265-83.

Van Essen, D.C., W.T. Newsome, J.H. Maunsell and J.L. Bixby (1986). The projections from striate cortex (V1) to areas V2 and V3 in the macaque monkey: asymmetries, areal boundaries, and patchy connections. Journal of Comparative Neurology **244**: 451-80.

Van Essen, D.C. and S.M. Zeki (1978). The topographic organisation of rhesus monkey prestriate cortex. Journal of Physiology, London **277**: 193-226.

Vieth, G.A.U. (1818). Über die Richtung der Augen. Annalen der Physik **28**.

Von Bonin, G., H.W. Garol and W.S. McCulloch (1942). The functional organization of the occipital lobe. Biological Symposia **7**: 165-92.

Von der Heydt, R., C. Adorjani, P. Hanny and G. Baumgartner (1978). Disparity sensitivity and receptive field incongruity of units in the cat striate cortex. Experimental Brain Research **31**: 523-45.

Waugaman, W.R. and S.D. Foster (1991). New advances in anesthesia. Nursing Clinics of North America **26**: 451-61.

Weorgoetter, F. and U.T. Eysel (1991). Axial responses in visual cortical cells: Spatio-temporal mechanisms quantified by Fourier components of cortical tuning curves. Experimental Brain Research **83**: 656-64.

Wheatstone, C. (1838). Contributions to the physiology of vision. -Part the first: On some remarkable, and hitherto unobserved, Phenomena of

Binocular Vision. Philosophical Transactions of the Royal Society of London, B 2: 371-94.

Whitteridge, D. (1965). Area 18 and the vertical meridian of vision. Functions of the corpus callosum. E.G. Ettliger. London, Churchill: 115.

Wiesel, T.N. and D.H. Hubel (1963). Single cell responses in striate cortex of kittens deprived of vision in one eye. Journal of Neurophysiology **26**: 1003-17.

Wiesel, T.N. and D.H. Hubel (1965). Extent of recovery from the effects of visual deprivation in kittens. Journal of Neurophysiology **28**: 1060-72.

Wiesel, T.N. and D.H. Hubel (1966). Spatial and chromatic interactions in the lateral geniculate body of the rhesus monkey. Journal of Neurophysiology **29**: 1115-56.

Wiesel, T.N., D.H. Hubel and D.M.K. Lam (1974). Autoradiographic demonstration of ocular-dominance columns in the monkey striate cortex by means of transneuronal transport. Brain Research **79**: 273-9.

Wong Riley, M.T. and E.W. Carroll (1984). Quantitative light and electron microscopic analysis of cytochrome oxidase-rich zones in V II prestriate cortex of the squirrel monkey. Journal of Comparative Neurology **222**: 18-37.

Wong-Riley, M.T.T. (1979). Changes in the visual system of monocularly sutured or enucleated cats demonstrable with cytochrome oxidase histochemistry. Brain Research **171**: 11-28.

Yang, Y. and R. Blake (1991). Spatial frequency masking of human stereopsis. Vision Research **31**: 1177-89.

Zeki, S.M. (1969). Representation of central visual fields in prestriate cortex of monkey. Brain Research **14**: 271-91.

Zeki, S.M. (1970). Interhemispheric connections of prestriate cortex in monkey. Brain Research **19**: 63-75.

Zeki, S.M. (1973). Colour coding in rhesus monkey prestriate cortex. Brain Research **53**: 422-7.

Zeki, S.M. (1974a). Cells responding to changing image size and disparity in the cortex of the rhesus monkey. Journal of Physiology, London **242**: 827-41.

Zeki, S.M. (1974b). Functional organization of a visual area in the posterior bank of the superior temporal sulcus of the rhesus monkey. Journal of Physiology, London **236**: 549-73.

Zeki, S.M. (1975). The functional organization of projections from striate to prestriate visual cortex in the rhesus monkey. Cold Spring Harbour Symposia on Quantitative Biology **40**: 591-600.

Zeki, S.M. and D.R. Sandeman (1976). Combined anatomical and electrophysiological studies on the boundary between the second and third visual areas of rhesus monkey cortex. Proceedings of the Royal Society of London. B **194**: 555-62.

Zeki, S.M. (1977a). Colour coding in the superior temporal sulcus of rhesus monkey visual cortex. Proceedings of the Royal Society of London. B **197**: 195-223.

Zeki, S.M. (1977b). Simultaneous anatomical demonstration of the representation of the vertical and horizontal meridians in areas V2 and V3 of rhesus monkey visual cortex. Proceedings of the Royal Society of London. B **195**: 517-23.

Zeki, S.M. (1978a). Functional specialization in the visual cortex of the monkey. Nature (London) **274**: 423-8.

Zeki, S.M. (1978b). The third visual complex of rhesus monkey prestriate cortex. Journal of Physiology, London **277**: 245-72.

Zeki, S.M. (1978c). Uniformity and diversity of structure and function in rhesus monkey prestriate cortex. Journal of Physiology, London **277**: 273-90.

Zeki, S.M. (1979). Functional specialization and binocular interaction in the visual areas of rhesus monkey prestriate cortex. Proceedings of the Royal Society of London. B **204**: 379-97.

Zeki, S. (1980a). A direct projection from area V1 to area V3A of rhesus monkey visual cortex. Proceedings of the Royal Society (London) B **207**: 499-506.

Zeki, S. (1980b). The representation of colours in the cerebral cortex. Nature (London) 284: 412-8.

Zeki, S. (1982). Binocular cells of monkey striate cortex that receive conflicting information from the two eyes. Journal of Physiology, London 336: 26-7 P.

Zeki, S. (1983). The distribution of wavelength and orientation selective cells in different areas of monkey visual cortex. Proceedings of the Royal Society (London) B 217: 449-70.

Zeki, S. (1986). The anatomy and physiology of area V6 of macaque monkey visual cortex. Journal of Physiology, London 381: 62P.

Zeki, S. and S.D. Shipp (1987). Functional segregation within area V2 of macaque monkey visual cortex. Seeing contour and colour. J.J. Kulikowski, C.M. Dickinson and I.J. Murray. Manchester, Pergamon: 120-4.

Zeki, S. and S. Shipp (1988). The functional logic of cortical connections. Nature (London) 335: 311-7.

Zeki, S. (1990). A century of cerebral achromatopsia. Brain 113: 1721-77.

Zeki, S. (1991). Cerebral akinetopsia (visual motion blindness). Brain 114: 811-24.

Zeki, S. (1992). The visual image in mind and brain. Scientific American 267: 68-76.

Zihl, J., D. Von Cramon and N. Mai (1983). Selective disturbance of movement vision after bilateral brain damage. Brain 106: 313-40.